

# Functional polymer layers with protected amines

## DISSERTATION

zur Erlangung des akademischen Grades

Doktor rerum naturalium

(Dr. rer. nat.)

vorgelegt

der Fakultät Mathematik und Naturwissenschaften

der Technischen Universität Dresden

von

**mgr ing. Barbara Sieczkowska**

geboren am 04 Dezember 1977 in Radom, Polen

Gutachter: Prof. Dr. B. Voit (Dresden)  
PD. Dr. M. Mertig (Dresden)  
Prof. Dr. W. Binder (Halle)

Eingereicht am: 03.02.2009

Tag der Verteidigung: 08.05.2009

## Acknowledgments

I would like to express my deep gratitude to Prof. Dr. Brigitte Voit for giving me the opportunity to work in her research group and also for this interesting topic. I want to thank for her supervision and patience, constant support, valuable advises, constructive suggestions and comments. She opened up the fascinating and challenging field of chemistry for me.

I was glad to have the opportunity to be engaged with the Dr. Michael Mertig group from Technical University Dresden, Max Bergman Center for Biomaterials. I would like to thank Dr. Joerg Opitz for his scientific advices, interesting and productive discussions during our meetings. I gratefully acknowledge Mr. Jan Voigt for the help with the labeling experiments and the microscopy.

My gratitude goes to the IPF co-worker, who contributed to this work by performing analytical measurements and helped me in data interpretation as well for the helpful discussions: Mrs. Liane Häußler and Mrs. Kerstin Arnhold for the DSC and TGA measurements, Mr. Andreas Janke and Mrs. Nicole Petong for the help in the AFM analysis, Dr. Peter Simon and Mr. Dieter Pleul for XPS measurements, Mr. Roland Schulze for the ellipsometric measurements.

I am very grateful Dr. Hartmut Komber for his help in the interpretation of the NMR spectra. Mr. Dieter Voigt, Mrs. Petra Treppe, Mrs. Christina Harnisch for SEC measurements.

A big “thank you” goes to my best friend Mrs. Monika Molenda for her kindly attendance and great help by the syntheses, for her friendliness, cares and readiness to help in any situation.

The special thanks goes to Mr. Martin Gernert, Mrs. Elena Zelentsova, Dr. Marta Millaruelo-Boira, Dr. Martin Messerschmidt, Dr. Aleksandra Mendrek, Dr. Sebastian Mendrek for their friendship, moral support, discussions and having good times in Dresden.

I also wish to convey my sincere thanks to all colleagues which created friendly and pleasant atmosphere of work: Dr. habil. Doris Pospiech, Dr. Dietmar Appelhans, Dr. Felix Braun, Mrs. Carmen Krause, Mrs. Beate Weiße, Dr. Katrin Stumpe, Dr. Senta Reichelt, Dr. Sven Fleischmann, Andreas Korwitz, Dr. Ewa Pavlova, Dr. Falko Schallausky, Dr. Arnulf Scheel, Vicky Rose, Dr. Zeynep Özyürek, Dr. Renata Kęska, Dr. Naranayan Radha Krishnan, Ute Leuteritz, Dr. Yulia Mikhaylova, Dr. Thorsten Hoffman, Dr. Ulrich Schulze, Saija Ptacek, Mrs. Kathrin Eckstein, Mr. Helfried Kunath.

Most of all I would like to thank to my parents Anna and Wiesław and to my sister and brother: Małgorzata and Jacek for their constantly support and for their encouragements to finish my study abroad, who has always been there for me.

I dedicate this work to my daughter Victoria Anna for her endless loves, laughs and smile that made all of the above possible and really delight me during a hectic and hart time.

The financial support by Deutsche Forschungsgemeinschaft (DFG) is gratefully acknowledged.

---

<b>1</b>	<b>INTRODUCTION.....</b>	<b>4</b>
<b>2</b>	<b>THEORETICAL PART.....</b>	<b>6</b>
<b>2.1</b>	<b>THIN ORGANIC FILMS AND PATTERNING.....</b>	<b>6</b>
2.1.1	Langmuir and Langmuir-Blodgett films (LB film).....	6
2.1.2	Self-assembled monolayers .....	9
2.1.3	Thin organic polymer films by spin-coating.....	11
2.1.4	Comparison of thin film preparation.....	14
2.1.5	Patterning techniques.....	17
2.1.5.1	Conventional Lithography.....	17
2.1.5.2	Alternative Lithographies.....	20
2.1.6	Characterisation of thin organic films.....	23
<b>2.2</b>	<b>THIN ORGANIC FILMS ON GOLD SUBSTRATES.....</b>	<b>29</b>
2.2.1	Gold in technical application.....	29
2.2.2	Anchoring groups to gold.....	31
<b>2.3</b>	<b>TERPOLYMER CONCEPT .....</b>	<b>34</b>
2.3.1	Photo labile protecting group for amine .....	36
2.3.2	Free radical polymerisation .....	43
2.3.3	Living/controlled radical polymerization .....	48
2.3.3.1	Nitroxide mediated living free radical polymerization (NMRP).....	48
2.3.3.2	Atom transfer radical polymerization (ATRP) .....	54
2.3.3.3	Reversible addition-fragmentation chain transfer polymerization (RAFT) .....	57
2.3.4	Polymeranalogous reaction – “Click chemistry” .....	61
<b>3</b>	<b>AIM OF THE WORK .....</b>	<b>64</b>
<b>4</b>	<b>RESULT AND DISCUSSION.....</b>	<b>67</b>
<b>4.1</b>	<b>SYNTHESIS AND CHARACTERISATION OF AMINO TERPOLYMES .....</b>	<b>67</b>
4.1.1	Synthesis of dithiolate monomers.....	67
4.1.2	Synthesis of N-(N-NVOC-aminopropyl)methacrylamide (NVOC) .....	72

---

4.1.3	Synthesis of co- and terpolymers by FRP .....	74
4.1.4	NVOC deprotection .....	78
<b>4.2</b>	<b>COMBINING NMRP AND CLICK CHEMISTRY FOR THE PREPARATION OF MULTIFUNCTIONAL POLYMERS .....</b>	<b>81</b>
4.2.1	Multifunctional polymer through precursors.....	81
4.2.1.1	Synthesis of starting precursor polymer by NMRP for click reaction	81
4.2.1.2	Copolymerisation of active ester .....	88
4.2.1.3	Postmodification through 1,3-dipolar cycloaddition .....	90
<b>4.3</b>	<b>THIN FILM PREPARATION AND PATTERNING .....</b>	<b>100</b>
4.3.1	Film preparation.....	100
4.3.2	Patterned thin films.....	108
4.3.2.1	Labelling of patterned films with fluorescent marker YOYO-1 ...	109
4.3.2.2	Site-specific binding of $\lambda$ -DNA.....	112
4.3.2.3	End-specific binding of $\lambda$ -DNA.....	113
<b>5</b>	<b>SUMMARY.....</b>	<b>115</b>
<b>6</b>	<b>EXPERIMENTAL PART .....</b>	<b>122</b>
<b>6.1</b>	<b>MATERIALS AND METHODS.....</b>	<b>122</b>
6.1.1	Materials.....	122
6.1.2	Instruments.....	124
<b>6.2</b>	<b>SYNTHESIS .....</b>	<b>129</b>
6.2.1	Synthesis of dithiolate monomers.....	129
6.2.2	Synthesis of N-(N-NVOC-aminopropyl)methacrylamide (NVOC) .....	132
6.2.3	Synthesis of co- and terpolymers by FRP .....	135
6.2.4	Click-chemistry .....	145
6.2.4.1	Synthesis of copper(I) catalyst .....	145
6.2.4.2	Synthesis of functional azides .....	146
6.2.5	Synthesis of starting precursor polymer by NMRP .....	153
6.2.5.1	Synthesis of poly(styrene-r-4-acetoxy-styrene) .....	153
6.2.5.2	Synthesis of poly(styrene-r-4-hydroxy-styrene).....	154

---

6.2.5.3	Synthesis of poly[styrene-r-4-propargyl-oxy-styrene)] .....	155
6.2.6	Multifunctional polymer through precursor by 1,3-dipolar cycloaddition	156
<b>7</b>	<b>LIST OF SYMBOLS AND ABBREVIATIONS .....</b>	<b>165</b>
<b>8</b>	<b>REFERENCES.....</b>	<b>169</b>

## 1 INTRODUCTION

Both patterning of ultrathin films and selective functionalisation of surfaces and their properties become more and more essential for the development of novel devices in micro- and nanotechnology [Dai03], [Jen04], [Mau05]. Micro- and nanopatterned material surfaces have attracted the attention of many researchers in industry and academia as a consequence of the promising applications in different areas such as optoelectronic devices, communications technology or semiconductor industry or biomedicine. Here new concepts of the patterning of surfaces with functional groups based on photoactive polymers are required.

In parallel during the last ten years there is a rising demand to obtain functional polymers with well defined and controllable structures, specially in nanoscience and nanotechnology, where the structure of the materials assumes a crucial role because of the small size scales involved [Lan04]. Lithographic patterning techniques as well as the bottom-up approach using nanostructure formation by self-assembly are used widely in this respect. In order to combine pattern formation with functionality, special functionalised polymers can be used. Here, photoremovable protecting groups can have a key role to the novel techniques of light directed synthesis, whereby the preparation of large arrays consisting of thousands of biopolymer sequences can be accomplished. Patterned functional polymer surfaces on gold are of special interest for use in sensoric and diagnostic. However, the films used have to be covalently attached to the gold covered substrate to allow use in liquid media.

Nowadays there is a wide range of techniques grouped under the name controlled radical polymerization (CRP) adequate for the preparation of polymers with assorted macromolecular architectures, controlled molecular weight, polydispersity index, and specific end-functional groups, allowing the targeting of materials with tunable properties and hence specific applications. They all constitute an exciting research field and attract substantial interest, both from an industrial and academic point of view. Among them, NMRP has appeared as an important synthetic tool whose development has been extremely rapid with exciting possibilities for the future [Haw01]. Both the mentioned techniques and highly efficient cycloaddition reactions, known as click chemistry, have been recently applied in the area of macromolecular science in the modification of surfaces, and also the synthesis of a variety of

materials of different nature, as polysaccharides, conjugated polymers, hydrogels, adhesives, supramolecular structures, and different polymeric architectures.

Click chemistry allows the preparation of multifunctional materials in simultaneous combination with other synthetic transformations, allowing at the same time absolute fidelity and quantitative yields of the new materials. Development of cascade and simultaneous functionalization approaches for the preparation of multifunctional materials has been explored by Malkoch et al. [Mal05] in which a combination of previously functionalized and non functionalized monomers is used for the preparation of materials ready for further modifications using the mentioned strategies.

Here an approach is presented combining the advantages of controlled radical polymerization (NMRP) and click chemistry for the synthesis of side-functionalized copolymers. These functionalized surfaces prepared by photolabile random terpolymers which covalently tethered to the gold substrate with the possibility for patterning by means of UV or laser irradiation are of high interest.

Thus, in this work the extension of click chemistry is shown for the preparation of structural near-perfect polymers consisting of simple units, with great potential for use in lithographic functional patterning and nanotechnology.



## 2 THEORETICAL PART

### 2.1 THIN ORGANIC FILMS AND PATTERNING

Organic thin films, self-assembled monolayer (SAM) and multilayer films are of interest for both fundamental studies and technological applications. Such films can be used in thin film optics, sensors and transducers, as protective layers, for high-resolution imaging materials, and for functionalized surfaces with specific chemical, biological, or adhesive properties [Rob90, Swa87, Whi90]. SAM-forming materials may be physisorbed layers, such as Langmuir-Blodgett films, or chemisorbed layers, such as organothiols bound to Au or organosilanes bound to silica. Both types of SAM films inherently offer a high degree of control in the direction normal to the plane of the film and substrate. Chemisorbed films are more versatile and stable, because the interaction between the film precursor and the surface is much stronger than in physisorbed film.

#### 2.1.1 Langmuir and Langmuir-Blodgett films (LB film)

Langmuir-Blodgett films (LB films) denote monolayers and multilayers of amphiphilic molecules transferred from the water-air interface (or liquid-gas interface in general) onto a solid substrate. The amphiphilic molecule is a molecule that is insoluble in water. One end is hydrophilic, and, therefore, is preferentially immersed in the water, and the other is hydrophobic, and preferentially resides in the air (or in the nonpolar solvent). The amphiphilic molecules are first dissolved in an organic solvent that is immiscible with water, spread on the water surface, and compressed by decreasing the area in which the molecules are confined, to form a monolayer at the air-water interface. These successive deposition steps lead to formation of multilayer films, or LB films which are the product of the individual molecular chain length and the number of times that the substrate has crossed the air-water interface [Ngu97]. The monolayer can be transfer onto a solid substrate either by dipping the substrate through the interface or by touching it to the interface. The procedure can be used to obtain ultrathin films with the structure and thickness (monolayer or multilayer) controlled at molecular level.

### *LB film deposition onto a substrate*

Two types of surfaces can be coated by the LB technique - hydrophobic (water repelling) and hydrophilic (water attracting). Deposition onto a hydrophobic surface always takes place on the down path while for a hydrophilic surface, deposition always takes place on the up path.

The surface of a substrate being coated with a LB film changes from hydrophobic to hydrophilic with every layer. Thus when a hydrophobic surface is immersed and coated with a monolayer, it will be completely hydrophilic while it is immersed. Then, when it is withdrawn from the subphase and a second layer is deposited, the surface will be hydrophobic again.

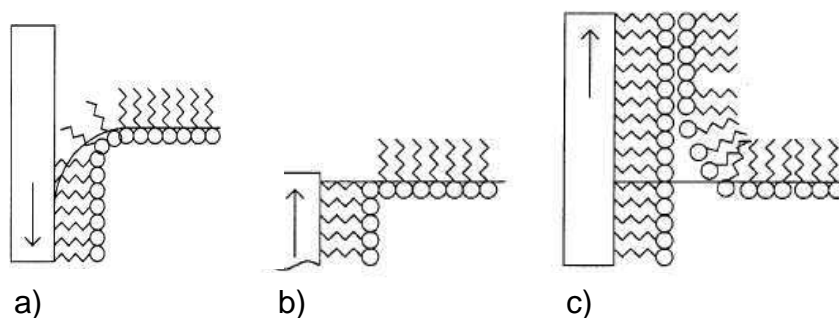


**Figure 2-1.** where:

*(a) Deposition of the first monolayer onto a hydrophobic substrate (a).*

*(b) The substrate reverses and the second layer is deposited (c).*

Hence, for deposition to occur, the prime criterion is that the curvature of the meniscus at the liquid/substrate boundary and the direction of motion coincide. It is easy to determine what type of surface you have - just immerse the substrate in the subphase. If the meniscus curves down, the surface is hydrophobic - if it curves up then the surface is hydrophilic. A hydrophobic substrate will result in deposition on the first down pass, the hydrophobic hydrocarbon tails adhering to the hydrophobic substrate. With a hydrophilic substrate, no ordered deposition will occur until the first up-stroke because the hydrophobic tails are repelled by the hydrophilic substrate as it is immersed in the water. Therefore an even (2, 4, 6...) number of layers is always

deposited onto a hydrophobic surface and an odd (1, 3, 5...) number onto hydrophilic surfaces.

The surface quality and composition of the substrate controls the nature of subsequently deposited layers. The deposition of the first layer is also of importance as this predetermines the manner in which subsequent layers are laid down. For consistent film quality, the monolayer must be kept at a constant pressure, even when transfer is actually occurring.

### *Application*

The LB-technique is one of the most promising techniques for preparing such ultrathin films as it enables the precise control of the monolayer thickness, homogeneous deposition of the monolayer over large areas and the possibility to make multilayer structures with varying layer composition [Ulm91]. An additional advantage of the LB technique is that monolayers can be deposited on almost any kind of solid substrate. Many possible applications of Langmuir-Blodgett films in the fields of electronics, optics, molecular electronics and biotechnology are currently being investigated by research groups throughout the world. Some examples are:

**Biology:** Cure for 'blue baby' syndrome. Some babies are born without the ability to breathe. This is because their lungs cannot absorb oxygen just after birth. Surfactants are being developed to be sprayed into the lungs to absorb oxygen. Once this process is stimulated, it is self regenerating. Surfactants are being designed by testing Langmuir monolayers for this oxygen absorbing ability.

**Chemistry:** Sensors - to have chemical sensors (such as gas detectors) it is best to have a large surface to bulk ratio. This gives higher signals for lower concentrations of gas and can improve reversibility of the detection process. LB layers are ideal candidates.

**Physics:** Optical waveguides and devices are being developed for computing and communications applications. The capability of fabricating dimensions to monomolecular tolerances and their ability to incorporate different molecular architecture give LB films some unique advantages in this field.

### 2.1.2 Self-assembled monolayers

Self-assembled monolayers (SAMs) are organic assemblies formed spontaneously by the absorption of molecular constituents from solution or the gas phase onto the surface of solids or in regular arrays on the solution of an active surfactant in an organic solvent (Figure 2-2) [Big46, Zis64]. The adsorbates organize spontaneously (and some-times epitaxially) into crystalline (or semicrystalline) structures. The molecules or ligands that form SAMs have a chemical functionality, or “headgroup”, with a specific affinity for a substrate; in many cases, the headgroup also has a high affinity for the surface and displaces adsorbed adventitious organic materials from the surface. There is a number of headgroups that bind to specific metal, metal oxides, and semiconductors.

The most famous include organosilicones on hydroxylated surfaces ( $\text{SiO}_2$  on Si,  $\text{Al}_2\text{O}_3$  on Al, glass, etc.) [Sag80, Coh86, Til89]; alkanethiols on gold [Bai89, Whi90, Str88]; silver [Ulm89]; copper [Ste86, Bla57, Bla57a]; dialkyl sulfides on gold [Tro88]; dialkyl disulfides on gold [Nuz87]; alcohol and amines on platinum [Tro88]; and carboxylic acids on aluminum oxide [All85, All85a, Oga85] and silver [Sch86], phosphates and phosphonate on  $\text{Al}_2\text{O}_3$  and on  $\text{TiO}_2$  [Zhu04].

In all these cases there are very strong molecule-substrate interactions. The apparent formation of chemical bonds at the substrate-monolayer interface is the result of these interactions. In such spontaneous adsorption reactions, molecules try to occupy every available binding site on the substrate, and in this process they push together molecules that have already adsorbed, thus eliminating free volume. This exothermic reaction may be compared to the pressure that the barrier in a Langmuir trough applies on the amphiphilic molecules at the water-air interface. A common feature of these systems is the spontaneous adsorption at the organic material-substrate interface, together with the strong van der Waals attraction amongst the alkyl chains, which are the driving force for the formation of highly ordered, and dense packed systems.

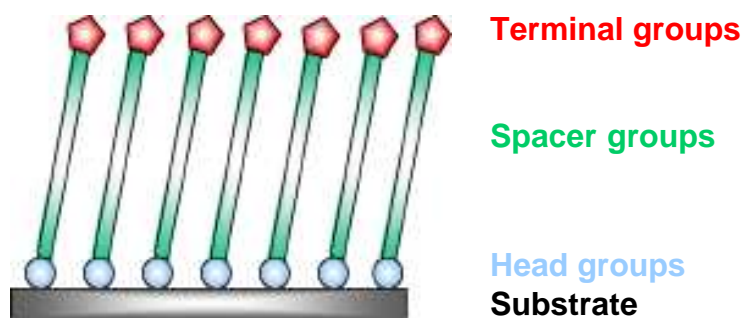


**Figure 2-2.** Scheme of monolayer structure.

Two families of SAMs attracted most of the attention of the researcher. The first is based on the reaction of (tri)chloro- or (tri)alkoxysilanes with a hydroxylated silicon surface [Mao88] and the second, conveniently prepared by exposure of gold surface to organosulfur (thiol or disulfide) solution, relies on the strength of sulfur-gold interactions [Nuz83, Jun98] (Figure 2-3). The latter is most investigated system because it is an ideal model system for studying the self-assembly process.

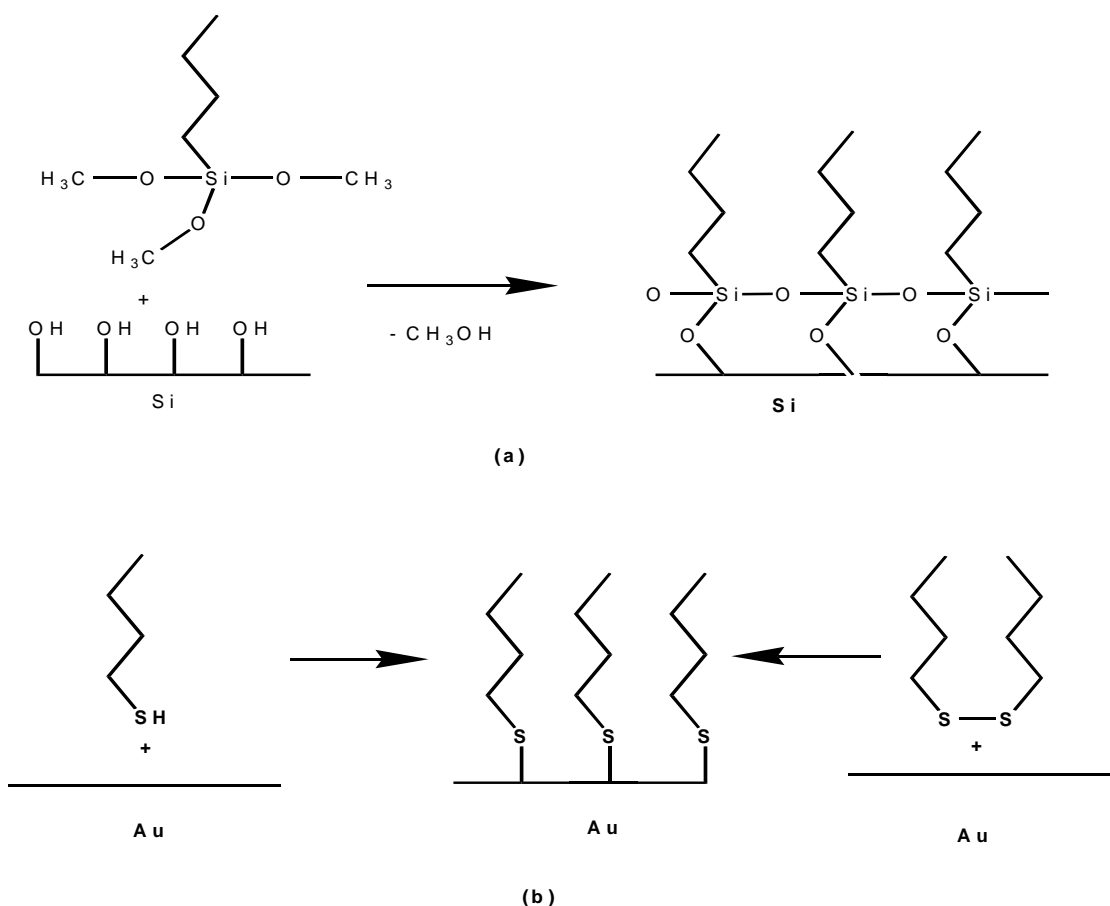


**Figure 2-3.** Formation of trialkoxysilane- SiO<sub>2</sub> (a) and gold-thiol (b) monolayers.

## *SAMs in Nanotechnology*

SAMs are themselves nanofilms with a number of useful properties and advantages i.e. like:

- easiness of the preparation, no requirement for example of ultrahigh vacuum (UHV) or other specialized equipment like i.e. in LB preparation techniques.
- they coat on objects of all sizes and are critical components for stabilizing and adding function to preformed, nanometer scale objects like thin films, nanowires and other nanostructures (their thickness is about 1-3 nm).
- they can connect the external environment with the electronic (current-voltage responses, electrochemistry) and optical (local refractive index, surface plasmon frequency) properties of metallic structures.
- they link molecular-level structures to macroscopic interfacial phenomena, such as wetting, adhesion, and friction.

These features make SAMs useful in organic synthesis providing a convenient, flexible, and simple system in order to tailor the interfacial properties of metal, metal oxides, and semiconductors. SAMs can be fabricated into pattern (in 10-100 nm dimension) in the plane of a surface by using microcontact printing [Xia98, Mic01], scanning probes [Liu00, Kra03, Gin04], beams of photons [Sha04, Sun02, Beh96], electrons [Gey01], or atoms [Ber95, Cha03].

### 2.1.3 Thin organic polymer films by spin-coating

Organic and polymer thin films play a important role in the development of electronic devices, passivation coatings, and chemical and biological sensors. However, in order to improve device and system performance and to meet future demands, new approaches are needed to grow thin films on wafer surfaces or small component areas with accurate thickness control. Depending on the particular application, one may want to deposit films containing single or multilayer structures of different organic or polymeric materials, homogeneous composite materials, or materials with graded compositions. In many situations, it will be necessary to deposit these materials discretely, achieve conformal coverage, and provide highly uniform films, especially with regard to surface coverage and thickness control.

Thin films of polymeric, inorganic, and organic materials also play an important role in batteries, organic transistors, high-performance dielectrics, optical data storage and communications, and displays based on organic electroluminescent materials. Polymeric and lower molecular weight organic materials are essential as coatings for chemical and biochemical sensors. In the biomedical field, the use of polymers is important for applications ranging from passivation films for prosthetic devices to smart coatings for drug-delivery systems.

Currently, thin films of organic and polymeric materials are processed by various techniques that differ in complexity and applicability. The selection of a deposition technique depends on the physicochemical properties of the material, the required film tolerances, the substrate to be coated, and the costs. The simplest methods of applying a thin organic film are solution casting, inkjet, aerosol, dip-, and spin-coating. In these techniques, a solution of the coating material in a volatile solvent is dispersed on a substrate surface. When the solvent evaporates, it leaves behind a coating of the polymer. Other techniques include in situ polymerization using plasma, electrochemical, catalytic, or photo-activated processes to coat directly onto the substrate surface.

In this work the spin-coating technique was used to produce the photolabile thin polymer films and two approaches were chosen to realize thin functional films, grouped into the two classes of polymers which are activated or deactivated by UV-irradiation. In the first concept pendant photolabile amino functions are incorporated into the polymer structure. Terpolymer containing the photolabile protected amino groups and sulfide units which allow the covalent attachment to gold substrates were synthesized via free radical polymerization. Thin films from these terpolymers were structures by UV-irradiation in order to create defined functional areas ready for further modification and attachment of biotemplates like DNA. In the second concept a highly efficient polymer-analogous modification was developed which allows the introduction of a variety of functional groups through the postfunctionalized reactions as well as better controllable structure of polymers and almost quantitative yield under mild conditions. Nitroxide mediated radical polymerization (NMRP) was used for the synthesis of the starting precursor polymer: poly(styrene-*r*-propargyl-oxystyrene). The material was modified by polymer analogous reactions using Cu(I) catalyzed 1,3 dipolar cycloadditions. A series of azides containing sulfide units was designed for the incorporation of fragments with

specific properties into the material like our earlier mentioned photoremovable amino protecting group which leads to the release of amino functions after selective UV/laser irradiation. The so obtained polymers are suitable to produce thin organic films by dip- and spin-coating.

### *Spin-Coating*

Spin-coating is a process used for fabricating thin polymer films from solution. A drop of the polymer solution is dispensed onto a substrate, which is held fixed by means of vacuum onto a substrate holder (disc). The disc with the sample is then rotated at a high speed (from hundreds up to several thousands revolutions per minute). The spinning motion causes the solution to spread out and form a thin solid film on the substrate. After the initial deposition of the solution onto the substrate, the process can be broken down into three stages (Figure 2-4) [Law88].

1. Acceleration
2. Film thinning
3. Drying

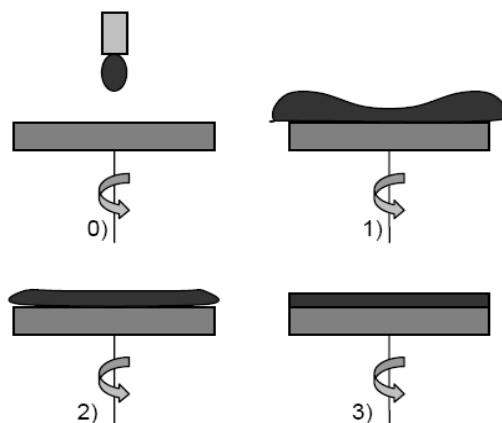


**Figure 2-4.** *The stages of spin-coating, 0) deposition of solution, 1) spreading during acceleration to final spin speed, 2) film thinning by outflow and evaporation, 3) drying by evaporation.*

During the acceleration stage (1) excess fluid (~90%) is slung off until the film is thin enough to co-rotate with the substrate. The dispensed volume of solution and the



acceleration rate have little effect on the final thickness and uniformity of the film unless the acceleration rate is slow (~10 seconds or longer for the acceleration stage) [Fla84]. In the next stage (2) viscous forces control the thinning process of the film as fluid flows off the substrate and solvent evaporates. It is in this stage that the final thickness and homogeneity of the film is determined. When the viscosity is so high throughout the whole film that the flow is drastically reduced, solvent evaporation becomes the dominant mechanism (stage 3) [Law88].

#### 2.1.4 Comparison of thin film preparation

With the increasing importance of thin film work, the need has arisen for the development of methods for film formation and for the investigation of thin films.

The most common methods for the formation organic thin films can be grouped as “dry” and “wet” methods. Dry processes, which include: plasma assisted deposition, physical vapor deposition, and chemical vapor deposition, organic molecular beam epitaxy (OMBE) etc. are techniques that have been adapted from solid-state materials processing [Sch99], [Scho99]. Wet methods usually require amphiphilic and organic or water-soluble polymers and monomers. Spin-coating, solution casting and dip-coating are three of the most important wet processes [Fla84].

As outlined before important techniques that have gained significant interest for the last thirty years are molecular, macromolecular, and supramolecular wet assembly methods. These assemblies are defined as the application of solution or interfacial techniques at the molecular level where molecules or macromolecules are observed to self-assemble or form ordered monolayers at the range of less than one to less than several nanometers per layer. The advantage of this method is the potential to “tailor” layer ordering, thickness, and orientation at the molecular level on a monolayer basis with short and long range or covalent and non-covalent interactions. Subsequently, multilayers can be built on solid support substrates. A uniform microstructural arrangement at the nanometer level is critical to achieve adequate control of layer dimensions. Because these techniques involve adsorption (physisorption or chemisorption) in solution or at the air-water (solvent) interface, they are distinctly different from solvent casting and conventional vacuum evaporation deposition.

However, despite the wide range of techniques by which thin films of organic and polymeric compounds can be deposited, the utility of each process is restricted to certain types of materials.

An organized self-assembly monolayer (SAM) is a single layer of molecules on a substrate in which the molecules exhibit a high degree of orientation, molecular order and packing. There are two common methods for depositing a monolayer, namely Langmuir-Blodgett and self-assembly technique, as described before.

The drawbacks of using LB technique are that it is a time-consuming process and films tend to be fragile and mechanically instable. The self-assembly technique offers an alternative route to prepare monolayer thin films of highly ordered multifunctional compounds in a more effective and time saving manner. This technique is more advantageous than the LB technique in the sense that each layer in self-assembly (SA) film can be covalently linked and no excessive deposition can take place as it is limited by the reactive sites on the layer surface [Li93]. In self-assembly technique, monomolecular films of a surfactant are spontaneously formed on a substrate upon exposure of surfactant solution. Depending on the structure of the surfactant, these films can be disordered (liquid-like) or well-packed, resembling the organization of crystals. The degree of order in a monolayer is the product of many factors, including geometric considerations, electrostatic and dipole-dipole interactions within the monolayer, affinity of the head group of the surfactant to the surface, etc. A successful self-assembly requires a relatively strong bond between the substrate and an atom or moiety in the surfactant, and an additional lateral interaction between molecules in the monolayer. The strength of the head group-substrate bonds and the lateral interactions lead to the monolayer resistance towards removal by a solvent rinse. SAMs provide facile means of defining the chemical composition and structure of a surface, therefore, they have become the focus of intensive investigation. Potential technological applications can be found in areas such as wetting, lubrication, adhesion, corrosion, biocompatibility, catalyst, and chemical sensing and nanoscale lithography. When SAMs are used in areas of adhesion, such surfactants are called adhesion promoters.

Spin-coating is the preferred fabrication technique for polymer thin films since it does not require very high temperatures and creates films of the necessary range with thickness. Ultrathin films have thickness of a few to several hundred nanometers, in variations of the substrate. Spin coating method is an easy and general process for

coating polymer material or photoresist on silicon, glass and gold wafers. After dropping the coating solution onto the wafer, the degree of coating is controlled by the centrifugal force derived from the rotation perpendicular to the wafer. At low rotation speed, the coating solution spreads out on the wafer, and at high rotation speed (generally 2,000 ~ 4,000 rpm) thin films are formed. As described above, the spin coating method, distinctively compared to the conventional physical and chemical method, is a quite simple and effective way of making thin films with varying its thickness by just controlling parameters such as the time and speed of rotation as well as the viscosity and the density of the coating solution. Beyond that, thin polymer films obtained by spin-coating technique exhibit high flexibility and functionality because it is possible to form those films on all substrates which are mechanically quite stable. Polymer spin coatings have been widely used in the microelectronics industry for fabrication of photolithographic and resist patterns but have limited applications for large area displays.

When the choice of technique in the generation of thin organic films becomes an issue the question arises which organic material is appropriate for which substrate, and which preparation method. The general three techniques used in nanotechnology and other applications are outlined in the Table 2-1.

**Table 2-1.** *The main division of thin organic films.*

<b>TYPE</b>	<b>MOLECULES</b>	<b>SUBSTRATE</b>
Langmuir - Blodget	Alkyl-acids (R-COOH) others	Metal-oxides, Al <sub>2</sub> O <sub>3</sub> , AgO Any polar or ionic surface
Self Assembly	Thiols (R-SH) Phosphonates (R-PO <sub>3</sub> H) Silanes (R-SiX <sub>3</sub> )	Au, Ag, Cu Ta <sub>2</sub> O <sub>5</sub> ; TiO <sub>2</sub> ; Al <sub>2</sub> O <sub>3</sub> ; .... Many substrates
(Ultra)Thin films	Organic and inorganic polymer; biopolymer	All substrates

## 2.1.5 Patterning techniques

The trend in electronics fabrication is continuously going towards smaller and smaller structures. Downscaling the size of the components increases their performance and density, lowers the power consumption and the cost. The dimensions in microfabrication are typically 0.1 – 100  $\mu\text{m}$ . Microfabrication techniques are increasingly being used also outside traditional microelectronics, including microfluidics, microelectromechanical systems, such as microsensors, microactuators and micro-optics. Most research in microfabrication is still silicon-based, originating in microelectronics, but new materials and areas of research are also increasing like the use of gold substrate. Top down nano-fabrication is an extension to microfabrication, defined as the process of fabricating structures with the dimensions of 1 - 100 nm. The field of nanotechnology is growing rapidly, and new ideas are being introduced frequently.

Many lithography methods such as photolithography, electron-beam lithography, micro-contact printing, nanoimprint lithography, and scanning probe lithography are being used to fabricate structures and patterns on substrates from the micro- to the nanoscale. Very few methods offer the ability to work routinely in the sub-50-nm regime with control over the feature size and interfeature distance, especially when such features are made of both hard and soft materials.

### 2.1.5.1 Conventional Lithography

When the features are miniaturized, the fabrication becomes challenging. The conventional way of patterning structures in microfabrication is lithography. Lithographic techniques are used to create patterns on substrates. Thanks to lithography, a wide variety of devices can be made. Lithography is a process in which the substrate to be patterned is covered with a layer of radiation-sensitive polymer, a photoresist. The resist is locally exposed to radiation, which modifies the structure of the polymer chain to change its solubility properties. After exposure, the resist is developed in a suitable solution, and the desired pattern is created onto the substrate. Conventional lithography includes photolithography and beam (electron or ion) lithography.

## *Photolithography*

In photolithography, the substrate is covered with a photoresist and a photomask above it, having dark and bright parts, letting the radiation through selected areas. With a positive photoresist, the bright parts of the mask, where the radiation gets through, cause the resist material to become soluble in a developer solution, while the dark parts are protected and insoluble and thus remain on the substrate after development in the appropriate solution. In a negative photoresist, the exposed parts become insoluble and unexposed parts are soluble in the developer solution. After development, the pattern of the mask is portrayed by the remaining resist on the substrate. The resist can be used as a mask in subsequent etching or deposition steps. The photolithography process is presented in Figure 2-5. In Figure 2-5a, the mask is in proximity contact with the resist, with a gap in between the mask and resist, usually in the range of 3 - 50  $\mu\text{m}$ . The mask can also be in hard contact, with no gap in between, or in projection mode, (Figure 2- b) using a lens system that allows for example a 1:4 reduction in feature size. The hard mode offers better resolution than proximity mode, but the masks get damaged in the contact, shortening the mask lifetime.

In photolithography, the exposing radiation is typically ultraviolet (UV) having the wavelength of 365 - 436 nm. Smaller resolution can be achieved with deep ultraviolet (DUV), wavelength of 193 - 248 nm, or extreme ultraviolet (EUV), wavelength of 10–14 nm. In projection mode the size is also decreased using reduction optics. With EUV, the reflective optics have to be specially fabricated, to avoid the problem of absorption in these short wavelengths, as most materials strongly absorb them. Even better resolution can be achieved with X-rays, using high energy and thus short wavelength, around 1 nm. The reduction optics cannot be used with X-ray lithography; it is used in proximity mode. Also mask fabrication is problematic with X-ray lithography [Fra04, Div04].

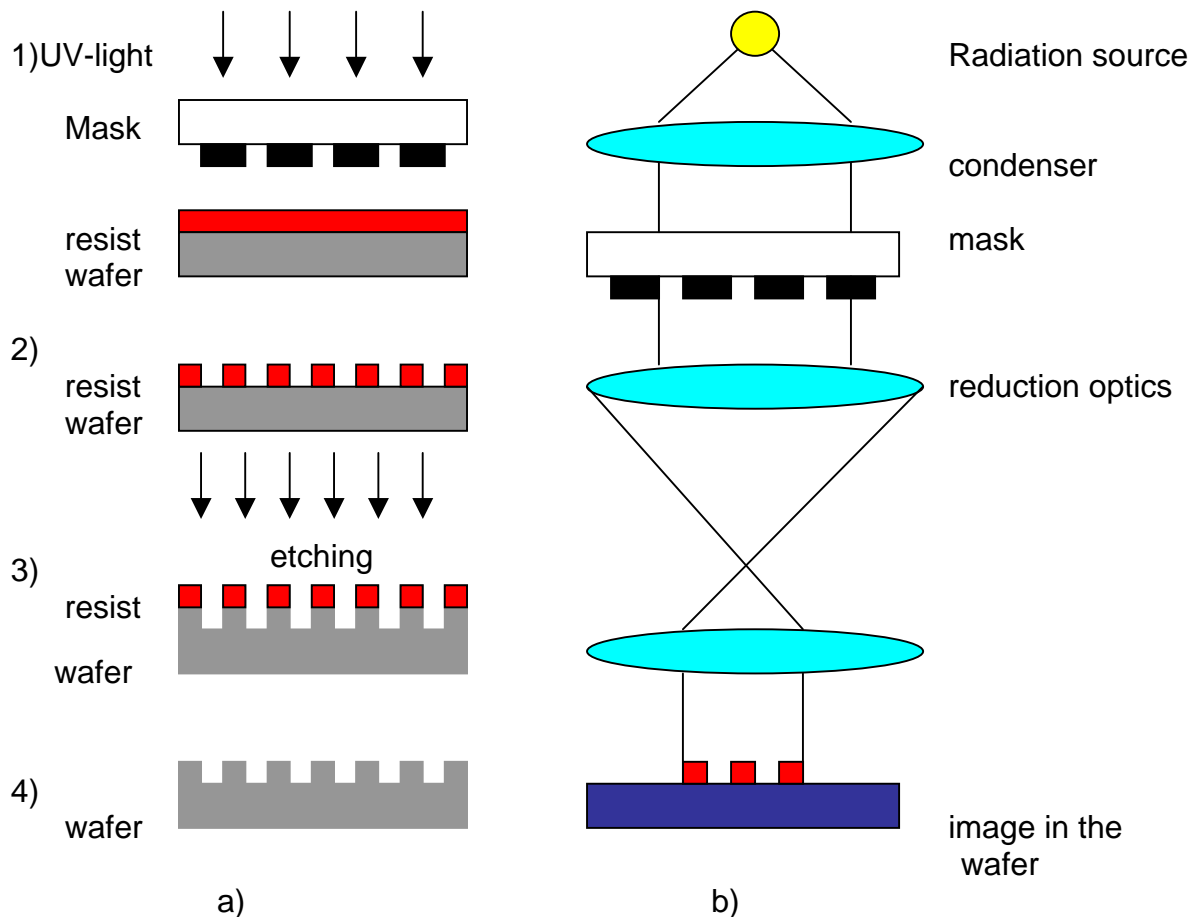


**Figure 2-5.** a) Principle of proximity photolithography. a1) A mask is placed on top of the resist-coated wafer, and exposed to UV light, letting the light expose the resist through the holes in the mask. In the next step a2), the resist is developed, in order to remove exposed parts (positive resist) creating a resist pattern on the wafer. a3) the resist pattern can act as a mask in a subsequent etching step, a4) after the removal of resist, wafer has the etched mask pattern. b) The principle of projection lithography with reduction optics in order to reduce the feature size in the wafer. The drawings are not in scale.

### Scanning Beam Lithography

Scanning beam lithography is a maskless process, including electron beam lithography (EBL) and focused ion beam lithography (FIB). The sample is covered by an electron or ion sensitive resist layer, a focused beam scans across the sample, and turns on and off according to the data input, exposing the resist point-by-point to produce the image. This is called direct writing. In EBL, the beam consists of electrons;

and in FIB the beam consists of ions, typically gallium, ( $\text{Ga}^+$ ). With FIB, direct removal of particles by sputtering the substrate without a resist is also possible.

In EBL the resolution is limited by the scattering of electrons, whereas in FIB the ion scattering from the resist and backscattering from the substrate is very low. The major problem in FIB is the damage to samples caused by high energy ions. FIB has higher resist exposure sensitivity than EBL, but throughput of FIB is lower than with EBL because of the much lower velocity of charged ions with respect to electrons when accelerated to comparable energies [Div04].

With scanning beam techniques, a smaller resolution can be achieved than with photolithography, but the downside is its slowness. Photolithography is a parallel technique, meaning that the whole area is exposed simultaneously, through the mask, scanning beam lithography techniques are serial; point-by point exposure is quite slow, and it is better suitable for research purposes than batch production. EBL is usually used for producing the photomasks for photolithography [Xia99, Div04, Gat05] and scanning beam lithography using lasers is used for microfabrication and offset printing. Using relatively cheap laser diode arrays (up to 254) speeds up the process.

### 2.1.5.2 Alternative Lithographies

One of these unconventional lithographies is called soft lithography. It is a family of techniques that use organic, soft materials to perform replication and pattern transfer. The term refers to a soft stamp or a soft substrate, such as polymers or self assembled monolayers. Soft lithography techniques are based on molding, replication and pattern transfer. These are alternative lithographic techniques, since instead of radiation exposure they use physical deforming or material transfer to replicate the patterns. Soft lithographic techniques are promising methods for parallel patterning, since they could allow higher throughput, and do not require expensive equipment.

Microcontact printing ( $\mu\text{CP}$ ) consists of depositing an ink that forms a SAM on a substrate with the help of a soft stamp by simple contact [Jac95]. It is a direct patterning method that permits working on non-flat surfaces. As the deposited ink molecules are highly ordered, they allow controlling the surface chemistry of substrates, and they can be used to form resist masks for etching. Using this technique, surfaces can be functionalized with small molecules (thiols on gold), precursors (catalyst, functionalized polymers) as well as biological molecules

(proteins, DNA) [Mic02]. An advantage of  $\mu$ CP is that it is possible to print on flexible substrates. The resolution is limited by the size of the stamp features, the stability of the flexible stamp structures and ink diffusion. The usual feature sizes produced by  $\mu$ CP are on the micrometer scale, but sub-micrometer features, down to about 100 nm have been created by using fine-tuned processes [Xia98a].

The soft lithographic techniques enable the fabrication on non-planar surfaces with a wide range of materials. These are relatively new technologies still at the stage of research. Usually the first step in soft lithography, the master fabrication, needs the use of conventional lithography, so it cannot be done completely without cleanroom and high-cost equipment. High-cost, high-resolution, slow-throughput equipment can be used in the master fabrication, and low-cost soft lithography can be in replication of the features of the master [Xia98, Xia99].

While top-down techniques are based on making existing patterns smaller and smaller, the alternative and very promising bottom-up approach relies on spontaneous formation, or self-assembly, of nanosized structures. Self assembly is a bottom-up production technique in which atoms or molecules arrange themselves into ordered nanoscale structures by physical or chemical interactions between the units. The goal of the bottom-up approach is to mimic nature's building process using various kinds of self-assembly techniques. These approaches may be classified as being either chemical or biological. Single molecule research began with biomolecules, like DNA, not only because they are the "building blocks of life", but also because of their large size, which facilitates their visualization. Self assembly of proteins like S-layer [Mer07], [Ryz07]. The chemical approaches apply the rules of bonding and kinetics for chemical objects to form stable and useful structures. Most of the current self-assembly methods produce 2-dimensional surfaces or interfaces. For example, thiol (SH) bonds attached to molecular groups are used to form a self-assembled monolayer (SAM) on metal surfaces with desired surface properties. The advantage of bottom-up techniques is the straightforward application of the associated self-assembly processes such as immersion, drop-casting, spin-coating, dip-coating, etc. It also allows large area processing but the choice of patterns is limited to periodic structures with homogeneous sizes as well self assembly of block copolymers [Che06].



### *Bottom-up and top down approach*

Micro- and nanostructures are usually patterned by photolithography and etching, based on removal of material, so called top-down approach. These techniques are highly developed and widespread. They have their limitations, however. The patterning of nanoscale dimensions means higher equipment cost with conventional techniques, and going to smaller dimensions requires scanning beam serial techniques, which have a low throughput. Nanotechnology requires lithography techniques with improved resolution down to the sub-100 nm scale. The unconventional techniques provide an alternative way to fabricate small structures. The techniques of nanofabrication comprehend top-down and bottom-up approaches. In the top-down approach, a bulk material is patterned laterally while in the bottom-up approach, molecules or particles self-assemble on a surface.

Creating patterns of self-assembled monolayers (SAMs) using top-down and bottom-up approaches has received a rising interest. Such methods allow to chemically pattern a substrate, opening new possibilities for etch resists [Abb94, Mico1] or to control the position and attachment of molecules and particles with different functionalities on a substrate. Different applications have been demonstrated for patterned functionalized SAMs. For instance, the use of functionalized molecules has made it possible to fabricate sensors [Vee00] and molecular electronic devices [Che03,Zho97]. Working with proteins, biological arrays can be prepared [Zhu03] and, employing (non-functionalized) nanoparticles, photonic crystals can be fabricated [Kal03, San03]. Controlling the functionality of the chemical pattern allows to build-up complex systems [Aul04].

In the Table 2-2 we show some of the types of materials and products of both methods.

**Table 2-2.** *The use of bottom-up and top-down techniques in manufacturing.*

Bottom-up			Top-down	
Chemical synthesis	Self-assembly	Positional assembly	Lithography	Cutting, Etching, Grinding
Particles Molecules ↓	Crystals Films, Tubes ↓	Experimental atomic or molecular devices	Electronic devices chips, masks ↓	Precision engineered surfaces ↓
Cosmetics, fuel additives	Displays		Quantum well lasers, computer chips MEMS	High quality optical mirrors

### 2.1.6 Characterisation of thin organic films

Along with the successful preparation of thin organic films on gold, glass, and metal oxides in the early 1980s, analytical techniques have been developed with sufficient sensitivity to allow the detailed characterization of thin layers. Thorough investigation on, in particular, SAMs on gold has led to a basic understanding of their growth and final structure.

The total amount of organic material in a well-packed monolayer of alkanethiols on gold is approximately  $8.3 \times 10^{-10}$  mol cm<sup>-2</sup>. Such small quantities of material make it impossible to find a single analytical technique that is capable of giving a complete picture of the SAM. Therefore, it is essential to use a variety of characterization techniques that are able to determine certain properties of the layer (e.g., thickness, chemical composition, packing density, etc.). Only the combined information of these measurements eventually leads to an accurate molecular picture of the SAM and other thin organic layers. Some of the more frequently used techniques for thin layer characterization have been divided into five groups and are summarized in Table 2-3.

**Table 2-3.** Analytical techniques for organic thin layer characterization.

Analytical technique [a]	Structural information
<u>General</u>	
Contact angle	Hydrophobicity, order
QCM/SAW	Changes in mass
<u>Optical</u>	
IR spectroscopy	Functional groups, molecular orientation
UV-vis spectroscopy	Density of adsorbates
Ellipsometry	Layer thickness
SPR	Layer thickness
<u>Vacuum methods</u>	
XPS	Elemental composition
AES	Elemental composition
SIMS	Molecular mass of adsorbate (+ fragments)
<u>Microscopy</u>	
AFM	Molecular packing, homogeneity, surface roughness
STM	Molecular packing
<u>Electrochemical</u>	
Cyclic voltammetry	Thickness, order/defects
Impedance spectroscopy	Thickness, order/defects

[a] QCM = quartz crystal microbalance, SAW = surface acoustic wave, SPR = surface plasmon resonance, XPS = X-ray photoelectron spectroscopy, AES = Auger electron spectroscopy, SIMS = secondary ion mass spectroscopy, AFM = atomic force microscopy, STM = scanning tunneling microscopy.

Some of the methods also used in this work will be briefly described in the following:

### Contact angle measurements ( $\theta_{eq}$ ),

are widely used to characterize the particular solid/liquid interaction and this is a simple and effective method to obtain a first impression about the structure and composition of the monolayer. Therefore, the contact angle serves as an indication of wettability of a solid by a liquid. Classically, the contact angle is described in two ways: firstly, a force balance method and secondly, the energetic description. When in statistic equilibrium the line which delimits the wetted and the dry part of the surface, the contact line, has to remain fixed. In the horizontal direction this is fulfilled by a simple force balance illustrated in Figure 2-6. Therefore, drop of a liquid forming

such angle may be considered as resting in equilibrium by balancing three forces which are correlated by Young's equation (Eq. 2-1) [KWO 99]:

$$\gamma_{lv} \cos(\theta_{eq}) \approx \gamma_{sv} - \gamma_{sl} \quad (\text{Eq. 2-1})$$

where  $\Theta$  is the contact angle of a liquid droplet on a solid surface.  $\gamma_{lv}$ ,  $\gamma_{sv}$  and  $\gamma_{sl}$  are the liquid/vapor, solid/vapor and solid/liquid- interfacial tensions, respectively.

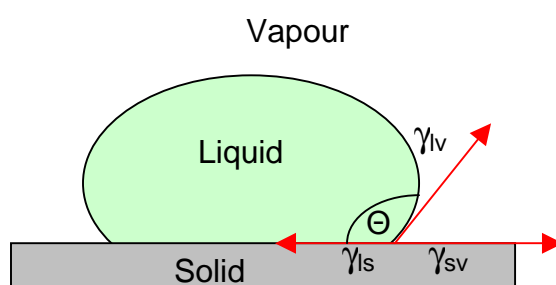


**Figure 2-6.** Scheme of three-phase contact of a droplet on a solid.

### *Infrared (IR) spectroscopy*

is a very powerful tool for the characterization of thin organic films. The spectra of SAMs on gold are usually studied in the grazing angle reflection configuration, where the incoming light is reflected under a large angle of incidence ( $>80^\circ$  relative to the surface normal) to maximize the absorbance by the monolayer. Due to the metallic substrate, only transition dipoles with a component perpendicular to the surface can be observed.

### *UV-vis absorption spectroscopy*

With this method thin layers of chromophoric adsorbates can be analyzed. Ultraviolet/visible spectroscopy involves the absorption of ultraviolet or visible light by a molecule causing the promotion of an electron from a ground electronic state to an excited electronic state. The absorption spectra, which are due to the light absorption, are then measured. The spectral range is from 200 to 800 nm, where the intensity of

the absorption bands can be related to the surface density of adsorbates by means of the Lambert- Beer law (Eq. 2-2):

$$\rho \approx \frac{A}{\varepsilon} \quad (\text{Eq. 2-2})$$

where:

$\rho$  is the film density of the chromophore,

$A$  is the absorbance of the organic layer,

$\varepsilon$  is the molar absorption coefficient.

### *Ellipsometry*

is the most common optical technique that uses polarised light to probe the dielectric properties of a sample and to estimate the thickness of thin organic films. It makes use of the fact that the polarization state of light may change when the light beam is reflected from a surface. It is based on a plane-polarized laser beam that is reflected by the substrate, which results in a change of the phase ( $\Delta$ ) and amplitude ( $\Psi$ ) of the light (Eq. 2-3). The polarization change is quantified in terms of the fundamental equation of ellipsometry. These parameters are related to the sample properties by:

$$\tan \psi \exp(i\Delta) \approx \frac{R_p}{R_s} \quad (\text{Eq. 2-3})$$

, where  $R_p$  and  $R_s$  are the complex reflection coefficients for the parallel and perpendicular polarization component, respectively [Tom99]. The parallel and perpendicular direction are defined with respect to the plane of incidence, which is the plane defined by the surface normal and the incident beam. The complex reflection coefficients describe how the linear polarization component in question changes in amplitude and phase factor due to the interaction with the sample. Therefore,  $\Psi$  basically describes the relative change in amplitude of the two

components, while  $\Delta$  describes the relative change in phase of the two linearly polarized components [Tom99].

### *X-ray photoelectron spectroscopy (XPS)*

is a surface analytical technique in which the sample is irradiated with monochromatic X-rays, which leads to the emission of core electrons (photoelectrons). An analyzer collects the escaping photoelectrons and measures their abundance as a function of their kinetic energy. The kinetic energy is defined by the energy of the X-rays ( $E_{x\text{-ray}}$ ), the binding energy of the electron ( $E_b$ ), and the workfunction of the spectrometer ( $\Phi$ ) (Eq. 2-4)

$$E_{kin} \approx E_{x\text{-ray}} - E_b - \Phi \quad (\text{Eq. 2-4})$$

Since the binding energies depend on the element and its oxidation state, XPS can be used to determine the elemental composition of the outer few nanometers of solid samples.

During XPS measurements, core-level electrons are emitted, thus creating a vacancy that is filled by an electron from the outer shells. The released energy during this process can be used to emit one of the outer electrons (Auger electron)  $\longrightarrow$  AES.

### *Atomic force microscopy (AFM)*

is a microscopy technique that allows the characterization of organic films with molecular resolution. Three fundamental operating techniques are usually performed with AFM, namely the contact, the non-contact mode, and the intermittent contact mode (also referred to as tapping mode). Contact mode is usually applied to "hard" materials where the rather large force does not damage the surface. For soft materials, such as colloids and polymers, non-contact or intermittent contact mode is used.

Atomic force microscopy probes the surface of a sample with a sharp stylus, called a tip. The tip is a few microns long and located at the end of a cantilever that is 100 to 200  $\mu\text{m}$  long. It is usually made of Si or  $\text{Si}_3\text{N}_4$  and is capable of measuring forces between  $10^{-12}$  to  $10^{-9}$  N. Forces between the tip and the sample surface cause the cantilever to bend or deflect. A laser beam is reflected from the back side of the cantilever and is focused on a photodiode sensor. When the cantilever is deflected the position of the laser spot on the detector changes. The force acting on the cantilever is proportional to the deflection. Therefore by adjusting a force setpoint, the force between tip and sample is also adjusted. This results in a signal, which is recorded in a computer (Figure 2-7). The feedback of the computer controls the z translator (called piezoelectric scanner) to adjust the tip or sample up or down in order to restore the tip to its original deflection. The computer stores the vertical position of the z translator at each point and assembles the image [Ulm 91].

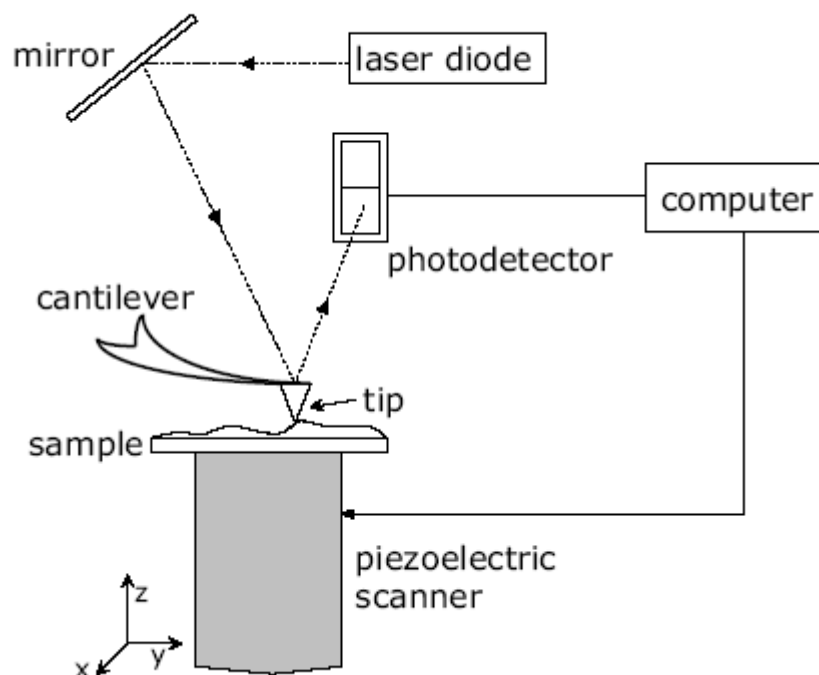


**Figure 2-7.** *The sample is positioned on the piezoelement that can be moved in xyz. As a raster-scan drags the tip over the sample, the photodetector measures the vertical deflection of the cantilever due to upwards or downwards deflection of the laser beam. The photodiodes can measure displacements of light smaller than 10 Å.*

## 2.2 THIN ORGANIC FILMS ON GOLD SUBSTRATES

### 2.2.1 Gold in technical application

Gold is important metal not only for the industry but also for medicine. Some characteristics make gold an ideal material for wide-ranging application in nanotechnology. At the nanoscale, gold displays properties and attributes that make it an important material for numerous nanotechnology-related products and process. The nobility of gold and its resistance to surface oxidation is one important material characteristic as well as good electrical and thermal conductivity.

The optical properties of gold at the nanoscale are also exciting, because gold nanoparticles have a colour varying from red to purple depending on particle size. These properties can be successfully exploited in a range of applications. Based on these unique properties exciting new nanotechnology applications using gold are being developed in various branch of industry like:

- **ELECTRONICS**

Gold and gold alloys have been key materials within the electronics and semiconductor industry for many years. Specific use of gold include contact and connector coatings for printed circuit boards (PCBs), component leads, gold bonding wires and sputtering targets. These uses are related to gold's outstanding corrosion resistance, ability to form metallurgical bonds by soldering or cold welding, ease of fabrication and good electrical and thermal conductivity.

- **CATALYST**

Nanosized gold can be used as a catalyst in chemical processing, pollution control and fuel cell applications. Indeed, its use requires preparations of gold of a very small particle size (less than 5 nm) on appropriate oxide support material. One of the most exciting aspect about catalysis by gold is the low temperature that can be used (the temperature at which the catalys becomes functional).

- **BIOMEDICINE**

Recently, gold prepared at the nanoscale was used and investigated for a variety of biomedical applications and devices. There have been direct applications of "bulk" gold in medical devices including wires for pacemakers, gold plated tents used to inflate and support arteries in the treatment of heart disease and implants that are at high risk of infections , such as the inner ear.



For example, the high opacity of gold to X-rays means that gold nanoparticles are being considered for use as intravenous contrast enhancers in medical imaging. In many instances, the potential application of gold is related to the interesting optical properties of the metal at the nanoscale and its biocompatibility.

Recently, Nippon Paint in Japan have developed a novel method to prepare concentrated and stable dispersions of gold nanoparticles having diameters of 5 - 15 nm. This involves two key nanotechnologies: the protection of particles from agglomeration by using a comb-shaped block copolymer to stabilize the particles and, secondly the use of an amine reduction method to yield gold nanoparticles under industrial conditions. They have reported the successful preparation of nanoparticulate pastes containing up to 95 % of metal particles. By selection the polarity of the protective polymer, the pastes remain stable when diluted or mixed with aqueous and non- aqueous media.

There are a few important reasons, which make gold very useful in the current modern technology:

- Gold is easy to obtain, both as a thin film by physical vapour deposition, sputtering, or electro-deposition and as a colloid, which is commercially available.
- Gold is easy to pattern by a combination of lithographic tools (photolithography, micromachining and others).
- Gold is a reasonably inert metal, it does not oxidize at temperatures below its melting point; it does not react with most chemicals. These properties make it possible to handle and manipulate samples under atmospheric conditions instead of under UHV.
- Thin films of gold are common substrates used for a number of existing spectroscopy and analytical techniques, including SPR spectroscopy, quartz crystal microbalances (QCM), RAIRS, and ellipsometry. Their characteristics are particularly useful for applications of SAMs for the studies of surface interactions.
- Gold is compatible with cells, that is, cells can adhere and function on gold surfaces without evidence of toxicity.

With the development of surface chemistry, many efforts have been made to achieve the real-time sensing and long-term monitoring of biomolecule interaction. Future biosensor are expected to maximize the use of signal amplification, fabrication and diagnostic processing. To this end, the attachment of biomolecule like DNA, nanotubes to microelectronics-compatible material such as gold has been developed.

In addition, a lot of compounds like thiols, disulfides, sulfides can be deposited in the form of thin organic films. The unique properties of gold make it an attractive substrate for chemical and biochemical modifications.

### 2.2.2 Anchoring groups to gold

It is known from the literature that sulfur compounds coordinate very strongly to silver [Ulm89, Wal91, Ihs94], GaAs [She92] and InP [Gu95] surfaces, nanosize  $\gamma\text{-Fe}_2\text{O}_3$  particles [Bru94] and colloidal gold particles [Bru94]. Sulfur as well as phosphorus make strong interaction with the gold substrate that promote the formation of a close-packed, ordered monolayers in opposite to the isocyanide which coordinates good to gold, too, but forms poorly packed monolayers. There is a number of reported surface active organo-sulfur compounds that form monolayers (Figure 2-8).

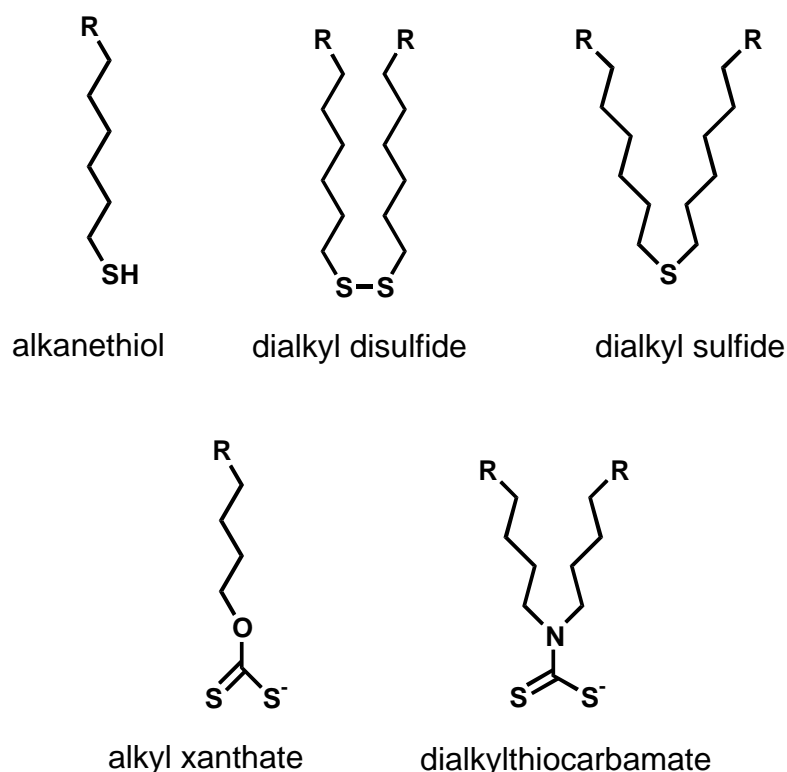


**Figure 2-8.** Surface active organosulfur compounds.

These include di-n-alkyl sulfide [Tro88, Kat92], di-n-alkyl-disulfides [Nuz83], thiophenols [Sab93, Bry92], mercaptopyridines [Bry92], mercaptoanilines [Hil93], thiophenes [Li84], cysteines [Coo93, Uvd92], xanthates [Ihs93], thiocarbaminates

[Arn89], thiocarbamates [Mie91], thioureas [Edw89], mercaptoimidazoles [Ard90, Xue91, Bha93].

It is a fact that alkanethiols and dialkyldisulfides can both physisorb on gold through van der Waals interactions which can be changed by varying the chain length and chemisorb through the sulfur bond.

Adsorption of organosulfur compounds on gold is an easy route to form self-assembled monolayers (SAM). The work of Bain et al. showed at relatively dilute solution ( $10^{-3}$  M) two distinct adsorption kinetics steps [Bai89] for the adsorption of alkanethiols on gold:

- 1) a very fast step which takes a few minutes, by the end of which the contact angles are close to their limiting values and the layer thickness reaches about 80 - 90 % of its maximum [Ulm91a].
- 2) a slow step, which lasts several hours, at the end of which the layer thickness and the contact angles reach their final values.

The initial step is depended on concentration of the sulfur compounds and is described by diffusion-controlled Langmuir adsorption [Bai89]. The second step can be described as a surface crystallization process, where alkyl chains get out of the disordered state and into unit cells, thus forming a two-dimensional crystal.

Therefore, the kinetics of the first step is governed by the surface-head group reaction, and the activation energy may depend on the electron density of the adsorbing sulfur. The kinetics of the second step is related to chain disorder (e.g. gauche defects), the different components of chain-chain interaction (VDW, dipole-dipole, etc.) and the surface mobility of chains [Ulm96].

Chemisorption of alkenethiols as well as di-n-alkyl disulfides on clean gold gives indistinguishable monolayers. The reaction of dialkyldisulfides with gold (0) is an oxidative addition one, forming gold(I)thiolate ( $RS^-$ ) species:



The reaction mechanism of disulfides on gold is not completely understood. The formation of  $RS^-Au^+$  requires the loss of the SH hydrogen, but it has not been determined yet, whether this proton is lost as  $H_2$ , either via the reductive elimination reaction of the gold (II) hydride ( $RS^-Au^{2+}-H^-$ ), formed by oxidative addition of the alkanethiol, or by another unknown reactions:



or as H<sub>2</sub>O, either via the reaction of the gold (II) hydride or another unknown species with trace of oxidant.



The bonding of the thiolate group to the gold surface is very strong (homolytic bond strength is approx. 40 kcal<sup>-1</sup>) [Dub92]. On the basis of the bond energies of RS-H, H<sub>2</sub> and RS-Au (87, 104, and 40 kcal mol<sup>-1</sup>, respectively), the net energy for adsorption of alkenethiolates on gold would be approx. -5 kcal mol<sup>-1</sup> (exothermic).

Adsorption energy of dialkyl disulfide is approx. -24 kcal mol<sup>-1</sup>, or -12 kcal mol<sup>-1</sup> per RS<sup>-</sup> [Sch95].

The rate of formation of thin organic films from dialkyl disulfides or alkanethiols were indistinguishable but the rate of replacement of molecules by thiols were much faster than by disulfides.

The structure of the alkanethiolates on gold was studied in detail by many researcher for example Strong and Whitesides and have thoroughly characterized SAMs using a large number of surface analytical tools like infrared spectroscopy, ellipsometry, studies of wetting by different liquids, X-ray photoelectron spectroscopy, electrochemistry, and scanning probe measurements. They have used these techniques to study the molecular packing of monolayer and multilayers organic film.

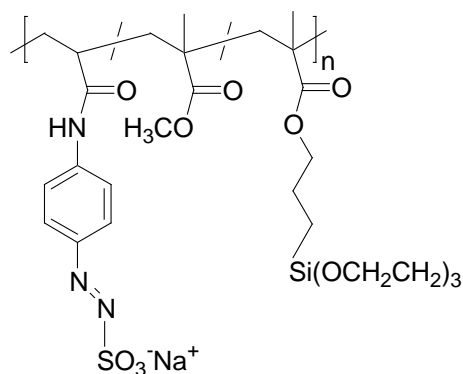
A variety of other methods have been developed for assembling metal and semiconductor colloids into nanomaterials. These methods have focused on the use of covalent linker molecules that possess functionalities at opposing ends with chemical affinities for the colloids of interest. One of the most successful approaches to date, Brust et al. [Bru95], involves the use of gold colloids and well-established thiol adsorption chemistry [Bai89a], [Dub92]. In this approach, linear alkanedithiols are used as the particle linker molecules. The thiol groups at each end of the linker molecule covalently attach themselves to the colloidal particles to form aggregate structures. An other example is the use as "crosslinker" highly branched macromolecules for gold nanoparticles. A high thiol- (aliphatic polythioether) or sulfide- (aromatic poly(phenylene sulfide)) group concentration on individual highly

branched macromolecules seems very attractive as it guarantees a strong binding between the organic crosslinker and the gold nanoparticles [Hie06]. The latter would ensure a well defined structure of the film and thus better control e.g. on sensor performance.

## 2.3 TERPOLYMER CONCEPT

Polymerization reactions can proceed by various mechanisms using various initiators. For addition polymerization of single compounds, initiation of chains may occur via radical, cationic, anionic or coordination-initiators, but some monomers will not polymerize by more than one mechanism.

Copolymerisation of several monomers can lead to multifunctional polymers also suitable for the preparation of patternable thin organic films. In previous work a so-called "terpolymer" concept was developed, where film forming monomers were combined with monomers which allow for surface anchoring and those which allow surface patterning by lithographic methods. By this method the fabrication of diazosulfonate terpolymers [Bra02] was demonstrated which allowed to be covalently attached as thin films to glass and silicon substrate after spin-coating (Scheme 2-1).

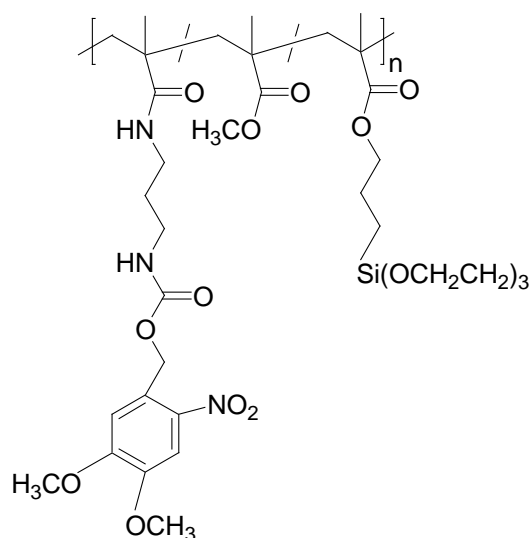


**Scheme 2-1.** Chemical structure of the terpolymer APAS/MMA/TMSPMA. The molar ratio of APAS = 20 % (sodium-4-acryloyl-aminophenyldiazosulfonate) , MMA = 75 % (methylmethacrylate) and TMSPA = 5 % (3-(trimethoxysilyl)propylmethacrylate).

For this, terpolymers containing the photolabile and charged diazosulfonate units, as well as anchoring groups (TMSPMA) have been synthesized via free radical polymerisation. Thin films from these terpolymers were structured imagewise by laser

light irradiation in order to create defined functional areas at the template surface ready for further modification and attachment of nanostructures.

An other alternative to obtain thin functional films was the incorporation of photolabile amino protecting groups in the polymer enabling the release of functional group by means of UV irradiation and which are suitable for further modification like attachment of colloid, metallization or DNA strands [Opi04], [Voi02]. Terpolymers containing the photolabile protected amino function introduced by N-(N-nitroveratryloxycarbonyl-aminopropyl)methacrylamide as well as (trimethoxysilyl)-propylmethacrylate and MMA have been synthesized via free radical polymerization and have been prepared similarly to the diazosulfonate films by spin-coating. Scheme 2-2 shows the resulting polymer structure.



**Scheme 2-2.** Chemical structure of the terpolymer NVOC/MMA/TMSPMA. The molar ratio of NVOC = 33,3 % (4,5-dimethoxy-2-nitrobenzyl-oxycarbonyl), MMA = 33,3 % (methylmethacrylate) and TMSPA = 33,3 % (3-(trimethoxysilyl)propyl-methacrylate).

By imaging the film, the protecting groups are removed and the free amine groups can be used to attach functional nanoelements like DNA strands.

### 2.3.1 Photo labile protecting group for amine

Protecting groups have an important role in organic chemistry. In order to find wide application these groups must fulfill several criteria:

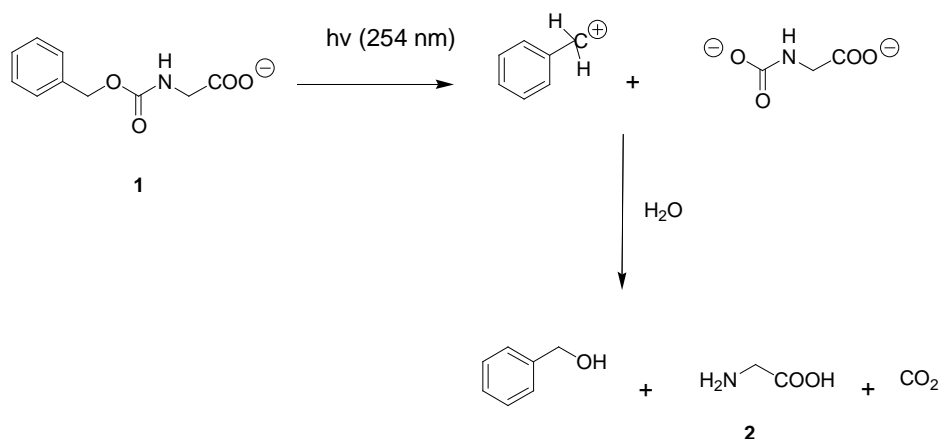
- react selectively in good yield to give a protected substrate that is stable to the projected reactions.
- has to be introduced into the molecule to be protected under mild conditions in a selective manner and in high yield; functional groups other than that to be protected must not be attacked.
- has to be stable under all the conditions used during the synthesis, including those of the purification steps, up to the step in which the protecting group is removed on purpose.
- the protecting group should have a minimum of additional functionality to avoid further sites of reaction.
- should be easy produceable and cheap.
- has to be cleavable under very mild conditions in a highly selective manner and in the high yield; other protecting groups present in the molecule and unprotected functionalities should not be affected by the cleavage conditions.
- should be introduced and removed with the help of readily available reagents, such that in both transformations the products can be easily purified.
- neither possess nor introduces a chiral centres.

The protection is usually accomplished directly by converting the particular group into a derivate which is known to be stable under the experimental conditions to be used and from which the original group may be regenerated without affecting the synthesized molecule.

Only a few protecting groups meet all of these demands and in most cases a compromise must be found, in which the most important criteria are addressed. In most cases guaranteeing that the protecting group is very stable and, at the same time, easily liberated when wanted is the crucial problem and overshadows the requirements for efficient introduction and the provision of desirable physical and chemical properties.

In the following, protecting groups especially for amino functions which can be removed photochemically will be described since those are of interest for the purpose of this work.

The first photoremovable protecting group (PRPG) was discovered by Baltrop and Schofield in 1962 [Bar62]. They found that upon irradiation with light of 254 nm of benzyloxycarbonyl glycine (1) is converted in a basic solution to the free amino acetic acid (Scheme 2-3).



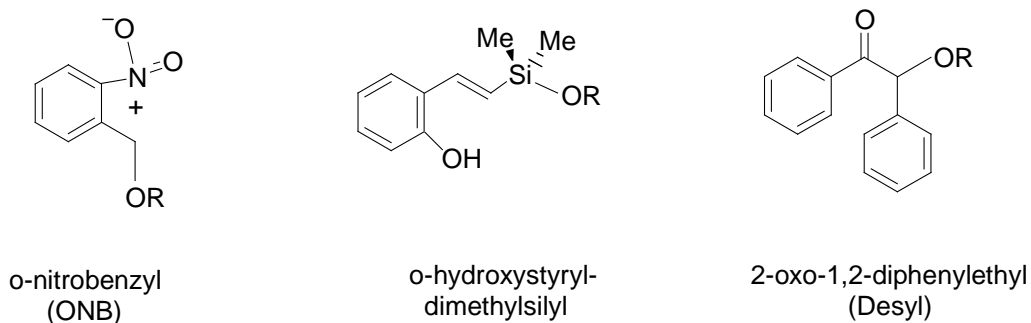
**Scheme 2-3.** Reaction paths for amino-glycoside.

Gradually many new photoremovable protecting groups have been developed for various functional groups like amines including carbamates (>NCO<sub>2</sub>R) and amides (>NCOR), hydroxyls, carbonyls, thiols and another, used more widely in syntheses of alkaloids and for the protection of the nucleic acids like adenine, cytosine, and guanine in nucleotide syntheses.

A photoremovable protecting group contains a chromophore which is sensitive to light, but relatively stable to most of the wide variety of chemical reagents. Therefore it can be selectively activated by irradiation with light of suitable wavelength. The wavelength of the light to be used must be such that it will be absorbed only by the protecting group and will not affect other parts of the molecule.

Of the many known photolabile protecting groups, the *o*-nitrobenzyl group has been often used in the form of ethers, esters, carbonates, carbamates, and acetals [Bar66]. Two further interesting photolabile protecting groups are the 2-oxo-1,2-diphenylethyl (Desyl) group [Giv93] and the *o*-hydroxystyryldimethylsilyl group [Pir93] (Scheme 2-4).

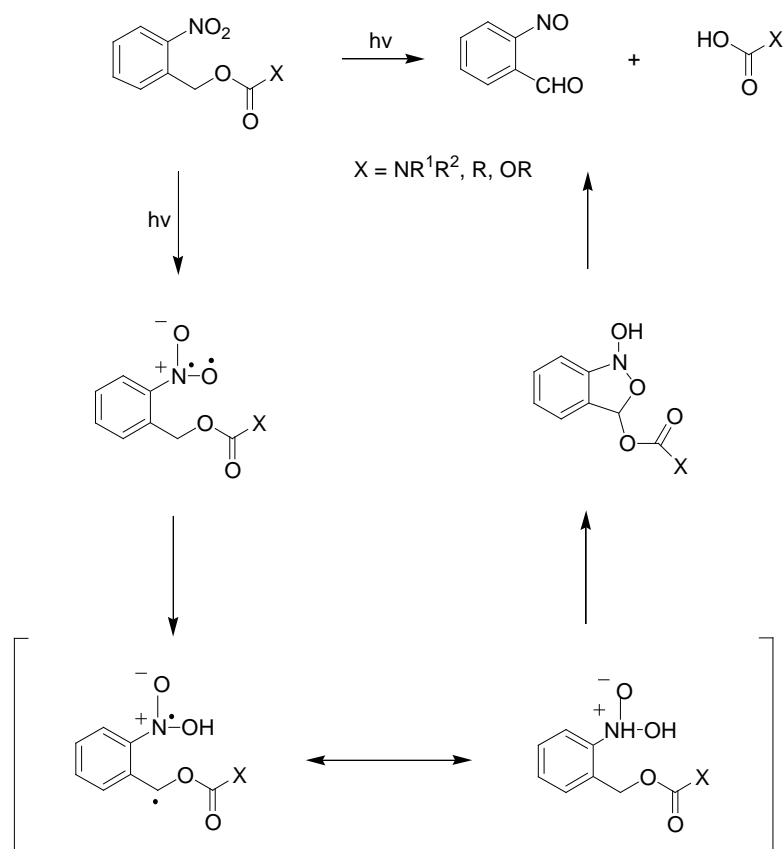




**Scheme 2-4.** A some example for photolabile protecting group.

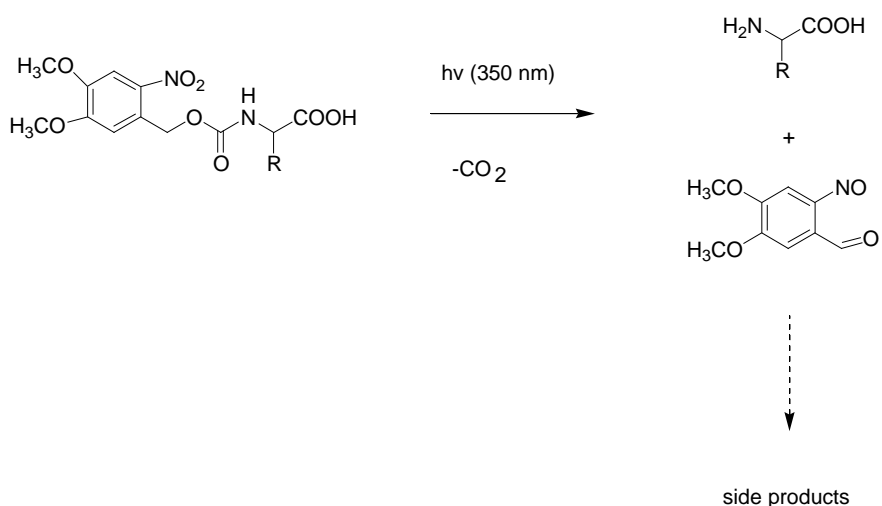
Photochemical reactions provide a convenient tool for activating important functional groups. In the photochemical activation approach the functional group is derivatized with a light-sensitive chromophore, which can serve as a latent activator of the functional group. On irradiation with light of suitable wavelength the functional group is converted to an active form and the light-sensitive chromophore is removed. The active species in which the functional group possesses enhanced reactivity towards the desired reaction permits synthesis under mild, neutral conditions. Such mild and neutral photochemical activation approaches have been found to offer effective synthetic methods for peptides, macrolides and carbohydrates.

The most popular photolabile protecting group for amines is undisputedly the 6-nitroveratryloxycarbonyl group (NVOC). First this group was introduced by Patchornik and his group in 1970 [Pat70]. It is based on the photochemically-induced photoisomerisation of o-nitrobenzyl alcohol derivatives into o-nitrosobenzaldehyde (Scheme 2-5).



**Scheme 2-5.** Mechanism of photorelease in *o*-nitrobenzyl derivatives.

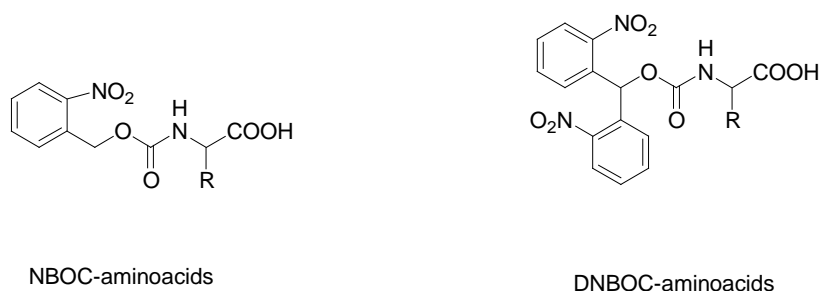
Carbamates, carbonates and esters are thus converted into an acetal derivative that spontaneously collapses into an aldehyde and spontaneous decarboxylation leads to the free amine. Although the vast majority of the systems involve the ortho isomer, photoisomeration of meta and para nitrobenzyl alcohols has been observed [Wan86]. Next, the two methoxy groups were introduced to increase to absorbance at wavelength longer than 320 nm. Under these conditions, even the most light-sensitive amino acid, tryptophan, was not affected (Scheme 2-6).



**Scheme 2-6.** Decomposition mechanisms of nitroveratryl carbamates through irradiation with UV light.

However, the desirable amount of the amino acid was not obtained even though the carbon dioxide evolution was quantitative. A serious side reaction is the formation of an imine, resulting from the reaction of the released amine with the aldehyde photoproduct. This could be suppressed by adding a carbonyl scavenger, such as semicarbazide hydrochloride to the reaction mixture. With this additive the yields are consistently quantitative [Boc02].

The use of additives with another *o*-nitrophenyl group to the benzylic methylene group should prevent the formation of diastereoisomers. In this case, the photolysis led to the release of a ketone, much less prone to imine formation than aldehydes. Hence, the di(nitrobenzyl)oxycarbonyl (DNBOC) group gave yields higher than 70%. The NVOC/NBOC groups were also used for the protection of the hydroxyl groups in carbohydrates. In many cases, the NVOC chloride (a chloroformate) is used to protect amines or alcohols (Scheme 2-7).



**Scheme 2-7.** Chemical structure of two protecting groups: NBOC and DNBOC.

All other criteria for an ideal protecting group apply to the photosensitive blocking group also. The photochemical reaction of the protecting group chromophore should in no way affect the substrate molecule and the protecting group photoproduct should be readily separable from the deprotected compound. The protecting group should be capable of being introduced and cleaved from the functional group in essentially quantitative yield.

Another important factor to be considered in the selection of a photosensitive masking group is the lifetime of the excited species that is responsible for the particular photoreaction. Thus, if the protected substrate has a long excited state lifetime before cleavage occurs, the chances for undesirable quenching processes to reduce the efficiency of the cleavage reaction are greater.

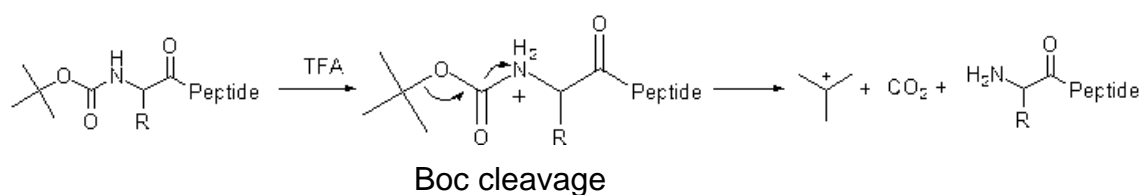
This would hinder the removal of the protecting group and also might labilise the quenching species such energy dissipation processes might result in some undesired changes in the substrate. Therefore, it would seem a distinct advantage to design a protecting group with a chromophore characterized by a short-lived excited state.

Photolabile protecting groups play an important role in synthetic organic chemistry, for caging of biologically active molecules, for light directed, combinatorial solid-phase synthesis of biopolymers and for UV-light patterning of SAMs [Wal01].

As recently reported UV-light patterning of ultrathin self-assembling monolayers (SAMs) of organic molecules for SAMs prepared from amines protected with photolabile groups allows to fabricate a chemical surface pattern or even direct deposition of molecules onto a substrate in one step by means of microcontact printing [Fod91], [Kru02]. In previous work we demonstrated a novel method to fabricate a functional surface pattern for a site-specific deposition of charged nanoparticles and biomolecules, based on optical exposure of a thin, spin-coated aminoterpolymer film, and intrinsically capable of massive parallel processing. The amino groups of the polymer film are protected by UV-labile nitroveratryloxycarbonyl (NVOC) groups [Bra03]. Thus, the film surface can be easily chemically patterned by applying UV light which causes photo-cleavage of the NVOC groups. As a result, the amino function is created at the UV-light exposed area, ready to use for a site-specific immobilization of nanoparticles.

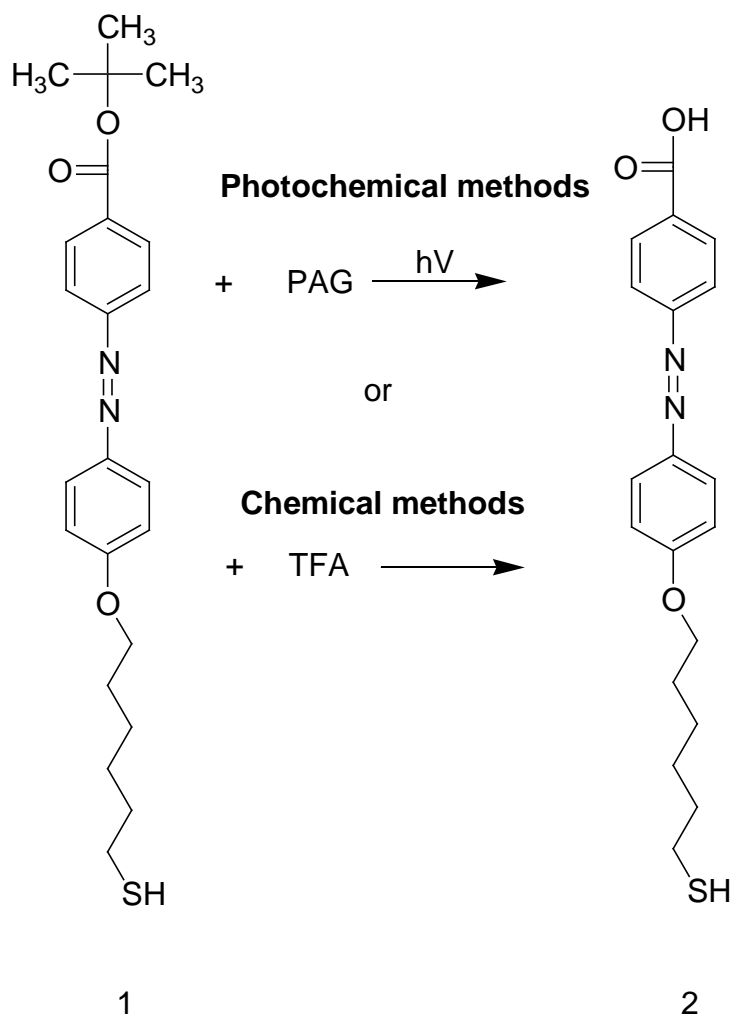
The t-butylcarbamate (BOC) groups is one of the acid-labile protecting group which is characterized by the formation of stabilized cations upon cleavage. Its cleavage liberates the tert-butyl cation. The BOC group is used extensively in peptid synthesis

for the amines, thiols, alcohols and carboxylic acids protection. It is not hydrolysed under basic conditions and is inert to many other nucleophilic reagents. In order to remove BOC from a growing peptide chain acidic conditions (usually TFA) are necessary. Removal of side-chain protecting groups and the peptide from the resin at the end of the synthesis is achieved by incubating in hydrofluoric acid. For this reason BOC chemistry is generally disfavoured. However, when synthesizing nonnatural peptide analogs which are base-sensitive (such as depsi-peptides), t-BOC is necessary.



**Scheme 2-8.** Deprotection of Boc-group by TFA.

In new photolithographic techniques a photo-acid generator (PAG) is used for direct photochemical modification and patterning of thin organic films as well as self-assembled mono-layers (SAMs) [Ulm96]. This specific technology employs PAG, a chemical species that releases a proton upon photolysis, to hydrolyze terminal hydrophobic tert-butyl ester groups to a reactive hydrophilic carboxylic acid group. When exposed to UV light, the PAG produces a proton that catalyzes the deprotection of the tert-butyl ester (compound 1) to form a carboxylic acid (compound 2) and butylene gas. Photodeprotection of the hydrophobic *tert*-butyl ester to form a carboxylic acid offers a photochemical alternative to more traditional chemical deprotection methods, such as hydrolysis with trifluoroacetic acid [Lee04], also shown in Scheme 2-9. Both of these deprotection schemes occur readily in solution to produce an acid-terminated azobenzene alkanethiol compound but can also be applied on SAMs on gold of the discussed molecules.



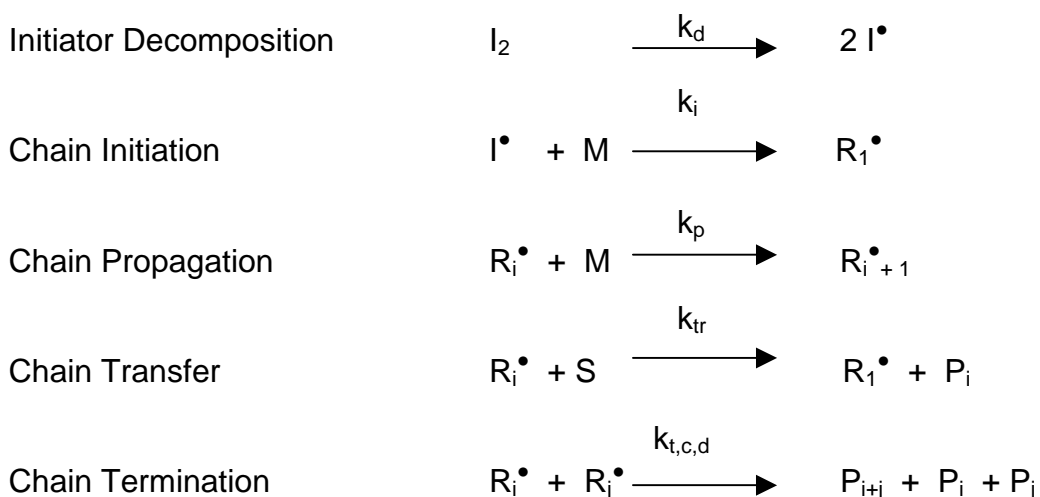
**Scheme 2-9.** A tert-butyl ester azobenzene alkanethiol derivative can be either photochemically or hydrolytically converted to a carboxylic acid derivative.

### 2.3.2 Free radical polymerisation

Conventional free radical polymerisation (FRP) has been known for a long time. This kind of polymerisation has many advantage over other polymerization processes i.e. like anionic or cationic polymerization. FRP does not require stringent process conditions and can be used for the (co)polymerization of a wide range of vinyl monomers.

The mechanism of free radical polymerization consists of three primary process: initiation, propagation and termination.

The processes may be described via a simplified set of fundamental reaction:



Where:

$R_i^\bullet$  - a radical of chain length  $i$ ,

$I_2$  - the initiator,

$M$  - the monomer,

$S$  - a transfer agent

$P$  - polymer

**Scheme 2-10.** *General mechanism of free radical polymerisation.*

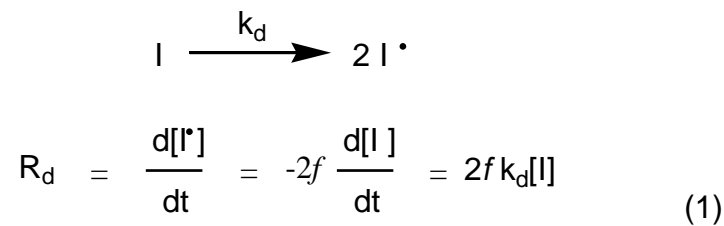
Each reaction given in Scheme 2-10 is associated with a kinetic rate law expression that contains a specific rate coefficient. The kinetic of the initiation process - its rate and effectiveness - are the fundamental importance in commercial applications.

The first reaction step-initiation-leads to the generation of (primary) radicals. Initiating radicals are rarely formed by monomers but rather via thermal decomposition using azo- and peroxy-type compounds as well as electrochemically or photo-chemically.

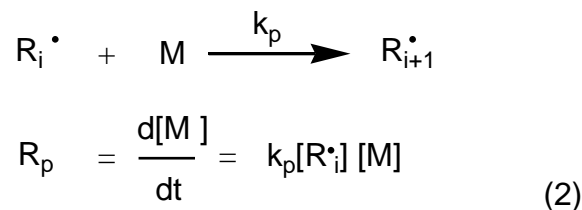
Initiation in a free-radical polymerization consists of two steps:

- 1) Dissociation of the initiator to form radical species,
- 2) Addition of a single monomer molecule to the initiating radical (association step).

The rate of dissociation of initiators,  $I$ , usually follows 1st order kinetics and is dependent upon the solvent present and the temperature of polymerization as well.



After the initiation reactions, addition monomer units are added sequentially to the initiated monomer species during subsequent propagation steps and this is described via the following rate law expression (2):



where:

$k_p^i$  – the propagation rate coefficient of a macroradical with chain length  $i$ ,  $R_i$ .

It is generally accepted that the propagation reaction is chemically controlled up to high monomer conversion i. e. high viscosities of the reaction medium. This implies that the propagation rate coefficient is independent of monomer conversion  $\leq 80\%$ .

The next step in the free radical polymerisation is the chain transfer. It is the reaction of a propagating radical ( $R_i \cdot$ ) with a transfer agent ( $S$ ) to yield dead polymer ( $P_i$ ) and a small radical ( $R_1 \cdot$ )



The radical center is transferred from the polymer end to another molecule, and the number of unpaired electron thus remains unchanged.

The radical site is transferred to the chain-transfer agent  $R_1 \cdot$  to continue the polymerization process. The number-average degree of polymerization decreases if transfer reactions show strongly their presence.

Figure 2-9 shows schematically ideal chain transfer in which the kinetic chain length is identical in the presence and absence of  $T$ . The degree of polymerisation



decreases and the number of polymer molecules increases as a result of chain transfer.

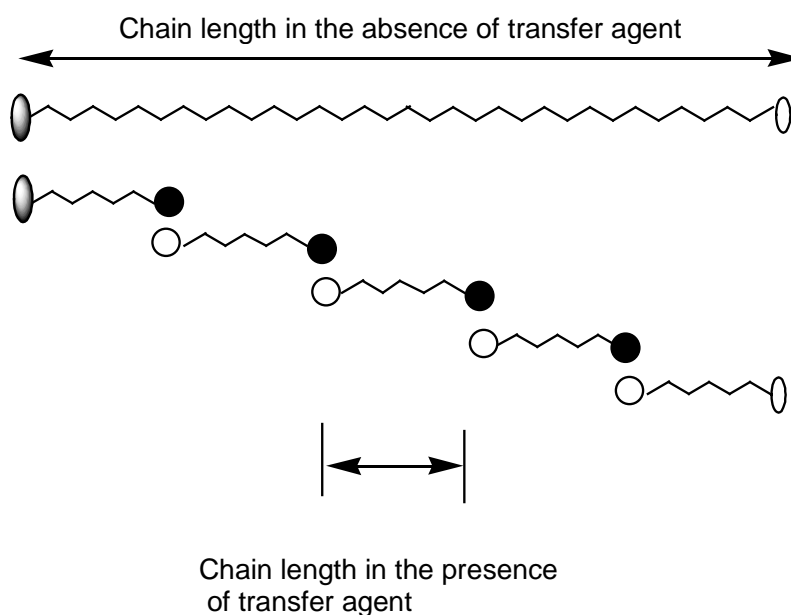


**Figure 2-9.** Schematic description of chain transfer :  $\text{O}$  and  $\text{O}$  denote end groups in the absence of transfer agent, and  $\text{O}$  and  $\bullet$  denote end groups in the presence of transfer agent.

Chain transfer can occur to all the substances present in a polymerization system and T can be employed to effectively reduce the molecular weight or to introduce designated end groups.

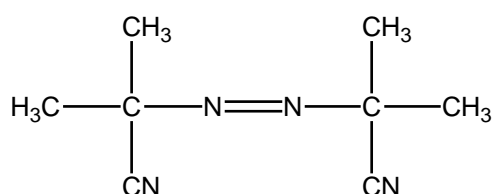
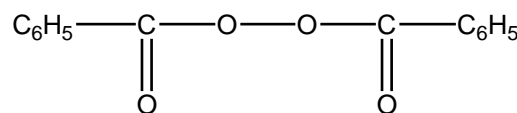
Chain transfer will continue until some termination process occurs. Termination is perhaps the most complex of the elementary reactions in free radical polymerisation as it constitutes the consecutive events of polymer radicals undergoing translational diffusion to come into relative proximity of one another, segmental diffusion whereby the chain ends approach one another, and finally chemical reaction. Termination can occur by combination, by disproportionation or by chain transfer reactions. Termination by combination occurs when two propagating radical chains of arbitrary degrees of polymerization meet at their free-radical ends. Termination by disproportionation gives two terminated chains. One terminated chain will have an unsaturated carbon group while the other terminated end is saturated. Termination by chain transfer can be achieved by hydrogen abstraction from an initiator, monomer, polymer or solvent molecule.

*INITIATORS IN FRP*

Thermal initiators are most widely used to generate radicals to initiate polymerization for commercial polymerization as well as for the theoretical studies.

Thermally decomposing initiators fall into two classes: azo- [Eng80, Min96, Qui85] and peroxy-type molecules [Dix99, Moa89].

Some common thermal initiators are: 2,2'-azo-bis-isobutyronitrile (AIBN); t-butyl hydroperoxide; cumyl peroxides; benzoyl peroxide (BPO); t-butyl peroxide; lauroyl peroxide, dipotassium persulfate.

**AIBN****BPO**

**Scheme 2-11.** *Two most common thermal initiators AIBN and BPO in FRP.*

They generate carbon-centered and oxygen-centered radicals by the homolysis of the C-N (dialkyl diazenes) and O-N (dialkyl hyponitrides) bonds. The major driving force for the dissociation by azo initiators is the formation of the highly stable nitrogen molecule. Various initiators are used at different temperatures depending on their rates of decomposition. For example the azobisisobutyronitrile (AIBN) is commonly used at 50 - 70 °C, acetyl peroxide at 70 - 90 °C, benzoyl peroxide at 80 - 90 °C, and dicumylor di-t-butyl peroxide at 120 - 140 °C [Eas76, Eas76b, Eas76c].

An important property of a thermal initiator is its half-life,  $t_{1/2}$ , (at a certain temperature), given by Eq.(1); the half-life is the time period during which half of the initiator molecules initially present are decomposed:

$$t_{1/2} = \frac{\ln 2}{k_d} \quad (1)$$

At choosing an initiator it is important to consider possible side reactions, that monomer and initiator can undergo, as well as the transfer ability of the initiator molecule, which may limit the accessible molecular weight range. An attractive alternative to thermally decomposing initiators are photoinitiators that decay on irradiation with UV or visible light.

### 2.3.3 Living/controlled radical polymerization

As already outlined conventional free radical polymerization (FRP) has many advantages over other polymerization processes. Nearly 50 % of all commercial synthetic polymers are prepared using radical chemistry, providing a spectrum of materials for a range of markets [Mat02a]. However, the major limitation of FRP is poor control over some of the key elements of the process that would allow the preparation of well-defined polymers with controlled molecular weight, polydispersity, composition, chain architecture, and site-specific functionality.

Controlled radical polymerization (CRP) provides such control, leading to an unprecedented opportunity in materials design, including the ability to prepare bioconjugates, organic/inorganic composites, and surface-tethered copolymers [Mat05]. A number of CRP methods have been developed and the three most promising are: stable free radical polymerization (SFRP), the most common of it is nitroxide mediated polymerization (NMP) [Geo93, Haw01] but may also include organometallic species [Way94]; transition-metal-catalyzed atom transfer radical polymerization (ATRP) [Kat95, Wan95]; and degenerative transfer with alkyl iodides [Mat28], methacrylate macromonomers [Moa96], and dithioesters via reversible addition-fragmentation chain transfer (RAFT) polymerization [Chie98, Des00].

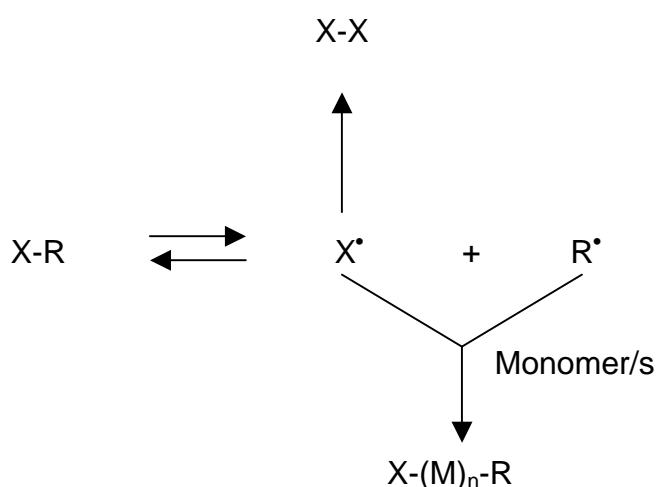
#### 2.3.3.1 Nitroxide mediated living free radical polymerization (NMRP)

Nitroxide mediated controlled radical polymerization, involving stable nitroxyl radicals and alkoxyamines was demonstrated first by Rizzardo and Salomon in 1986 [Sal86, Riz87]. The first use was limited to form a variety of vinyl polymers with low-molecular weight. Next Georges and co-workers demonstrated the polymerisation of styrene in the presence of TEMPO. Alkoxyamines have been employed to control the polymerization of styrene [Geo93, Geo93a, Geo93b]. The NMRP process is carried

out in principle with a unimolecular- or with a biomolecular system. The first system was introduced by George et al. [Geo93, Geo93a, Ver93]. A free radical initiator, such as 2,2'-azobisisobutyronitrile (AIBN) or benzoyl peroxide (BPO) is used in conjunction with TEMPO. The second system is a "unimolecular system", in which alkoxyamine dissociates to produce both the initiating radical and the mediating nitroxide radical [Haw96, Haw96a, Tsa02].

NMP is based on a kinetic effect, so called: "the persistent radical effect" [Fis86, Fis97, Fis99, Fis01 ] (Scheme 2-12).

Initially, through decomposition of an initiator two radicals are formed: persistent radical (R) and a propagating radical (transient radical) – (X). Whereas the transient radical may undergo irreversible radical-radical termination reaction (self-combination) or reversible reaction with the persistent radicals, the persistent radical can only undergo a reversible recombination reaction with the transient radical. Thus, every irreversible self-termination reaction of transient radicals eliminates the transient radicals from the reaction medium and leads to buildup of excess of persistent radicals that increase with the reaction time. At elevated concentration of the persistent radicals they will undergo reversible deactivation to form the dormant species and this reaction will be favored over the irreversible self-combination reaction of the transient radicals. Thus, the irreversible reaction will be suppressed and the control over the polymerization will be achieved [Fis01], [Lut01]. In general we can introduce the mechanism of NMRP as follows.



**Scheme 2-12.** Principle of persistent radical effect.

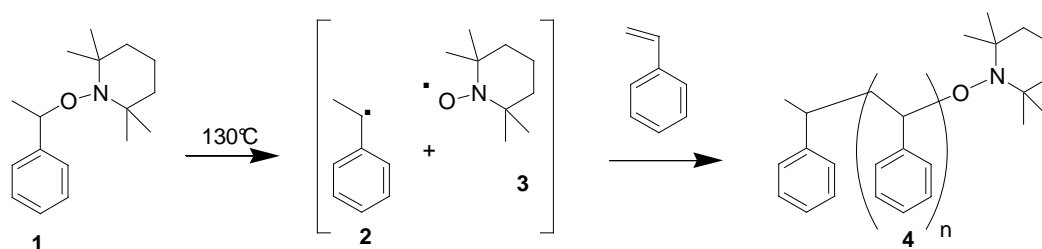
### *Bimolecular system*

At the beginning of the 90 s, George and his group tried the polymerizations of styrene derivatives at 130 °C in bulk, containing an initiating system composed of benzoyl peroxide and a stable nitroxide (TEMPO) in a molar ratio of 1.3:1 [Geo93]. At these elevated temperatures the C-O bond in the formed alkoxyamine becomes unstable, releasing the nitroxide, which now can act as a polymerization mediator, not as an inhibitor as it is at low temperatures. They obtained high molecular weight and low polydispersity materials. A linear increase of molecular weight with conversion typical for a living polymerization procedure was observed. The PD (PD = 1.2 - 1.3), which was significantly lower than the theoretical limits for a free radical process of 1.5 and the typical values of ca. 2.0 for free radical systems. At the propagating step the concentration and reactivity of radicals is significantly reduced but therefore terminations reactions can still occur.

### *Unimolecular alkoxyamine initiators*

The first investigation in the controlled free radical polymerization were based on the use of a bimolecular initiating system consisting of benzoyl peroxide and a stable nitroxide, typically TEMPO.

The desire to develop a simple and versatile method for the preparation of wide variety of well-defined polymeric materials led Hawker et al. to unimolecular initiators for the NMP [Haw94]. The structure of these initiators was based on a specially designed alkoxyamine functionality that is present at the chain end of the growing polymer during its dormant phase. The principle of design of NMP initiators is that the C-O bond of the small molecule alkoxyamine derivatives **1** is thermolytically unstable and decomposes on heating to give initiating **2** and mediating nitroxide radicals **3** in the correct 1:1 stoichiometry; next the initiation of polymerization follows and one receives the polystyrene derivatives **4** (Scheme 2-13).

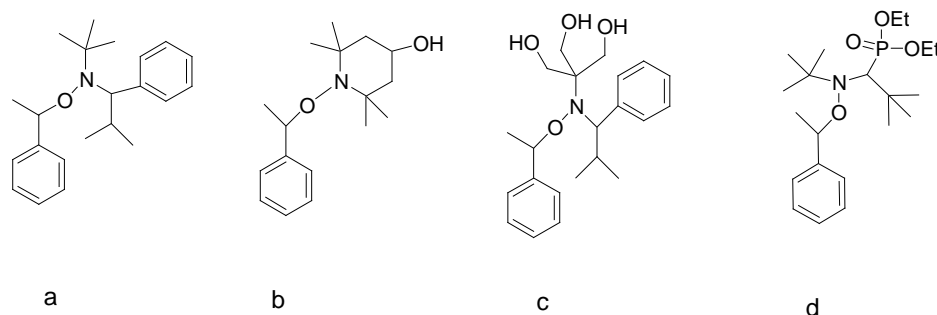


**Scheme 2-13.** *Synthesis of unimolecular initiator by means of NMRP.*

The advantage of the unimolecular initiator is that:

- the structure of the polymer can be prepared with better control,
- can be functionalized at the chain ends of the macromolecules,
- allows for the preparation of block copolymers and other complex architectures.

A list of unimolecular initiators is shown in Scheme 2-14.



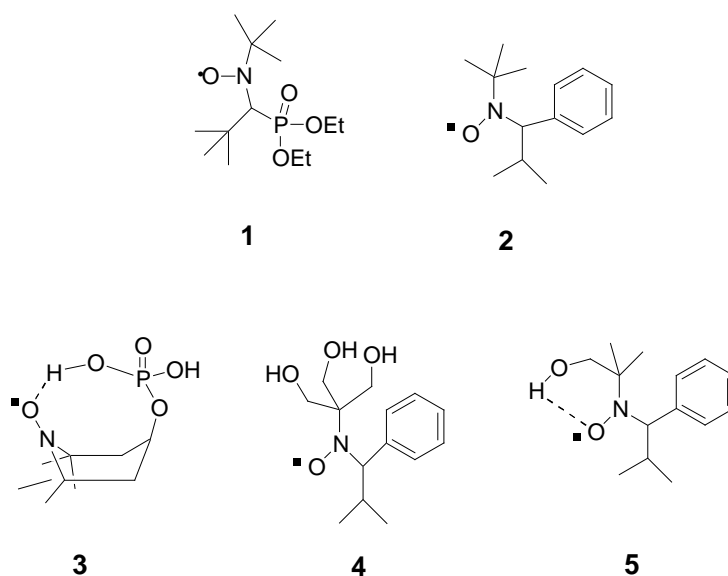
**Scheme 2-14.** *Unimolecular initiators for CRP.*

### *Selection of nitroxides*

Until 90 years TEMPO was the standard compound used for the trapping of free radicals because it was relative cheap and commercially available. Unfortunately, there were serious deficiencies and problems with the use for a living radical procedure, for instance, the necessity to use high polymerization temperature (125 - 145 °C), long reaction time (24 - 72 h) and an incompatibility with many important monomers [Haw96].

The Xerox group made the first attempts to develop a new better system which relied on the use of nitroxides other than 2,2,6,6-tetramethylpiperidinoxy (TEMPO). They have polymerized acrylates at elevated temperatures (145 - 155 °C) in the presence of 4-oxo-TEMPO, as the mediating nitroxide.

However the polydispersities were still between 1.40 - 1.67 and the living nature of the polymerization was questionable [Keo98]. Recently, the same group has introduced the use of reducing additives such as hydroxyacetone as a method for controlling the concentration of free nitroxide. The most breakthrough in the design of improved nitroxides was the use of alicyclic nitroxides, which bear a structural resemblance to TEMPO. In fact, their most striking difference was the presence of a hydrogen atom on one of the  $\alpha$ -carbons, in contrast to the two quaternary  $\alpha$ -carbons present in TEMPO and its derivatives. The best examples of these new materials are the phosphonate derivative, **1**, **3** introduced by Gnanou and Tordo [Ben00, Mat95a] and the family of arenes **2**, **4**, **5** presented by Hawker [Ben99, Har01] (Scheme 2 - 15). The new initiators such as **1** and **2** permit the polymerization with high control of molecular weights and polydispersities as low as 1.06.

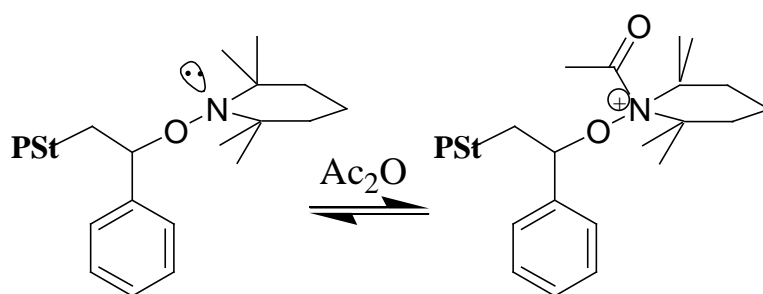


**Scheme 2-15.** Common nitroxides for CRP.

One of the major disadvantage of NMRP is the long reaction times and elevated temperatures. Typically “living” free radical polymerization are proceeded by heating a bulk mixture of the initiator and monomer at 120 - 130 °C for 36 - 72 hours. Unfortunately, so high temperature contributes to the autopolymerization and can be a

significant problem leading to loss of the “living” character of the polymerization process and an inability to achieve high molecular weights (app. 200 000). From an industrial point of view, so long reaction times are not economically attractive therefore we need simple rate accelerating additives which should result in significant rate enhancements, give reaction times of hours not days, providing the same high level of control over molecular weight and polydispersity, being compatible with a wide range of functional groups, and being easily removed. Malmström et al. studied rate-accelerating effect on the polymerization and showed how a different additives influence this process [Mal97]. They found that simple anhydrides such as acetic anhydride or benzoic anhydride as well as also acid chlorides led to an accelerating effect.

Since acetic anhydride is a cheap, readily available reagent and is simple to remove due to its volatility, it became a new class of rate accelerating agent for nitroxide-mediated free radical polymerization. E. Malmström et al. found that only addition of 1 weight percent of acetic anhydride decreases significantly the reaction time from 48 to 5 hours. This decrease in reaction time leads to increased control over the polymerization process with low polydispersity materials (polydispersities less than 1.30). A possible explanation for this effect is acylation of the alkoxyamine nitrogen. The lone electron pair on the alkoxyamine nitrogen is undergoing a reversible acylation reaction (Scheme 2-16). The coordination of this acyl group to the nitrogen atom induces a partial positive charge resulting in a polarization of the N-O bond towards the nitrogen. This leads to weakness of the C-O bond promoting the thermal dissociation of the C-O bond which increases the polymerization rate.



**Scheme 2-16.** Proposed acylation of alkoxyamine end groups leading to increased reactivity [Mal97], [Mat 95], [Bau01].



### *Applications of NMRP*

NMRP is one of the most successful CRP techniques and can be used to synthesize many of new materials like homopolymers, linear block copolymers, and more complex macromolecular architectures such as star copolymers [Haw01, Geo93, Ber96, Mal98], with well-defined end groups and narrow PDIs.

The synthesis of functionalized unimolecular initiators permits the preparation of a wide range of different materials which are either difficult to prepare or not available via other polymerization processes. Using living free radical polymerization such features of polymers as the architecture, the topology (i.e., comb, star dendritic etc.) [Wei97, Gay 96], composition of the backbone (i.e., random, gradient, or block copolymer) [Kaz97, Lii97], inclusion of functionality (i.e, chain-end, site-specific, etc.) [Kim98, Had97] can be manipulated.

#### 2.3.3.2 Atom transfer radical polymerization (ATRP)

Many researchers tried to find a system leading to better control of “living” radical polymerization system [Ots82], [Sol85], [Geo93], [Way94], [Gay95], [Riz95], [Arv94], [Har96], [Wun96] but these have generally poor control of molecular weights [Ots82], [Gay95], [Har96], [Wun 96] or were successful for only one class of monomer, e. g. only styrenes [Geo93], acrylates [Way94], [Arv94] or methacrylates [Riz95].

The first successful addition of halogenated compounds to alkenes via radical intermediates under photochemical conditions (atom transfer radical addition (ATRA)) was provided by Kharash [Kha45]. This ATRA process was gradually converted to a much more efficient metal - catalyzed reaction by Minisci [Min75], Vofsi [Vof63] and others during the 1960s.

In 1982 Otsu, for the first time, provided a model for a living radical polymerization. He described MMA polymerization in the presence of phenylazotriphenylmethane and benzyl dithiocarbamate [Ots82a]. In analogy with iniferters used in carbocationic system it was proposed that dithiocarbamates act as iniferters, namely, agents that initiate, transfer, and terminate [Ots82]. The Otsu model is very similar to modern CRP.

In 1995 Matyjaszewski and his co-workers described a promising system for controlling radical polymerizations. It was based on the catalytic system used by

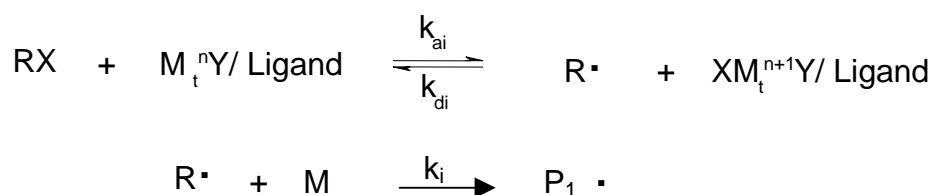
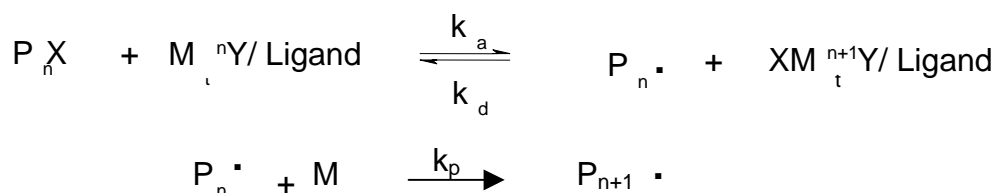
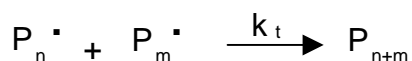
organic chemists for ATRA and therefore was termed atom transfer radical polymerization (ATRP). One of those systems was proposed by Sawamoto in 1994. The living polymerization of methyl methacrylate (MMA) was based on ruthenium(II) complex ( $\text{RuCl}_2$ ) as catalyst coupled with carbon tetrachloride ( $\text{CCl}_4$ ) as the initiator [Kat95]. A very similar mechanism has been applied by Matyjaszewski [Mat02b]. It was based on a  $\text{CuX/bpy}$  (copper chloride/ bipyridine) catalyst, which had also been successfully used in many ATRA reactions [Wan95].

ATRP allows for the controlled polymerization of styrenes, acrylates, methacrylates, acrylonitrile and other monomers [Wan95a], [Mat98].

### *General mechanism of ATRP*

ATRP is a complex process based on several elementary reactions. Success depends on controlling all of them as well as on controlling the concentrations and reactivities of the involved species. The whole process of ATRP is described by Scheme 2-17.

The process occurs when a growing radical or an active species ( $\text{R}^*$ ) generated from an organic halide ( $\text{RX}$ ,  $\text{X}$  = halogen) in the presence of a metal catalyst  $\text{M}_t\text{Y/L}$  attacks an unsaturated compound to form an adduct with a carbon-halogen bond. The metal catalyst thus undergoes a reversible one-electron redox reaction via abstraction of the halogen ( $\text{X}$ ) from the initiator or dormant species ( $\text{RX}$ ), followed by a one electron reduction by release of the halogen back to the resulting species ( $\text{R}^*$ ). The reversible process then switches the polymer chain ends from a dormant state to an active and propagating state. In this process the oxidized metal complex ( $\text{XM}_t\text{Y/L}$ ) is used as persistent radical and reduces the stationary concentration of growing radical, therefore minimizes termination by generating a steady low concentration of short-lived active radical chain ends. Termination reaction occurs mainly through radical coupling and disproportionation in ATRP.

**Initiation:****Propagation:****Termination:**

- X,Y = Cl, Br  
 Ligand = Bipy, PMDETA,  
 M<sub>t</sub> = Cu, Fe, Ru, Rh, Mo, Cr, Ni, ...  
 k<sub>a</sub> – rate constant of activation  
 k<sub>d</sub> – rate constant of deactivation  
 k<sub>p</sub> – rate constant of propagation  
 k<sub>t</sub> – rate constant of termination

**Scheme 2-17.** *General mechanism of ATRP.**Features of ATRP*

ATRP is a rather complicated method, where the choice of the components is of extreme importance for the achievement of the desired products therefore a few basic requirements must be fulfilled in order to achieve the successful ATRP process [Mat02] :

- 1) It should adsorb initiator at the early stages and generate propagating chains leading to polymers with degrees of polymerization predetermined by the ratio of concentrations of converted monomer to the introduced initiator ( $DP = \Delta[M]/[I]_0$ ).
- 2) The number of monomer molecules added during one activation step should be small, resulting in polymers with low polydispersities.
- 3) The contribution of chain breaking reactions (the transfer and termination step) should not have any influence to yield polymers with high degrees of end-functionalities and block copolymers.

In order to reach this aim, it is necessary to select proper structure of reagents and good reaction conditions. The transition-metal complex is also the key to the successful ATRP process because it determines the position of the atom transfer equilibrium and the dynamics of exchange between the dormant and active species. Most often in ATRP process copper catalyst is used as well as others metal complexes like molybdenum [Bra99], rhenium [Kot99], ruthenium [Kat95], iron [Mat97], rhodium [Moi98], nickel [Ueg97, Moi99] and palladium [Lec97]. However, the main roles for the ligands are the control of the solubility of the transition metal and ensuring the stability of the complex in different monomers, solvents and at different temperatures.

### 2.3.3.3 Reversible addition-fragmentation chain transfer polymerization (RAFT)

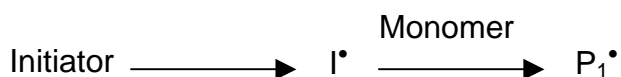
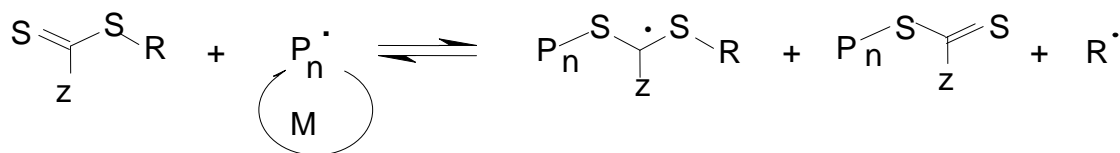
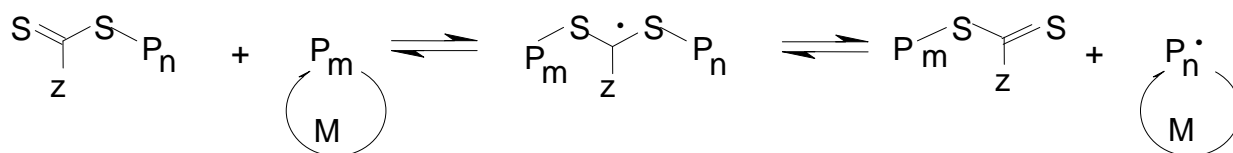
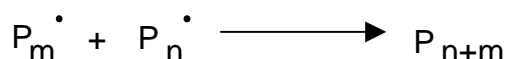
The reversible addition-fragmentation chain transfer process is the most recent of the controlled radical system leading to a wide range of polymers with narrow polydispersities (usually  $< 1.2$ ). The first report about the possibility of controlled radical polymerization using dithiocarbonyl was described by Chiefari and co-workers in 1998 [Chi98]. The interest in developing new radical process with living character for the synthesis of well-defined architectures was shown by the increasing number of publications [AhT04, Aro02, Bar01, Bar03, Don02, May99, May00, Shi01, Sum01].

### *General mechanism of RAFT*

First Rizzardo demonstrated that dithiocarbonyl compounds, with a weak carbon-sulphur bond, confer living characteristics to radical polymerization [Le98, Chi99], which he termed RAFT polymerization.

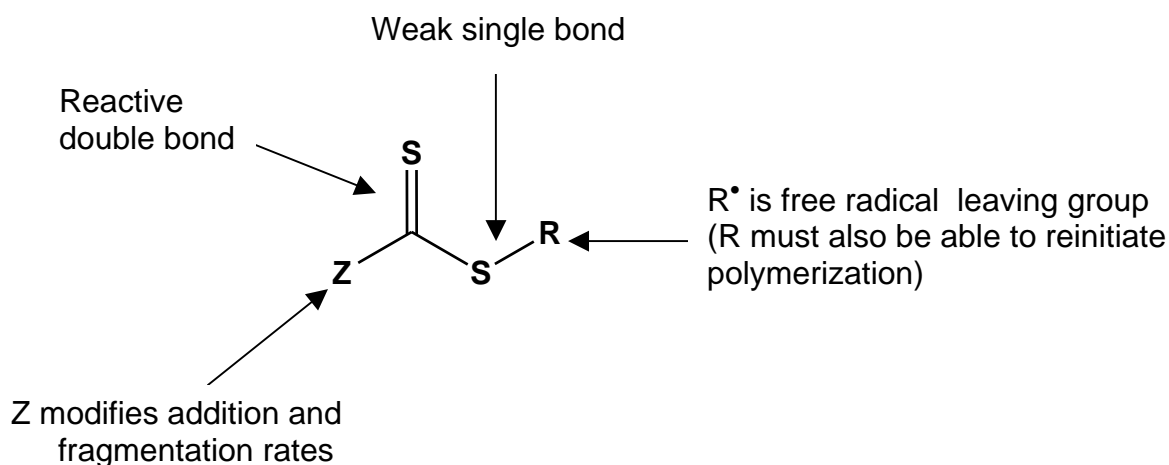
The RAFT polymerization mechanism is based on the reversible addition and fragmentation of the propagating radical to dithioesters [Chi98], dithiocarbamates [May99] or trithiocarbonates [May00].

In this process, a chain transfer agent (CTA),  $S = C(Z)-SR$ , reacts with either the primary radical derived from an initiator or propagating polymer chain ( $P^*$ ), forming a new CTA and eliminating  $R^*$ , which is able to re-initiate the polymerization (Scheme 2-18). The polymerization is controlled by the transfer of the CTAs between dormant and active chain and because of that maintains the living character of the polymerization. Molar mass control can be adjusted by the relative amount of reagents involved in the polymerization. The end functionality of the resulting chain is controlled by the nature of the substituents Z and R on the CTA.

**(I) Initiation****(II) Chain transfer****(III) Reinitiation****(IV) Chain equilibration****(V) Termination****Scheme 2-18.** General mechanism of RAFT polymerization.*Controlling agents of RAFT*

After Rizzardo demonstrated that dithiocarbonyl compounds performed as *Chain Transfer Agents* (CTA) in RAFT process [Le98, Chi99], dithioester [Chi98], trithiocarbonates [May00], and certain aromatic dithiocarbamates [Bar01, Des00] were successfully employed as CTA to obtain narrow polydispersity for styrene and (meth)acrylates in batch polymerization. In Scheme 2-19 the general structure of CTA is shown. Choice of Z and R is crucial to the success of the RAFT process. Suitable Z groups are aryl or alkyl that govern the reactivity of the C=S moiety (should activate the C=S double bond) towards radical addition and R should be a

good free-radical leaving group (e.g. cumyl, cyanoisopropyl) which is capable to reinitiating the polymerization.



Where:

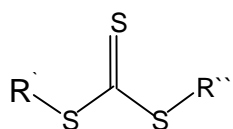
$Z$  = aryl, alkyl,  $NR'_2$ ,  $OR'$ ,  $SR'$

$R$  = homolytic leaving group

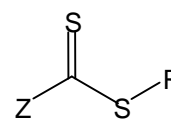
**Scheme 2-19.** General structure of CTA.

In the Scheme 2-20 some of the best chain transfer agents with the most common leaving group ( $R$ ) shown.

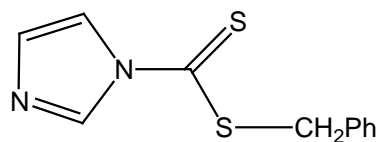
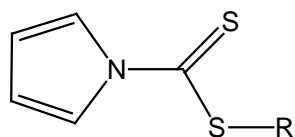
Trithiocarbonates



Dithioesters



Dithiocarbamates



$R = CH_2Ph$  or  $C(CH_3)CN$

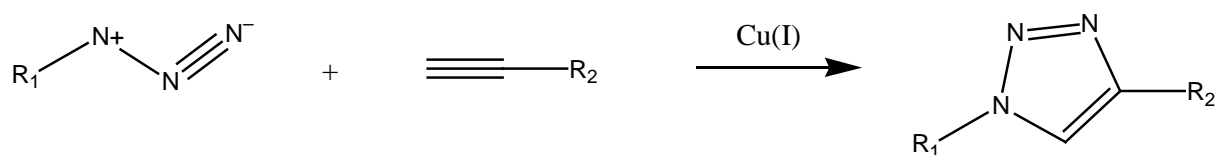
**Scheme 2-20.** Possible RAFT mediating agents (CTAs).

CTA have to fulfill a few requirements in order to achieve well-defined products. First, CTA should have a high transfer constant relative to the monomers being polymerized, which means a high rate of addition and a suitable leaving group for the propagating radical. The second important quality of the CTA is the ability to form intermediates that fragment rapidly, giving no side reaction.

### 2.3.4 Polymeranalogous reaction – “Click chemistry”

Click chemistry is a concept introduced by K. Barry Sharpless in 2001 [Kol01], and it denotes a growing family of powerful chemical reactions that are based on “spring-loaded” energy-intensive substrates that can under the right conditions unload their energy to form stable products in high selectivity. Sharpless and co-workers described the Cu(I)-catalysed synthesis of 1,2,3-triazoles from azides and terminal alkynes catalyzed by Cu(O) as well as by CuSO<sub>4</sub>/sodium ascorbate [Ros02], [Tor02]. In both cases it was suggested that the Cu(O) and Cu(II) precursors are oxidized or reduced to give the active Cu(I) catalytic species. This type of effective organic reaction found rapidly also entrance in polymer science, for building up polymers, make block-copolymers or for effectively modifying polymers [Mos02].

The most studied example of click chemistry for polymer analogous reaction is again Huisgen 1,3-dipolar cycloaddition of azides and terminal alkynes via copper(I) catalyst.



**Scheme 2-21.** Huisgen 1,3-cycloaddition of azides to terminal alkynes catalyzed by Cu(I).

This reaction tolerates a variety of functional groups, is insensitive to water and oxygen and gives easy access to regiospecific 1,4-disubstituted 1,2,3-triazole. The reaction is catalyzed by Cu(I) species that are either added directly as cuprous salts (with or without ligands) [Lew04], or generated by the reduction of Cu(II) salts, or by the in situ oxidation of copper metal to give Cu(II) species. The last option is



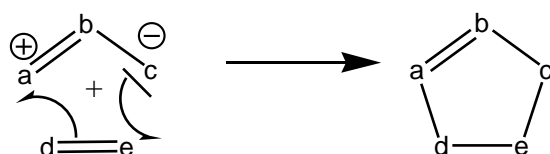
particularly attractive, as copper metal is inexpensive, and there is no need for a reducing agent as in the case of Cu(II). However, the reaction is relatively slow and require a significant amount of catalyst. These drawbacks are increasingly important when large-scale production is considered.

This kind of reaction is useful in various applications ranging from bio-orthogonal bioconjugation [Dei03], [Lin03], [Spe03], [Wan03] polymer [Mes08], [Sche04], and dendrimer [Mal05], [Voi07] syntheses to the construction of peptide bond surrogates [Lin04a] and for the powerful synthesis of pharmacophores [Kol03].

### *Mechanism of 1,3-dipolar cycloadditions*

The term “1,3-dipolar addition” is derived from the fact that compounds which can only be represented by zwitterionic all-octet resonance structures are ambivalent in the 1- and 3-position, thus displaying electrophilic as well as nucleophilic activity.

A cycloaddition can be described as the number of new  $\sigma$ -bonds formed or according to the size of the ring, like the uncharged five-membered ring, which is formed on fusion of the 1,3-dipole  $a$ - $b$ - $c$  with the dipolarophile  $d$ - $e$ . The bonds are closed simultaneously or one after the other.



**Scheme 2-22.** *Mechanism of 1,3-dipolar cycloaddition.*

In most frequent case, two reactants unite to form the cyclic compound creating two new  $\sigma$ -bonds at the expense of two  $\pi$ -bonds [Hui97].

1,3-cycloadditions follow the scheme  $3+2 \rightarrow 5$  and leads to an uncharged 5-membered ring. It cannot occur with octet-stabilized reactants which have no formal charges. The 1,3-dipole,  $a$ - $b$ - $c$ , must be defined in a way that atom  $a$  possesses an electron sextet, i.e. an incomplete valence shell combined with a positive formal charged center, and that the negatively charged center has an unshared electron pair. Combination of such a 1,3-dipole occurs with a multiple bond system  $d$ - $e$ ,

termed the dipolarophile. The dipolarophile may be any double or triple bond. Compounds containing an electron sextet at a carbon, nitrogen, or oxygen atom are not stable. Stabilization is possible if an unshared pair of electrons at atom *b* can relieve the electron deficiency at the center *a* by formation of an additional bond. In the new mesomeric formula, in which *b* now has the positive charge, all the centers have completely filled valence shells. Such system will be designated as 1,3-dipoles with internal octet stabilization.

### 3 AIM OF THE WORK

This work refers to the area of bio-nanotechnology and concerns the selective immobilization of DNA or other bio-template on microstructured gold contacts and which then permit a coordinated cooperation of several of these nanotemplate, e.g., within a microreactor (Figure 3-1). Within the frame of the DFG Forschergruppe "Nanostrukturierte Funktionselemente in makroskopischen Systemen" the immobilization of such nano-objects should be realized through functional thin polymer films which provide binding groups.

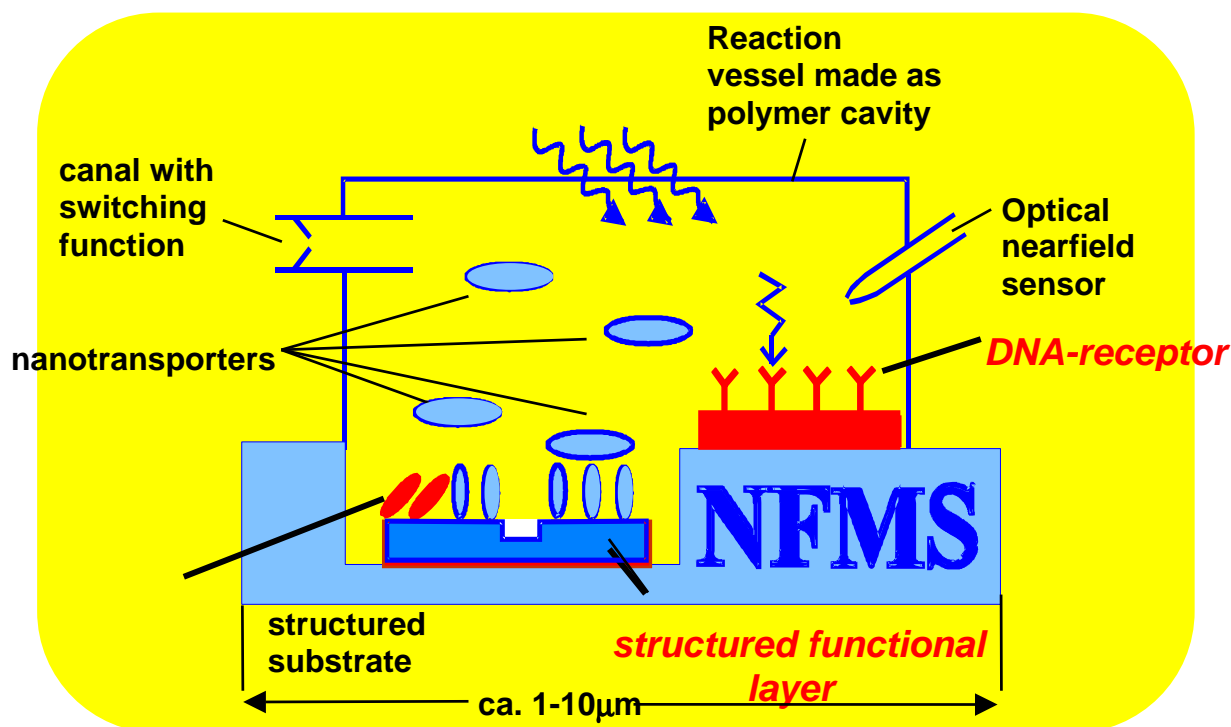


**Figure 3-1.** Schematic structure of a microreactor with active nanoelements.

Thus, the main aim of this work is the development of polymeric thin films which permit the area-selective attachment of a wide variation of functional elements or metal structures on different substrates e.g. by structuring/irradiation through optical grid methods. Thin functional layers play a determining role in micro- and nanotechnology. The areas of application pass from modern communications-technologies, computer technologies and memory technologies to micro and

nanoreaction techniques. Among others special polymers are used which are prepared on planar substrates (e.g. gold coated wafer).

It was decided to build-up on the knowledge of the Voit group where a polymer system based on a photolabile protected amine was developed which was suited for the layer formation glass and silicon wafers and which could be patterned with ultraviolet light (by laser writing or mask-irradiation).

An important new feature was firstly, to allow now immobilization on a gold substrates which needs the use of different anchor groups, and secondly, to find new and better ways to prepare well-defined multifunctional polymers.

For that a terpolymer system was aimed for which consists of three components with particular functions in suitable molar ratios, which allow to tune the properties of the materials, and provide: amino photolabile protected groups for the photolithographic creation of patterned areas with free amino groups, which are available for further modifications like attachment of colloids, metallization or attachment of DNA strands; disulfide derivative anchor groups providing anchoring capacity for gold surface and spacer groups for adjusting the film quality. The anchoring capacity for gold surfaces should be provided by a to be developed lipoic acid derivative monomer. The photolabile capacity by the monomer {N-(N-NVOC-aminopropyl)methacrylamide}, simply assigned as **NVOC** and spacer groups by the methyl methacrylate (MMA) or styrene (S).

These multifunctional terpolymers should be synthesised by free radical polymerisation of suitable monomers. However, there are also problems involved when free radical polymerisation is applied for functional monomers referring e.g. to thermosensitivity of some monomer or the resulting polymer when highly reactive monomers are used. Hence, a highly efficient polymer-analogous modification should also be developed which allows to introduce the functionalities after the polymer construction reactions. For this the 1,3-dipolar cycloaddition reaction of alkinen and aziden was chosen.

The aim of this work should be achieved through the following investigations:

- synthesis of photolabile co- and terpolymers ((meth)acrylate type) by classical free radical polymerisation designed for the covalent attachment onto gold substrates and

available for subsequent photo-patterning.

- optimizing the polymerization reaction conditions.
- synthesis of random copolymers poly(styrene-r-(4-propargyl(-oxystyrene) (3) by nitroxide mediated radical polymerisation.
- synthesis of a series of azides required for the incorporation into the polymer (3).
- postfunctionalization of (3) with azides by polymeranalogous reactions and via Cu(I) catalyzed 1,3-dipolar cycloaddition (click chemistry approach) to provide a family of photo patternable functional polymers.
- full structural characterization of the various products and prove of the efficiency of the postmodification.
- preparation of thin protected aminoterpolymer films (optimizing the process condition and preparation technique).
- UV-deprotection of aminoterpolymer in the solution and on the film.
- Patterning and further modification of the polymer films allowing anchoring biotemplates like DNA.

## 4 RESULT AND DISCUSSION

As outlined before, sulphur containing compounds are very suited for direct binding to gold surfaces. Therefore, we chose sulphur-compounds for our anchoring groups in the terpolymer concept.

The thiol-gold bridge is very stable. This direct binding of thiol-groups to gold contacts is a known procedure. Unfortunately, thiols are well known transfer agents of radicals and can be used only in protected form in free radical polymerisation. Hence, the DL- $\alpha$ - lipoic acid (LA, Scheme 4-1) or its reduced form, the dihydrolipoic acid (DHLA) were used, which can be bound, e.g., to hydroxyethylmethacrylate or acrylate to produce polymerizable monomers with anchoring groups. They appear as specially interesting candidates. LA is commonly used for electrochemical studies of biomolecules or for the elaboration of biological sensors because the carboxylic acid group allows the immobilization of a biomolecule on an electrode surface. From the chemical point of view LA is characterized by an endocyclic disulfide bond available for the formation of a double bridge over the metal substrate, and the absence of free thiol groups avoids chain transfer reactions in free radical polymerization. On the other hand the versatility of the carboxylic group allows the incorporation of the dithiolane moieties to already existing polymers or to precursor monomers as it is described in this work.



**Scheme 4-1.** DL- $\alpha$ - Lipoic acid (LA) and dihydrolipoic acid (DHLA).

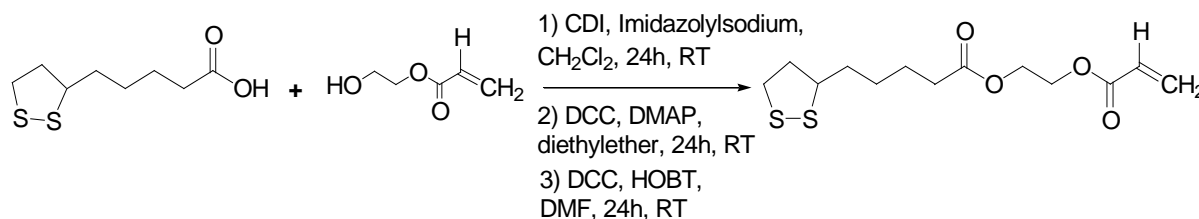
### 4.1 SYNTHESIS AND CHARACTERISATION OF AMINO TERPOLYMES

#### 4.1.1 Synthesis of dithiolate monomers

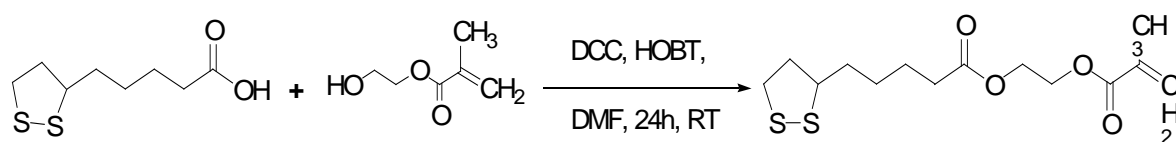
The anchoring capacity for gold surfaces is provided by the lipoic acid derivative monomers, 1,2-dithiolane-3-pentanoic acid - 2 -[(2-methyl-1-oxo-2-propenyl)oxy]-

ethyl ester and 1,2-dithiolane-3-pentanoic acid-2-[1-oxo-2-propenyl]oxy]ethyl ester designed respectively as LM and LA (Figure 1 and 2, bottom).

1) 1,2-dithiolane-3-pentanoic acid -2-[(1-oxo-2-propenyl)oxy]ethyl ester (LA)



2) 1,2-dithiolane-3-pentanoic acid-2-[(2-methyl-1-oxo-2-propenyl)oxy]ethyl ester (LM)



Due to the anchoring capacity of molecules containing lipoic acid units onto gold, as widely demonstrated in the attachment of single molecules in SAMs [Lin04] or in the stabilization of gold nanoparticles [Fre73], this moiety was selected to be included in the objective monomers for the covalent attachment of our polymers to gold surfaces. There is a strong preference of the disulfide group to attach to the gold surface relative to a wide variety of polar and non polar groups, as hydroxyl, amino, carbonyl, chloro, alkyl, phenyl, nitro, or even other sulfur containing functional groups such as thiols and sulfides even though they are less competitive in the absorption process rate relative to disulfides [Bee04]. Lipoic acid has to be connected to a polymerizable unit, in this case an acrylate or methacrylate moiety, via an esterification step.

A number of esterification methods are known [Tur53]. In most cases the presence of strong acids, the isolation of intermediate acyl derivatives or the application of heat is required. The basis of the mild procedures is the activation of the acid group, usually as an acyl chloride or anhydride, accompanied sometimes of an activator or a catalyst, that reduces the formation of side products and increases the yield of the

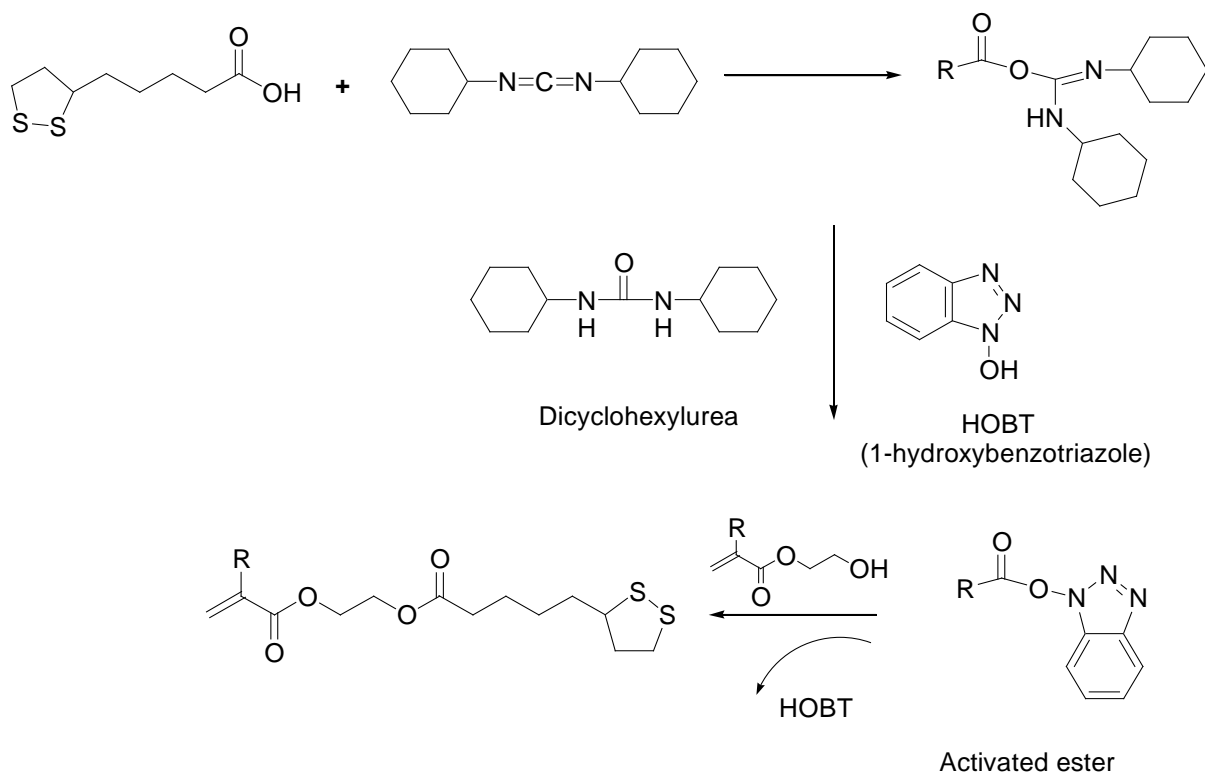
esterification. With the purpose of synthesizing our monomers under mild conditions, the esterification was performed using the coupling agent DCC (dicyclohexylcarbodiimide) in presence of DMAP (dimethylaminopyridine), choosing as reaction medium dry diethyl ether [Zie79]. In presence of the catalyst, the carboxylic acid is converted by DCC to anhydride and acylpyridinium species are formed with the catalyst. The formation of the ester is finally performed by the nucleophilic attack of the RO<sup>-</sup> on the acyl group with the subsequent generation of the objective ester and the regeneration of the catalyst. The presence of both reagents has been reported to provide the esters in high yields. The formation of side products is suppressed and even sterically demanding esters can be formed in good yields at room temperature. This reaction afforded the monomers **LA/LM** in 70 - 75 % yield, which fits with the yields previously reported in the literature for other species (70 - 90 %).

Another reactant employed for the synthesis of esters under mild conditions is N,N'-carbonyldiimidazol which is allowed to react together in equimolar amounts of carboxylic acid and the alcohol in inert solvents, providing the esters in particularly mild reaction condition [Sta62]. Besides, catalytic amounts of sodium ethoxide accelerate the ester synthesis to such an extent that even at rt the esterification is complete after a very short time. Imidazolyl sodium or other alkali metal compounds are capable of converting alcohols to alkoxides, and may be used in place of ethoxide to initiate the catalytic cycle. We tried the synthesis of **LM/LA** in presence of imidazolyl sodium as reported and the aimed for materials were obtained only in approximately 15 % yield.

In another trial it was intended to perform the activation of the carboxylic function by means of diisopropylcarbodiimide (DIPC). As catalyst was used 4-(N,N'-dimethyl)aminopyridinium tosylate (DPTS) as described by A. Hult et al. [Hul98]. The application of these reaction conditions afforded the pursued product in 76 % yield.

Finally, the activation of the carboxylic function with DCC in presence of 1-hydroxybenzotriazole (HOBT) was tried [New91]. In this case the complex formed with DCC and the acid is attacked by HOBT which activates the ester and in presence of the alcohol (Scheme 4-2) finally the monomers were provided in very high yields (95 – 98 %). The prepared monomers (LA and LM) were characterized by <sup>1</sup>H NMR and <sup>13</sup>C NMR.





**Scheme 4-2.** Reaction mechanism of the synthesis of LA/LM under mild conditions using DCC/HOBT.

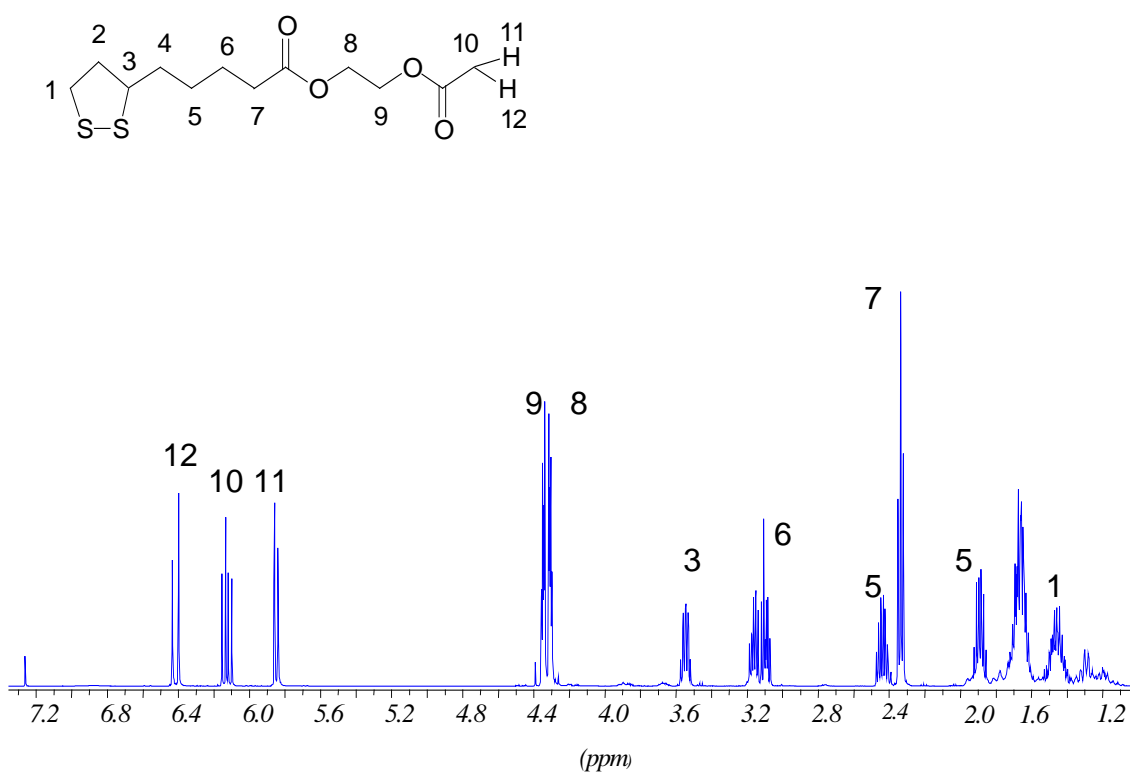


**Figure 4-1.**  $^1\text{H}$  NMR spectrum of LA in  $\text{CDCl}_3$ .

The  $^1\text{H}$  NMR spectrum of  $\alpha$ -LA sample is shown in Figure 4-1. The spectrum shows clearly the signals of protons present at different positions. The two characteristic signals for the double bond is obviously at 6.41 ppm (12) and 5.87 ppm (11) as well as a signal of the proton of the methin (CH) group at 6.14 ppm (10). The  $^{13}\text{C}$  NMR spectrum of LA confirms the esterification of this compound by the shift ( $\Delta 2$  ppm) of the carbonyl carbon ( $\delta$  172.65) ppm (8) and the presence of another carbonyl ester at 165.31 ppm (11) (Figure 4-2).

The signals of disulfide units are not be observed in  $^1\text{H}$  NMR spectrum. With the help of Raman spectroscopy the S-S, SC and C=C bonds are, however, easily recognized. The S-S unit was found at  $506\text{ cm}^{-1}$ , the C-S unit at  $676\text{ cm}^{-1}$  and C=C unit at  $1651\text{ cm}^{-1}$  (Figure 4-3).

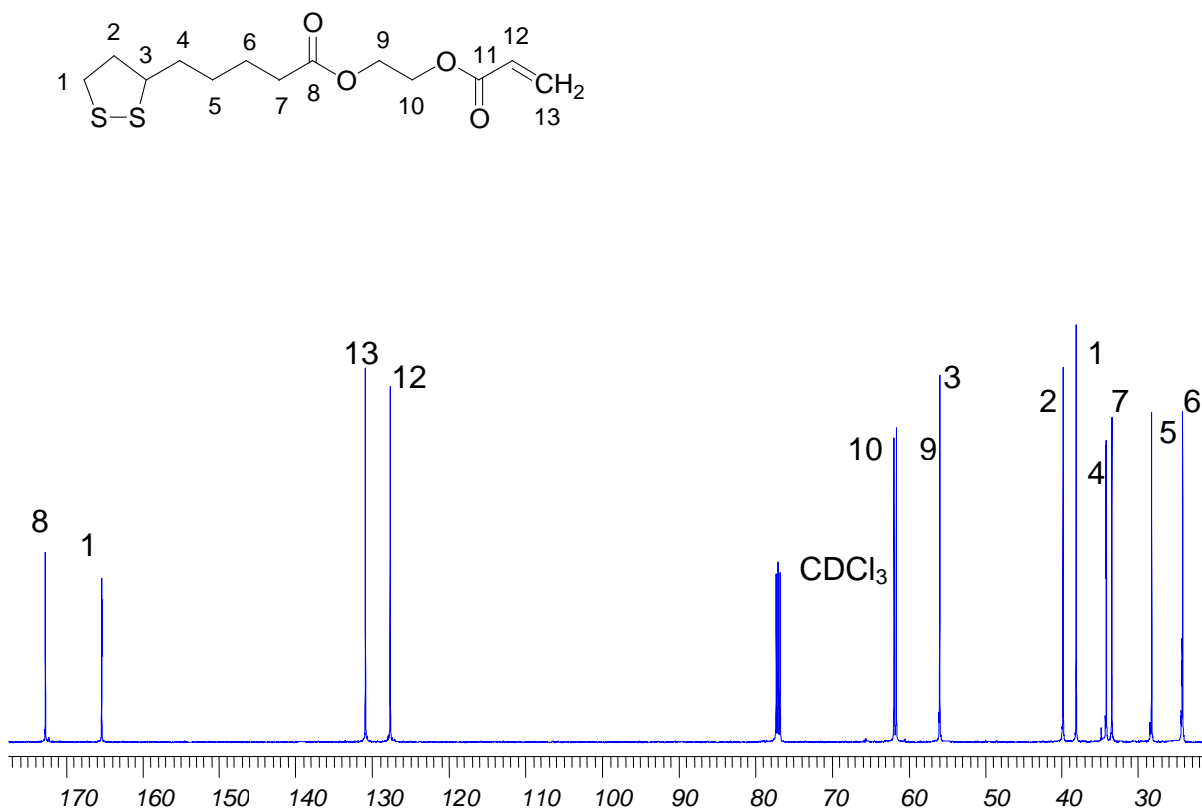


**Figure 4-2.**  $^{13}\text{C}$  NMR spectrum of LA in  $\text{CDCl}_3$ .

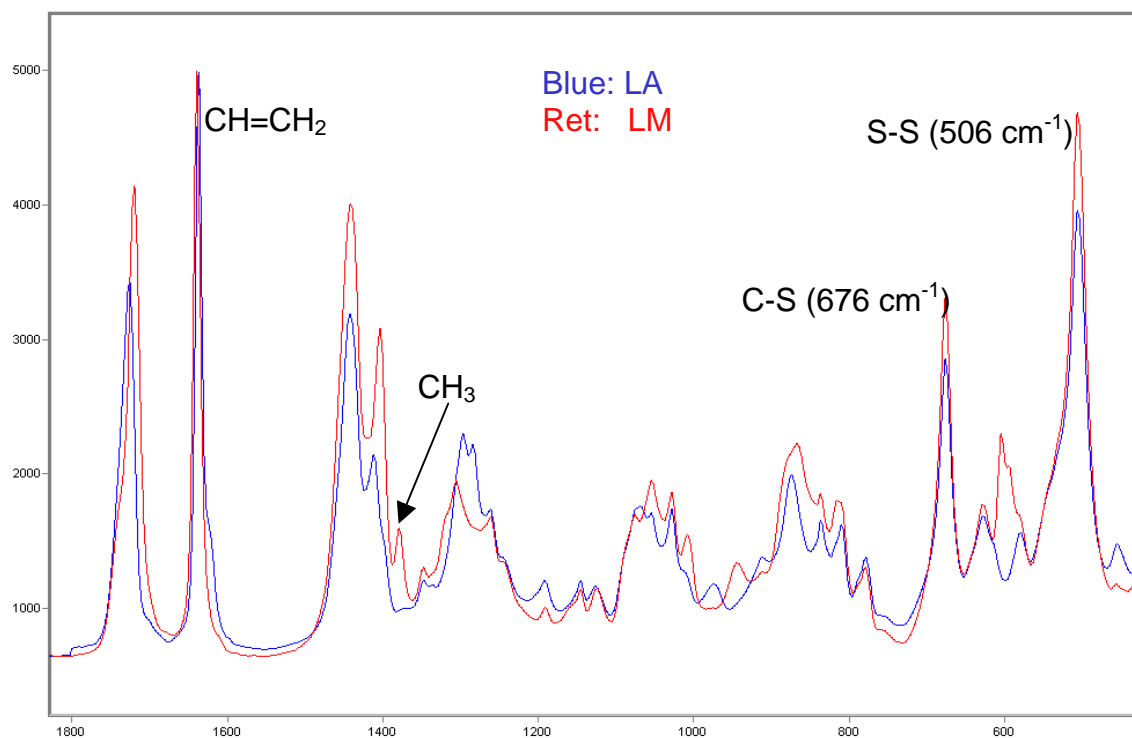
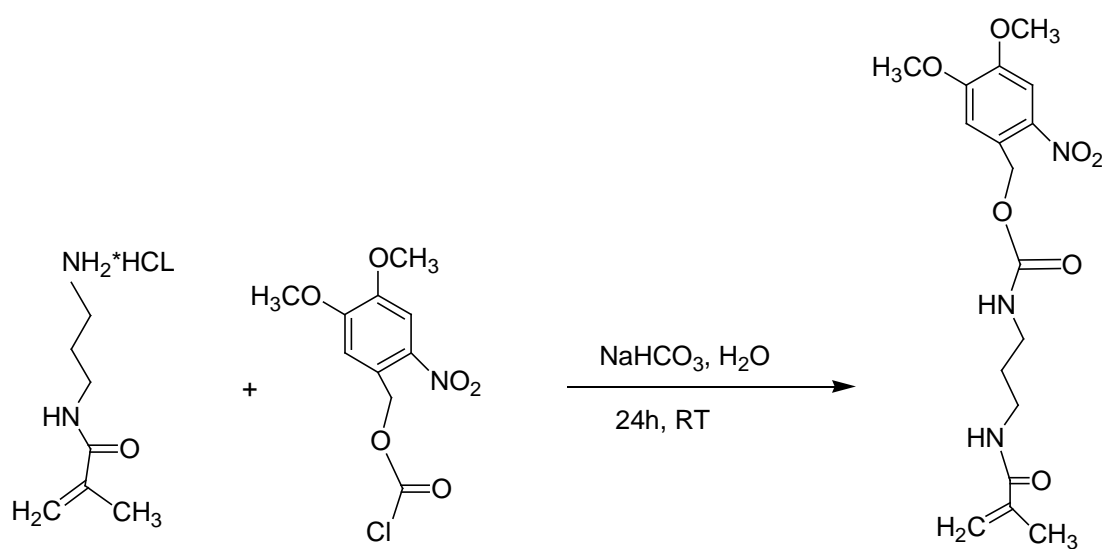


**Figure 4-3.** Raman spectrum of LA and LM monomers.

#### 4.1.2 Synthesis of N-(N-NVOC-aminopropyl)methacrylamide (NVOC)



**Scheme 4-3.** Synthesis of protected amine monomer (NVOC).

One of the most frequently used photolabile protecting group for amines is the 6-nitroveratryloxycarbonyl (NVOC) group. The monomer (NVOC) was synthesized using as starting materials N-(3-amino-propyl)methacrylamide hydrochloride with 1.1 excess NVOC in the mixture of dioxane and water as described previously by Braun [PhD Thesis]. The NVOC protected monomer was prepared in 83 % yield. We used this monomer in previous research for similar purposes: selective irradiation through a mask or direct laser irradiation was used for the patterning of surfaces with free amino groups, but at that time these units were part of terpolymers appropriately designed for the anchoring on silicon substrates.

The characterisation of these monomers was performed by conventional techniques like  $^1\text{H}$  NMR,  $^{13}\text{C}$  NMR, IR, EA.

The  $^1\text{H}$  NMR spectrum shows clearly the signal of the formed carbamate bond at 7.40 ppm (4) (Figure 4-4).

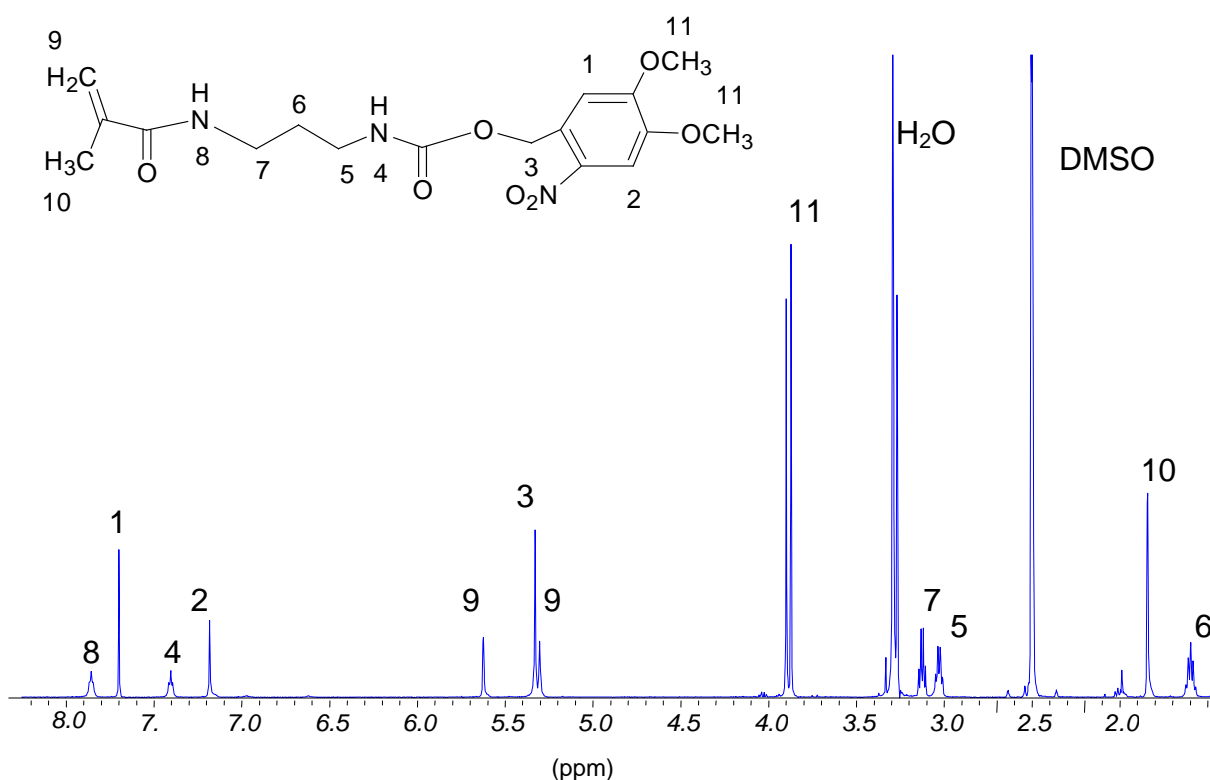


**Figure 4-4.**  $^1\text{H}$  NMR spectrum of protecting amine monomer (NVOC) in  $\text{DMSO-d}_6$ .

The signals for the methoxy groups of the protective NVOC group was seen as double peak at 3.88 ppm (11). The methylene signal was observed at 5.32 ppm (3) and the aromatic protons at 7.69 ppm (1) as well as at 7.18 ppm (2).

The Figure 4-5 shows the  $^{13}\text{C}$  NMR spectrum of NVOC. All peaks in the  $^{13}\text{C}$  NMR spectrum were clearly assigned to each C atoms. The most important signal (the carbamat group (8)) was found at 155.85 ppm.

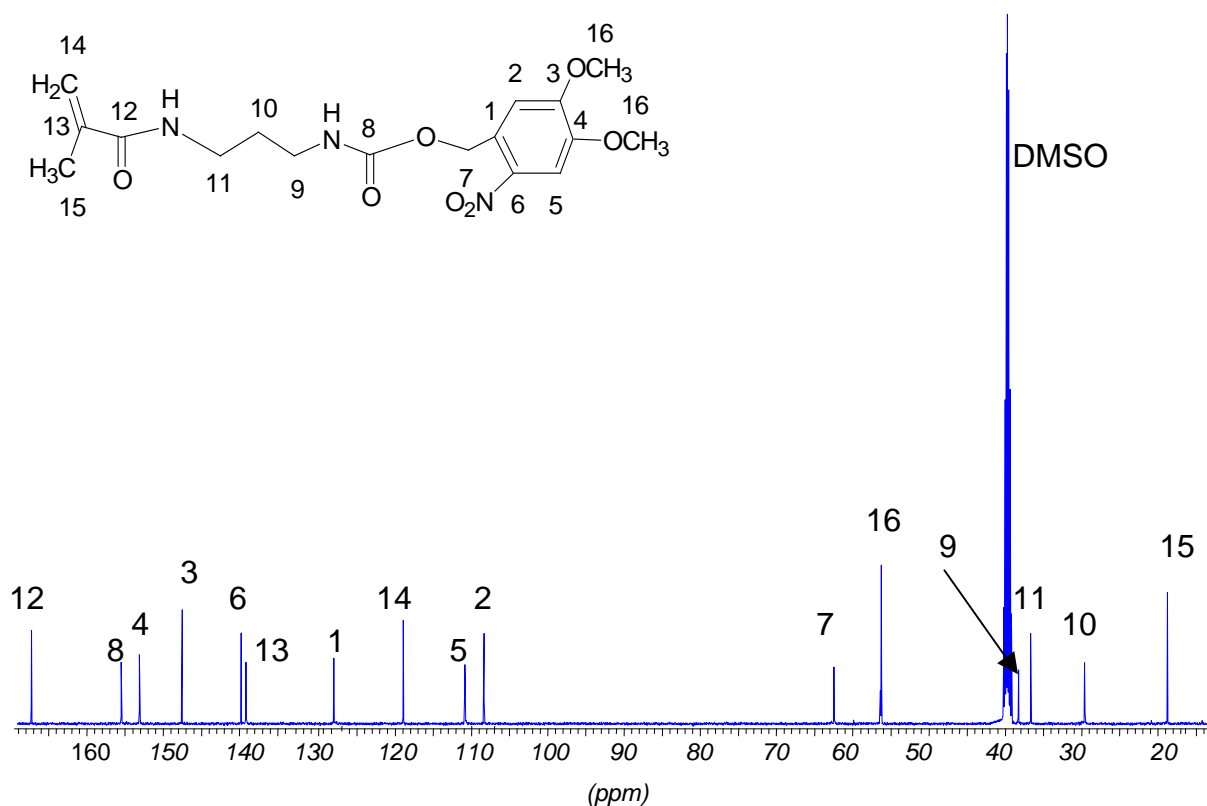
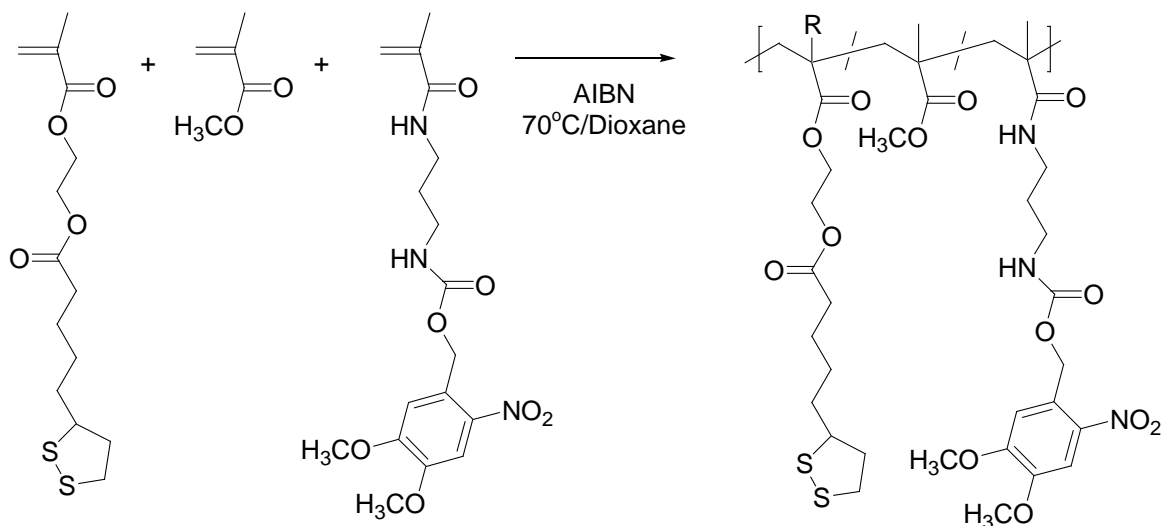


**Figure 4-5.**  $^{13}\text{C}$  NMR spectrum of protecting amine monomer (NVOC) in  $\text{DMSO-d}_6$ .

#### 4.1.3 Synthesis of co- and terpolymers by FRP

The combination of these monomers with specific functions together with methyl methacrylate or styrene via free radical polymerization yielded terpolymers suitable for the formation of thin films of high quality. Also copolymers including the monomers LM/LA and only MMA or S were synthesized for comparison reason. The synthesis of these polymers was performed by free radical polymerization of the monomers included in the adequate proportion in the feed in presence of AIBN as thermal initiator, heating at 70 °C under inert atmosphere, and using as solvent dry dioxane previously distilled (20%w solution) (Scheme 4-4). For the synthesis of the copolymers 2 mol% AIBN were used. The obtained materials have molar masses  $M_n$  between 10000-15000 g/mol,  $M_w$  between 30000 - 40000 g/mol, and relatively broad PDIs around 3 (obtained by GPC, polystyrene calibration) maybe due to presence of

a small amount of SH groups resulting from the opening of the disulfide ring (Table 4-1). With the help of Raman Spectroscopy (Figure 4-6) the presence of disulfide units in the polymers can be confirmed.



**Scheme 4-4.** Schematic example of terpolymer (LM/MMA/NVOC 5/75/20) synthesis by free radical polymerization.

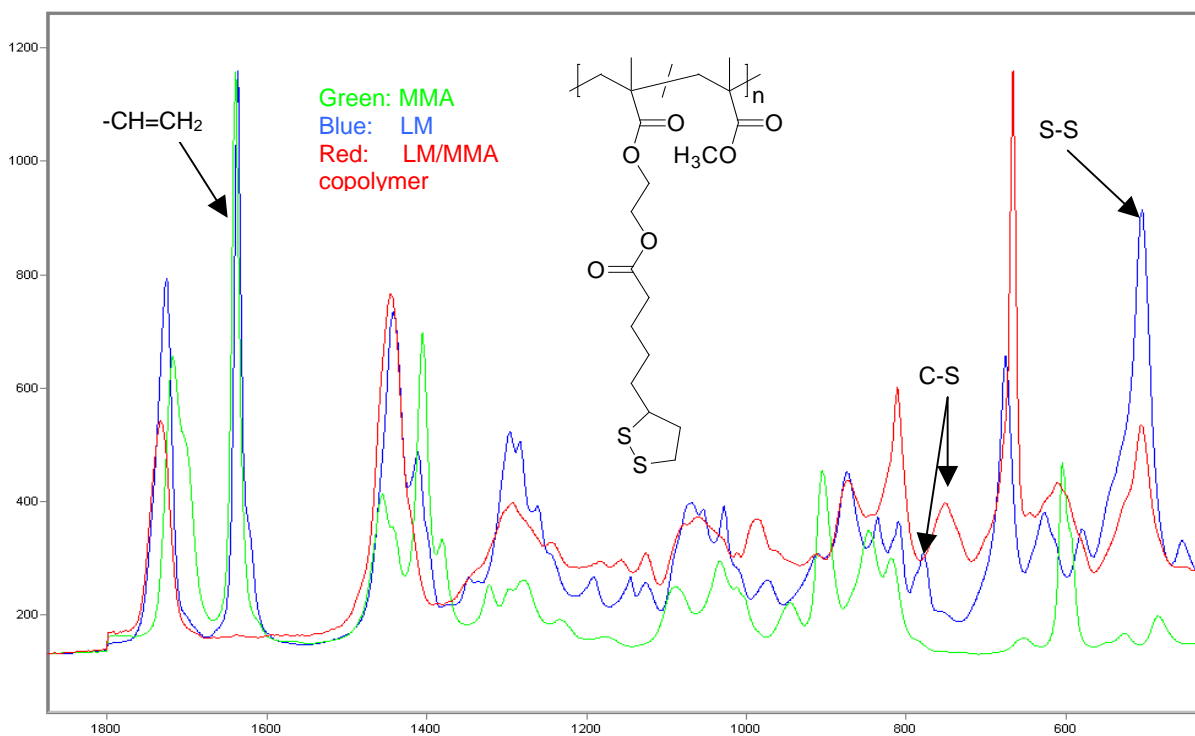


**Figure 4-6.** Raman spectrum of LM copolymer with MMA (25/75) and of the corresponding monomer.

In the particular case of the terpolymers, a high amount of 10 mol% AIBN was used to start the reaction due to the fact that the presence of NO<sub>2</sub> group in the monomer NVOC leads to radical trap reactions. In this case, as expected, lower molar masses were achieved (M<sub>w</sub> between 3000 - 8000, M<sub>n</sub> of around 2000 - 4500) but the PDI was around 2 (Table 4-1) and high polymer yields could be obtained.

Characterization of the resulting polymers was performed through <sup>1</sup>H NMR, <sup>13</sup>C, EA, GPC, TG, DSC and is summarized in Table 4-1. All the characterization techniques evidence the accordance of the chemical structures of these materials with the ones expected from the monomer feed ratio. As an example, the <sup>1</sup>H NMR spectra of the terpolymer LM/MMA/NVOC 5/75/20 is shown in Figure 4-7.

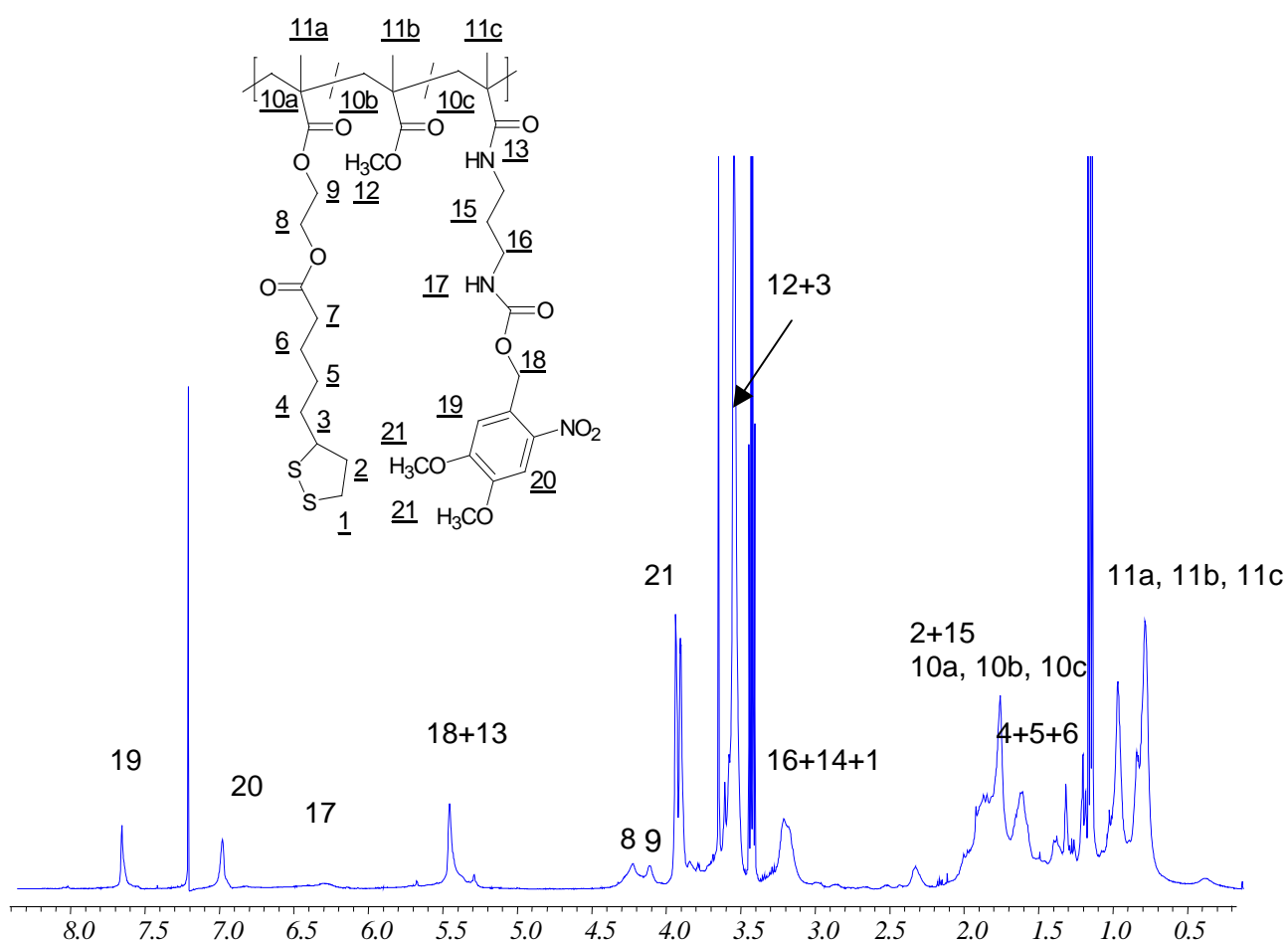


**Figure 4-7.** <sup>1</sup>H NMR spectra of the terpolymer LM/MMA/NVOC 5/75/20 in CDCl<sub>3</sub>.

The real composition of the polymers was calculated through integration in the <sup>1</sup>H NMR spectra of isolated bands characteristic for every unit: dimethylene bridge in the case of LM and LA monomers, methoxy group for MMA, aromatic hydrogens for

styrene, and methoxy groups for the monomer NVOC. All the spectra were recorded in  $\text{CDCl}_3$  with the exception of the co- and terpolymers containing styrene (those spectra were recorded in  $\text{DMSO-d}_6$ ), since overlapping of the aromatic signals from styrene with  $\text{CDCl}_3$  signal did not allow the integration of isolated bands. As it can be observed in Table 4-1, the real compositions of all the polymers are in reasonable good accordance with the monomer composition in the reaction mixture.

**Table 4-1.** Summary of the characteristics of the co- and terpolymers synthesized (polymerization in dioxane,  $70^\circ\text{C}$ , 24 hrs).

Polymer	Determined composition <sup>1</sup>	Yield (%)	GPC			TGA	DSC
			Mw	Mn	PI	$T_{(10\% \text{ loss})}$ ( $^\circ\text{C}$ )	$T_g$ ( $^\circ\text{C}$ )
LA/MMA 25/75 <sup>2</sup>	18/82	75	34000	15000	2.3	279	48
LM/MMA 25/75 <sup>2</sup>	24/76	63	40000	9500	3.6	335	66
LA/S 25/75 <sup>2</sup>	16/84	90	---	---	---	319	65
LM/S 25/75 <sup>2</sup>	22/78	83	33000	11000	3.0	297	47
LA/MMA/NVOC 5/75/20 <sup>3</sup>	4/25/71	64	8000	4500	2.2	284	96
LM/MMA/NVOC 5/75/20 <sup>3</sup>	4/18/78	49	9700	4300	1.7	256	80
LA/S/NVOC 5/75/20 <sup>3</sup>	6/30/64	22	3200	2000	1.6	268	84
LM/S/NVOC 5/75/20 <sup>3</sup>	5/13/82	23	4500	2200	2.1	266	64

<sup>1</sup>Calculated by <sup>1</sup>H NMR integration; <sup>2</sup> 2 mol% AIBN; <sup>3</sup> 10 mol% AIBN.

The thermal stability and glass transition temperatures of the objective materials was studied by TGA and DSC, respectively. TGA analysis demonstrates the sufficiently high thermal stability of these materials, as in all the cases the temperatures  $T_{10\% \text{ loss}}$  are above  $255^\circ\text{C}$ . In general higher stability is exhibited by the copolymers, probably due to the higher molecular weight. Between the copolymers, those containing the styrene unit display higher  $T_{10\% \text{ loss}}$  ( $>297^\circ\text{C}$ ) and also those containing the methacrylate LM ( $>297^\circ\text{C}$ ) units compared to the acrylate LA ( $>279^\circ\text{C}$ ). The polymer LA/S 25/75 seems to be an exception to this behavior which can be explained by the difference between the expected composition and the one determined by <sup>1</sup>H NMR integration. The higher amount of styrene incorporated into the polymer chain



increases the thermal stability. With regard to the glass transition temperatures, terpolymers exhibit higher values, comprised between 65 - 96 °C compared to the copolymers with  $T_g = 47 - 66$  °C, probably due to the bulky nitroveratryl group, however, further conclusions can not be drawn due to overlapping effects of the acrylate, methacrylate and styrene unit, the functional side group and the molar masses. From the obtained values, however, it can be concluded that the thermal properties of the polymers are adequate for our purposes.

Finally the solubility of co- and terpolymers was checked in different solvents. The results are shown in Table 4-2. Most of the polymers are soluble in DMF, dioxane, THF and chloroform, even though in some cases some traces of flocculation were observed, specially noticeable for the copolymers LA/S 25/75 and LM/MMA 25/75. Ethanol, however, does not solubilize any polymer.

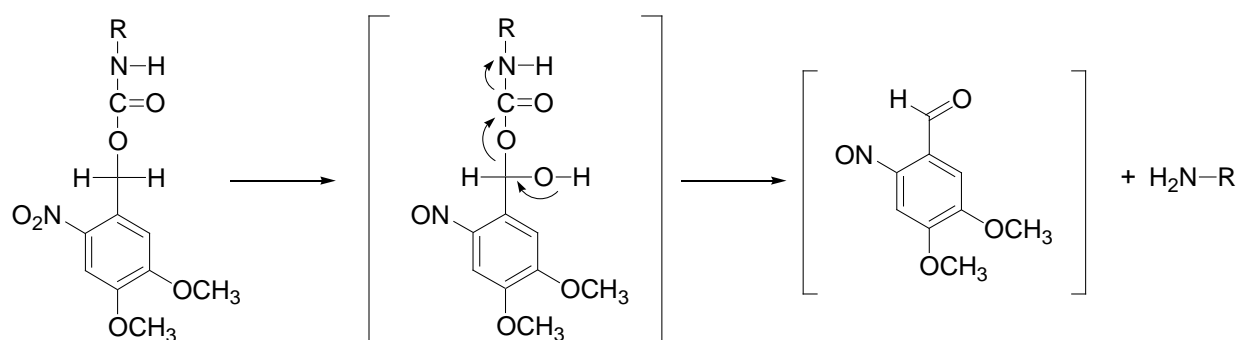
**Table 4-2.** Solubility of the polymers in different solvents (*f* = traces of flocculation; *ns* = not soluble).

Polymer	DMF	Dioxane	Ethanol	Ethyl acetate	THF	CHCl <sub>3</sub>
LM/MMA 25/75	f	f	ns	f	f	+
LA/MMA 25/75	+	f	ns	+	+	+
LM/S 25/75	+	+	ns	+	+	+
LA/S 25/75	f	f	ns	f	f	f
LM/MMA/NVOC 5/75/20	+	+	ns	+	+	+
LA/MMA/NVOC 5/75/20	+	+	ns	+	+	+
LM/S/NVOC 5/75/20	+	+	ns	+	+	+
LA/S/NVOC 5/75/20	+	f	ns	+	+	+

#### 4.1.4 NVOC deprotection

The deprotection of the NVOC protection group under UV-exposure (UV light between 200 – 400 nm) leads to an intramolekularen relocation where the nitro-group is reduced to a nitroso-group and an oxygen in the CH group in 2 position is introduced. The free amino group and the nitrosobenzaldehyd are the end products of this process (Scheme 4-5). The irradiation with UV light of this group provides in high yields the amino functionality following the mechanism depicted in Scheme 4-5. Removal of these groups from amino-terpolymers was achieved easily by UV light at

350 nm wavelength, firstly in solution, as shown by the reduced UV absorption of the aromatic protecting group (Figure 4-8).



**Scheme 4-5.** Decomposition mechanism of nitroveratryl carbamates through irradiation with UV light.

Spectra in DMSO solution of all the terpolymers containing **NVOC** were recorded and irradiation of the samples using a Hg-Xe lamp was performed. In Figure 4 - 9 the decrease of the absorption band at 350 nm provided by the presence of **NVOC** unit of the polymer **LM/MM/NVOC 5/75/20** can be observed. The deprotection occurred, as expected, relatively fast in solution (Figure 4-8), where the disappearance of the absorption band occurred in a few minutes.

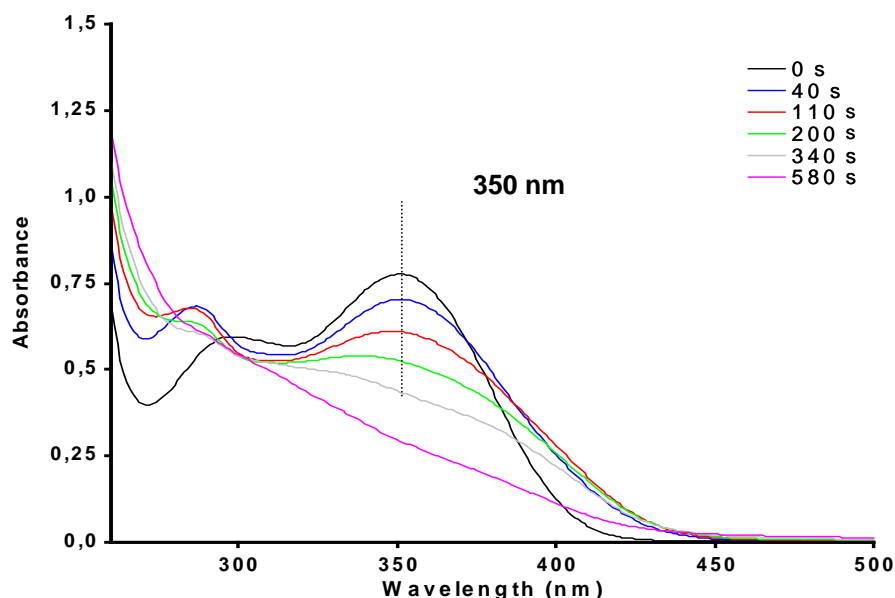


**Figure 4-8.** UV spectrum of terpolymer **LM/MMA/NVOC 5/75/20**,  $10^{-4}$  M solution in DMSO, upon irradiation with a Hg/Xe lamp (300 W).

Spectra on a film of all the terpolymers containing **NVOC** were recorded and irradiation of the samples using a Hg-Xe lamp was performed. The irradiation was performed on films obtained by spin coating at 2000 r.p.m from 3 wt.-% solution (dioxane) of aminoterpolymers (approx. thickness 20 - 25 nm). Also in the film, the disappearance of the absorption band occurred in a few minutes, even though the reaction is some what slower in the film compared to the reaction in solution. This rate is acceptable for the deprotection in thin films, since only the superficial functional groups need to be addressed.

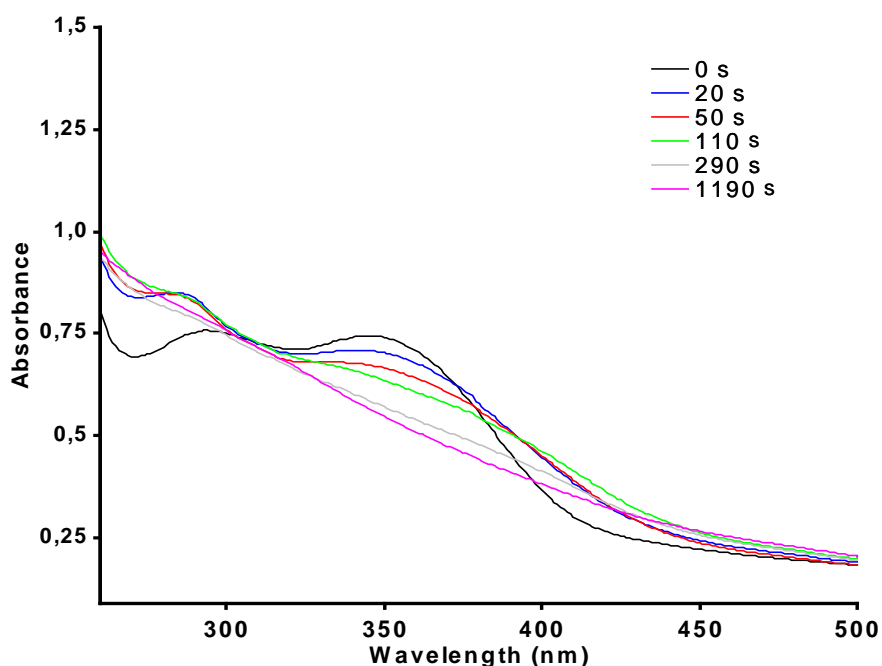


**Figure 4-9.** UV spectrum of the terpolymer **LM/MMA/NVOC 5/75/20**, cast as film, upon irradiation with a Hg/Xe lamp ( $100\text{mW}/\text{cm}^2$ ).

Thus, together with the good thermal properties, other properties of these materials can be highlighted as the anchoring capacity to gold substrates and the photolabile behaviour, which make these polymers attractive for patterning and subsequent functionalization. The easiest way to demonstrate the availability of these polymers for the functionalization of surfaces through irradiation is to study how deprotection of the cage groups occurs upon irradiation. Studies on this work are shown in chapter 2.3.1.

## 4.2 COMBINING NMRP AND CLICK CHEMISTRY FOR THE PREPARATION OF MULTIFUNCTIONAL POLYMERS

### 4.2.1 Multifunctional polymer through precursors

#### 4.2.1.1 Synthesis of starting precursor polymer by NMRP for click reaction

As already it was mentioned in this work, we also want to presented an approach combining the advantages of controlled radical polymerization (NMRP) and click chemistry for the synthesis multifunctional of side-functionalized copolymers. We have chosen as starting material the random copolymer poly[styrene-*r*-(4-acetoxystyrene)] obtained from styrene and 4-acetoxystyrene, monomers which can be easily polymerized by NMRP and with the advantage that they can be commercially purchased. The subsequent polymer is transformed by further cascade reactions into an adequate precursor polymer for the performance of click reactions, which: poly(styrene-*r*-4-propargyl-oxystyrene). Later on a family of azides has been selected to modulate the properties of the polymers using the “click chemistry approach”. The incorporation of photolabile amino protecting groups in the materials enables the release of functional groups by means of UV/laser irradiation. On the other hand the incorporation of sulfide derivatives as anchoring groups allows the covalent attachment of the materials onto gold substrates. This feature will allow further reactivity or modifications of the functional groups of thin polymer films in liquid media, for example, for the formation of supramolecular interactions or the attachment of nanoelements. Even though in this work only random copolymers are prepared, the controlled character of NMRP allows also for the formation of blockcopolymers and thus nanostructure formation by self-assembly.

As a starting precursor polymer, random poly[styrene-*r*-(4-acetoxystyrene)] (**1**) was synthesized by NMRP using 2,2,5-trimethyl-4-phenyl-3-azahexane-3-nitroxide as initiator (Figure 4-10). This nitroxide-adduct developed by Hawker et al. [Haw01] allows to polymerize a wide variety of monomers in a controlled fashion, as acrylates, styrene derivatives, acrylamides, 1,3-dienes and so on, and it also allows to perform

the polymerization under relative mild conditions. The most striking difference of the chosen structure is the presence of a hydrogen atom on one of the  $\alpha$ -carbons, in contrast to the two quaternary  $\alpha$ -carbons present in the traditional TEMPO and other nitroxides.

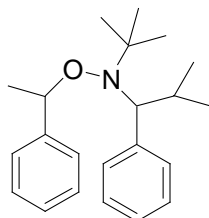


**Figure 4-10.** Chemical structure of the initiator 2,2,5-trimethyl-4-phenyl-3-azahexane-3-nitroxide.

The initiator was synthesized following the experimental conditions described in the literature [Beo00]. It is well known that many styrene derivatives can be polymerized by NMRP keeping the control over the reaction. One example is 4-acetoxystyrene, which is a good precursor for hydroxyl groups in position 4, ready for further modification. Thus, the monomers styrene and 4-acetoxystyrene were mixed in a given feed ratio (9:1) with acetic anhydride together with the initiator (Figure 4 - 10) and the polymerization was carried out in the bulk under inert atmosphere at 120 °C similar as described previously [Mes04, Leu02]. Acetic anhydride was used to accelerate the reaction time. Polymerisation time was 17 hours and monomer conversion obtained was according to the NMR integration 90%. The purification of the polymer was performed by subsequent precipitation in ethanol. The reactivity ratios of styrene and 4-acetoxystyrene (1.02 and 0.80 respectively) [Bar98], [Gra04] indicate that the final polymer should exhibit a structure with high tendency to randomness.  $^1\text{H}$  NMR spectrum (Figure 4-11) shows clearly the signal of the acetyl groups at  $\delta = 2.25$  ppm, which overlaps with the very wide signal of the aromatic hydrogen atoms of the polymer chain. However, the overlapping of the signals in the CH, CH<sub>2</sub> region of the  $^{13}\text{C}$  NMR, do not allow to establish definitive conclusions about the microstructure of the polymer.

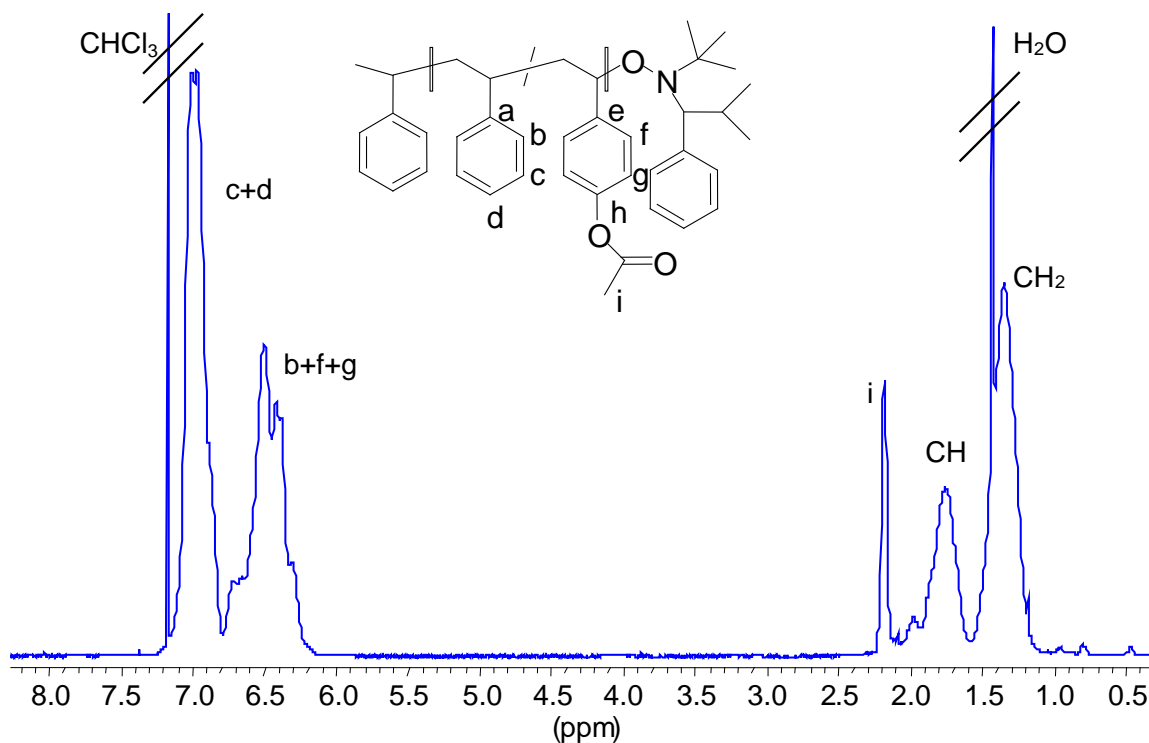


**Figure 4-11.** <sup>1</sup>H NMR spectrum of poly[styrene-*r*-(4-acetoxystyrene)] (1) in CHCl<sub>3</sub>.

The polymer (1) was obtained with a narrow molar mass distribution and a polydispersity index of  $\sim 1.17$  ( $\overline{M}_n = 27,100$  g/mol) as determined by GPC. The calculated molar mass based on monomer/initiator ratio and the obtained conversion was in the order of 27,000 g/mol which indicates that the polymer was obtained with a good control of the molar mass and PDI. This result is in accordance with previous experiments performed on NMRP in our laboratories [Mes06].

Later on, the hydrolysis of the acetyl group was carried out under basic conditions to provide free phenolic groups (Scheme 4-6, b). This reaction led to poly[styrene - *r* - (4-hydroxystyrene)] (2). A number of procedures have been described for such an hydrolysis reaction using different bases [Bar98], [Che99]. Comparative studies have demonstrated that for the removal of the acetyl groups, reactions with hydrazine hydrate are better than those with NaOH, as hydrazine monohydrate often provides deacetylated materials free of any side reactions which might lead to crosslinked products. For this reason hydrazine monohydrate was chosen as hydrolyzing agent.

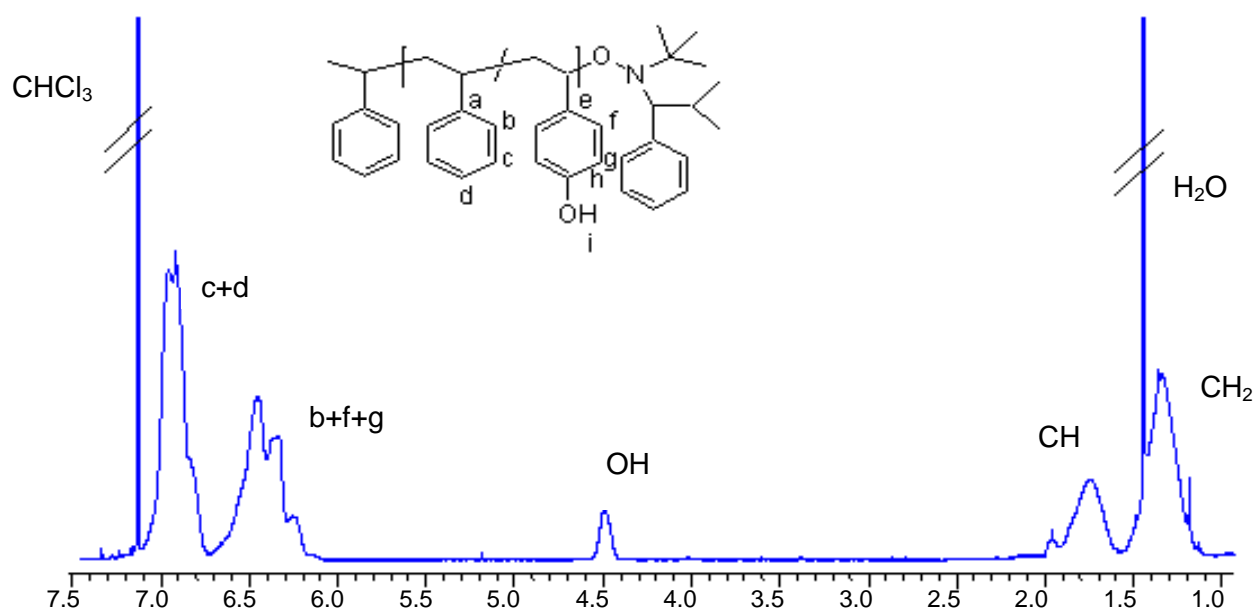
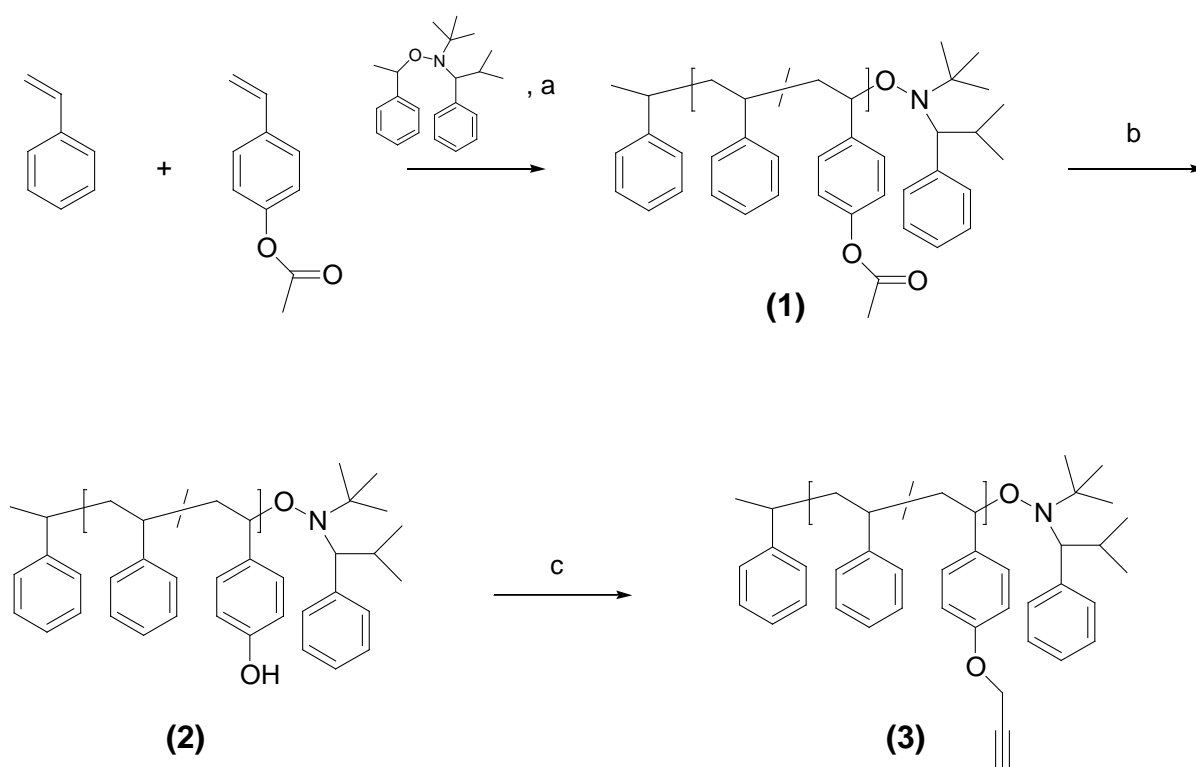


**Figure 4-12.**  $^1\text{H}$  NMR spectrum of poly[styrene-*r*-(4-hydroxystyrene)] (**2**) in  $\text{CHCl}_3$ .

The quantitative removal of the acetyl group can be observed in the  $^1\text{H}$  NMR spectrum (in  $\text{CDCl}_3$ ) (Figure 4-12) by the disappearance of the peak corresponding to the acetyl group at 2.27 ppm, and by the appearance of a broad signal at 4.80 - 4.35 ppm corresponding to the hydroxy group. This polymer was obtained with a narrow molar mass distribution, too. In a second step, the alkyne modified polymer (**3**) was obtained by treatment of polymer (**2**) with propargyl bromide together with potassium carbonate in DMF solution leading to ether formation as described in the literature [Bar98,Che99] (Scheme 4 - 6, c). DMF was selected as a solvent because it owns dipolar aprotic character and accelerates considerably the reaction. In the choice of the solvent its character as well as the solubility to all components is important. Because the solubility of potassium carbonate is very low, 18-crone-6 was used as a phases transfer catalyst in very small quantity (catalytic amount). In the  $^1\text{H}$  NMR spectra (Figure 4-14a) of (**3**) one can observe the propargyl group with a peak at  $\delta = 2.46$  ppm ( $\text{C}\equiv\text{C-H}$ , 1H) and another at  $\delta = 4.60$  ppm ( $\text{O-CH}_2\text{-C}\equiv\text{C-H}$ , 2H). The integration of both signals with respect to the aromatic groups indicates the quantitative character of the reaction. From the relative integration between the aromatic units from styrene and the propargyl group a ratio 89/11 was obtained,

which is in accordance with the monomer ratio in the feed of the starting polymer **(1)** (Scheme 4-6).



**Scheme 4-6.** Synthesis of the copolymer poly(styrene-*r*-4-propargyl-oxystyrene) **(3)** by NMRP and subsequent polymer analogous reactions: a) NMRP, nitroxide-adduct, acetic anhydride, 120 °C; b)  $\text{NH}_2\text{NH}_2 \cdot \text{H}_2\text{O}$ , dioxane, rt; c) propargyl bromide, DMF, rt.

In the  $^{13}\text{C}$  NMR spectra (Figure 4-14b) the signals at  $\delta_1 = 55.9$ ,  $\delta_2 = 79.0$  and  $\delta_3 = 75.2$  ppm corresponding to the three atoms of the propargyl group ( $-\text{C}_1-\text{C}_2\equiv\text{C}_3-$ ), respectively, demonstrate the success of the reaction. Additionally an enlargement is shown of the area 1.1-0.3 ppm of the  $^1\text{H}$  NMR spectra (Figure 4-13), in which protons corresponding to nitroxide initiator (TPPA) fragments included in the polymer are exhibited.

Both modified copolymers **(2)** and **(3)** were also characterized using GPC, which revealed  $\overline{M}_n = 26,000$  g/mol and  $\overline{M}_n = 27,000$  g/mol, respectively, and PDI = 1.20 and 1.21. Comparing these values versus  $\overline{M}_n = 27,100$  g/mol and PDI = 1.17 of the starting material **(1)**, we can see that the narrow molar mass distribution was



retained, which points to the fact that the polymer analogous reactions proceeded efficiently.

The molar mass and polydispersity of all three copolymer were determined by means of GPC in THF as an eluent. The obtained values are shown together in the Table 4-3.

**Table 4-3.** Molar mass and polydispersity index of precursor copolymers.

Copolymer	Calculated $M_n$	$M_n$	PDI
<b>1</b>	27100	26400	1.17
<b>2</b>	26000	27900	1.20
<b>3</b>	27000	27000	1.21

The corresponding GPC traces are shown in Figure 4 - 13 which also indicate narrow monomodal distributions.

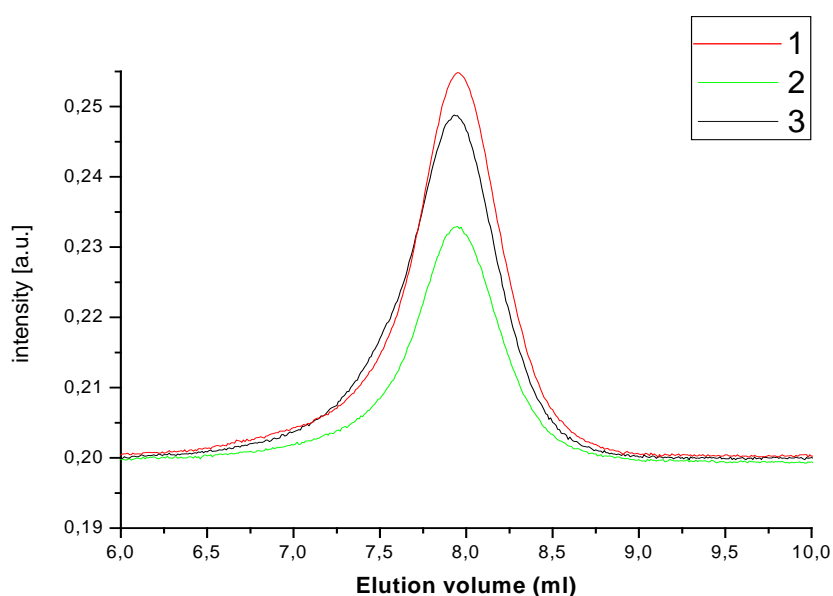


**Figure 4-13.** GPC traces of precursor copolymers in THF.

Copolymer (**3**) was thought to be a good platform for further modification of the propargyl group by means of click reactions (1,3-dipolar Cu catalyzed cycloaddition reactions) as pendant terminal alkynes are suitable for reacting with azides in the presence of Cu(I) catalyst.

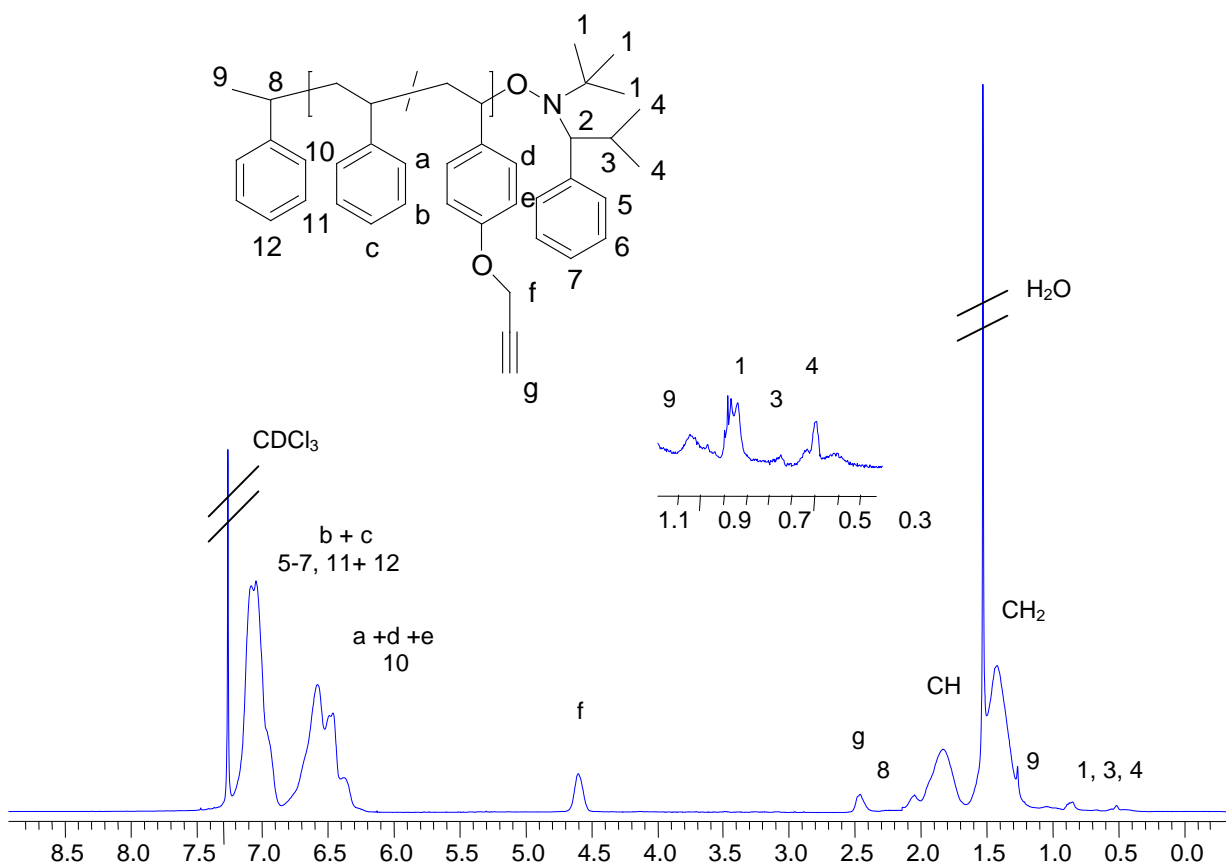


Figure 4-14a.  $^1\text{H}$  spectrum of poly[styrene-*r*-(4-propargyl-oxystyrene)] (3) in  $\text{CDCl}_3$ .

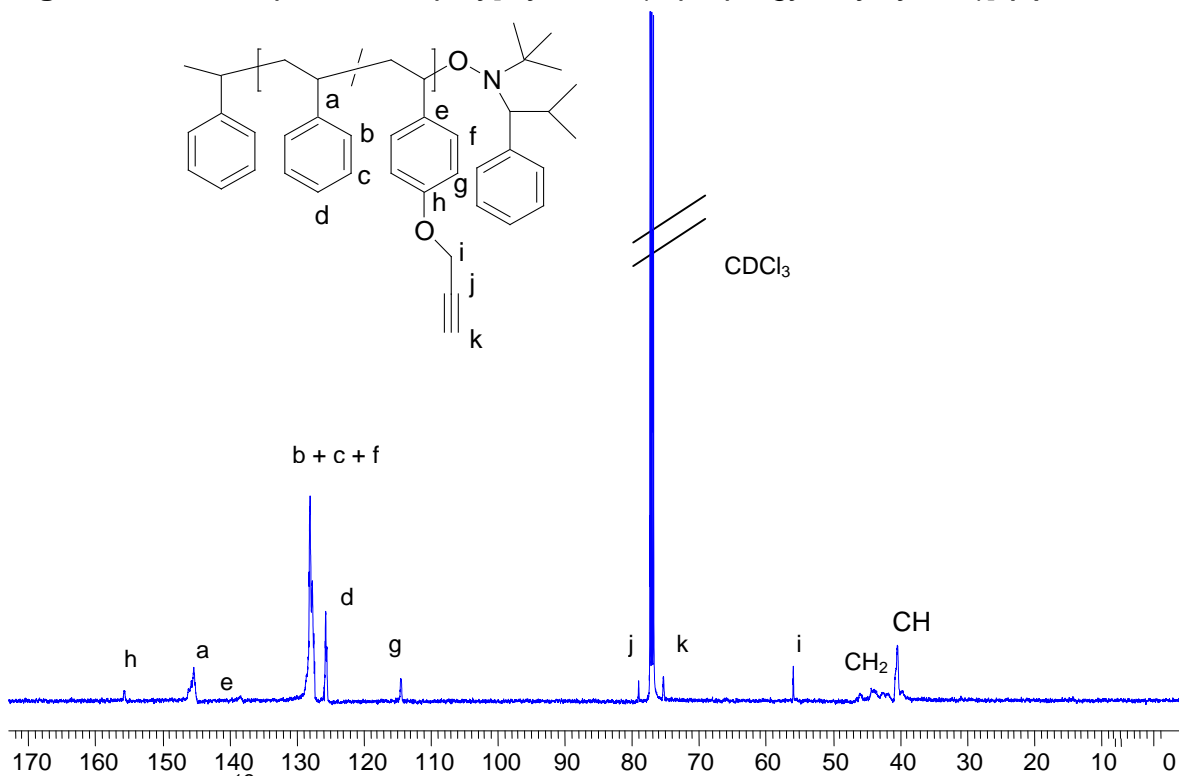


Figure 4-14b.  $^{13}\text{C}$  NMR spectrum of poly[styrene-*r*-(4-propargyl-oxystyrene)] (3) in  $\text{CDCl}_3$ .

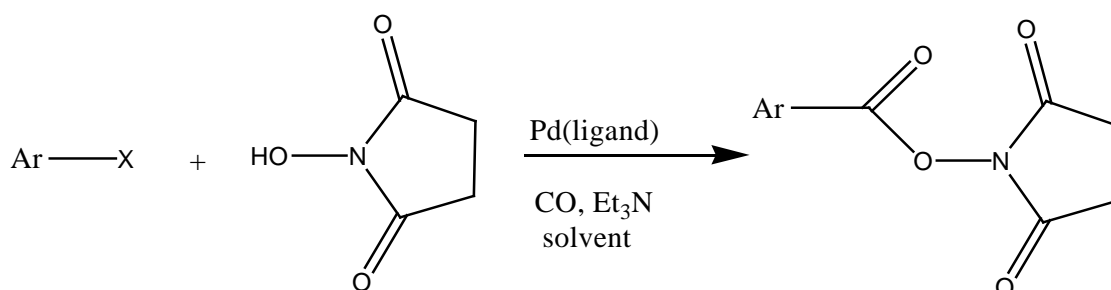
#### 4.2.1.2 Copolymerisation of active ester

In this work, two general approaches were considered for the postmodification- the 1,3 dipolar cycloaddition and the use of active ester.

Tailoring polymer properties for increased functionality is very important to all areas of polymer science [Coe01, Lia05]. The polymerisation of active ester monomers for free radical polymerisation and postpolymerisation modification are attracting increased attention [God01, Mon04, Rel04]. It has been successfully applied to many homogeneous polymerization systems: free radical [Giz01], nitroxide-mediated controlled radical polymerization (CRP) [Chau00], atom transfer radical polymerization (ATRP) [Mig05], step-growth reactions [Far05], simultaneous determination of average composition and mass distributions in free radical copolymerization [Cat02] for continuous reactors [Gra01] and inverse emulsion polymerization [Alb06].

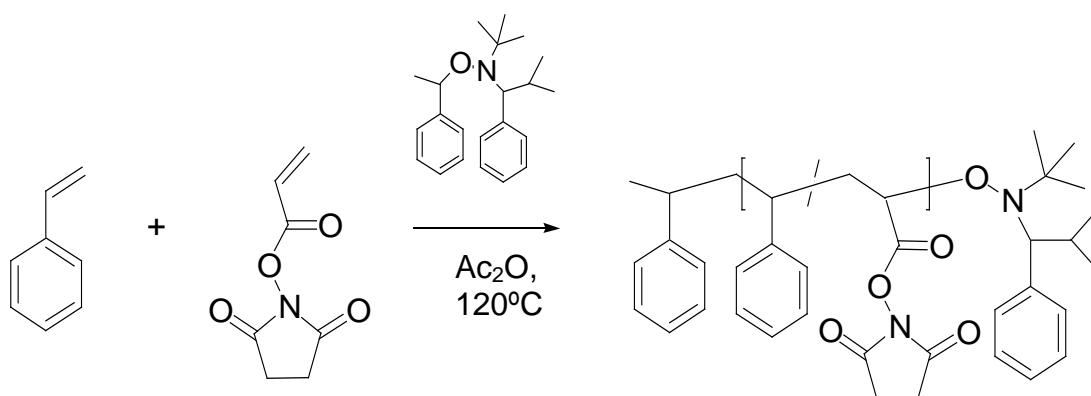
These active ester polymers appear to be excellent candidates for generating a host of novel polymers with applications from biology to electronic materials [Ber98, Sav04, Shu05]. The use of active esters for bioconjugation has been studied for many years, including the attachment of peptides for polymer therapeutics [God01]. More recently, the use of these monomers has been extended to more traditional polymer areas [Shu05, Shu05a].

The classical method for making N-hydroxysuccinimido esters involves the reaction of the sodium, potassium, silver or thallium salt of NHS with an acyl chloride [Neu70, Bau57] (Scheme 4-7). Another common methods of preparation, which is used in this work, involves esterifying an acryloyl chloride with NHS in the presence of 4-dimethylaminopyridine in dry THF.



**Scheme 4-7.** Preparation of N-hydroxysuccinimide ester via Pd-catalyzed carbonylation of aryl triflates and aryl halides.

Carboxylic acid ester of N-hydroxysuccinimide (NHS) have been widely used in organic synthesis as reactive acylating reagents (active esters). These active esters are especially useful as intermediates in the synthesis of peptides and proteins via N-acylation [Hyp97, Sag93]. In addition, a number of biologically important molecules such as receptor antagonists [Ros99, Siv94], nucleotides [Sen00, Kol00] and labelling reagents [Ada99, May99] have been chemically modified using N-hydroxy-succinimido ester intermediates. More recently, N-hydroxysuccinimido esters have been used to acrylate other nucleophiles such as alcohols [Tur00] and a hydroxylamine. As part of this work was the synthesis of functional stable terpolymer by "living free radical polymerisation". The preparation of these random copolymers containing active ester was one way to get it this kind of functional product. In this case the copolymerization of 250 equiv of a 9:1 mixture of styrene and acrylate-based active ester monomer in the presence of the nitroxide-initiator at 120°C for 6h gave 82% yield of the desired random copolymer PS-EA in Scheme 4-8. The chemical stability of our alkoxyamine initiator allowed the introduction and manipulation of numerous functional groups and the introduction of acetic anhydride as accelerating agent reduced significant the long reaction times of this polymerization. The prepared copolymer PS-EA was characterized by  $^1\text{H}$  NMR (Figure 4-15). The spectrum shows clearly the signals of protons of the active ester peak at 2,8 ppm.



**Scheme 4-8.** Synthesis of active ester functionalised polymers (PS-EA) by NMRP.

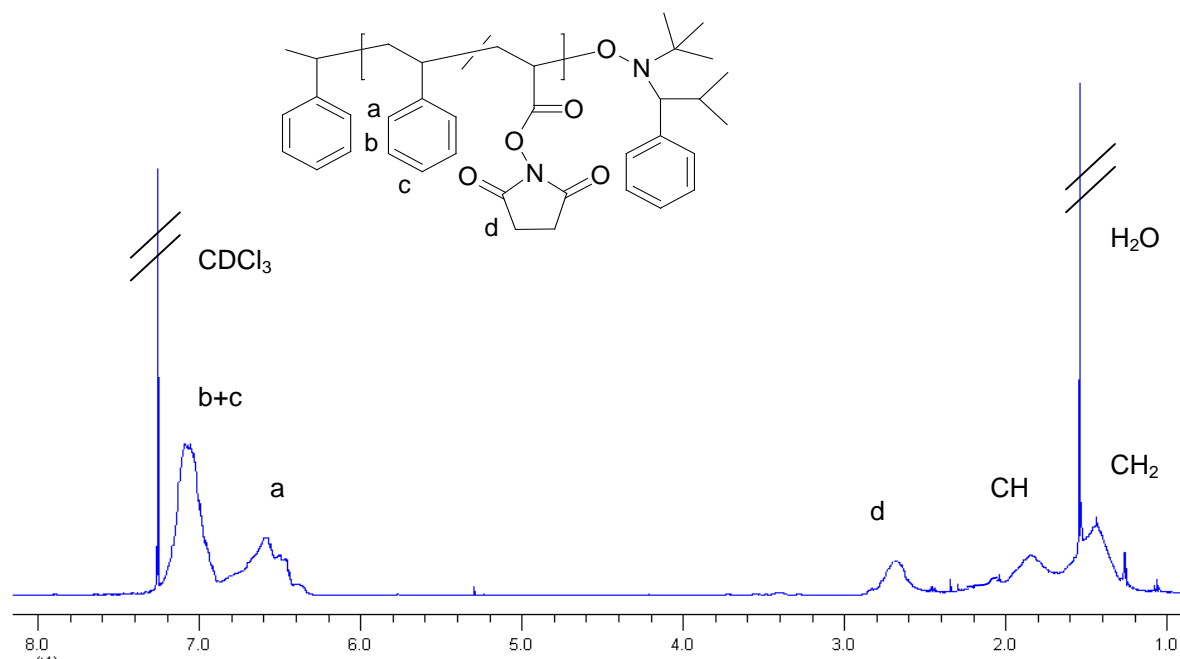
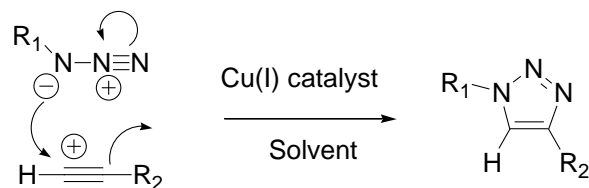


**Figure 4-15.**  $^1\text{H}$  spectrum of active ester functionalised polymer PS-EA in  $\text{CDCl}_3$ .

#### 4.2.1.3 Postmodification through 1,3-dipolar cycloaddition

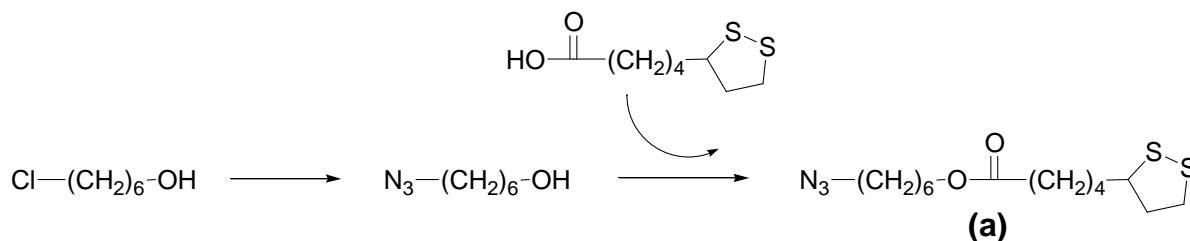
The first reaction have shown that the postmodification through 1,3 dipolar cycloaddition are very efficient and more versatile than the active ester postmodification. This in the following the focus will be solely one the modified of the alkyene copolymer with various azides. Several functional azides were used to introduce a variety of functionalities in the materials. Some of them were synthesized for this work and others could be purchased. One of the most efficient click reactions is the Cu(I) catalyzed Huisgen 1,3-dipolar cycloaddition between terminal acetylenes and azides to yield a stable 1,4-disubstituted 1,2,3-triazol ring (Scheme 4-9).



**Scheme 4-9.** *Cu(I) catalyzed 1,3-dipolar cycloaddition between azides and alkynes providing 1,4-regioselective triazoles.*

Click chemistry allows the preparation of multifunctional materials in simultaneous combination with other synthetic transformations, allowing at the same time absolute fidelity and quantitative yields of the new materials. Development of cascade and simultaneous functionalization approaches for the preparation of multifunctional materials have been explored by Malkoch et al. [Mal05] in which a combination of previously functionalized and non functionalized monomers is used for the preparation of materials ready for further modifications using the mentioned strategies.

As outlined earlier, this work is focused on the preparation of polymers adequate for surface patterning, preferably onto gold substrates. Thus, some azides were designed for this purpose allowing e.g. the incorporation of a sulfide derivative anchoring group. In the first part of the work a family of side chain polymers obtained by free radical polymerization were reported in which lipoic units were introduced by copolymerization of specially designed monomers for covalent anchoring onto gold [Sie05]. Now, 5-[1,2]-dithiolan-3-yl-pentanoic acid 6-azido-hexyl ester (**a**) was obtained by esterification of lipoic acid and 6-azido-1-hexanol (Scheme 4-10). The esterification process was performed in presence of DCC and DMAP, which provided the final ester compound in high yields (90%) and under mild conditions as reported. The precursor 6-azido-1-hexanol was synthesized from 6-chloro-hexanol and NaN<sub>3</sub> following a procedure described in the literature [Dav99] (Scheme 4-10).



**Scheme 4-10.** Synthesis of the azide 5-[1,2]dithiolan-3-yl-pentanoic acid 6-azido-hexyl ester **(a)**.

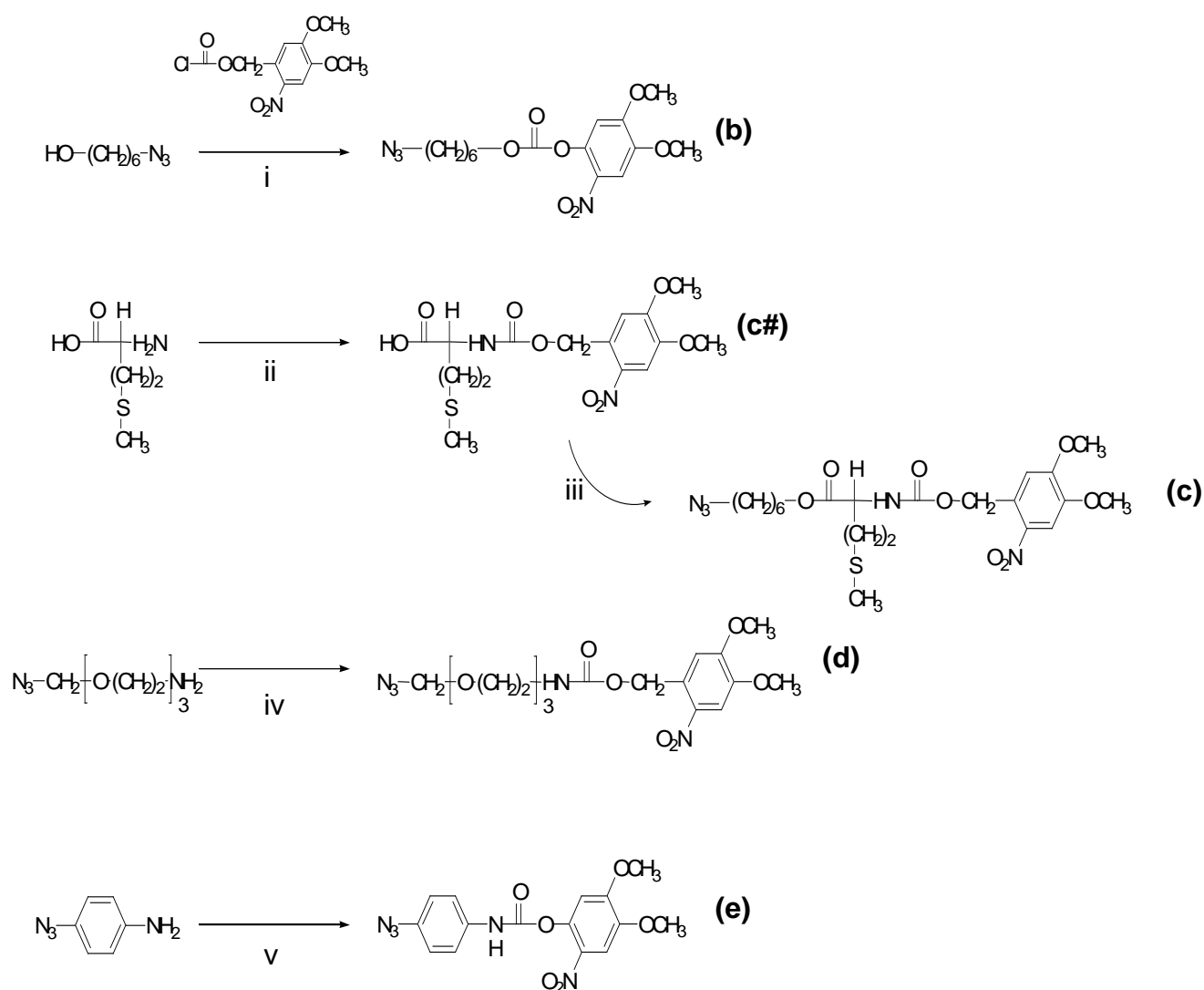
In order to obtain photolabile polymers for patterning applications, azide **(b)** was synthesized from 6-chlorohexanol and 2-nitroveratryl chloroformiate as depicted in Scheme 4-11, i.

An azide derivative from an amino acid was synthesized later on following the route as depicted in Scheme 4-11, ii, iii. Amino acids are well known not only because they are constituents of proteins and typical biological polymers, but also because they are useful substances for chiral auxiliaries, and building blocks used in organic synthesis for the incorporation of a variety of chemical and biochemical functions. This aroused the interest in the design of an azide including both a photolabile and an anchoring group for gold, enabling the incorporation of two specific properties in one step. For this purpose the amino acid methionine was selected. Although S-S is reported to be a more effective anchoring group, anchoring groups for gold containing the moiety methylsulfide  $\text{CH}_3\text{-S-}$  have been also described [Lov05]. The amino group from methionine enables an easy protection by the photolabile unit of choice, nitroveratryl oxycarbonyl (NVOC) in a first step, and the carboxylic group remains as a functional branch in which an azide moiety can be easily incorporated (Scheme 4-11, iii). This group was esterified with 6-azido-1-hexanol which provided the multifunctional azide 2-(4,5-dimethoxy-2-nitro-benzyloxycarbonyl-amino)-4-methylsulfanyl-butyrac acid 6-azido-hexylester, depicted as **(c)**. The conditions used for the esterification were analogous as those used for the synthesis of azide **(a)**.

Another photoactive azide having a longer spacer and thus a more flexible structure, was obtained from the reaction of 11-azido-3,6,9-trioxane 1-amine and 2-nitroveratryl chloroformiate (Scheme 4-11, iv), depicted as **(d)**.

From 4-azido-aniline and nitroveratryl chloroformiate (Scheme 4-11, v) the azide (4-azido-phenyl)-carbamic acid-4,5-dimethoxy-2-nitro-benzyl ester **(e)**, as described in

the experimental part, was synthesized also for this work. As mentioned before, the nitroveratryl group has been used in previous investigations in which comb type terpolymers were obtained by free radical polymerization and later on were used for selective patterning of ultrathin films anchored onto silicon wafers [Bra03]. Selective irradiation in presence of a mask freed amino groups which were used for the attachment of gold colloids or nanoelements [Opi04, Voi04].

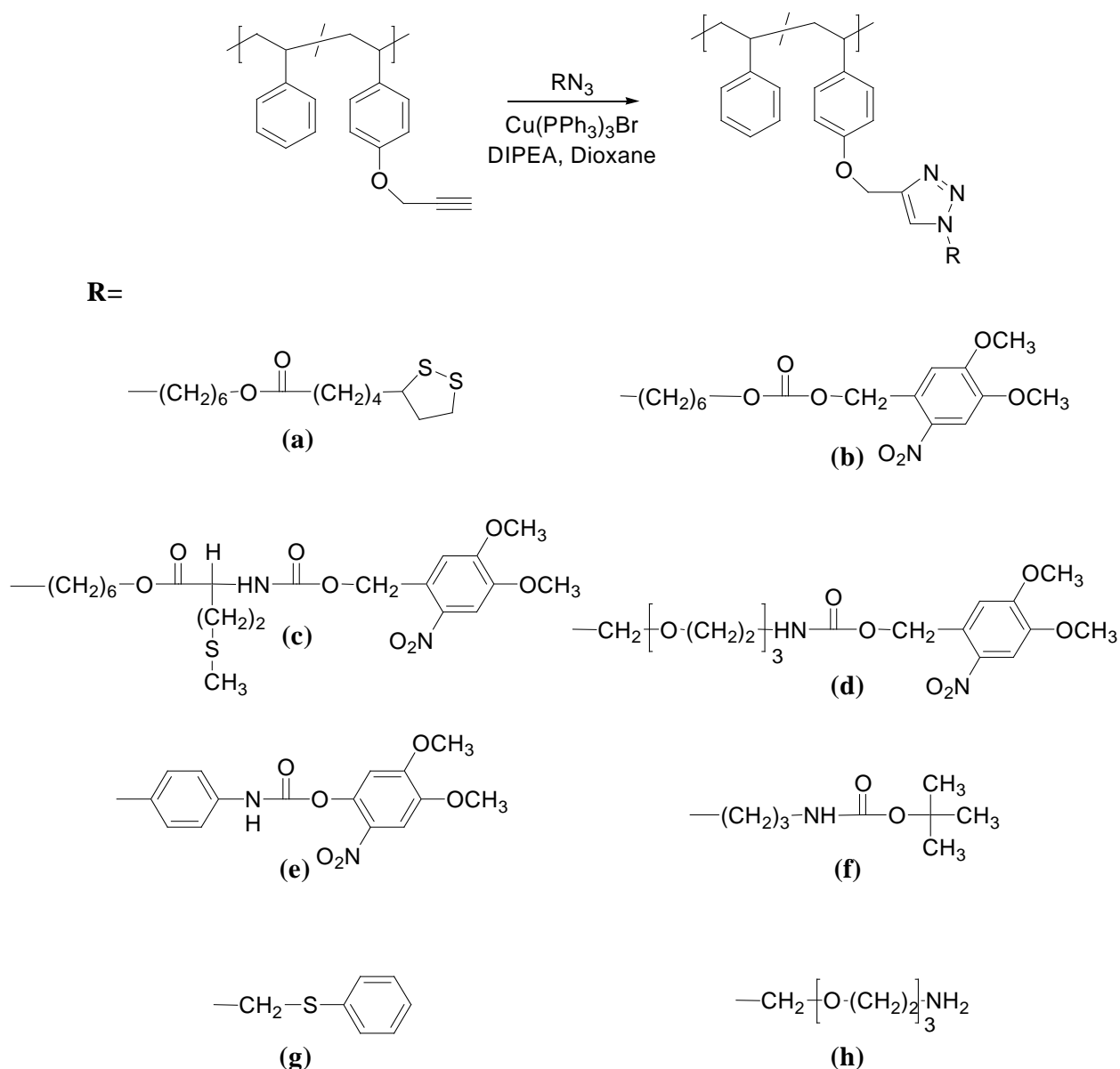


**Scheme 4-11.** Synthesis of photolabile NVOC-derivative azides.

In addition to the mentioned designed compounds, some commercially available azides with interesting properties were also used for our purposes. One of them was 3-azido-propyl-carbamic acid *tert.*-butyl ester. The *t*-butyloxycarbonyl group (*t*-BOC) is well known as a protective group for OH and amino functions. This group is



extensively used in phenolic polymers for lithographic and photoresist applications [Ree78], and it allows the release of the functional groups after irradiation in presence of a photoacid generator (PAG). These molecules (PAG) provide strong acidic species ( $H^+$ ) after irradiation with UV light which promote the release of the protecting group after a postbaking process. Although the yield in the deprotection of  $NH_2$  is not so high as for OH groups,  $NH_2$  groups can also be obtained in moderate yields in presence of triphenyl sulfonium triflate as it was recently investigated [Mil07]. Azide azidomethyl-phenylsulfide (**g**) was also chosen, in order to study the anchoring capacity of this moiety to gold substrates, as well as 11-azido-3,6,9-trioxane -1 - amine (**h**) which supplies directly free amino functionalities in the polymer (**3-h**).



**Scheme 4-12.** Post-modified polymers by click reactions with functional azides.

The 1,3-dipolar Cu catalyzed coupling of azides to alkynes is often performed using mild conditions. Some well known catalysts systems for the performance of these cycloaddition reactions are  $\text{Cu(I)}\cdot\text{P}(\text{OEt}_3)/\text{DIPEA}$ ,  $\text{CuSO}_4\cdot 5\text{H}_2\text{O}/\text{sodium ascorbate}$ ,  $\text{CuI}/\text{DIPEA}$  or  $\text{CuI}/\text{DBU}$  (1,8-diazabicyclo[5,4,0]undec-7-ene). Due to solubility reasons,  $\text{Cu}(\text{PPh}_3)_3\text{Br}/\text{DIPEA}$  was chosen as catalyst system, and dioxane as reaction media. The reaction mixtures were stirred at rt for 3 days under nitrogen atmosphere, and by precipitation in ethanol the desired materials were obtained without further purification steps in high yields (70 - 95 %) (Table 4-4). Their chemical structures are shown in Scheme 4-12.

In Figure 4-16a the FTIR spectrum of polymer **(3)** is shown, where the bands corresponding to the propargyl group can be seen at  $2092\text{ cm}^{-1}$  ( $\text{C}\equiv\text{C}$ ) and  $3013\text{ cm}^{-1}$  ( $\equiv\text{C-H}$ ). In Figure 4-16b the spectrum of a modified material **(3-a)** is shown, in which one can confirm that these bands disappeared. Together with the spectrum of **(3-a)**, the spectrum of the precursor azide is shown as dashed line. The absence of  $\text{N}_3$  band in **(3-a)** FTIR is observed but the presence of bands at  $1239$  and  $1169\text{ cm}^{-1}$  characteristic for the azide are visible indicating that the incorporation of the azide has been successful. Some significant bands of the polymers are indicated in the represented spectra and more in detail for all the materials in the experimental part.

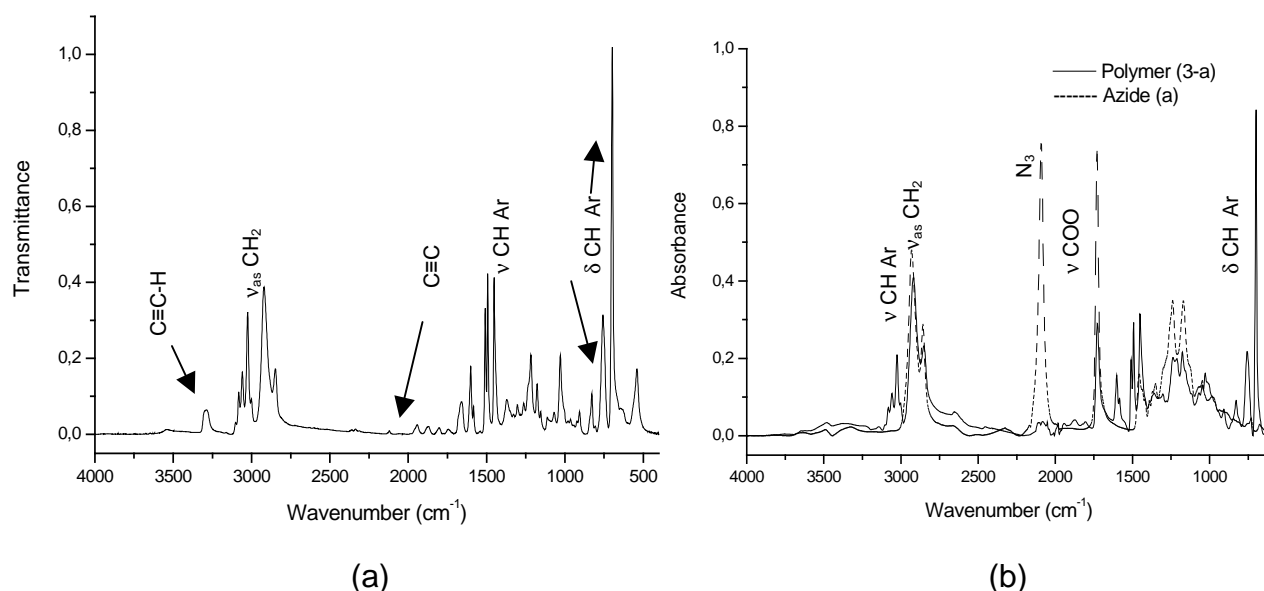


**Figure 4-16.** FT-IR spectra of polymers precursor polymer **(3)** shown in (a), and product **(3-a)** shown in (b) (together with the spectrum of azide (a)).

The effectiveness of the reactions was proven also by  $^1\text{H}$  NMR and  $^{13}\text{C}$  NMR. In Figure 4-17 the  $^1\text{H}$  NMR spectra of polymer **(3-d)** is shown. Two signals are significant in the determination of the new materials, one is a broad peak found at around 5 ppm corresponding to the  $-\text{CH}_2-$  group bonded to the triazol ring, and the other is the peak appearing at around 7.5 ppm corresponding to the aromatic proton of the triazol ring. The remaining signals in the spectra could be fully assigned and are in correspondence with the proposed polymer structures.

In the example shown **(3d)** (Figure 4-17) no peak corresponding to the propargyl group is shown which indicates that the reaction proceeded in this case quantitatively according to the NMR accuracy. A yield  $\geq 95\%$  has been assumed to calculate the theoretical molar masses of the final materials in the cases in which no remaining propargyl group was detected.

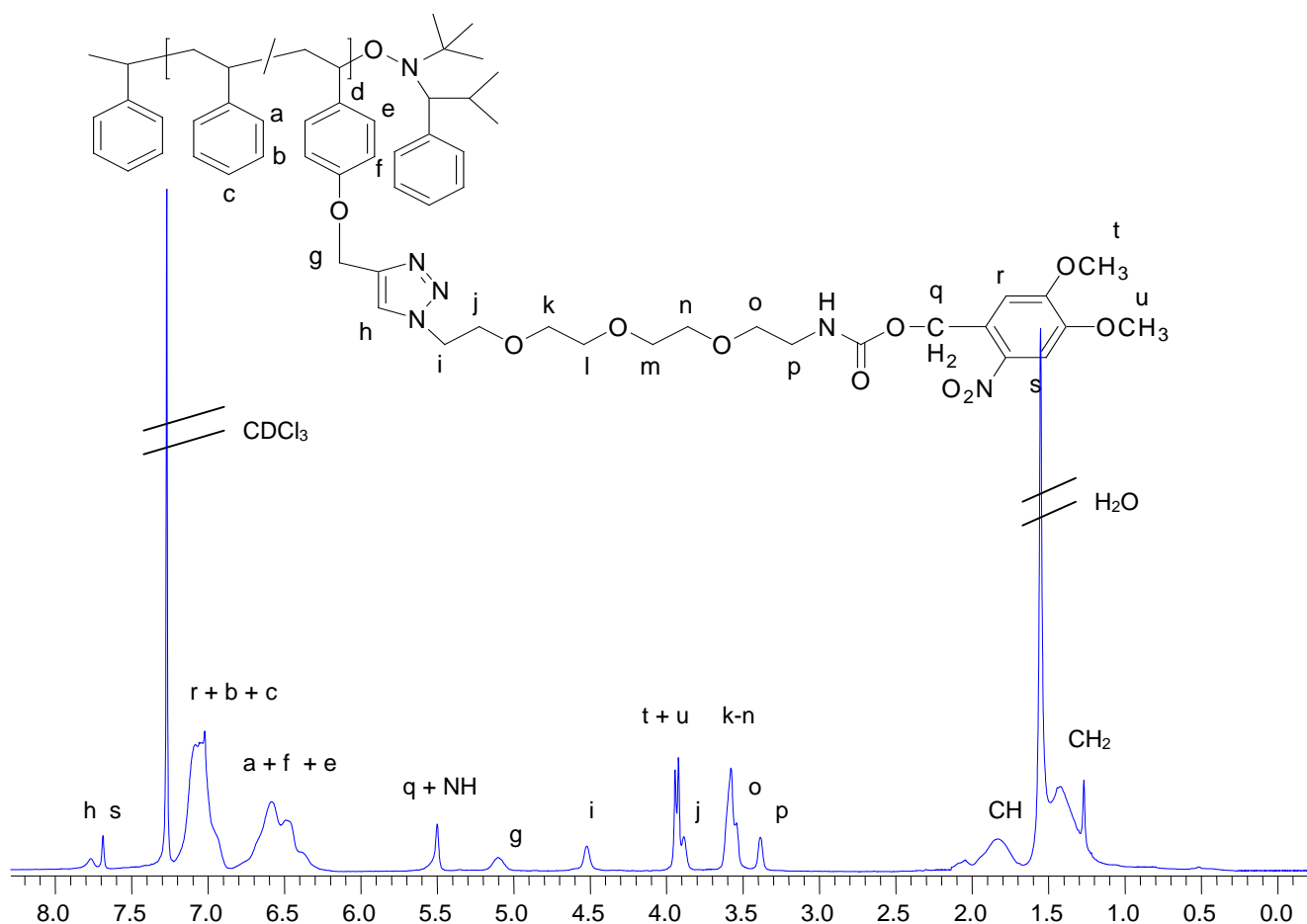
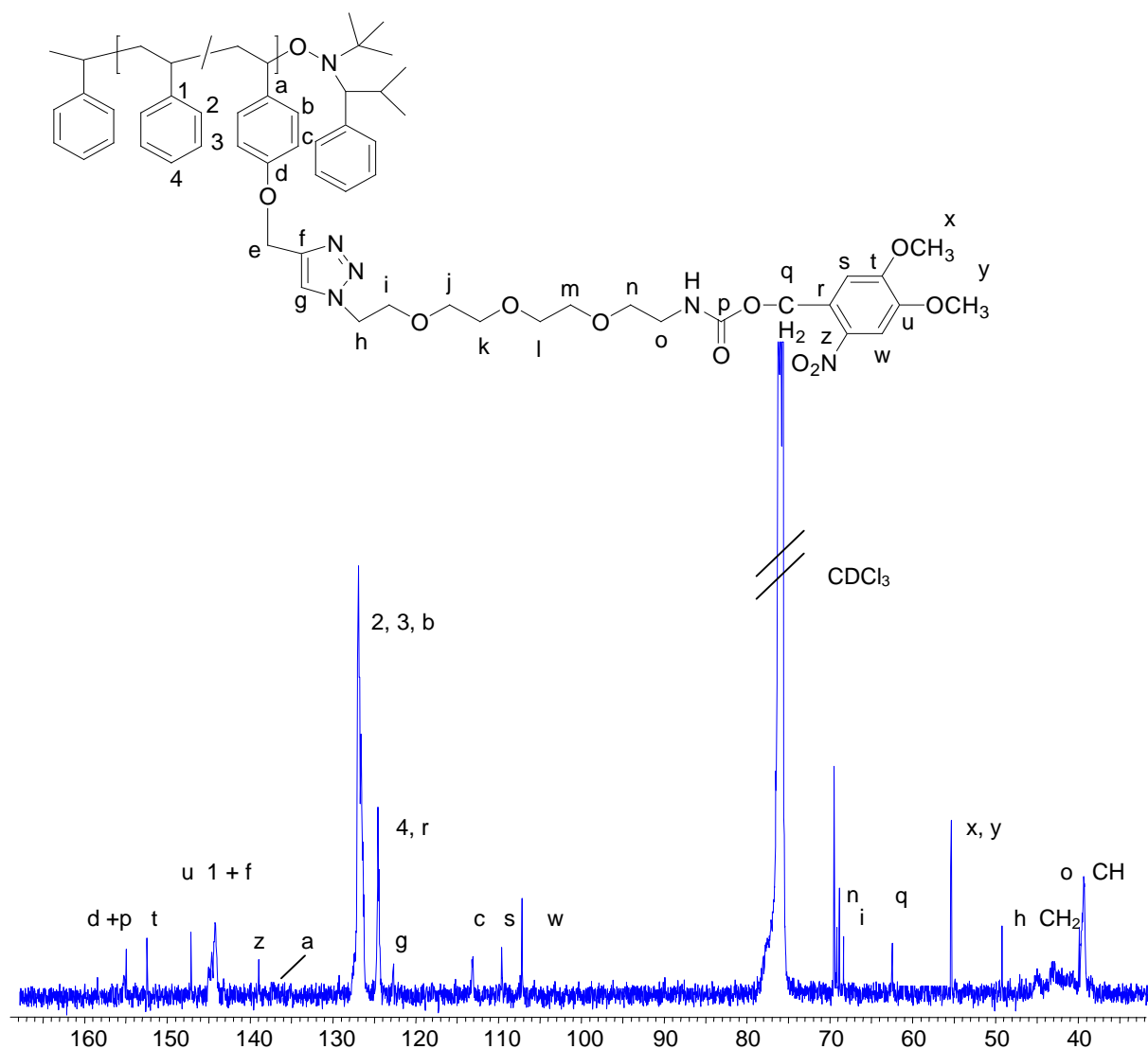


Figure 4-17.  $^1\text{H}$  NMR spectra of the copolymer **(3-d)**.

Finally, in  $^{13}\text{C}$  NMR spectra of polymer **(3-d)** (Figure 4-18) the absence of peaks at  $\delta_1 = 55.9$ ,  $\delta_2 = 79.0$ , and  $\delta_3 = 75.2$  ppm corresponding to the propargyl group is observed, versus the appearance of peaks designed as e, f, g assigned to the modified polymer as specific of the triazol ring and adjacent  $-\text{CH}_2-$  group. Similarly, also the  $^1\text{H}$  NMR spectrum proves the structure of polymer **(3-d)** (Figure 4-17).



**Figure 4-18.**  $^{13}\text{C}$  NMR of polymer **(3-d)** in  $\text{CDCl}_3$ .

Full characterization of all the obtained polymers by a combination of spectroscopic and chromatographic techniques demonstrated the efficiency of this functionalization strategy. In Table 4-3 the main properties of the copolymers are summarized. At first, it is interesting to observe the influence of the post modification reaction on the molecular weight of the materials. The incorporation of the functional azides into **(3)**

leads to an increase in the molecular weight. In most cases the obtained  $\overline{M}_n$  are in accordance with the predicted  $\overline{M}_n$  calculated for each polymer. Small increases in the polydispersity indices are in general observed, but they remain mostly below 1.3 (PDI value). Polymer **(3-a)** exhibits a higher increase in the polydispersity index (up to 1.44) with bimodal distribution (Figure 4-18), and surprisingly the obtained molar mass is higher than it was expected. It is possible that the complexation affinity of the Cu(I)-catalyst Cu(PPh<sub>3</sub>)Br to the disulfide is promoting the formation of small amount of polymeric complexes providing higher increase of the polydispersity in the modified material, as well as  $\overline{M}_n$  higher than expected, due to a small amount of chain combination. Polymers **(3-c)** and **(3-d)** exhibit polydispersity indexes of 1.32 and 1.39 and the difference of  $\overline{M}_n$  between expected and obtained molar masses is slightly higher. Glaser analogous coupling reactions could be a reason for this small increases in the polydispersity [Boc06]. In Figure 4 several representative GPC curves of the copolymers are shown in which the mentioned effects can be observed.

**Table 4-4.** Characteristics of the polymer obtained through polymer analogous reaction.

Polymer	Calculated $\overline{M}_n$ (g/mol)	Conversion* (%)	$\overline{M}_n$ (g/mol)	PDI	T <sub>g</sub> (°C)	T <sub>1%loss</sub> (°C)	T <sub>10%loss</sub> (°C)
<b>(1)</b>	27,100	90	26,400	1.17	105	256	355
<b>(2)</b>	26,000	95	27,900	1.20	110	206	362
<b>(3)</b>	27,000	95	27,000	1.21	99	231	396
<b>(3-a)</b>	35,500	95	37,800	1.44	72	215	342
<b>(3-b)</b>	35,000	78	34,000	1.24	92	213	344
<b>(3-c)</b>	37,400	75	31,800	1.32	75	155	287
<b>(3-d)</b>	38,200	95	27,600	1.39	77	83	267
<b>(3-e)</b>	35,300	85	30,200	1.25	110	210	280
<b>(3-f)</b>	32,100	94	30,700	1.23	131	196	305

<b>(3-g)</b>	31,300	95	29,600	1.29	78	152	266
<b>(3-h)</b>	32,300	95	28,300	1.23	107	313	368

\* Calculated according to  $^1\text{H}$  NMR integration. According to the accuracy of the NMR technique, conversions higher than 95% can not be confirmed.

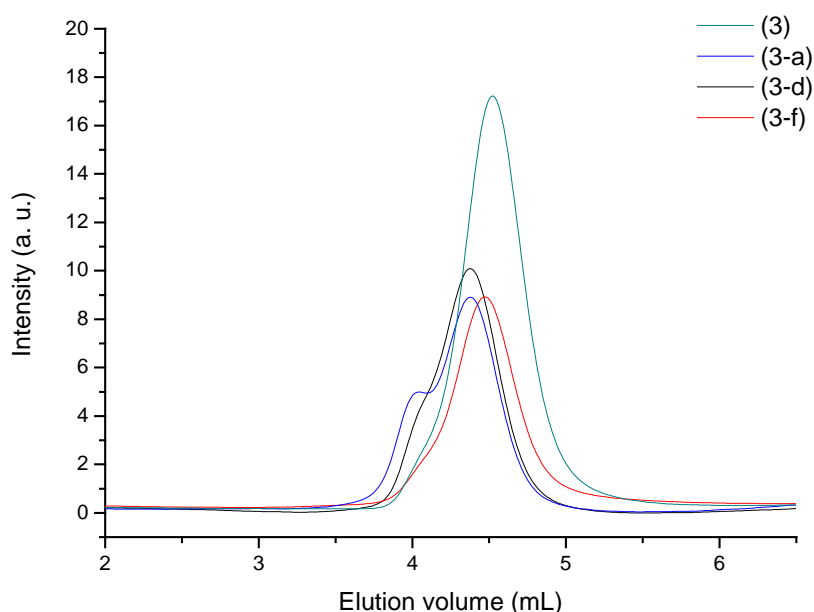


**Figure 4-19.** GPC traces of some of the obtained polymers **(3)** in  $\text{CHCl}_3$ .

Thermal properties of the materials were studied by DSC and TGA. All the materials exhibit a glassy amorphous behaviour. Polymer **(1)** displays a glass transition of 105 °C which increased up to 110 °C after the hydrolysis of the acetyl group. Interactions among OH groups are probably the reason for this increase. These interactions are again eliminated with the incorporation of the propargyl group which as expected provided a glass transition (99 °C) slightly lower than **(1)**.

For the modified materials a general decrease in the glass transition was observed. Polymers **(3-a)**, **(3-d)**, **(3-c)** and **(3-g)** exhibited glass transitions around 75-78 °C. Polymer **(3-b)** exhibits a glass transition of 92 °C. In comparison with polymer **(3-d)** this increase can be explained by the shortening of the alkyloxy chain. For polymer **(3-g)** a glass transition of 107 °C was obtained. Polar interactions between amine groups can be responsible for this rather high Tg, that becomes even higher for polymer **(3-e)**, up to 110 °C, as a consequence of the aromatic ring introduced. The

highest glass temperature is observed in the case of copolymer **(3-f)**, with 131 °C, due to the presence of the bulky <sup>t</sup>BOC group.

On average  $T_{10\% \text{ loss}} > 340$  °C were founded for most of the polymers. Exceptions are **(3-f)** with  $T_{10\% \text{ loss}} = 305$  °C, and polymers **(3-d)**, **(3-e)**, **(3-c)** and **(3-g)** with  $T_{10\% \text{ loss}}$  between 260-280 °C due to the labile protecting groups.  $T_{1\% \text{ loss}}$  is in general higher than 150 °C, with the exception of polymer **(3-d)** in which the small weight loss at 83 °C could be due to the presence of traces of solvents. In general we can say that the thermal stability of the obtained materials is adequate for the use in thin functional films.

### 4.3 THIN FILM PREPARATION AND PATTERNING

#### 4.3.1 Film preparation

The gold surface anchoring capability of the chosen anchor group based on lipoic acid was proven by SAM studies. Surface modification by using  $\omega$ -functionalized self-assembled monolayers (SAMs) on gold or other noble metals is a simple way to create flat, chemically-, or biologically-functionalized surfaces. Alkyl-thiol derivatives are often used for the preparation of carboxyl terminated SAMs. However lipoic acid has distinct advantages for surface modification. The disulfide-containing base gives added stability, and yields two gold-sulfur bonds per molecule in surface-attached species.

This anchoring group adsorbed well on gold and formed films with thickness approx. 1 nm (this was determined with ellipsometrie) and with XPS the film formation was confirmed. X-ray photoelectron spectroscopy (XPS) gives the opportunity to establish the atomic composition and to study the chemisorptive properties of organosulfur species on gold surface, in the studied case of disulfide and dithiols units (Figure 4-20). The grafting of these molecules onto the gold surface by both atoms depends on their structure and involves the cleavage of the S-S bond providing two monothiolated fragments which do not adsorb adjacent to each other (Figure 4-20).

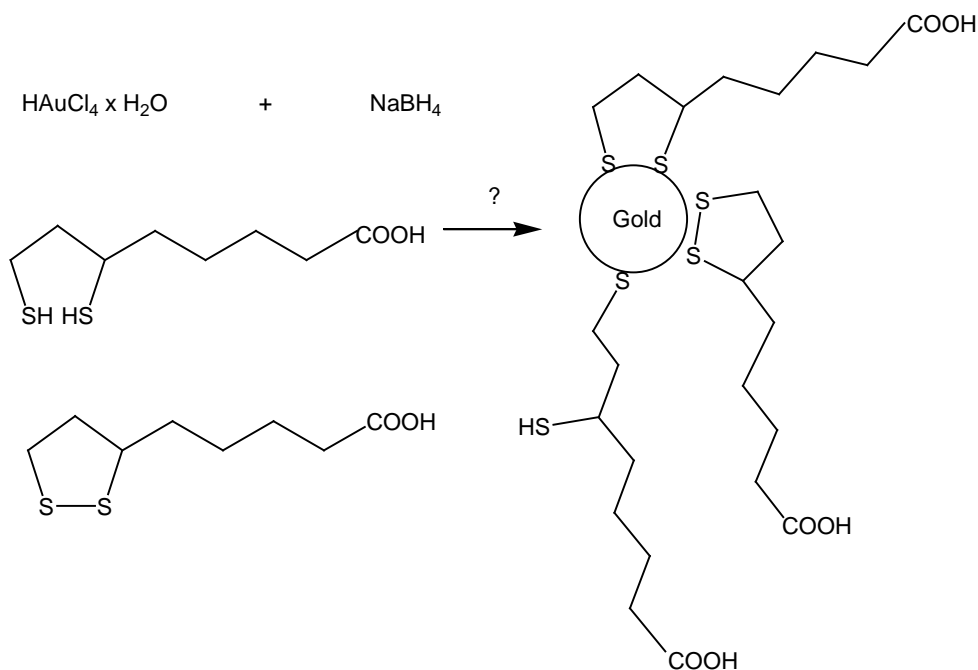


**Figure 4-20.** *The grafting of LA or DHLA molecules on gold surface.*

The spiroalkanedithiols (DHLA) and the endocyclic disulfides (LA), thanks to their peculiar structure, generate chelating monolayers which are more robust than those derived from alkanethiols of similar chain length because both sulphur ends probably attach to gold.

In Figure 4-21 Schematically the preparation of thin patterned monolayers is shown. In the first step the surface of a PDMS (polydimethylsiloxane) is treated with a chemical compound necessary for local surface modification, in the following called ink. For chemisorption on a surface, the ink molecules are terminated with the anchor group (Figure 4-20) which are the disulfide units from lipoic acid.



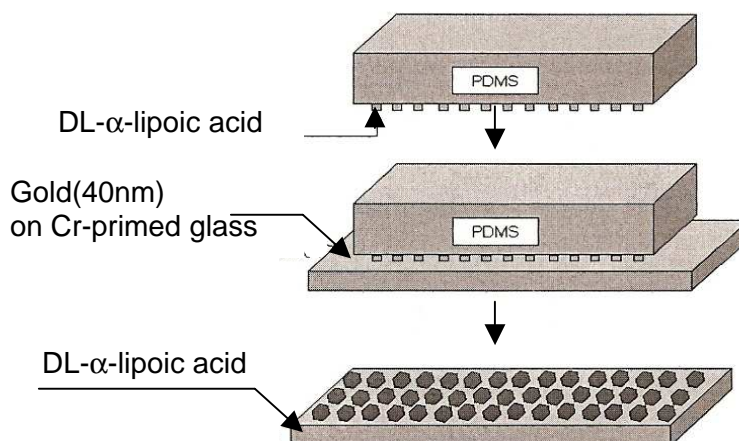


**Figure 4-21.** Schematic representation of the preparation of thin patterned monolayers by microprinting.

Using this method we have been able to pattern gold surfaces with DL- $\alpha$ -lipoic acid. By the microprinting process the molecules were transferred by interaction of the disulfide groups with gold atoms. As substrate gold layers of 40 nm thickness were prepared by thermal evaporation of gold with an evaporation rate of 0.03 nm/s onto glass substrate which were precoated with a 2 nm Cr layer as adhesive interface. The glass substrates were cleaned according to standard procedures before the Cr and the gold was deposited. The stamps were wetted with a few drops of a  $10^{-3}$  mol/l ethanol solution of DL- $\alpha$ -lipoic acid (Fluka). Excess solvent was removed with nitrogen gas. For micro-printing the impregnated stamp was contacted with gold surfaces for about 2 min. PDMS stamps and structured polymer films were investigated by scanning electron microscopy (LEO Gemini DSM 982) at low voltages (0.3 KeV-1 KeV) because of the low penetration depth of the electrons. Under these conditions charging of the uncoated samples was avoided. The control of the condensation process of micro-droplets on the patterned surface is an important step before film formation. The droplets act as substitutes for the holes during film formation. Shape, periodicity and coalescence of the droplets determine the corresponding hole structure in the film. Successive states of condensation on hexagonal modified surfaces are shown in Figure 4-22 a-b and this means that a bonding of DL- $\alpha$ -lipoic acid to the gold surface was achieved.

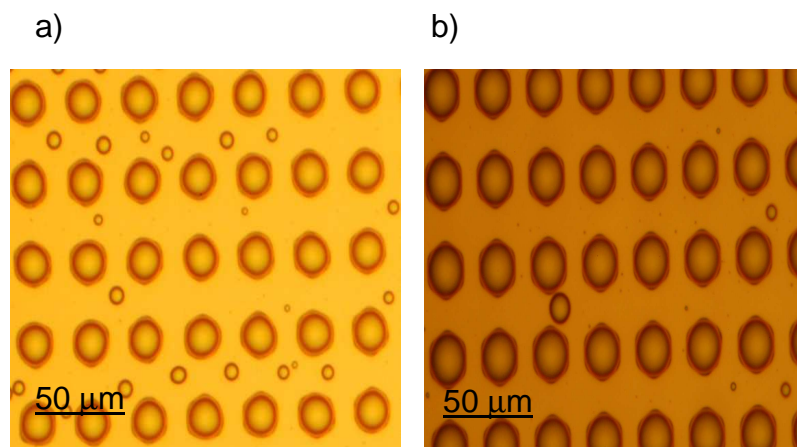


**Figure 4-22.** Formation, growth and coalescence of *DL-α-lipoic acid (LA)* droplets (transferred via soft lithography) on gold coated surface.

Also, the XP Spectrum of LA of S 2p (Figure 4-23) shows the presence of three chemically different sulphur species. Each of the three species shows according to the spin road coupling for 2p orbital a fragmentation in S 2p<sub>3/2</sub> and S 2p<sub>1/2</sub> Peak. The energy distance of  $\Delta BE = |BE(S\ 2p_{3/2}) - BE(S\ 2p_{1/2})| = 1.18\ eV$  agrees with the corresponding literature values [Bea92]. The intensity relations  $I(S\ 2p_{3/2}):I(S\ 2p_{1/2}) = 2:1$  correspond to the expected intensity distribution. On account of the position of the components peak maxima the following bonding states could be assigned the sulphur species:

- 1) the component peaks A:  $R-\underline{S}\cdots\{Au\}_x$  or  $R-\underline{S}H$
- 2) the component peaks B:  $R-\underline{S}-\underline{S}-R$  or  $R-\underline{S}-\underline{S}-R$   
 $\vdots$   
 $\{Au\}_x$
- 3) the component peaks C:  $-\underline{S}O_3^-$  or  $\underline{S}O_4^{2-}$

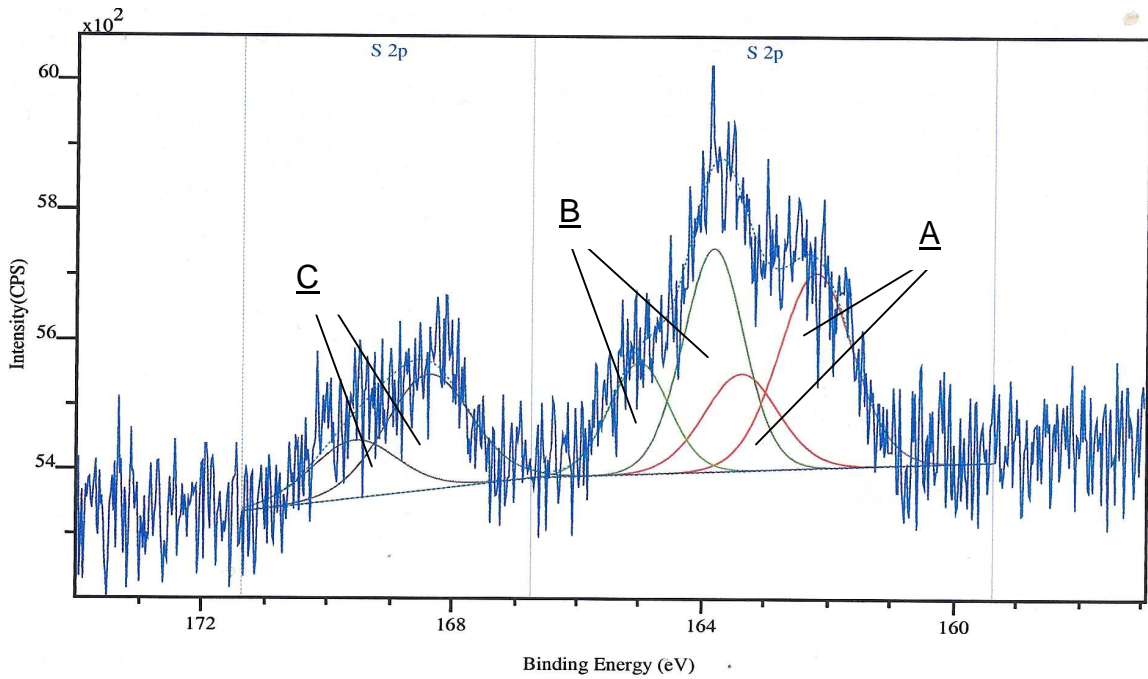


**Figure 4-23.** XPS-S 2p spectrum of 1 mM DL- $\alpha$ -lipoic acid adsorbed on gold.

In the overview spectra can prove the other elements of the lipoic acid monomer, like: carbon, oxygen as well as sodium traces and gold were observed (Figure 4-24).

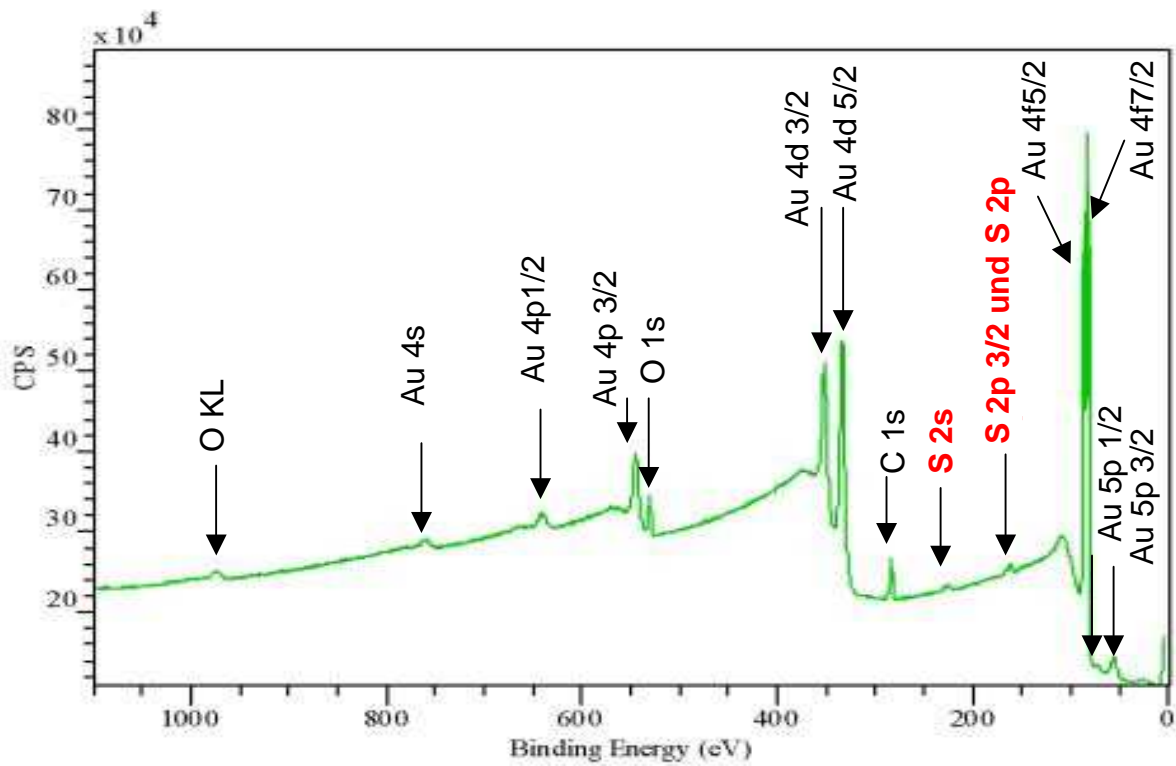


**Figure 4-24.** XPS- Overview spectrum of 1mM DL- $\alpha$ -Lipoic acid adsorbed on gold.

The XPS studies showed that the surface composition of the monomer film largely correlates with the stoichiometry of the applied monomer.

In the next step the terpolymer were prepared as thin films on gold coated glass substrates. The polymer was deposited from diluted DMSO or THF solution by means of spincoating or dipcoating on the gold contacts of the size 24 mm x 24 mm. The annealed and unannealed coated substrates were washed by sonication in THF and Millipore water for 5 min, and dried again at 50 °C under vacuum. After the cleaning the layers were stable and showed a constant layer thickness. Thin layers were formed from the aminopolymers LA/MMA/NVOC and LM/MMA/NVOC.

The film preparation of the polymers was optimized by varying the physical parameter of the spincoating process (Rotation speed, between 2000-5000 rpm) and by varying the concentration of the polymer solution. In principle the polymers having different concentration form reasonable films once the condition for spin-coating had been optimized. The solution was dropped on the rotating substrate. Highly concentrated solutions (5 wt.-%) lead to rejections in the layer, above all, the edge areas were not homogeneous. In addition, bigger particle were often enclosed. Best result were obtained using a 2 wt.-% solution in THF and rotation speed of 4000 rpm. The covalent bond to the substrate is strong enough to allow the treatment of the polymer films with water or organic solvent. This is important for subsequent chemical modification. Washing of the films directly after preparation with THF allows any residues of unattached polymer to be removed. The produced layers, after the washing step, are very homogeneous and smooth in surface topography as shown in the AFM image in Figure 4-25. Consecutively, the films were annealed for 2h at 120 °C under high vacuum. Unattached polymer was removed by sonication in Milipore-wafer for 15 min at room temperature and dried for 2h at 50°C under ambient conditions.

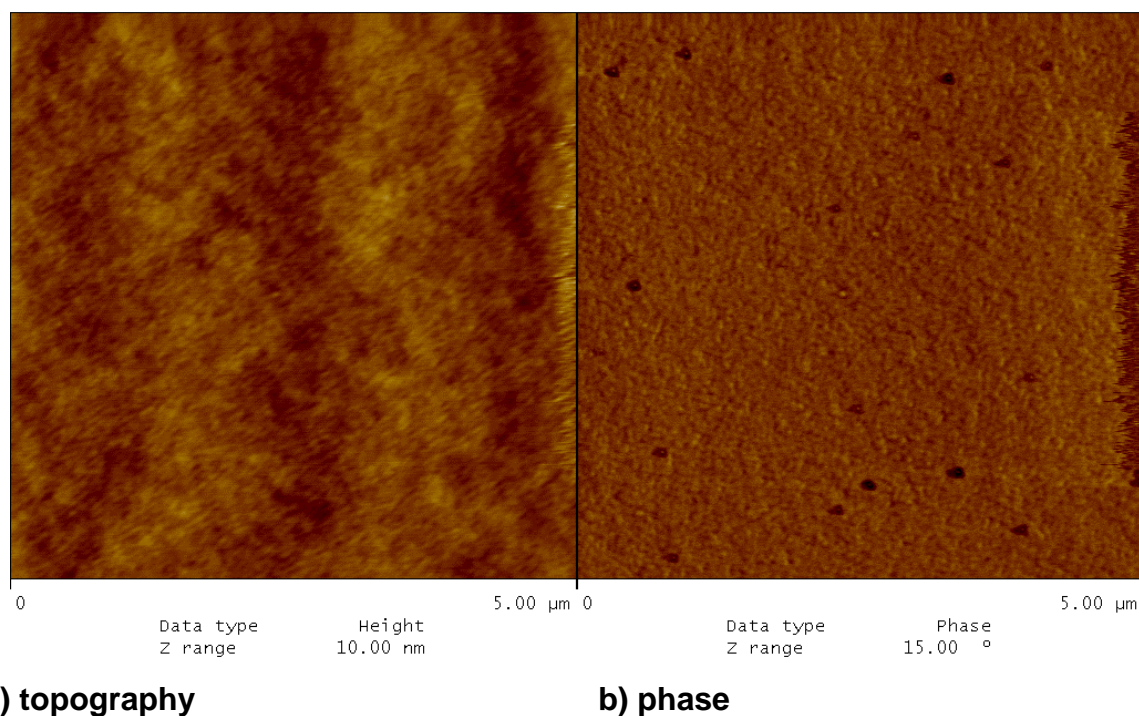


**Figure 4-25.** AFM picture (topography and phase) of spin-coated annealed LA/MMA/NVOC terpolymer.

Figure 4-25 shows the height and phase image of the annealed aminoterpolymer (LA/MMA/NVOC) with a very low roughness of  $\sim 0,3 - 0,4$  nm (rms). For unannealed samples the roughness was between  $\sim 1 - 3$  nm measured over a  $5 \times 5 \mu\text{m}^2$  area (Figure 4-26). In both cases a homogeneous structure was observed. Some defects are caused by the preparation procedure. The film thickness was determined before and after the annealing process by ellipsometry. The film thickness of unannealed layers was decreased from 25 - 30 nm to 8 - 12 nm in annealed layers. Otherwise variations in film thickness result not only from difference in the amount of polymer that was initially dropped onto the substrate but also from solvent, concentration of solution and used technique.

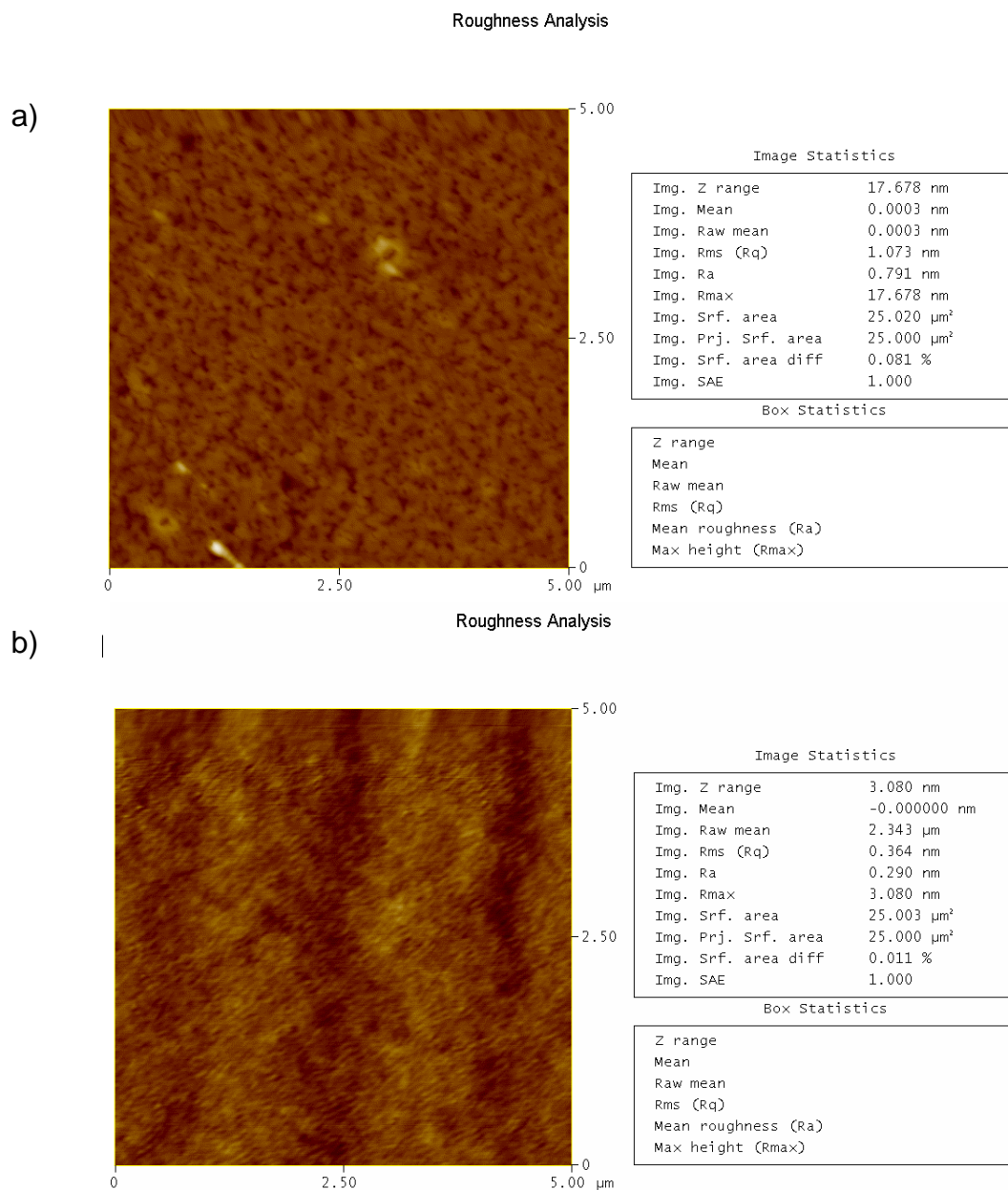


**Figure 4-26.** Roughness as analysed by AFM (topography) of unannealed (a) and annealed (b) amine polymer film (LA/MMA/NVOC).

The layer thickness for the amino terpolymer depends also on the rotating speed and was examined with ellipsometry measurements using a 2 wt.-% solution THF for generating the layers. The results are shown in Table 4-5.

**Table 4-5.** *The influence of the rotating speed on the layer thickness of the amino polymer(LA/MMA/NVOC) layers produced by spin-coating of the 2 wt.-% in THF.*

Rotating speed of the substrate in rpm	Layer thickness in nm (certainty about ellipsometry)
2000	35-40
3000	15-25
4000	8-12
5000	7-10

This study showed that the chosen anchor group based on lipoic acid is very well suited to prepare stable SAM but also to anchor successfully thin films of our multifunctional polymers.

#### 4.3.2 Patterned thin films

The final goal of this work was to show the possibility to prepare selectively patterned amino functional surfaces e. g. to attach nano-sized objects, e.g. DNA strands or end-functionalized nanotubes. Photolabile terpolymers have been designed to be used for the preparation of thin organic films covalently attached to gold substrates. For this, terpolymers containing photolabile as well as anchoring units have been synthesized via free radical polymerisation. Thin films from these terpolymers were now structured by UV- light irradiation in order to create defined functional areas at the template surface ready for further modification and attachment of nanostructures. By irradiation with UV light between 320-400 nm the NVOC protecting group is decomposed and the free reactive amino group is regenerated and prepared for further modification steps (Figure 4-27), in this case to connection with DNA-units.

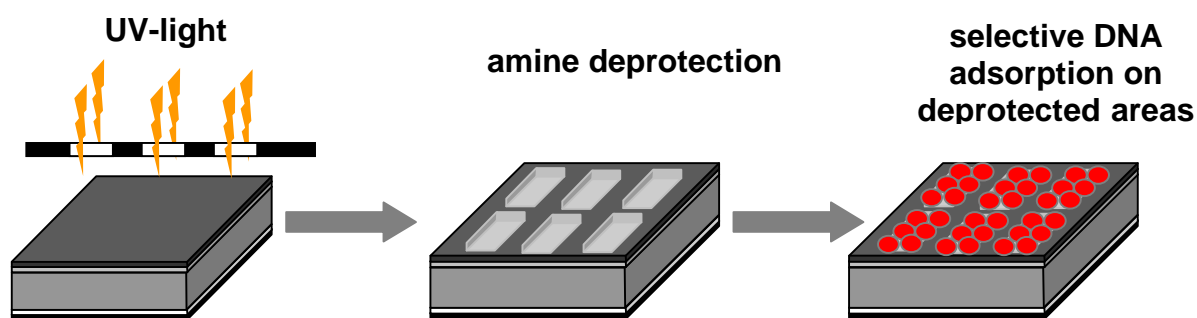


**Figure 4-27.** Schematic representation of the selective DNA adsorption on the deprotected amino areas.

#### 4.3.2.1 Labelling of patterned films with fluorescent marker YOYO-1

For this it was necessary to prove that before UV irradiation no reactive amino groups are present on the film surface or within the polymer film structure whereas on imaged areas sufficient and reactive amino groups are created for further modification steps. Therefore the presence of free amino groups was verified by treatment of the polymer film with a fluorescence marker which reacts quite selectively with amino functions. For the selective labelling of free amino groups within irradiated film parts the fluorescence marker YOYO-1 (1mM solution in DMSO) was used on gold contacts on glass substrates as shown in Figure 4-28.

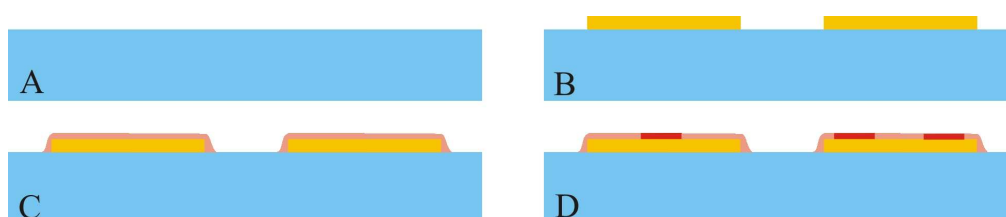


**Figure 4-28.** Schematic view of the selective deprotection of a thin amino terpolymer by UV irradiation through an optical mask. A – glass substrate; B - Carrier structure with gold contact structures; C – deposition of amino terpolymer on gold contact structures; D – selective deprotection of polymer by UV irradiation through an optical mask.



Pursuing this goal thin film of the terpolymer LA/MMA/NVOC were prepared as described in experimental part of this work and irradiated with a Hg-Xe lamp (Oriol 6000) in the presence of a mask (TEM grid 400 lines/inch). Afterwards, the samples were treated with 100 mL of a YOYO-1 solution.

YOYO-1 is high-affinity cyanine dyes for the visualisation of the dynamics of single DNA molecules through a fluorescence microscope. In particular, YOYO-1 (1,1'-(4,4,7,7 - tetramethyl - 4,7 - diazaundecamethylene) - bis - 4 - [3 - methyl - 2,3 - dihydro - (benzo-1,3-oxazde) - 2- methylidene] - quindinium tetraiodide) which are largely non-fluorescent in aqueous solution form a very stable, highly fluorescent complex with double stranded DNA undergoing about 500-fold fluorescence enhancement upon binding and improving dramatically the quality of the images [Gic05,Kap95].

Several of these fluorescence dyes like ethidium bromide, acridine orange or fluorescein isothiocyanate (FITC) [Bra03] were tested for DNA imaging application. In spite of that FITC reacts quite selectively with amino functions as already shown by Fodor et al. [Fod91].

YOYO-1 is positively charged dye suitable for the interaction of deprotected,  $\text{NH}_2$  containing areas and the shortest wavelength member of a series of oxazole yellow dimers. When YOYO-1 is bound to double-stranded DNA it is spectrally similar to fluorescein with excitation at 491 and emission at 509 nm. Its chemical structure is shown in Figure 4-29.

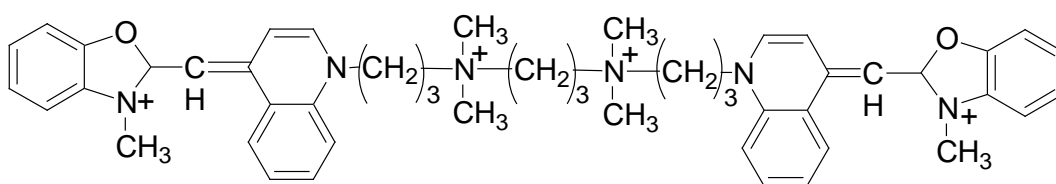


**Figure 4-29.** Chemical structure of the fluorescent marker YOYO-1.

Due to the presence of four positive charges in the molecule (Figure4-31), YOYO-1 is characterised by a very high electrostatic binding affinity for DNA ( $6 \times 10^8$ ), about 3-4 orders of magnitude higher than for example ethidium bromide or acridine orange. Also, compared with ethidium bromide, YOYO-1 bound to double stranded DNA has a 20-fold higher increase in fluorescence upon binding to DNA [Gur97], [Sin94].

Finally, YOYO-1 has 30-fold higher extinction coefficient and a 3-fold higher fluorescence quantum yield than ethidium bromide.

Moreover, the high affinity of YOYO-1 toward DNA made it possible to use very low DNA and dye concentration (DNA =  $5 \times 10^{-9}$  mol of bp/liter, YOYO-1 =  $1 \times 10^{-9}$  M), resulting in the presence of a few bright molecules in the field of view of microscope, increasing the contrast and avoiding confusion between molecules.

In Figure 4-29 the image observed by fluorescent microscopy of the mentioned terpolymers after 1 min of selective irradiation through a TMS 400 grid and post exposition to the mentioned YOYO-1 solution is shown. The 1 min of irradiation is enough that amino groups are available for reaction with the fluorescent marker molecule and a good patterning of the films following the outline of the mask grid is achieved. The attachment of the fluorescent dye to the irradiation locations at the surface is clearly visible and accurate.

On the picture 4-30 we can observe a field of gold structures  $52 \times 52 \mu\text{m}^2$  with an interdistance of  $12 \mu\text{m}$ . The amine polymer was exposed to UV light by a mask with the same geometry, however, the alignment was twisted and shifted with regard to the gold structures. The fluorescence image shows that the protected polymer (A) on the ground of unspecific interaction by YOYO-1 to the polymer appear bright, whereas the unprotected parts of the polymer (B) are darker, because here, on due to the positive charged surface the unspecific interaction with YOYO-1 (positively charged) is strongly reduced. In the areas (C) between the golden contacts is no polymer (pure substrate surface on which no gold is). Consequently these areas seem black, because there is no interaction between YOYO and the polymer film.

We assume that this selective staining effect is caused by a repulsion of the YOYO dyes from the irradiated, charged amino terpolymer areas.

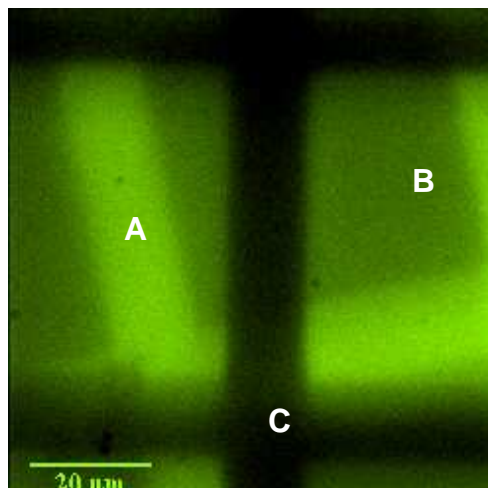


**Figure 4-30.** *Fluorescence microscopy image of a patterned amino polymer film, labelled with a very diluted YOYO-1 solution.*

The quality of fluorescence images of individual DNA molecules is mostly controlled by those factors that determine the fluorescence intensity of DNA molecules as well as the fluorescence of the surrounding background. The binding affinity of the dye for the DNA and the enhancement in the dye fluorescence upon binding to DNA are the critical factors determining the contrast, i. e., the intensity of the signal over the background. Instead, the extinction coefficient and the fluorescence quantum yield are the critical factors determining the overall brightness of a fluorescently labelled DNA molecules.

Salmon sperms-DNA (Sigma) and Lambda Phagen DNA (New England Biolabs GmbH) were used in order to proof the possibility of the specific binding of biomolecules on our terpolymer films. The length of the salmon sperms-DNA amounts between 500 and 5000 base pairs (bp). DNAs with an average molecule length of about 2000 base bp, corresponding to about 600 nm, were used in the decoration experiments.

#### 4.3.2.2 Site-specific binding of $\lambda$ -DNA

It could be shown that a highly site-specific binding of biomolecules to locally unprotected golden contacts is possible. For this the 2  $\mu\text{g/ml}$  solution from salmon sperms-DNA was incubated for 60s on the structured layers. To proof this, the

dependence of the binding on the pH value of the buffer was studied varying it between 7.5 and 8.8. In this pH area the DNA binds specifically to the unprotected areas (Figure 4-31a). It results a direct image of the mask on the golden structures, because the fluorescence signal of the specifically coloured DNA excels far the unspecific colour the protected DNA. The potential of the structural width is limited at the moment by the lithography used to about hundred nanometers like expected.

#### 4.3.2.3 End-specific binding of $\lambda$ -DNA

Because through the pH of the buffer the protonation of the amino groups on the surface can be controlled. It is also possible that the site-specific binding can be determined by the control of the process parameters of the specific binding behaviour of DNA and another biomolecules.

This was shown in the model system of  $\lambda$ -DNA. For a 100 mM Tris - HCl - buffer in the pH area 7.0 - 7.5 the DNA anchors in the unprotected areas through the whole length (Figure 4-31). For pH 8.0 - 8.5 the molecules bind primarily by the end caps. With it the rest of the molecule stands by disposal for an additional manipulation. This was shown by stretching of the molecule to the contour length with the help of a receding meniscus [Ben94, Hau02]. For our experiments about 48502 bp (48 kbp) long  $\lambda$ -DNA with a length of about 16.1  $\mu\text{m}$  is used. In this connection the wafers were immersed into 3.3  $\mu\text{g/ml}$  DNA-solution. After the incubation time of 10 s they were removed very slowly (a speed of approx. 10 mm/s) from the solution. The applied forces lie between 10 and more than 400pN [Opt04]. The binding forces between molecule and surface are bigger, therefore an end of the DNA remains linked with the surface and the rest of the molecule can be stretched in the meniscus. The  $\lambda$ -DNA has therefore the possibility to anchor through the tip of the molecule in the unprotected areas (Figure 4-31 b). A relatively concentrated solution of  $\lambda$ -DNA was used. Thus, no individual molecules can be visualized in the pictures 4-31, rather a continues fluorescence of the DNA modified in protected areas can be seen.

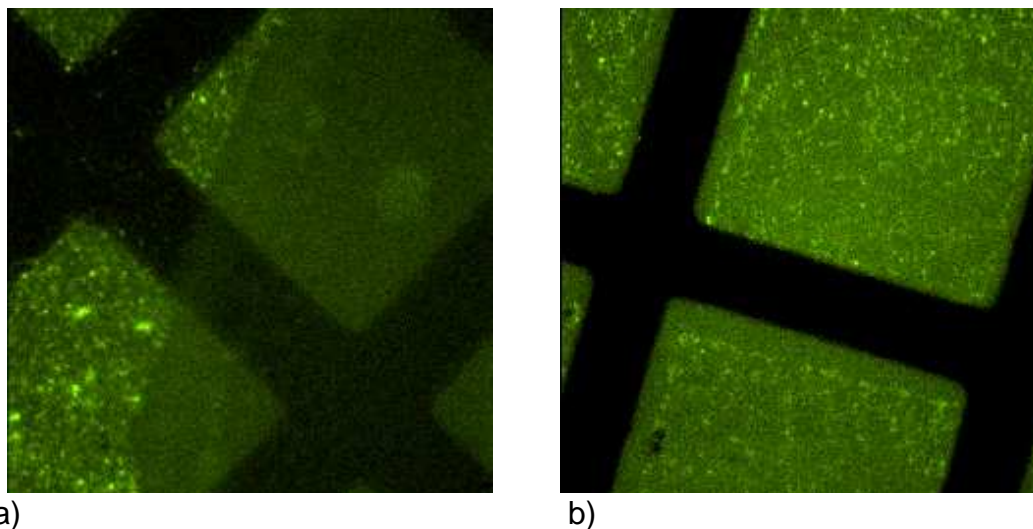


**Figure 4 - 31.** *Imagewise structuring by UV light using a TEM grid as a mask (squares: 51  $\mu\text{m}$ , grids: 11  $\mu\text{m}$ ); Fluorescence-microscopic image to the binding of salmon sperms-DNA. Left area of the sample: In the unprotected areas binds the DNA. Right area of the sample: This area was covered with the exposure. It is protected, consequently binds there no DNA (Figure 4-31a). Binding of lambda-DNA in completely unprotected golden contacts by means of UV irradiation (Figure 4-31b).*

A site-specific deposition of charged nanoparticles and biomolecules based on optical exposure of thin spin-coated aminoterpolymer film is one of the methods to fabricate a functional surface. The binding of DNA onto patterned aminoterpolymer film and these investigations allowed us to answer the question of whether deprotected amino groups are exposed to the surface upon UV-irradiation to obtain a strong binding with DNA. This highly site-specific binding of DNA to the patterned aminoterpolymer layer showed in general that patterned aminofilms are well suited for a site-specific immobilization of negatively charged biomolecules. In this approach the patterning shown not only changes in chemistry but also with regard to changes in surface charge. The surface charge of deprotected aminofilms areas can be tuned to obtain a highly selective, end-specific DNA binding. The obtained binding forces are large enough to allow single molecule manipulation of DNA which is one important prerequisite for biological or bio-physical studies at single molecule level.

## 5 Summary

The main aim of this work was the development of polymeric materials for thin functional films which permit to deposit on different substrates a wide variation of functional elements or metal structures and to achieve a pattern formation using optical grid methods. In order to realize this concept it was necessary to design and develop a polymer system based on suitable photolabile units and in addition having anchoring groups which attach on specific substrates like gold. A covalent attachment of the final polymer film to substrate is essential in order to allow further modification and use of the films in fluidic media. A polymer approach has the advantage that the different units can be incorporated by co- or terpolymerization and in addition, stable functional polymer thin films may be prepared by an easy spin-coating step.

In this work, two approaches were chosen to realize thin functional films, grouped into the two classes of polymers which have been prepared by free radical polymerisation (FRP) or by combining of nitroxide mediated radical polymerization (NMRP) and click chemistry. In the first concept the pendent photolabile protected amino functions are incorporated directly into the polymer structure and can be activated or deactivated by UV irradiation. By imaging the film, the protecting groups are removed and the free amine groups can be used to attach functional nanoelements like DNA strands. In the second concept, the synthesized precursor polymer (3) is transformed by further cascade reactions in order to prepare side-functionalized copolymers. In this concept a novel extension of click chemistry for the preparation of structural near-perfect multifunctional polymers with great potential for use as thin films with great potential in lithographic functional patterning and nanotechnology was demonstrated.

### *Amino terpolymers through copolymerization*

The organic films which are aimed for should contain the following functional units:

- 1) Adhesive groups like thiol or disulfide for covalent anchoring on gold contacts.

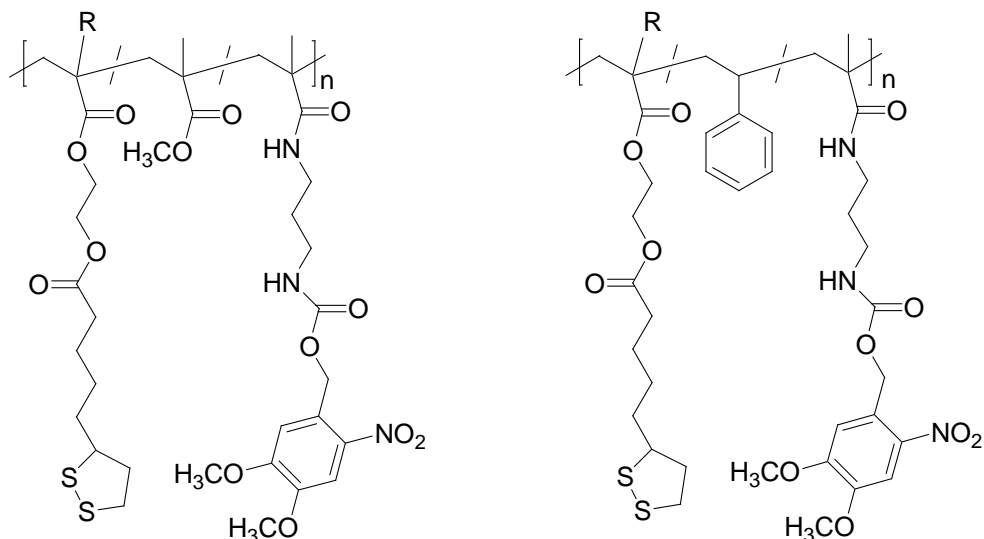
- 2) Amino group, photolabile protected e.g. by NVOC for photolithographic patterning.
- 3) MMA or Styrol as a spacer for the improvement of the quality of the films.

Corresponding materials were appropriately designed in the first approach through copolymerization using up to three acrylate/methacrylate components. The anchoring capacity for gold surfaces is provided by the lipoic acid derivative monomer, {1,2-dithiolane-3-pentanoic acid-2-[(2-methyl-1-oxo-2-propenyl)oxy]ethyl ester} and {1,2-dithiolane-3-pentanoic acid-2-[1-oxo-2-propenyl]oxy]ethyl ester} assigned, respectively, as **LM** and **LA**.

The photolabile capacity is provided by the monomer {N-(N-NVOC-aminopropyl)-methacrylamide}}, simply assigned as **NVOC** (Figure 5-1), developed in our group in previous work [Bra03]. By irradiation with UV light ( $400\text{nm} > \lambda > 320\text{ nm}$ ) the NVOC protecting group is decomposed and the free amino group is regenerated. The presence of the photolabile amino protecting group nitroveratryl in analogous terpolymer film prepared for anchoring onto silicon allowed the creation of patterned areas with free amino groups. Finally a third component, methyl methacrylate (**MMA**) or styrene (**S**), was eventually incorporated in the appropriate proportion ensuring the formation of films with good quality and sufficient mechanical stability. Materials including the three components were synthesized by means of free radical polymerization. For the comparison reason also copolymers containing the monomers **LA** or **LM** and methyl methacrylate or styrene were prepared.

The presence of the nitro group containing monomer results in a reduced polymerization rate. Therefore, 10mol% AIBN had to be used to start the reaction. As expected, relatively low molar mass products were achieved ( $M_w = 3\text{-}8\text{ kg/mol}$ ,  $M_n = 2\text{-}4,5\text{ kg/mol}$ ) but PDI was around 2 and high polymer yields could be obtained.

A terpolymer prepared from a molar monomer feed ratio of 5:75:20 (anchoring monomer, spacer, protected amine) was used in film preparation. Spin coated on gold substrates, the polymers formed thin homogeneous films of about 10 nm thickness and with surface roughness below 1 nm. It was not expected to achieve any ordered film structure and thus, the functional units will be distributed evenly on the surface as well as within the polymer bulk.



LA/MMA/ NVOC 5/75/20, R=H

LM/MMA/ NVOC 5/75/20, R=CH<sub>3</sub>

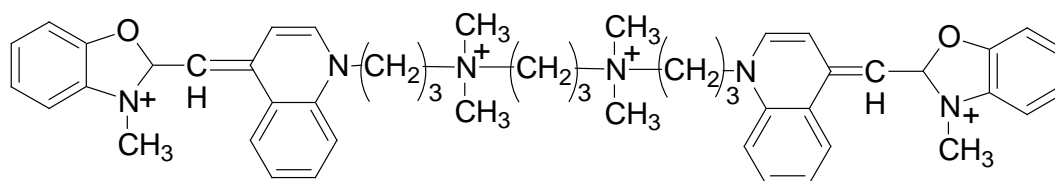
LA/S/ NVOC 5/75/20, R=H

LM/S/ NVOC 5/75/20, R=CH<sub>3</sub>

**Scheme 5-1.** Chemical structure of the synthesized terpolymer.

Removal of the protecting group was achieved by UV irradiation, both in solution and for the thin polymer films. The deprotection in film is as expected slower than in solution and therefore, a longer irradiation time is necessary using a HgXe UV lamp (100 mW/cm<sup>2</sup> at the sample) in order to achieve full deprotection.

The regeneration of the free amino group in the polymer films was proven and visualized by the labeling of the released amino groups within irradiated films parts using the fluorescence marker YOYO-1 (Figure 5-1). Schema 5-2 shows the chemical structure of YOYO-1, a marker which specifically reacts with amines.



**Scheme 5-2.** Chemical structure of the fluorescent marker YOYO.



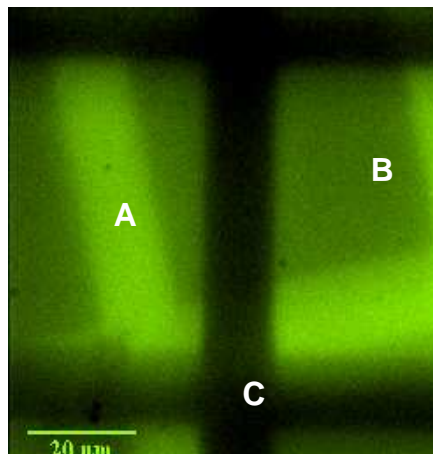


**Figure 5-1.** *Fluorescence microscopy image of a patterned amino polymers film, labelled with a very diluted YOYO-1 solution.*

### *Multifunctional polymers through click reaction*

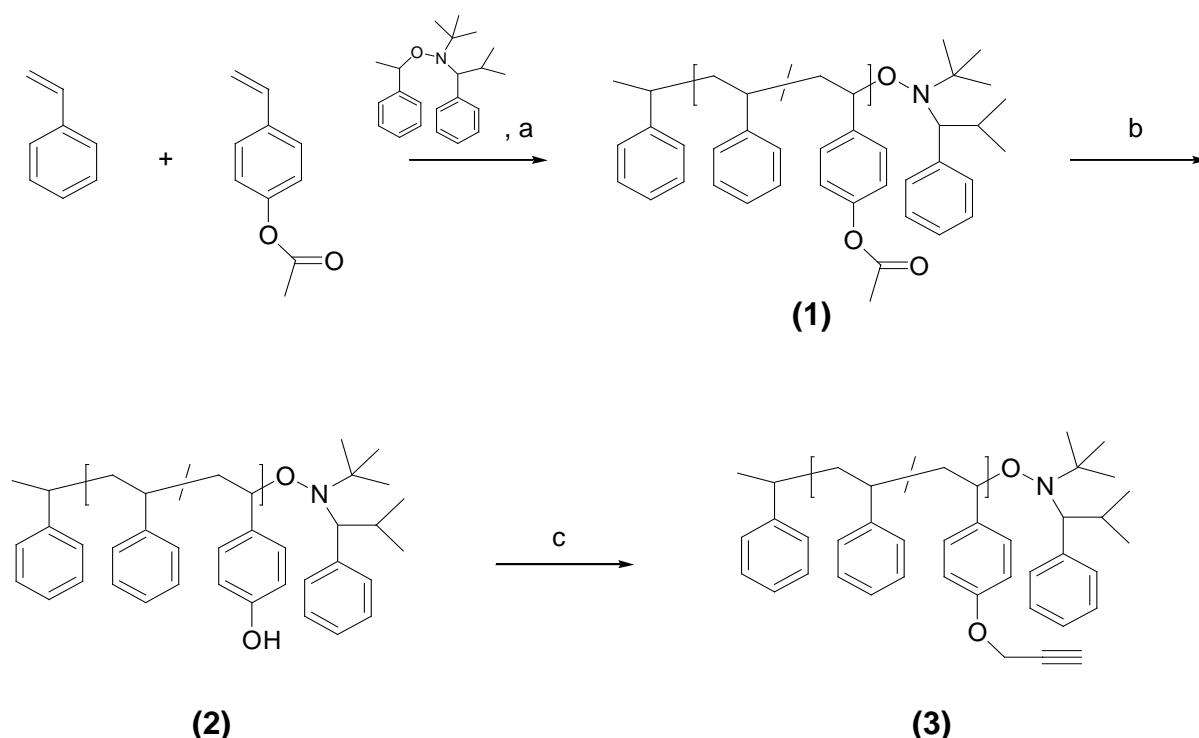
The so far described approach leads to multifunctional polymers through radical copolymerisation. However, there are, as usual, problems especially with termolabile and highly reactive functionalities. To avoid these problems and to improve the present system, a new concept was introduced in the polymerization process like long reaction times and low molar masses of the products based on polymer analogous reactions. A highly efficient polymer-analogous modification allows to introduce the functionalities after the polymer construction reaction. For this the 1,3-dipolar cycloaddition between alkynes and azides was used. The production of suitable prepolymers was carried out with the help of a controlled synthesis methodology "nitroxide mediate radical polymerization" followed by polymer analogous reaction using one of the most efficient click reactions, the Cu(I) catalyzed Huisgen 1,3-dipolar cycloaddition between terminal acetylenes and azides to attach further functionalities through the formation of a stable 1,4-disubstituted 1,2,3-triazol ring (Scheme 5-4) [Hui67].

Click reactions encompass a set of techniques which allow the functionalization or construction of macromolecules in nearly quantitative yields. They are well known for the broad tolerance towards functional groups, have low susceptibility to side reactions, and allow mild reaction conditions and easy work-up of final products. One of the most efficient click reactions is the Cu(I) catalyzed Huisgen 1,3-dipolar

cycloaddition between terminal acetylenes and azides to yield a stable 1,4-disubstituted 1,2,3-triazol ring (Scheme 5-3) [Hui67].

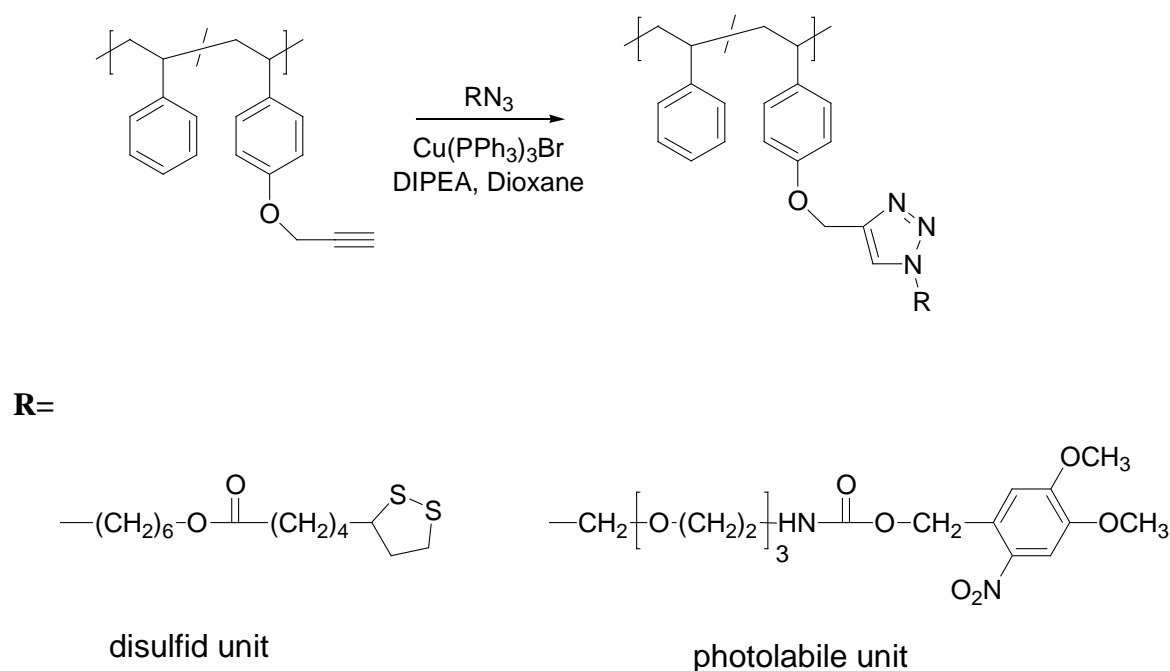
As a starting material the random copolymer poly[styrene-*r*-(4-acetoxystyrene)] was chosen obtained from styrene and 4-acetoxystyrene, monomers which can be easily polymerized by NMRP. The subsequent polymer is transformed by further cascade reactions into an adequate precursor polymer for the performance of click reactions, which was poly(styrene-*r*-4-propargyl-oxystyrene) (Scheme 5-3).

Thus, a series of azides was designed for the incorporation of subunits with specific properties into the materials. Photopatterning was made possible by the introduction of units with a photoremovable amino protecting group (PRG) (nitroveratryloxy-carbonyl, NVOC) which leads to the release of amino functions after selective UV/laser irradiation. Covalent attachment of the functional polymers onto gold is promoted by sulfide containing anchoring units again introduced as pending groups onto the polymer backbone via the 1,3-dipolar cycloaddition reaction (Schema 5-4). The modified materials were obtained in almost quantitative yields under mild conditions according to IR, NMR studies.



**Scheme 5-3.** Synthesis of the copolymer poly(styrene-*r*-4-propargyl-oxystyrene) (3) by NMRP and subsequent polymer analogous reactions: a) NMRP, nitroxide-adduct, acetic anhydride, 120 °C; b)  $\text{NH}_2\text{NH}_2 \cdot \text{H}_2\text{O}$ , dioxane, rt; c) propargyl bromide, DMF, rt.

Until now the synthetically demanding techniques, such as anionic, cationic or group-transfer polymerisation were the only available tools to accurately control structural features such a polydispersity, molecular weight, chain ends and macromolecular architecture. While these techniques are successful, they are limited by their complexity, rigorous synthetic demands, as well as incompatibility with many functional groups/monomers units.



**Scheme 5–4.** Post-modified polymers by click reactions with functional azides.

To overcome these difficulties a polymerisation technique based on “living” free radical polymerisation has been used in this work. It was shown that functional random copolymers suitable for further click chemistry could be successfully prepared by nitroxide mediated radical polymerisation. In NMRP the unimolecular initiator was taken to produce narrow polydispersity polymers with controlled molecular weights, chain ends and chain architectures. The chemical stability of these alkoxyamino initiators under a variety of reaction conditions permitted the introduction and manipulation of numerous functional groups, but this spectrum was further broadened by introducing even sensitive groups through an efficient post-modification reaction using click chemistry of functional azides. This technique allowed to produce

well-defined random copolymer but it could already be shown that also block copolymers can be prepared which give the chance to combine nanostructure formation. in block copolymers with special functionality.

In summary, in this work two different synthetic ways were developed successfully to prepare multifunctional polymers for the preparation of thin polymer films for photopatterning with functional and highly reactive amino groups. The additional incorporation of anchor groups for gold surfaces allows the use of these polymers with amino groups in further modification steps also in liquid media. In a first experiment and as proof of principle it was already shown that DNA strands can be selectively bound with the tip to the irradiated parts of an amino terpolymer film which nicely proved the high potential of these polymers in bionanotechnology. Thus, the special properties of these functional polymers like the capability for photopatterning and anchoring onto gold substrates make them very interesting for nanotechnology applications.

## 6 EXPERIMENTAL PART

### 6.1 MATERIALS AND METHODS

#### 6.1.1 Materials

---

Compound	Purity in %	Source
Acetic anhydride	99	Riedel-deHaen
Acetoxystyrene	96	Aldrich
Acryloylchloride	96	Fluka
N-acryloxysuccinimide	98	Acros Organic
N-(3-Aminopropyl)methacrylamide hydrochloride	98	Polysciences
4-Azidoaniline hydrochloride	97	Aldrich
Azidomethyl phenylsulfide	95	Aldrich
11-Azido-3,6,9-trioxaminedecene-1 amine	90	Fluka
2,2'-Azobis-(isobutyronitrile) (AIBN)	98	Fluka
1,1'-carbonyldiimidazole (CDI)	98	Fluka
6-Chloro-1-hexanol	99	Fluka
18-Crown(6)	99	Fluka
Copper(II)bromid	99	Fluka
1,6-Diaminohexane	99	Fluka
Dichloromethane	98	Fluka
N,N'-Dicyclohexylcarbodiimide (DCC)	99	Fluka
Diethyl ether	99,8	Fluka
Diisopropylcarbodiimide (DIPC)	99	Fluka
N,N-Diisopropylethylamine (DIPEA)	99	Fluka
Dimethylaminopyridine (DMAP)	99	Fluka
4-(Dimethylamino)pyridinium p-toluenesulfonate (DPTS)	99	Fluka
1,4-Dioxane	99,5	Fluka

---

---

Compound	Purity in %	Source
N,N-Dimethylformamide (DMF)	99,9	Fluka
Di-tert-butyl dicarbonate (BOC) <sub>2</sub> O	99,5	Fluka
Dimethyl sulfoxide-d <sub>6</sub> (DMSO-d <sub>6</sub> )	99,9	Fluka
Hydrazine monohydrate	99	Fluka
Hydrochloric acid	99,8	Fluka
1-Hydroxybenzotriazol (HOBT)	98	Acros
2-Hydroxyethyl acrylate	97	Fluka
2-Hydroxyethylmethacrylate	99	Fluka
2-Hydroxysuccinimide	97	Fluka
DL- $\alpha$ -Liponic acid	98	Fluka
Methanol	98	VWR
Methyl methacrylate	99	Fluka
6-Nitroveratryl chloroformate (NVOC-Cl)	97	Fluka
Potassium carbonate	99	Fluka
Propargyl bromide	80% in toluene	Acros
Pyridine	99,5	Fluka
Sodium azide (NaN <sub>3</sub> )	99,5	Fluka
Sodium borohydride	99	Fluka
Sodium bicarbonate	99	Riedel-deHaen
Sodium carbonate	99,5	Fluka
Sodium hydroxide	99,5	Fluka
Sodium sulfate	99,5	Fluka
Styrene	99,5	Fluka
Triethylamine	99	Fluka
Triphenylphosphine	99	Aldrich

---

## 6.1.2 Instruments

### *Nuclear Magnetic Resonance (NMR)*

$^1\text{H}$  NMR spectra were recorded on a Bruker DRX 500 NMR spectrometer (Bruker, Billerica, MA, USA) at 500.13 MHz and  $^{13}\text{C}$  NMR spectra were recorded at 125.74 MHz. All the spectra were measured in  $\text{CDCl}_3$  or  $\text{DMSO-d}_6$  and the solvent was used as a internal standard, for  $\text{DMSO-d}_6$  ( $\delta$  ( $^1\text{H}$ ) = 2.50 ppm;  $\delta$  ( $^{13}\text{C}$ ) = 39.70 ppm) and for  $\text{CDCl}_3$  ( $\delta$  ( $^1\text{H}$ ) = 7.26 ppm;  $\delta$  ( $^{13}\text{C}$ ) = 77.0 ppm). When necessary, the assignment of the peaks has been achieved performing two dimensional experiments as  $^1\text{H}$   $^1\text{H}$ -COSY,  $^1\text{H}$   $^{13}\text{C}$ -HMCQ and  $^1\text{H}$   $^{13}\text{C}$ -HMBC. In these cases the standard pulse sequences from Bruker's software package have been used.

### *FT-IR spectroscopy*

FTIR spectra were registered in a transmission mode using a Bruker IFS 66 v/s spectrometer (Bruker, Billerica, MA, USA) configured with a mercury/ cadmium/ tellurium (MCT) detector capable of detecting in the range of 4000 – 600  $\text{cm}^{-1}$ . The Attenuated Total Reflectance (ATR) FTIR technique was used from the company Harrick (Twin parallel mirror reflection attachment). A germanium ATR-crystal, 45° (i.e., the penetration depth of IR-rays depending on the wave length between 0.17 and 1.1  $\mu\text{m}$ ) was used for the experiments. The polymer samples were analyzed at 4  $\text{cm}^{-1}$  resolution and 32 scans per measurement. All sample collection and spectra data processing was handled using the OPUS software. Samples were measured in the solid and liquid form.

### Differential Scanning Calorimetry (DSC) / Thermogravimetric Analyse (TGA)

Microcalorimetric studies were performed using a DSC Q1000 (TA Instruments) with a heating rate of 20 K/min under  $\text{N}_2$  atmosphere (-60  $^\circ\text{C}$ -Ti). TGA was carried out

using a TGA Q500 (TA Instruments) at a heating rate of 10 K/ min under N<sub>2</sub> atmosphere (30-800 °C).

### *Elementary analysis (EA)*

EA analysis was performed with a Elementar Analyses System GmbH.

### *Gel Permeation Chromatography (GPC)*

The relative molecular weights of the polymers were determined using gel permeation chromatography (GPC) in chloroform using a modular Knauer system with a refractive index detector at ambient temperature. LIChrogel PS40- and a single PL Mixed-B column were used applying linear calibration with polystyrene standard. Sample concentration was  $c = 2$  g/L, the injection volume was 20  $\mu$ l and flow rate was 1ml/min.

### *Atom force microscopy (AFM)*

Atomic force microscopy was carried out with a Dimension 3100 system (DJ, Santa Barbara). The tip used for the experiments was an ultrasharp noncontact silicon cantilever (NSC 16) from micromash (Talliu, Estonia). The area of interest was scanned in the “ Tapping mode”.

### *X-ray photoelectron spectroscopy (XPS)*

The XPS investigations were obtained on an Axis Ultra (Kratos Analytical, England) photoelectron spectrometer with a monochromatic Al K $\alpha_{1,2}$  X-ray source with corresponding photon energy of 160 eV. The X-ray source was operated at 300W by 20mA.

The use of a monochromatic source is especially important for polymers to minimize sample radiation damage. All samples were analyzed at ambient temperature and exhibited no evidence of damage during measurements. The electron binding energy



is calculated from the photon energy ( $h\nu$ ) of incident x-rays and the kinetic energy of the emitted electron according to the following equation:

$$h\nu = E_b + E_{kin}$$

### *Ellipsometry*

Ellipsometric measurements were made with a Gaetner Variable Angle Ellipsometer L116B using a helium-neon laser and an incident angle of 70°. Automatic ellipsometry programs from Gaertner were used to calculate film thicknesses. An index of 1.46 was used for the films. In general, the thicknesses of at least 3 different points on each surface were measured and found to be within +/- 1Å° of the reported average. Sample to sample reproducibility is +/- 2Å°.

### *Microcontact printing ( $\mu$ CP)*

An elastomeric mold was fabricated from poly(dimethylsiloxane) (PDMS, Sylgard 184, Dow Corning) by casting PDMS against a master that contained a pattern complementary to that to be reproduced. Predetermined structural features were etched in silica wafers (etching depth 4  $\mu$ m) by conventional microfabrication techniques.

Systems were wetted with a few drops of 10<sup>-3</sup> mol/l ethanol solution of DL-  $\alpha$  - lipoic acid (Fluka). Excess solvent was removed with nitrogen gas. For microprinting the impregnated stamp was contacted with gold surfaces for about two minutes.

Gold layers of 50 nm thickness were prepared by thermal evaporation of gold with an evaporation rate of 0.03 nm/s onto glass substrates which were precoated with a 2 nm Cr layer as adhesive interface.

### *Scanning Electron Microscopy (SEM)*

PDMS stamps and structured polymer films were investigated by scanning electron microscopy (LEO GEMINI DSM 982) at low voltages (0.3 – 1 keV). Due to the low

penetration depth of electrons at these image conditions the contrast arising from ultrathin films was sufficient for SEM investigation.

### *UV- irradiation*

The UV spectra were recorded by a Perkin-Elmer Lambda 800 spectrometer (spectral range available 190-800 nm) applying a spectral resolution of 1 nm, both, in solution (dioxane) and in film (prepared by spin coating from 3 wt.-% dioxane solution at 2000 r.p.m, 500 r.p.m/s, 60 s). The irradiation experiments were carried out with a 300W high pressure HgXe lamp with a condenser (LOT Oriel, Stratford, CT / USA). A recipient with water between the irradiation source and the sample was placed to avoid the influence of IR light. The distance from the irradiation source to the solution was 5 cm and 35 cm to the films.

### *Contact angle measurements*

The measurements of static contact angle were carried out on treated substrates by sessile drop method [drop shape analysis (DSA)] using a G 40 apparatus (Krüss GmbH, Germany). A micro syringe was used to dispense a 4-5 $\mu$ l (approx.) droplet on the surface of the material. Distilled, deionized, and filtered water was used for the measurements. Each measurement was done few seconds after the drop was deposited to avoid evaporation. At least 5 readings on different surface locations were averaged for each sample. The typical standard variations of measurements were 1-2°.

### *Raman spectroscopy*

Spectra were collected using the Raman spectrometer Holoprobe 785 (Kaiser Optical Systems Inc). The system has a diode laser operating at 785 nm and a CCD camera as detector. The in-line probe was connected to the spectrometer by an optical fiber and directly immersed into the reaction medium. Cleaning of the probe head surface is required from time to time to avoid excessive fouling. Raman spectra were

continuously recorded for every 2 minutes, each scan had an integration time of 5 seconds and for one spectrum 10 scans were accumulated with a resolution of  $2\text{ cm}^{-1}$ .

### *Film Preparation*

The preparation of thin layers from amino polymer or from disulfide solution was achieved through spin-coating of diluted polymer solution on gold coated silicon or glass substrates. The anchorage of the gold to glass or silicon substrates was achieved by a previously deposited 3 nm thick chromium layer. First, the glass substrates or silicon wafer were cleaned by Piranha solution (75 % conc.  $\text{H}_2\text{SO}_4$ , 25 % conc.  $\text{H}_2\text{O}_2$ ) and sonicated for 15 min in acetone in the ultrasonic Bath (US) at  $70^\circ\text{C}$  using a standard procedure [Bra02]. The substrates were dried in a nitrogen stream. In the second step gold coated silicon or glass substrates were cleaned by means of Harrick plasma cleaner or by rinsing with ethanol and milipore water. Then the samples were dried in  $\text{N}_2$  and used immediately after cleaning. Thin polymer films of the amino terpolymers were produced by spincoating of the purified reaction solution (2 wt.-% in THF) at 4000 rpm for 30 s. Consecutively, the films were annealed for 30 min at  $80^\circ\text{C}$  and then for 2 h at  $120^\circ\text{C}$  under ambient conditions. Non-attached polymer was removed by rinsing a several times in THF at room temperature. Then the film was dried in vacuum.

### *Labelling of patterned films with fluorescent marker (YOYO-1)*

In this experiment the terpolymer film was marked with a fluorescence marker YOYO-1 solution prepared in the following way: At first, a buffer solution was prepared by dissolution of 1.21 g of Trizma® base (Sigma) in 100 ml of water. The pH was adjusted down to 8.8 by slow addition of HCl (37 %, Merck). Secondly, 300  $\mu\text{L}$  of this Trizma® base 8.8 buffer solution and 10  $\mu\text{L}$  of YOYO-1 were stirred together and 100  $\mu\text{L}$  of the mixture were added over the patterned terpolymer film. After 1 min of exposure the sample was rinsed three times with distilled water and dried under  $\text{N}_2$  stream. The sample finally was examined by fluorescence microscopy.

## Fluorescence microscopy

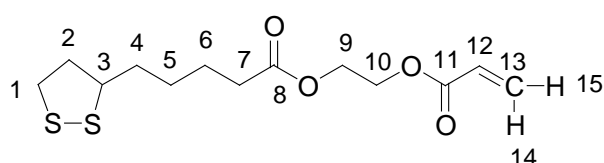
Fluorescent microscope images of the terpolymer films were made after selective irradiation through a TMS 400 grid and post exposition to the mentioned YOYO-1 solution. It was examined using a fluorescence microscope Axiovert 200 m (Carl Zeiss), mercury steam lamp (HBO 100) and the filter sentence 09 Carl Zeiss. The fluorescence-microscopic pictures were taken up with cascade 502B (RoberScientific) and quantifies the binding of the marker on the surface and the binding of the colouring was quantified on the surface

## 6.2 SYNTHESIS

### 6.2.1 Synthesis of dithiolate monomers

#### *1,2-Dithiolane-3-pentanoic acid, 2-[(1-oxo-2-propenyl)oxy]ethyl ester (LA)*

Variation A



LA

A reaction vessel was charged with  $\text{CH}_2\text{Cl}_2$  (15 ml), 5.75 mmol (1.19 g) of lipoic acid, 5.75 mmol (0.67 g) of 2-hydroxyethyl acrylate, 5.8 mmol (0.94 g) 1,1'-carbonyldiimidazole and 0.2 mmol (0.018 g) imidazolyl sodium. The solution was stirred at ambient temperature for 24 h, diluted with diethyl ether (50 ml), washed with water (2\*50 ml) and dried over  $\text{Na}_2\text{SO}_4$  and the solvent was removed under reduced pressure. The crude product was purified by distillation. Yield: 12 %.

## Variation B

A single-neck round flask was charged with 5.75 mmol (1.19 g) of lipoic acid, 5.75 mmol (0.67 g) of 2-hydroxyethyl acrylate, 1.21 mmol (0.36g) DPTS in 20 ml dry DMF. 8.05 mmol (1.02 g) DIPC was dissolved in 10 ml dry DMF and slowly added to the solution. Then the solution was stirred for next 12 hours at room temperature. The diisopropylurea was filtered off and the solvent was removed by rotary evaporation. Yield: 25 %

## Variation C

To a solution of 5 mmol (1.03 g) of lipoic acid dissolved in 10 mL of diethylether (anhydrous) 1 mmol (0.12 g) of DMAP and 6.6 mmol (0.77 g) of 2-hydroxyethyl acrylate was added and this mixture was cooled between  $-10$  and  $-5$  °C. Finally 1.2 mol (1.14 g) of DCC previously cooled to this temperature were added. The reaction mixture was stirred under these conditions for 1.5 h, then at  $5$  °C for 1.5 h and finally 4 h at rt. The white powder which appeared in the solution was filtered and the reaction mixture was diluted with diethylether (150 mL), washed with water (2x50 mL) and finally dried over  $\text{Na}_2\text{SO}_4$  anhydrous. After filtration the solvent was removed under reduced pressure. The monomer was obtained as yellow viscous liquids. Yield: 75 %

## Variation D

5 mmol (1.03 g) of lipoic acid, 6.6 mmol (0.77 g) of 2-hydroxyethylacrylate, 5.5 mmol (1.135 g) DCC and 5.5 mmol (0.147 g) HOBT in dry DMF (15 ml) were stirred for 2 h at  $-5$  to  $-10$  °C and then overnight at ambient temperature. After filtration of the DCC-urea, the solvent was removed in vacuum. The residue was dissolved in  $\text{CH}_2\text{Cl}_2$  (50 ml) and sequentially washed with cold aqueous HCl (10 %), water, saturated  $\text{NaHCO}_3$  and brine. The organic phase was dried over  $\text{Na}_2\text{SO}_4$ . After that the solvent was evaporated.

Yield: 96 %

Empirical formula: C<sub>13</sub>H<sub>20</sub>O<sub>4</sub>S<sub>2</sub> (Mr = 304,21 g/mol)

Elemental analysis: calculated: C 51,31 H 6,58 S 21,05

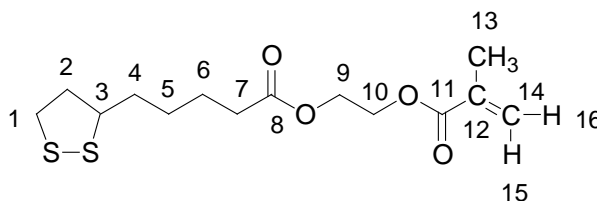
Found: C 52,50 H 6,91 S 20,11

<sup>1</sup>H NMR(DMSO): 6.41 (dd, 1H, H<sup>14</sup>), 6.14 (dd, 1H, H<sup>12</sup>), 5.87 (dd, 1H, H<sup>15</sup>), 4.35 (m, 2H, H<sup>10</sup>), 4.32 (m, 1H, H<sup>9</sup>), 3.55 (m, 1H, H<sup>3</sup>), 3.17 (m, 1H, H<sup>5</sup>), 3.11 (m, 1H, H<sup>6</sup>), 2.4 (m, 1H, H<sup>5</sup>), 2.34 (t, 2H, H<sup>7</sup>), 1.68 (m, 6H, H<sup>2</sup>, H<sup>4</sup>), 1.45 (m, 2H, H<sup>1</sup>).

<sup>13</sup>C NMR (DMSO): 172.65 (C<sup>8</sup>), 165.31 (C<sup>11</sup>), 130.87 (C<sup>13</sup>), 127.65 (C<sup>12</sup>), 61.87 (C<sup>10</sup>), 61.57 (C<sup>9</sup>), 55.89 (C<sup>3</sup>), 39.80 (C<sup>2</sup>), 38.09 (C<sup>1</sup>), 34.52 (C<sup>4</sup>), 33.42 (C<sup>7</sup>), 28.24 (C<sup>5</sup>), 24.19 (C<sup>6</sup>).

FT-IR (in cm<sup>-1</sup>): 2925 - 2851 (ν<sub>s,as</sub>CH<sub>2</sub>), 1728 (νC=O), 1635 (νC=C), 1447 (δ CH<sub>2</sub>), 1409 (δ CH<sub>2</sub>), 1269 (νCH Ar), 1169 (νC-O), 982 (δ C=C).

*1,2-Dithiolane-3-pentanoic acid, 2-[(2-methyl-1-oxo-2-propenyl)oxy]ethyl ester (LM)*



LM

To a solution of 5 mmol (1.03 g) of lipoic acid dissolved in 10 mL of diethylether (anhydrous) 1 mmol (0.12 g) of DMAP and 6.6 mmol (0.77 g) of 2-hydroxyethyl methacrylate was added and this mixture was cooled between -10 and -5 °C. Finally 1.2 mol (1.14 g) of DCC previously cooled to this temperature were added. The reaction mixture was stirred under these conditions for 1.5 h, then at 5°C for 1.5 h and finally 4 h at rt. The white powder which appeared in the solution was filtered off and the reaction mixture was diluted with diethylether (150 mL), washed with water (2x50 mL) and finally dried over Na<sub>2</sub>SO<sub>4</sub> anhydrous. After filtration the solvent was

removed under reduced pressure. The monomer was obtained as yellow viscous liquid.

Yield: 98 %

Empirical formula:  $C_{14}H_{22}O_4S_2$  (Mr = 318,22 g/mol)

Elemental analysis: calculated: C 52,79 H 6,91 S 20,11

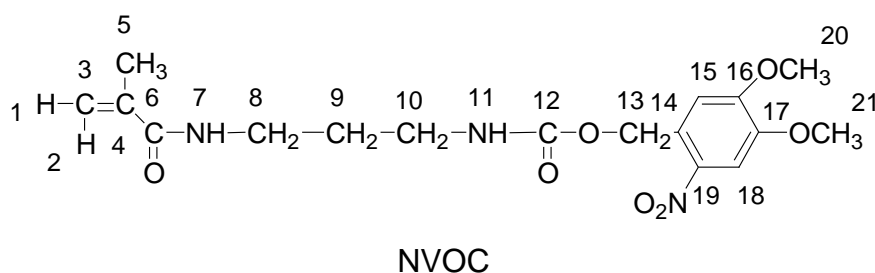
Found: C 51,50 H 6,80 S 19,71

$^1H$  NMR( $CDCl_3$ ): 6.12 (s, 1H,  $H^{15}$ ), 5.59 (s, 1H,  $H^{16}$ ), 4.34 (br, 4H,  $H^{9,10}$ ), 3.55 (m, 1H,  $H^3$ ), 3.17 (m, 1H,  $H^6$ ), 3.12 (m, 1H,  $H^6$ ), 2.45 (m, 1H,  $H^5$ ), 2.35 (t,  $J=7.6$ Hz, 2H,  $H^7$ ), 1.95 (s, 3H,  $H^{13}$ ), 1.90 (m, 1H,  $H^5$ ), 1.74-1.60 (m, 4H,  $H^{4,2}$ ), 1.31 (m, 2H,  $H^1$ ).

$^{13}C$  NMR ( $CDCl_3$ ): 172.80 ( $C^8$ ), 166.68 ( $C^{11}$ ), 135.66 ( $C^{12}$ ), 125.66 ( $C^{14}$ ), 62.14 ( $C^{10}$ ), 61.68 ( $C^9$ ), 56.10 ( $C^3$ ), 39.91 ( $C^2$ ), 38.20 ( $C^1$ ), 34.28 ( $C^4$ ), 33.57 ( $C^7$ ), 28.37 ( $C^5$ ), 21.38 ( $C^6$ ), 17.97 ( $C^{13}$ ).

FT-IR (in  $cm^{-1}$ ): 2928 - 2854 ( $\nu_{s,as}CH_2$ ,  $CH_3$ ), 1718 ( $\nu C=O$ ), 1637 ( $\nu C=C$ ), 1450 ( $\delta CH_2$ ), 1319 ( $\delta CH_3$ ), 1296 ( $\nu CH$  Ar), 1154 ( $\nu C-O$ ), 942 ( $\delta C=C$ ).

### 6.2.2 Synthesis of N-(N-NVOC-aminopropyl)methacrylamide (NVOC)



3 mmol (0.536 g) NAPMAAH and 10 mmol (0.84 g)  $NaHCO_3$  were dissolved in 150 ml water. 3.3 mmol (0.91 g) NVOC-Cl, dissolved in 57.5 ml dioxane were added at room temperature and the mixture was stirred at ambient temperature for 24 hours. The emerging precipitate was separated. Water was added to the resulting filtrate and extracted 5 times with 50 ml portions ethyl acetate. The combined organic fractions were washed with water, dried over  $Na_2SO_4$  and the solvent was removed

completely. The remaining residue was crystallized from a n-hexane / ethyl acetate [1:2, v/v] solution and the product was obtained as pale yellow needles.

Yield: 89 %

Empirical formula:  $C_{17}H_{23}N_2O_3$

Elemental analysis: calculated: C 53,54 H 6,08 S 11,02

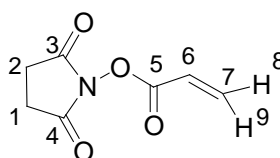
found: C 53,51 H 6,04 S 10,95

$^1H$  NMR(DMSO): 7.85 (br, 1H, H<sup>7</sup>), 7.69 (s, 1H, H<sup>15</sup>), 7.40 (br, 1H, H<sup>11</sup>), 7.18 (s, 1H, H<sup>18</sup>), 5.62 (s, 1H, H<sup>1</sup>), 5.32 (s, 2H, H<sup>13</sup>), 5.30 (s, 1H, H<sup>2</sup>), 3.89 - 3.87 (2s, 6H, H<sup>20,21</sup>), 3.11 (q, 2H, H<sup>8</sup>), 3.03 (q, 2H, H<sup>10</sup>), 1.84 (s, 3H, H<sup>5</sup>), 1.59 (m, 2H, H<sup>9</sup>).

$^{13}C$  NMR (DMSO): 167.63 (C<sup>6</sup>), 155.85 (C<sup>12</sup>), 153.48 (C<sup>16</sup>), 147.89 (C<sup>17</sup>), 140.18 (C<sup>19</sup>), 139.51 (C<sup>4</sup>), 128.00 (C<sup>14</sup>), 118.91 (C<sup>3</sup>), 110.80 (C<sup>15</sup>), 108.32 (C<sup>18</sup>), 62.43 (C<sup>13</sup>), 56.34 (C<sup>20</sup>), 56.23 (C<sup>21</sup>), 38.28 (C<sup>10</sup>), 36.65 (C<sup>8</sup>), 29.58 (C<sup>9</sup>), 18.74 (C<sup>5</sup>).

FT-IR (in  $cm^{-1}$ ): 3341 ( $\nu_{NH}$ ), 3104 ( $\nu_s C=CH$ ), 3003 ( $\nu_s Ar-H$ ), 2965, 2937, 2885 ( $\nu_s, asCH_2, CH_3$ ), 2848 ( $\nu OCH_3$ ), 1693 (amide I, -NH-CO-O), 165 (amide I, -NH-CO-C=), 1608, 1500 ( $\nu C=C$ , aromatic ring), 1583 (amid II), 1514 ( $\nu_{as} N=O$ ), 1461 ( $\delta CH_2$ ), 1327 ( $\nu_s N=O$ ), 1062 ( $\nu C-O$ ), 795 ( $\delta CH-Ar$ ).

### *N*-(acryloyloxy)succinimide



NASI

*N*-Hydroxysuccinimide (6.98 g, 60.7 mmol) and 4-dimethylaminopyridine (0.674 g, 5.52 mmol) were added to a solution of acryloyl chloride (5 g, 55.2 mmol) in dry THF. The solution was stirred at room temperature under nitrogen for 3 h and then



evaporated to dryness. The crude product was purified by flash chromatography, eluting with 1:1 petroleum ether/CH<sub>2</sub>Cl<sub>2</sub>, CH<sub>2</sub>Cl<sub>2</sub> and finally 5-10% ether in CH<sub>2</sub>Cl<sub>2</sub>.

Yield: 73 %

Empirical formula: C<sub>7</sub>H<sub>7</sub>NO<sub>4</sub>

Elemental analysis calculated: C 49,70 H 4,14 N 8,28

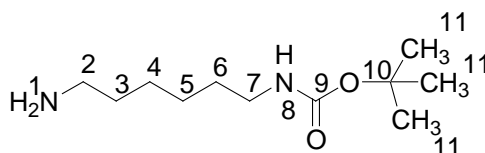
found: C 47,36 H 3,98 N 8,21

<sup>1</sup>H NMR (DMSO): 6.7 (dd, 1H, H<sup>8</sup>), 6.34 (q, 1H, H<sup>6</sup>), 6.16 (dd, 1H, H<sup>9</sup>), 2.85 (s, 4H, H<sup>1,2</sup>).

<sup>13</sup>C NMR (DMSO): 168.7 (C<sup>5</sup>), 165.82 (C<sup>3,4</sup>), 131.1 (C<sup>7</sup>), 126.3 (C<sup>6</sup>), 25.58 (C<sup>1,2</sup>).

FT-IR (in cm<sup>-1</sup>): 1800, 1775 (νCOO), 1735 (νC=O), 1327 (ν<sub>s</sub> N=O), 1260 (νCH Ar), 995 (δ C=C), 870 (δ CH-Ar).

### *(6-Amino-hexyl)-carbamic acid tert-butyl ester*



1,6-diaminohexane (1.16 g, 10 mmol) was dissolved in CH<sub>2</sub>Cl<sub>2</sub> (30 ml) and cooled in an ice bath to -5 °C. To the stirred solution 0.3 e q. di-tert-butyl bicarbonate (0.648 g, 3 mmol) was added slowly over a period of 1 h. The reaction was allowed to warm up to r.t., and proceeded overnight. The reaction mixture was extracted with saturated aqueous NaHCO<sub>3</sub> (50 ml, three times). The organic phases were pooled, dried, and evaporated under reduced pressure. The resulting oil was dissolved in 50 ml 1 N HCl and extracted with ether. The aqueous phase was washed with ether, made basic to a pH of 10 with aqueous 2 N NaOH, and extracted with ethyl acetate. The organic phases were pooled, dried, and evaporated under reduced pressure. The resulting oil was dissolved in 50 ml, 1 N HCl and extracted with ether. The aqueous phase was washed with ether, made basic to a pH of 10 with aqueous 2 N NaOH, and extracted with ethyl acetate. The organic extracts were pooled, dried over Na<sub>2</sub>SO<sub>4</sub> and evaporated to give yellow oil.

Yield: 82 %

Empirical formula:  $C_{11}H_{24}N_2O_2$

Elemental analysis: calculated: C 61,11 H 11,11 N 12,96

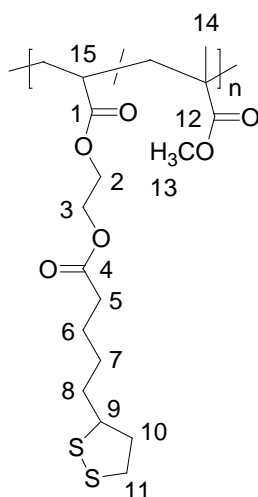
found: C 62,02 H 10,81 N 12,85

$^1H$  NMR (DMSO): 4.54 (br s, 1H, H<sup>8</sup>), 3.09 (dd, 2H, H<sup>2</sup>), 2.67 (t, 2H, H<sup>7</sup>), 1.68 (s, 2H, H<sup>1</sup>), 1.42 (br m, 13H, H<sup>3, 6, 11</sup>), 1.32 (m, 4H, H<sup>4, 5</sup>).

$^{13}C$  NMR (DMSO): 68.7 (C<sup>10</sup>), 55.82 (C<sup>9</sup>), 42.6 (C<sup>7</sup>), 40.3 (C<sup>2</sup>), 32.3 (C<sup>3</sup>), 29.58 (C<sup>6</sup>), 26.7 (C<sup>11</sup>), 25.1 (C<sup>4, 5</sup>).

### 6.2.3 Synthesis of co- and terpolymers by FRP

#### *Copolymer of LA/MMA 25/75*



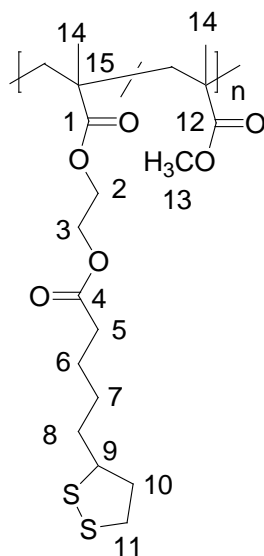
LA/MMA

2 mmol (0.608g) LA, 6 mmol (0.6g) MMA and 0.2 mmol (0.033g) AIBN were dissolved in 20 mL 1,4 dioxane. The temperature was set to 70 °C and the mixture was stirred for 24h under  $N_2$ .

The polymer was isolated by precipitation in ethanol and successive reprecipitations (2x) in  $CHCl_2$ /ethanol were performed for the purification of the material.

- Yield: 75 %
- $^1\text{H NMR}$  ( $\text{CDCl}_3$ ): 4.26 (br,  $\text{H}^2$ ), 4.16 ( $\text{H}^3$ ), 3.58 (m,  $\text{H}^9$ ,  $\text{H}^{13}$ ), 3.17 (m,  $\text{H}^{11}$ ), 3.12 (m,  $\text{H}^{11}$ ), 2.46 (m,  $\text{H}^{10}$ ), 2.0-1.4 (m,  $\text{H}^6$ ,  $\text{H}^8$ ), 1.4 - 0.95 (m,  $\text{CH}_2$ -chain), 0.94-0.75(m,  $\text{H}^{14}$ ,  $\text{H}^{15}$ ).
- $^{13}\text{C NMR}$  ( $\text{CDCl}_3$ ): 178.02( $\text{C}^1$ ), 177.76 ( $\text{C}^{12}$ ), 173.10 ( $\text{C}^4$ ), 62.22 ( $\text{C}^2$ ), 61.71 ( $\text{C}^3$ ), 56.28, 54.38 ( $\text{C}^9$ ), 51.73 ( $\text{C}^{14}$ ), 44.87 ( $\text{C}^{15}$ ), 44.52 ( $\text{C}^{16}$ ), 40.19 ( $\text{C}^{10}$ ), 38.45 ( $\text{C}^{11}$ ), 34.55 ( $\text{C}^8$ ), 33.74 ( $\text{C}^5$ ), 28.69 ( $\text{C}^7$ ), 24.49 ( $\text{C}^6$ ), 18.70 ( $\text{CH}_2$ -chain), 16.51 ( $\text{C}^{14}$ ).
- FT-IR (in  $\text{cm}^{-1}$ ): 2948 - 2850 ( $\nu_{\text{s, as}}\text{CH}_2$ ,  $\text{CH}_3$ ), 1722 ( $\nu\text{COO}$ ), 1436 ( $\delta\text{CH}_2$ ), 1385, 1239, 1143 ( $\nu\text{C-O}$ ), 985, 752 ( $\delta\text{CH-Ar}$ ).

### Copolymer of LM/MMA 25/75

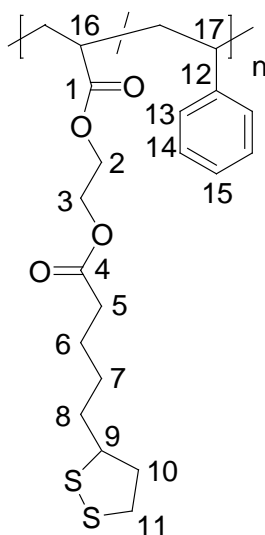


LM/MMA

2 mmol (0.636g) LM, 6 mmol (0.6g) MMA and 0.2 mmol (0.033g) AIBN were dissolved in 20 mL 1,4 dioxane. After three freeze and thaw cycles the temperature was set to 70 °C and the mixture was stirred for 24 h under  $\text{N}_2$ . The polymer was isolated by precipitation in the mixture methanol and water [1:1, v/v] and successive reprecipitations (2x) in dioxane and methanol/water were performed for the purification of the material. The product was obtained as white-yellow solid.

- Yield: 63 %
- $^1\text{H NMR}$  ( $\text{CDCl}_3$ ): 4.27 (br,  $\text{H}^2$ ), 4.15 (br,  $\text{H}^3$ ), 3.56 (br,  $\text{H}^9$ ,  $\text{H}^{13}$ ), 3.18 (m,  $\text{H}^{11}$ ), 3.13 (m,  $\text{H}^{11}$ ), 2.49 (m,  $\text{H}^{10}$ ), 1.94-1.71 (br,  $\text{H}^6$ ,  $\text{H}^8$ ), 1.51 - 1.37 (m,  $\text{H}^7$ ), 1.03 (br,  $\text{CH}_2$ -chain), 0.86 (br,  $\text{H}^{14}$ ).
- $^{13}\text{C NMR}$  ( $\text{CDCl}_3$ ): 177.71 ( $\text{C}^1$ ), 177.00 ( $\text{C}^{12}$ ), 173.17 ( $\text{C}^4$ ), 62.78 ( $\text{C}^2$ ), 61.46 ( $\text{C}^3$ ), 54.19 ( $\text{C}^9$ ), 51.78 ( $\text{C}^{14}$ ), 44.94 ( $\text{C}^{15}$ ), 44.58 ( $\text{C}^{16}$ ), 40.23 ( $\text{C}^{10}$ ), 38.49 ( $\text{C}^{11}$ ), 34.60 ( $\text{C}^8$ ), 33.76 ( $\text{C}^5$ ), 28.73 ( $\text{C}^7$ ), 24.57 ( $\text{C}^6$ ), 18.74 - 18.48 ( $\text{CH}_2$ -chain), 16.57 - 14.35 ( $\text{C}^{14}$ ).
- FT-IR (in  $\text{cm}^{-1}$ ): 2993 - 2946 ( $\nu_{\text{s, as}}\text{CH}_2$ ,  $\text{CH}_3$ ), 1722 ( $\nu\text{COO}$ ), 1435 ( $\delta\text{CH}_2$ ), 1386, 1240, 987, 751 ( $\delta\text{CH-Ar}$ ).

### Copolymer of LA/S 25/75



LA/S

2 mmol (0.608g) LM, 6 mmol (0.69g) styrene and 0.2 mmol (0.033g) AIBN were dissolved in 20 mL 1,4 dioxane. After three freeze and thaw cycles the temperature was set to 70 °C and the mixture was stirred for 24 h under  $\text{N}_2$ . The polymer was isolated by precipitation in methanol and successive reprecipitations (2x) in dioxane and methanol were performed for the purification of the material. The product was obtained as light yellow solid.

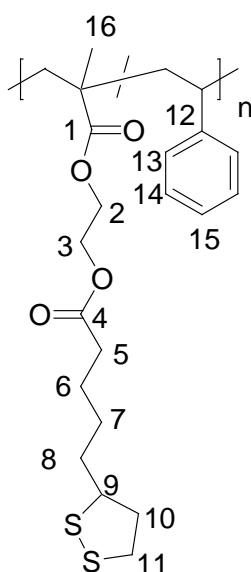
Yield: 90 %

$^1\text{H NMR}$  ( $\text{CDCl}_3$ ): 7.40 - 6.40 (m,  $\text{H}^{13}$ ,  $\text{H}^{14}$ ,  $\text{H}^{15}$ ), 4.12 - 3.84 (m,  $\text{H}^2$ ,  $\text{H}^3$ ), 3.51 (m,  $\text{H}^9$ ), 3.10 (m,  $\text{H}^{11}$ ), 2.45 - 2.10 (m,  $\text{H}^5$ ,  $\text{H}^{10}$ ), 1.84 - 1.82 (m,  $\text{H}^6$ ,  $\text{H}^8$ ), 1.62 - 0.70 (m,  $\text{H}^7$ ,  $\text{H}^{12}$ ,  $\text{CH}_2$ -chain).

$^{13}\text{C NMR}$ ( $\text{CDCl}_3$ ): 187.54 ( $\text{C}^1$ ), 173.28 ( $\text{C}^4$ ), 143.60 ( $\text{C}^{12}$ ), 128.69 ( $\text{C}^{13}$ ), 128.23 ( $\text{C}^{14}$ ), 127.90 ( $\text{C}^{15}$ ), 62.18 ( $\text{C}^2$ ), 61.97 ( $\text{C}^3$ ), 49.53 ( $\text{C}^9$ ), 44.20 ( $\text{C}^{16}$ ), 41.55, 40.55 ( $\text{C}^{17}$ ), 40.18 ( $\text{C}^{11}$ ), 38.72 ( $\text{C}^8$ ), 34.83 ( $\text{C}^5$ ), 34.20, 34.04, 33.45, 28.93 ( $\text{C}^7$ ), 25.22 ( $\text{C}^6$ ), 24.90 ( $\text{CH}_2$ -chain).

FT-IR (in  $\text{cm}^{-1}$ ): 2923 - 2853 ( $\nu_{\text{s, asCH}_2}$ ,  $\text{CH}_3$ ), 1731 ( $\nu_{\text{COO}}$ ), 1601 ( $\nu_{\text{C=C}}$ ), 1451 ( $\delta_{\text{CH}_2}$ ), 1371, 1150 ( $\nu_{\text{C-O}}$ ), 1067, 759, 750 ( $\delta_{\text{CH-Ar}}$ ).

### Copolymer of LM/S 25/75



LM/S

2 mmol (0.636g) LM, 6 mmol (0.69g) styrene and 0.2 mmol (0.033g) AIBN were dissolved in 20 mL 1,4 dioxane. After three freeze and thaw cycles the temperature was set to 70 °C and the mixture was stirred for 24 h under  $\text{N}_2$ . The polymer was isolated by precipitation in n-hexane and successive reprecipitations (2x) in dioxane and n-hexane were performed for the purification of the materials. The product was obtained as light yellow solid.

Yield: 83 %

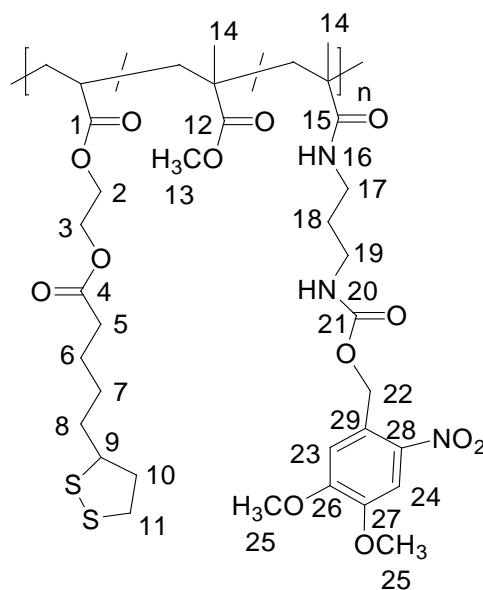
Empirical formula:  $[(C_{14}H_{22}O_4S_2) / (C_8H_8)]_n$

$^1H$  NMR ( $CDCl_3$ ): 7.40 - 6.40 (m,  $H^{13}$ ,  $H^{14}$ ,  $H^{15}$ ), 4.28 - 3.94 (m,  $H^2$ ,  $H^3$ ), 3.57 (m,  $H^9$ ), 3.14 - 3.09 (m,  $H^{11}$ ), 2.40-2.10 (m,  $H^5$ ,  $H^{10}$ ), 1.87 - 1.72 (m,  $H^6$ ,  $H^8$ ), 1.62 - 0.70 (m,  $H^1$ ,  $H^7$ ,  $H^{12}$ ,  $H^{16}$ ,  $CH_2$ -chain).

$^{13}C$  NMR( $CDCl_3$ ): 172.94 ( $C^1$ ), 156.84 ( $C^4$ ), 145.80 ( $C^{12}$ ), 128.69 ( $C^{13}$ ), 128.10 ( $C^{13}$ ), 127.77 ( $C^{14}$ ), 125.96 ( $C^{15}$ ), 67.03 ( $C^2$ ), 61.63 ( $C^3$ ), 49.19 ( $C^9$ ), 44.20 ( $C^{16}$ ), 41.55, 40.55 ( $C^{17}$ ), 40.18 ( $C^{18}$ ), 40.13 ( $C^{10}$ ), 38.45 ( $C^{11}$ ), 34.55 ( $C^8$ ), 33.81 ( $C^5$ ), 28.68 ( $C^7$ ), 25.55 ( $C^6$ ), 24.90 ( $CH_2$ -chain), 24.53 ( $C^{16}$ ).

FT-IR (in  $cm^{-1}$ ): 3026 ( $\nu_{Ar-H}$ ), 2926 - 2853 ( $\nu_{s,as}CH_2$ ,  $CH_3$ ), 1726 ( $\nu_{C=O}$ ), 1601 ( $\nu_{C=C}$ ), 1493 ( $\delta_{CH_2}$ ), 1451 ( $\delta_{CH_2}$ ), 1377, 1158 ( $\nu_{C-O}$ ), 1074 ( $\nu_{C-O}$ ), 759 ( $\delta_{CH-Ar}$ ), 750 ( $\delta_{CH-Ar}$ ).

### Terpolymer of LA/MMA/NVOC 5/20/75



### LA/MMA/NVOC

0.5 mmol (0.152 g) LA, 7.5 mmol (0.750 g) MMA and 2 mmol (0.763 g) AMIN-M2, 1 mmol (0.164 g) AIBN were dissolved in 50 mL 1,4 dioxane. After three freeze and thaw cycles the temperature was set to 70°C and the mixture was stirred for 24 h under N<sub>2</sub>. The polymer was isolated by precipitation in diethyl ether and successive

reprecipitations (2x) in dioxane and diethyl ether were performed for the purification of the material. The product was obtained as light yellow solid.

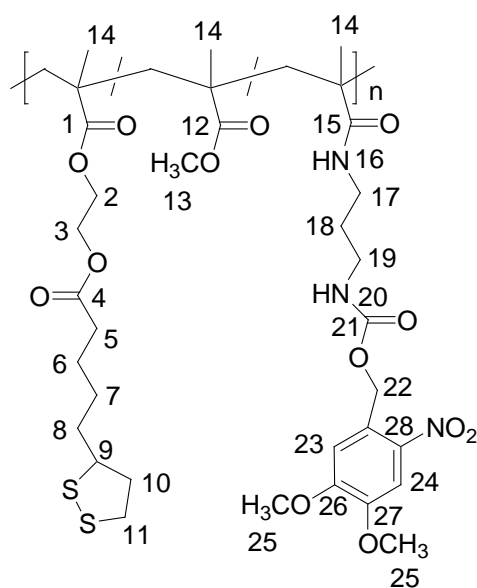
Yield: 64 %

$^1\text{H NMR}(\text{CDCl}_3)$ : 7.71 (s,  $\text{H}^{23}$ ), 7.03 (s,  $\text{H}^{24}$ ), 6.32 (m,  $\text{H}^{20}$ ), 5.51 (m,  $\text{H}^{16}$ ,  $\text{H}^{22}$ ), 4.26 – 4.15 (br,  $\text{H}^2$ ,  $\text{H}^3$ ), 3.99 (s,  $\text{H}^{25}$ ), 3.95 (s,  $\text{H}^{25}$ ), 3.59 (s,  $\text{H}^9$ ,  $\text{H}^{13}$ ), 3.26 (m,  $\text{H}^{17}$ ,  $\text{H}^{19}$ ), 2.58 (m,  $\text{H}^{11}$ ), 2.37 ( $\text{H}^5$ ), 2.10-1.58 (m,  $\text{H}^6$ ,  $\text{H}^8$ ,  $\text{H}^{10}$ ,  $\text{H}^{18}$ ,  $\text{CH}_2$ -chain), 1.43 (m,  $\text{H}^7$ ), 1.19-0.70 (m,  $\text{H}^{14}$ ).

$^{13}\text{C NMR}(\text{CDCl}_3)$ : 177.91( $\text{C}^1$ ), 177.63 ( $\text{C}^{12}$ ), 177.15 ( $\text{C}^4$ ), 173.03 ( $\text{C}^{15}$ ), 156.45 ( $\text{C}^{21}$ ), 153.41 ( $\text{C}^{26}$ ), 147.97 ( $\text{C}^{27}$ ), 139.57 ( $\text{C}^{28}$ ), 127.88 ( $\text{C}^{29}$ ), 110.17 ( $\text{C}^{23}$ ), 108.06 ( $\text{C}^{24}$ ), 63.36 ( $\text{C}^{22}$ ), 62.78 ( $\text{C}^2$ ), 62.66 ( $\text{C}^3$ ), 56.22 ( $\text{C}^{25}$ ), 55.89 ( $\text{C}^{25}$ ), 54.25 ( $\text{C}^9$ ), 51.58 ( $\text{C}^{13}$ ), 44.98 ( $\text{C}^{17}$ ), 44.80 ( $\text{C}^{30}$ ), 44.71 ( $\text{C}^{31}$ ), 44.36 ( $\text{C}^{10}$ ), 40.05 ( $\text{C}^{10}$ ), 38.30 ( $\text{C}^{11}$ ), 37.98 ( $\text{C}^{19}$ ), 36.42 ( $\text{C}^{17}$ ), 34.39 ( $\text{C}^8$ ), 33.60 ( $\text{C}^5$ ), 29.03 ( $\text{C}^{18}$ ), 28.52 ( $\text{C}^7$ ), 24.34 ( $\text{C}^6$ ), 18.57 - 18.55 ( $\text{CH}_2$ -chain), 16.76 - 16.32 ( $\text{C}^{14}$ ).

FT-IR (in  $\text{cm}^{-1}$ ): 3365 ( $\nu\text{NH}$ ), 2947 - 2848 ( $\nu_{\text{s, as}}\text{CH}_2$ ,  $\text{CH}_3$ ), 1721 ( $\nu\text{C=O}$ ), 1653, 1582, 1518 ( $\nu_{\text{as}}\text{NO}$ ), 1438 ( $\delta\text{CH}_2$ ), 1329 ( $\nu_{\text{s}}\text{NO}$ ), 1066 ( $\nu\text{C-O}$ ), 796 ( $\delta\text{CH-Ar}$ ).

### Terpolymer of LM/MMA/NVOC 5/20/75



LM/MMA/NVOC

0.5 mmol (0.152 g) LA, 7.5 mmol (0.750 g) MMA and 2 mmol (0.763 g) AMIN-M2, 1 mmol (0.164 g) AIBN were dissolved in 50 mL 1,4 dioxane. After three freeze and thaw cycles the temperature was set to 70 °C and the mixture was stirred for 24 h under N<sub>2</sub>. The polymer was isolated by precipitation in diethyl ether and successive reprecipitations (2x) in dioxane and diethyl ether were performed for the purification of the materials. The product was obtained as light yellow solid.

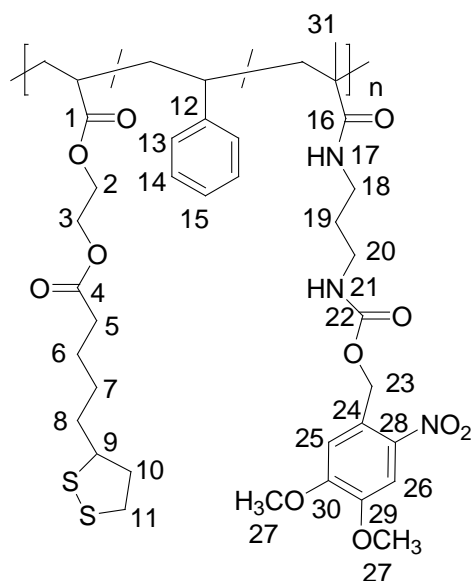
Yield: 49 %

<sup>1</sup>H NMR(CDCl<sub>3</sub>): 7.70 (s, H<sup>23</sup>), 7.03 (s, H<sup>24</sup>), 6.35 (m, H<sup>20</sup>), 5.51-5.40 (m, H<sup>16</sup>, H<sup>22</sup>), 4.27 - 4.16 (br, H<sup>2</sup>, H<sup>3</sup>), 4.16 (br, H<sup>10</sup>), 3.98 (s, H<sup>25</sup>), 3.95 (s, H<sup>25</sup>), 3.59 (m, H<sup>9</sup>, H<sup>13</sup>), 3.26 (m, H<sup>17</sup>, H<sup>19</sup>), 3.17 (m, H<sup>11</sup>), 2.38 (br, H<sup>6</sup>, H<sup>8</sup>, H<sup>10</sup>, H<sup>18</sup>), 1.96-1.64 (m, CH<sub>2</sub>-chain), 1.37 (m, H<sup>17</sup>), 1.10-0.78 (m, H<sup>14</sup>).

<sup>13</sup>C NMR(CDCl<sub>3</sub>): 177.90 (C<sup>1</sup>), 177.69 (C<sup>12</sup>), 176.83 (C<sup>4</sup>), 173.08 (C<sup>15</sup>), 156.48 (C<sup>21</sup>), 153.48 (C<sup>26</sup>), 148.08 (C<sup>27</sup>), 139.78 (C<sup>28</sup>), 128.00 (C<sup>29</sup>), 110.29 (C<sup>23</sup>), 108.15 (C<sup>24</sup>), 63.52 (C<sup>22</sup>), 56.39 (C<sup>25</sup>), 56.31 (C<sup>25</sup>), 54.30 (C<sup>9</sup>), 51.66 (C<sup>13</sup>), 44.98 (C<sup>30</sup>), 44.81 (C<sup>31</sup>), 40.14 (C<sup>10</sup>), 38.39 (C<sup>11</sup>), 38.11 (C<sup>19</sup>), 36.43 (C<sup>17</sup>), 34.49 (C<sup>8</sup>), 33.68 (C<sup>5</sup>), 29.13 (C<sup>18</sup>), 28.62 (C<sup>7</sup>), 24.47 (C<sup>6</sup>), 18.80 - 18.65 (CH<sub>2</sub>-chain), 16.75 - 16.43 (C<sup>14</sup>).

FT-IR (in cm<sup>-1</sup>): 3366 (νNH), 2947- 2848 (ν<sub>s,as</sub>CH<sub>2</sub>,CH<sub>3</sub>), 1722 (νCOO,COONH), 1656 (νC=C), 1582, 1519 (ν<sub>as</sub>NO), 1438 (δCH<sub>2</sub>), 1330 (ν<sub>s</sub>NO), 1068 (νC-O), 796 (δ CH-Ar).



*Terpolymer of LA/S/NVOC 5/20/75*

LA/S/NVOC

0.5 mmol (0.152 g) LA, 7.5 mmol (0.78 g) styrene and 2 mmol (0.763 g) AMIN-M2, 1 mmol (0.164g) AIBN were dissolved in 50 mL 1,4 dioxane. After three freeze and thaw cycles the temperature was set to 70°C and the mixture was stirred for 24h under N<sub>2</sub>. The polymer was isolated by precipitation in diethyl ether and successive reprecipitations (2x) in dioxane and diethyl ether were performed for the purification of the material. The product was obtained as light yellow grainy powder.

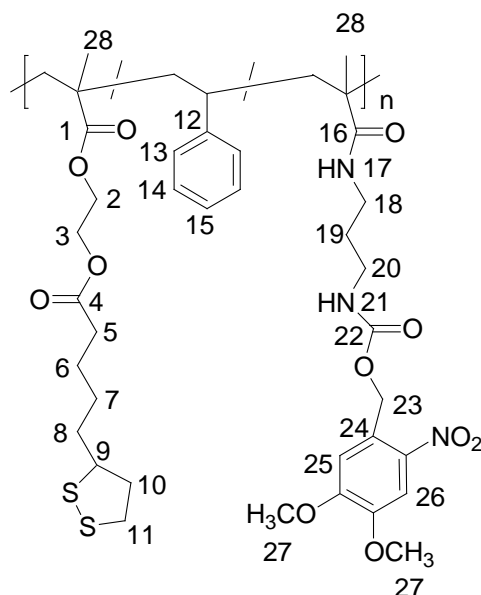
Yield: 22 %

<sup>1</sup>H NMR (CDCl<sub>3</sub>): 7.68 (s, H<sup>25</sup>), 7.42 (s, H<sup>26</sup>), 7.40-6.45 (m, H<sup>13</sup>, H<sup>14</sup>, H<sup>15</sup>), 5.32 (br, H<sup>17</sup>), 4.35 - 3.90 (m, H<sup>2</sup>, H<sup>3</sup>, H<sup>10</sup>), 3.85 (br, H<sup>27</sup>), 3.54 (m, H<sup>9</sup>), 3.22 - 2.68 (br, H<sup>18</sup>, H<sup>20</sup>), 2.44 (br, H<sup>11</sup>), 2.37 (H<sup>5</sup>), 2.10 (CH<sub>2</sub>-chain), 2 - 0.70 (br, H<sup>6-8</sup>, H<sup>10</sup>, H<sup>19</sup>, H<sup>31</sup>).

<sup>13</sup>C NMR (CDCl<sub>3</sub>): 178.29 (C<sup>1</sup>), 173.00 (C<sup>16</sup>), 156.62 (C<sup>22</sup>), 153.76 (C<sup>30</sup>), 148.31 (C<sup>29</sup>), 141.11 (C<sup>28</sup>), 128.28 (br, C<sup>24</sup>), 110.50 (C<sup>25</sup>), 108.36 (C<sup>26</sup>), 63.69 (C<sup>23</sup>), 62.95 (C<sup>2</sup>), 61.90 (C<sup>3</sup>), 56.70 (C<sup>27</sup>), 56.57 (C<sup>27</sup>), 54.80 (C<sup>9</sup>), 45.43 (C<sup>18</sup>), 38.50 (C<sup>11</sup>), 37.53 (C<sup>20</sup>), 35.65 (C<sup>18</sup>), 34.35 (C<sup>8</sup>), 33.68 (C<sup>5</sup>), 29.53 (C<sup>19</sup>), 28.58 (C<sup>7</sup>), 24.44 (C<sup>6</sup>), 18.43 (CH<sub>2</sub>-chain), 16.57 (CH-chain).

FT-IR (in  $\text{cm}^{-1}$ ): 3357 ( $\nu_{\text{NH}}$ ), 2934 ( $\nu_{\text{s,as}}\text{CH}_2, \text{CH}_3$ ), 1718 ( $\nu_{\text{COO}}, \text{COONH}$ ), 1649 ( $\nu_{\text{C=C}}$ ), 1517 ( $\nu_{\text{as}}\text{NO}$ ), 1452 ( $\delta_{\text{CH}_2}$ ), 1328 ( $\nu_{\text{s}}\text{NO}$ ), 1275, 1218, 1067 ( $\nu_{\text{C-O}}$ ), 702 ( $\delta_{\text{CH-Ar}}$ ).

*Terpolymer of LM/S/NVOC 5/20/75*



LM/S/NVOC

0.5 mmol (0.158 g) LM, 7.5 mmol (0.78 g) styrene and 2 mmol (0.763 g) AMIN-M2, 1 mmol (0.164 g) AIBN were dissolved in 50 mL 1,4 dioxane. After three freeze and thaw cycles the temperature was set to 70 °C and the mixture was stirred for 24 h under  $\text{N}_2$ . The polymer was isolated by precipitation in diethyl ether and successive reprecipitations (2x) in dioxane and diethyl ether were performed for the purification of the material. The product was obtained as light yellow grainy powder.

Yield: 23 %

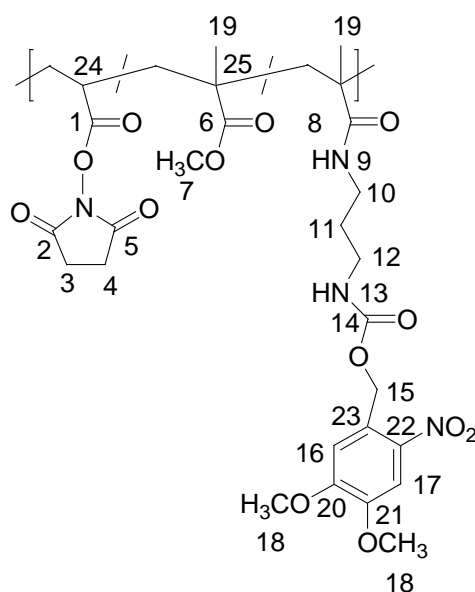
$^1\text{H}$  NMR ( $\text{CDCl}_3$ ): 7.70 (s,  $\text{H}^{25}$ ), 7.42 (s,  $\text{H}^{26}$ ), 7.40-6.30 (m,  $\text{H}^{13}$ ,  $\text{H}^{14}$ ,  $\text{H}^{15}$ ), 5.33 (br,  $\text{H}^{17}$ ), 4.35 - 4 (m,  $\text{H}^2$ ,  $\text{H}^3$ ,  $\text{H}^{10}$ ), 3.85 (br,  $\text{H}^{27}$ ), 3.55 (m,  $\text{H}^9$ ), 3.20 - 2.70 (br,  $\text{H}^{18}$ ,  $\text{H}^{20}$ ), 2.45 (br,  $\text{H}^{11}$ ), 2.37 ( $\text{H}^5$ ), 2.10 ( $\text{CH}_2$ -chain), 2.0-0.75 (br,  $\text{H}^{6-8}$ ,  $\text{H}^{10}$ ,  $\text{H}^{19}$ ,  $\text{H}^{31}$ ).

$^{13}\text{C}$  NMR ( $\text{CDCl}_3$ ): 178.19 ( $\text{C}^1$ ), 177.54 ( $\text{C}^4$ ), 172.98 ( $\text{C}^{16}$ ), 156.12 ( $\text{C}^{22}$ ), 153.49 ( $\text{C}^{30}$ ), 148.02 ( $\text{C}^{29}$ ), 139.73 (br,  $\text{C}^{28}$ ), 127.88 (br,  $\text{C}^{24}$ ), 110.15

(C<sup>25</sup>), 108.13 (C<sup>26</sup>), 63.42 (C<sup>23</sup>), 62.05 (C<sup>2</sup>), 61.69 (C<sup>3</sup>), 56.31 (br, C<sup>27</sup>), 54.78 (C<sup>9</sup>), 44.13 (br, C<sup>18</sup>), 38.39 (C<sup>11</sup>), 37.49 (C<sup>20</sup>), 35.80 (C<sup>18</sup>), 34.48 (C<sup>8</sup>), 33.70 (C<sup>5</sup>), 29.58 (C<sup>19</sup>), 28.60 (C<sup>7</sup>), 24.44 (C<sup>6</sup>), 18.53 (CH<sub>2</sub>-chain), 16.58 (CH-chain).

FT-IR (in cm<sup>-1</sup>): 3358 (νNH), 2926 - 2852 (ν<sub>s,as</sub>CH<sub>2</sub>,CH<sub>3</sub>), 1724 (νCOO,COONH), 1654 (νC=C), 1518 (ν<sub>as</sub>NO), 1451 (δCH<sub>2</sub>), 1328 (ν<sub>s</sub>NO), 1276, 1219, 1067 (νC-O), 751, 702 (δ CH-Ar).

### Terpolymer of AE/MMA/NVOC 10/20/70



### AE/MMA/NVOC

1 mmol (0.169 g) N-acryloxysuccinimide, 7.0 mmol (0.7 g) MMA and 2 mmol (0.763 g) AMIN-M2, 1 mmol (0.164 g) AIBN were dissolved in 50 mL 1,4 dioxane. After three freeze and thaw cycles the temperature was set to 75 °C and the mixture was stirred for 24h under N<sub>2</sub>. The polymer was isolated by precipitation in ethanol and successive reprecipitations (2x) in dioxane and ethanol were performed for the purification of the materials. The product was obtained as white powder.

Yield: 49.45 %

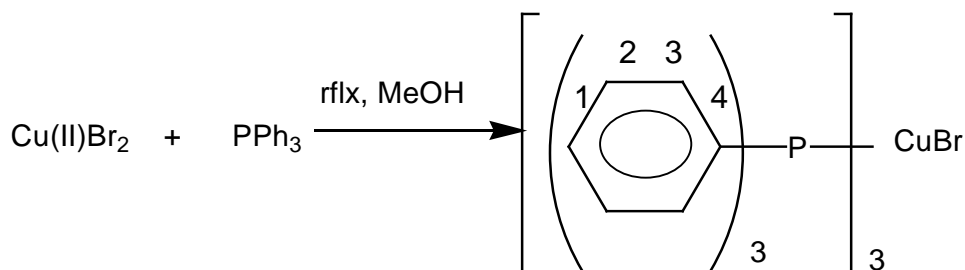
<sup>1</sup>H NMR (CDCl<sub>3</sub>): 7.67 (s, H<sup>16</sup>), 7.04 (s, H<sup>17</sup>), 6.34 (br, H<sup>13</sup>), 5.47 (s, H<sup>9</sup>, H<sup>15</sup>), 3.96 (s, H<sup>18</sup>), 3.93 (s, H<sup>18</sup>), 3.57 (br, H<sup>7</sup>), 3.21 (br, H<sup>10</sup>, H<sup>12</sup>), 2.88 (s,

H<sup>3</sup>, H<sup>4</sup>), 1.91-1.61 (br, H<sup>11</sup>, CH<sub>2</sub>-chain ), 1.00-0.81 (br, H<sup>19</sup>, CH-chain).

<sup>13</sup>C NMR (CDCl<sub>3</sub>): 177.71 (br, C<sup>6</sup>), 176.76 (br, C<sup>1</sup>), 173.05 (C<sup>8</sup>), 168.83 (C<sup>2</sup>, C<sup>5</sup>), 156.42 (C<sup>14</sup>), 153.45 (C<sup>20</sup>), 147.94 (C<sup>21</sup>), 139.66 (C<sup>22</sup>), 128.13 (br, C<sup>23</sup>), 110.25 (C<sup>16</sup>), 108.06 (C<sup>17</sup>), 63.41 (C<sup>15</sup>), 56.34 (C<sup>18</sup>), 56.26 (C<sup>18</sup>), 51.64 (br, C<sup>7</sup>), 44.97 (C<sup>24</sup>), 44.75 (C<sup>25</sup>), 38.13 (C<sup>12</sup>), 36.71 (C<sup>10</sup>), 30.08, 29.07 (C<sup>11</sup>), 25.49 (C<sup>3</sup>, C<sup>4</sup>), 18.62 - 18.25 (CH<sub>2</sub>-chain), 17.31 (C), 16.72 - 16.32 (CH-chain).

## 6.2.4 Click-chemistry

### 6.2.4.1 Synthesis of copper(I) catalyst



In an Erlenmeyer flask equipped with a Teflon stir bar, methanol (50ml) was heated to boiling and triphenylphosphine (11,2 mmol, 3 g) was slowly added to the stirring methanol. After the complete dissolution of triphenylphosphine, CuBr<sub>2</sub> (2,64 mmol, 0,62 g) was added as a solid, in portions. Upon addition of the copper bromide, a white precipitate was formed. After the completion of the addition, the contents were stirred for 10 min and the flask was allowed to cool to ambient temperature. The reaction mixture was then filtered and the white residue was washed repeatedly with ethanol and then with diethyl ether. The residue was dried under dynamic vacuum to yield 89% of a white solid.

Yield: 88,79 %

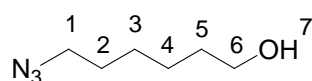
<sup>1</sup>H NMR (CDCl<sub>3</sub>): 7.36 (m, 18 H, H<sup>2</sup>), 7.33 (m, 9 H, H<sup>4</sup>), 7.22 (t, 18 H, H<sup>3</sup>).

$^{13}\text{C}$  NMR ( $\text{CDCl}_3$ ): 133.93 ( $^2J_{\text{PC}} = 15.3$  Hz,  $\text{C}^2$ ), 132.9 (br,  $\text{C}^1$ ), 129.70 ( $\text{C}^4$ ), 128.53 ( $^3J_{\text{PC}} = 9.2$  Hz,  $\text{C}^3$ ).

FT-IR (in  $\text{cm}^{-1}$ ): 3046 (Ar CH), 2975, 1584 (Ar), 1569, 1480, 1435, 1430, 1310, 1183, 1156, 1087, 1067, 1029, 996, 909, 758, 742, 643, 518, 508.

### 6.2.4.2 Synthesis of functional azides

#### 6-Azido-hexane-1-ol (N1)



N1

A triple-neck round flask was charged with 0.115 mol (7.47 g) of sodium azide, 0.036 mol (4.934 g) 6-chloro-hexanol-1-ol and  $2.5 \cdot 10^{-4}$  mol (0.66 g) of 18-crown(6) in 25 ml dry DMF. The solution was stirred for the next 2 days at 50 °C under  $\text{N}_2$ . The  $\text{NaN}_3$  was filtered and the solvent was removed by distillation at 45 °C,  $p = 8.0 \cdot 10^{-1}$  bar.

Yield: 82 %

Empirical formula:  $\text{C}_6\text{H}_{13}\text{N}_3\text{O}$

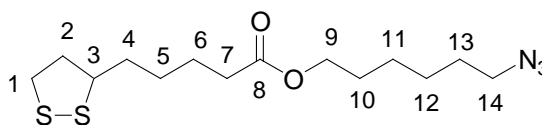
Elemental analysis: calculated: C 50,35 H 9,09 N 29,37

found: C 50,32 H 9,21 S 28,11

$^1\text{H}$  NMR (DMSO): 4.32 (t, 1H,  $\text{H}^7$ ), 3.38 (q, 1H,  $\text{H}^6$ ), 3.31 (t, 1H,  $\text{H}^1$ ), 1.53 (m, 1H,  $\text{H}^2$ ), 1.41 (m, 1H,  $\text{H}^5$ ), 1.32 (m, 2H,  $\text{H}^{3,4}$ ).

$^{13}\text{C}$  NMR (DMSO): 61.06 ( $\text{C}^6$ ), 51.10 ( $\text{C}^1$ ), 32.72 ( $\text{C}^2$ ), 28.73 ( $\text{C}^5$ ), 26.47 ( $\text{C}^3$ ), 25.45 ( $\text{C}^4$ ).

FT-IR (in  $\text{cm}^{-1}$ ): 3333 ( $\nu_{\text{OH}}$ ), 2932 – 2859 ( $\nu_{\text{s,as}}\text{CH}_2$ ), 2090 ( $\nu_{\text{N}_3}$ ), 1455 ( $\delta\text{CH}_2$ ), 1251, 1055 ( $\nu_{\text{C-O}}$ ).

*5-[1,2]Dithiolane-3-yl-pentanoic acid 6-azido-hexyl ester (N2)*

N2

To a stirred solution of 5 mmol (1.03 g) of lipoic acid dissolved in 10 mL of diethylether (anhydrous), 1 mmol (0.12 g) of DMAP and 6.6 mmol (0.945 g) of 6-chloro-1-hexanol were added and this mixture was cooled between  $-10$  and  $-5$  °C. Finally 5.5 mol (1.35 g) of DCC previously cooled to this temperature were added. The reaction mixture was stirred under these conditions for 1.5 h, then 4 h at rt. Precipitated urea is then filtered off and the filtrate was evaporated down in vacuo. The residue is taken up in  $\text{CH}_2\text{Cl}_2$  and, if necessary, filtered free of any further precipitated urea. The organic solution is washed twice with 0.5 N HCl and with saturated  $\text{NaHCO}_3$  solution, and finally dried over  $\text{Na}_2\text{SO}_4$  anhydrous. After filtration the solvent was removed under reduced pressure. The pure monomer was obtained on silica gel column (eluent: hexan: ethyl acetate v/v, 4/1) as yellow viscous liquids.

Yield: 63 %

Empirical formula:  $\text{C}_{14}\text{H}_{22}\text{N}_3\text{O}_4\text{S}_2$

Elemental analysis calculated: C 46,66 H 6,11 N 11,66 S 17,77

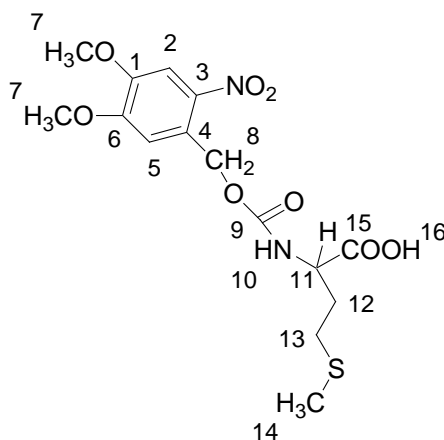
found: C 45,90 H 5,23 N 10,05 S 15,20

$^1\text{H}$  NMR( $\text{CDCl}_3$ ): 4.06 (t, 2H,  $\text{H}^9$ ), 3.54 (m, 1H,  $\text{H}^3$ ), 3.24 (t, 2H,  $\text{H}^{14}$ ), 3.15 (m, 1H,  $\text{H}^1$ ), 3.09 (m, 1H,  $\text{H}^1$ ), 2.43 (m, 1H,  $\text{H}^2$ ), 2.29 (t, 2H,  $\text{H}^7$ ), 1.88 (m, 2H,  $\text{H}^2$ ), 1.66-1.43 (m, 10H,  $\text{H}^{4,6,11,13}$ ), 1.37 (m, 4H,  $\text{H}^{11,12}$ ).

$^{13}\text{C}$  NMR ( $\text{CDCl}_3$ ): 173.38 ( $\text{C}^8$ ), 64.08 ( $\text{C}^9$ ), 56.24 ( $\text{C}^3$ ), 51.23 ( $\text{C}^{14}$ ), 40.11 ( $\text{C}^2$ ), 38.37 ( $\text{C}^1$ ), 34.49 ( $\text{C}^4$ ), 33.98 ( $\text{C}^7$ ), 28.64 ( $\text{C}^5, 13$ ), 28.42 ( $\text{C}^{10}$ ), 26.26 ( $\text{C}^{12}$ ), 25.44 ( $\text{C}^{11}$ ), 24.60 ( $\text{C}^6$ ).

FT-IR (in  $\text{cm}^{-1}$ ): 2931 - 2858 ( $\nu_{\text{s,as}}\text{CH}_2$ ), 2091 ( $\nu\text{N}_3$ ), 1729 ( $\nu\text{COO}$ ), 1456 ( $\delta\text{CH}_2$ ), 1239 ( $\nu\text{CH Ar}$ ), 1169 ( $\nu\text{C-O}$ ).

*2-(4,5-Dimethoxy-2-nitro-benzyloxycarbonylamino)-4-methylsulfanylbutyric acid (NVOC Me S)*



NVOCMeS

L-methionine (0.149 g, 1 mmol) and NaHCO<sub>3</sub> (0.21 g, 2.5 mmol) were dissolved in 20 mL of water. Then NVOC-Cl (0.304 g, 1.1 mmol) dissolved in 28 mL of dioxane was added to the solution under stirring. After 18 h, the solution was concentrated to approx. one-third of the volume under vacuum. The mixture was acidified with acetic acid and the precipitate obtained was filtered, washed several times with diluted acetic acid, and then dried under high vacuum. The product was isolated via chromatographic column using as eluent a mixture of ethyl acetate/hexane 2:3 (v/v). The product was obtained as a light yellow solid.

Yield: 79.8 %

Empirical formula: C<sub>15</sub>H<sub>20</sub>N<sub>2</sub>O<sub>8</sub>S

Elemental analysis calculated: C 49,39 H 5,15 N 7,22 S 8,24

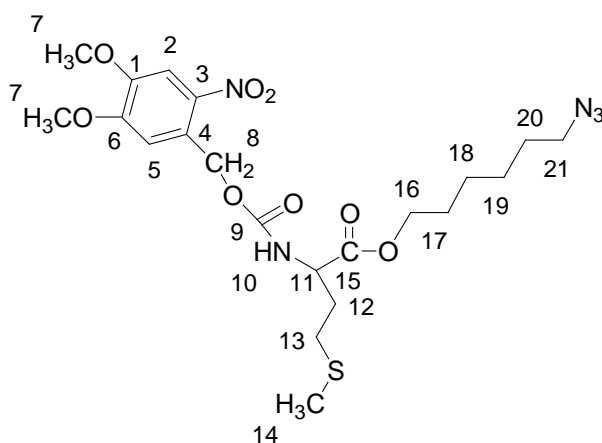
found: C 48,97 H 4,77 N 7,07 S 8,34

<sup>1</sup>H NMR(DMSO): 12.69 (br, 1H, H<sup>16</sup>), 7.84 (d, 1H, H<sup>10</sup>), 7.70 (s, 1H, H<sup>2</sup>), 7.18 (s, 1H, H<sup>5</sup>), 5.39 (q, 2H, H<sup>8</sup>), 4.11 (m, 1H, H<sup>11</sup>), 3.92 (s, 1H, H<sup>7</sup>), 3.87 (s, 1H, H<sup>7</sup>), 2.54 (m, 2H, H<sup>13</sup>), 2.03 (s, 3H, H<sup>14</sup>), 1.99 (m, 1H, H<sup>12</sup>), 1.90 (m, 1H, H<sup>12</sup>).

$^{13}\text{C}$  NMR (DMSO): 173.70 ( $\text{C}^{15}$ ), 155.93 ( $\text{C}^9$ ), 153.65 ( $\text{C}^6$ ), 147.87 ( $\text{C}^1$ ), 139.20 ( $\text{C}^3$ ), 128.34 ( $\text{C}^4$ ), 110.19 ( $\text{C}^5$ ), 108.31 ( $\text{C}^2$ ), 62.55 ( $\text{C}^8$ ), 56.25 ( $\text{C}^7$ ), 52.96 ( $\text{C}^{11}$ ), 30.59 ( $\text{C}^{12}$ ), 29.94 ( $\text{C}^{13}$ ), 14.64 ( $\text{C}^{14}$ ).

FT-IR (in  $\text{cm}^{-1}$ ): 3553 ( $\nu\text{OH}$ ), 3308 ( $\nu\text{NH}$ ), 3100 - 3019 ( $\nu\text{CH Ar}$ ), 2920 ( $\nu_{\text{s,as}}\text{CH}_2, \text{CH}_3$ ), 2851 ( $\nu\text{OCH}_3$ ), 1682 ( $\nu\text{COO}$ ,  $\text{COONH}$ ), 1581 (Amid II), 1517 ( $\nu_{\text{as}}\text{NO}$ ), 1440 ( $\delta\text{CH}_2$ ), 1423 ( $\delta\text{CH}$ ), 1381 ( $\delta_{\text{s}}\text{CH}_3$ ), 1324 ( $\nu_{\text{s}}\text{NO}$ ), 1270 ( $\nu\text{CO}$ ), 1064 ( $\nu\text{CO}$ ), 795-784 ( $\delta\text{CH Ar}$ ).

*2-(4,5-dimethoxy-2-nitro-benzyloxycarbonylamino)-4-methylsulfanyl-butyrac acid 6-azido-hexylester (N3)*



NVOCMeS Az ( $\text{N}_3$ )

NVOC MeS (0.388 g, 1mmol) and 1,1 -carbonyldiimidazol (CDI) (0.162 g, 1mol) were dissolved in 50 mL of dry THF and stirred at ambient temperature over night. Then 6-azido-1-hexanol (0.86 g, 6 mmol) was added to a stirred solution. The solution was stirred at 67 °C for 24 h under reflux and at last ethanol (40 ml) was added dropwise to the mixture. The reaction mixture was stirred under these conditions for 6 h. The solvent was removed by distillation and the product was purified by chromatographic column using as eluent a mixture of ethyl acetate/hexane 7:3 (v/v). The acid was obtained as a yellow solid.



Yield: 48 %

Empirical formula: C<sub>21</sub>H<sub>31</sub>N<sub>5</sub>O<sub>8</sub>S

Elemental analysis: calculated: C 49,12 H 6,04 N 13,64 S 6,24

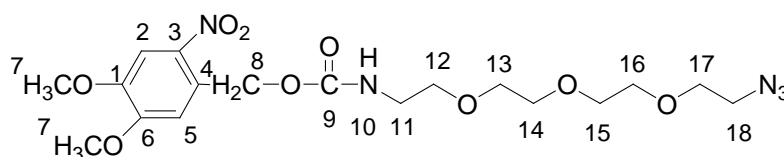
found: C 49,01 H 5,91 N 13,45 S 6,11

<sup>1</sup>H NMR(DMSO): 7.97 (d, 1H, H<sup>10</sup>), 7.71 (s, 1H, H<sup>2</sup>), 7.18 (s, 1H, H<sup>5</sup>), 5.38 (q, 2H, H<sup>8</sup>), 4.20 (m, 1H, H<sup>11</sup>), 4.05 (m, 2H, H<sup>16</sup>), 3.92 (s, 1H, H<sup>7</sup>), 3.87 (s, 1H, H<sup>7</sup>), 3.29 (t, 2H, H<sup>21</sup>), 2.53 (m, 2H, H<sup>13</sup>), 2.03 (s, 3H, H<sup>14</sup>), 1.95 (m, 1H, H<sup>12</sup>), 1.92 (m, 1H, H<sup>12</sup>), 1.54 (m, 2H, H<sup>20</sup>), 1.49 (m, 2H, H<sup>17</sup>), 1.30 (m, 4H, H<sup>18,19</sup>).

<sup>13</sup>C NMR(DMSO): 172.21 (C<sup>15</sup>), 155.88 (C<sup>9</sup>), 153.57 (C<sup>6</sup>), 147.89 (C<sup>1</sup>), 139.35 (C<sup>3</sup>), 127.96 (C<sup>4</sup>), 110.49 (C<sup>5</sup>), 108.33 (C<sup>2</sup>), 64.60 (C<sup>16</sup>), 62.67 (C<sup>8</sup>), 56.34 (C<sup>7</sup>), 56.24 (C<sup>7</sup>), 52.96 (C<sup>11</sup>), 50.69 (C<sup>21</sup>), 30.78 (C<sup>20</sup>), 30.42 (C<sup>12</sup>), 29.73 (C<sup>13</sup>), 28.22 (C<sup>17</sup>), 28.04 (C<sup>19</sup>), 25.80 (C<sup>18</sup>), 14.58 (C<sup>14</sup>).

FT-IR (in cm<sup>-1</sup>): 3308 (νNH), 3101 (νCH Ar), 2936 (ν<sub>s,as</sub>CH<sub>2</sub>, CH<sub>3</sub>), 2088 (νN<sub>3</sub>), 1740 (νCO), 1693 (νCOO, COONH), 1578 (Amid II), 1522 (ν<sub>as</sub>NO), 1437 (δCH<sub>2</sub>), 1423 (δCH), 1381 (δ<sub>s</sub>CH<sub>3</sub>), 1320 (ν<sub>s</sub> NO), 1275 (νCO), 1066 (νCO), 796 (δCH Ar).

*(2-{2-[2-(2-Azido-ethoxy)-ethoxy]-ethoxy}-ethyl)-carbamic acid 4,5-dimethoxy-2-nitro-benzyl ester (N4)*



NVOC TrO Az (N<sub>4</sub>)

11-Azido-3.6.9-trioxaneundecane-1-amine (0.22 g, 1 mmol) and NaHCO<sub>3</sub> (0.21 g, 2.5 mmol) were dissolved in water (20 mL) and under stirring a solution of NVOC-Cl (0.83 g, 3 mmol) in dioxane (28 mL) was added. The reaction mixture was kept under stirring for 18 h, and afterwards was diluted with ethyl acetate. The aqueous layer

was extracted (3x50 mL) with ethyl acetate, washed with water (2x50 mL) and finally dried over Na<sub>2</sub>SO<sub>4</sub> anhydrous. After filtration the solvent was removed under reduced pressure, and the product was isolated via column chromatography using as eluent a mixture of ethyl acetate/hexane 7:3 (v/v). The product was obtained as light yellow solid.

Yield: 47 %

Empirical formula: C<sub>18</sub>H<sub>27</sub>N<sub>5</sub>O<sub>9</sub>

Elemental analysis: calculated: C 47,26 H 5,9 N 15,32

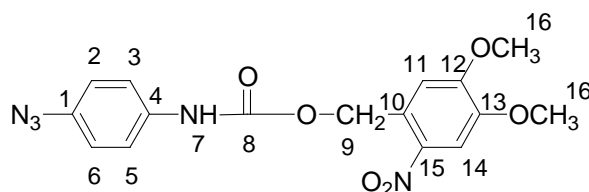
found: C 48,96 H 5,15 N 13,72

<sup>1</sup>H NMR(CDCl<sub>3</sub>): 7.69 (s, 1H, H<sup>2</sup>), 7.02 (s, 1H, H<sup>5</sup>), 5.5 (br, 3H, H<sup>8,10</sup>), 3.97-3.94 (s, 6H, H<sup>7</sup>), 3.66 (br, 4H, H<sup>13-16</sup>), 3.64 (br, 2H, H<sup>17</sup>), 3.57 (t, 2H, H<sup>12</sup>), 3.41 (q, 2H, H<sup>11</sup>), 3.36 (t, 2H, H<sup>18</sup>).

<sup>13</sup>C NMR (CDCl<sub>3</sub>): 156.0 (C<sup>9</sup>), 153.50 (C<sup>6</sup>), 148.20 (C<sup>1</sup>), 139.97 (C<sup>3</sup>), 125.48 (C<sup>4</sup>), 110.63 (C<sup>5</sup>), 108.20 (C<sup>2</sup>), 70.50 - 70.22 (br, C<sup>13-17</sup>), 69.90 (C<sup>12</sup>), 63.55 (C<sup>8</sup>), 56.45 (C<sup>7</sup>), 56.39 (C<sup>7</sup>), 40.98 (C<sup>11</sup>).

FT-IR (in cm<sup>-1</sup>): 3110 (νCH Ar), 2928 (ν<sub>s,as</sub>CH<sub>2</sub>, CH<sub>3</sub>), 2084 (νN<sub>3</sub>), 1736 (νCO), 1525 (ν<sub>as</sub>NO), 1437 (δCH<sub>2</sub>), 1423 (δCH), 1320 (ν<sub>s</sub> NO), 1275 (νCO), 1049 (νCO), 806 (δCH Ar).

*(4-Azido-phenyl)-carbamic acid 4,5-dimethoxy-2-nitro-benzyl ester (N5)*



(N<sub>5</sub>)

4-Azidoaniline hydrochloride (0.171 g, 1 mmol) and NaHCO<sub>3</sub> (0.21 g, 2.5 mmol) were dissolved in water (20 mL) and under stirring a solution of NVOC-Cl (0.304 g, 1.1 mmol) in dioxane (28 mL) was added. The reaction mixture was kept under stirring

for 24 h. The emerging precipitate was separated and afterwards was diluted with ethyl acetate. The aqueous layer was extracted (3x50 mL) with ethyl acetate, washed first time with 0.1 N HCl (50 ml) and then with water (50 ml) and brine. Finally dried over Na<sub>2</sub>SO<sub>4</sub> anhydrous. After filtration the solvent was removed under reduced pressure, and the product was isolated via column chromatography using as eluent a mixture of ethyl acetate/hexane 1:1 (v/v). The product was obtained as light yellow solid.

Yield: 58 %

Empirical formula: C<sub>16</sub>H<sub>15</sub>N<sub>5</sub>O<sub>6</sub>

Elemental analysis calculated: C 51,47 H 4,02 N 18,76

found: C 50,50 H 5,11 N 16,13

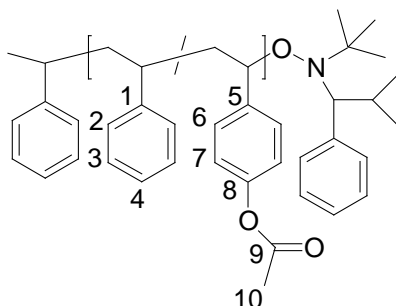
<sup>1</sup>H NMR (DMSO): 9.91 (s, 1H, H<sup>7</sup>), 7.72 (s, 1H, H<sup>14</sup>), 7.51 (d, 2H, H<sup>3,5</sup>), 7.28 (s, 1H, H<sup>11</sup>), 7.07 (d, 2H, H<sup>2,6</sup>), 5.45 (s, 2H, H<sup>9</sup>), 3.91 (s, 3H, H<sup>16</sup>), 3.88 (s, 3H, H<sup>16</sup>).

<sup>13</sup>C NMR (DMSO): 153.30 (C<sup>12</sup>), 153.04 (C<sup>8</sup>), 148.08 (C<sup>13</sup>), 139.82 (C<sup>15</sup>), 136.22 (C<sup>4</sup>), 133.45 (C<sup>1</sup>), 119.87 (br, C<sup>3</sup>), 114.57 (C<sup>2</sup>), 111.70 (C<sup>11</sup>), 108.32 (C<sup>14</sup>), 62.98 (C<sup>15</sup>), 56.37 (C<sup>16</sup>), 56.17 (C<sup>16</sup>).

FT-IR (in cm<sup>-1</sup>): 3065 - 3045 (νCH Ar), 2923 (ν<sub>s,as</sub>CH<sub>2</sub>, CH<sub>3</sub>), 2079 (νN<sub>3</sub>), 1735 (νCOO), 1523 (ν<sub>as</sub>NO), 1437 (δCH<sub>2</sub>), 1423 (δCH), 1328 (ν<sub>s</sub> NO), 1218 (νCO), 796 (δCH Ar).

## 6.2.5 Synthesis of starting precursor polymer by NMRP

## 6.2.5.1 Synthesis of poly(styrene-r-4-acetoxy-styrene)



PSPS4-OAc

Styrene (18.96 g, 0.18 mol), acetoxystyrene (3.28 g, 0.02 mol), nitroxide-initiator (0.46 g,  $7.4 \cdot 10^{-4}$  mol), and acetic anhydride (0.15 g,  $1.48 \cdot 10^{-3}$  mol) were introduced in a 250 mL flask. The mixture was degassed with freeze/thaw cycles (4) and then was kept under nitrogen atmosphere. The mixture was immersed in an oil bath preheated at 120 °C for 16 h, and then was cooled to room temperature, dissolved in  $\text{CH}_2\text{Cl}_2$  and precipitated in ethanol. The product was obtained as a white solid.

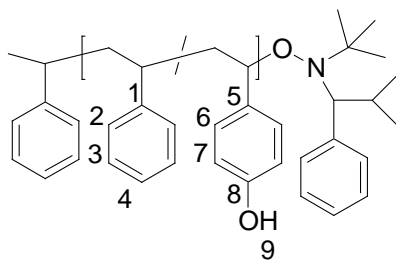
Yield: 97 %

$^1\text{H}$  NMR ( $\text{CDCl}_3$ ): 7.3 - 7.07 (br,  $\text{H}^3$ ,  $\text{H}^4$ ), 6.57 - 6.3 (br,  $\text{H}^2$ ,  $\text{H}^6$ ,  $\text{H}^7$ ), 2.26 (br,  $\text{H}^{10}$ ), 1.83 (br, CH-chain), 1.6 - 1.41 (br,  $\text{CH}_2$ -chain).

$^{13}\text{C}$  NMR ( $\text{CDCl}_3$ ): 169.20 ( $\text{C}^9$ ), 148.63 ( $\text{C}^8$ ), 145.31 ( $\text{C}^1$ ), 143.82 - 142.3 ( $\text{C}^5$ ), 129.08 - 127.96 ( $\text{C}^1$ ,  $\text{C}^2$ ,  $\text{C}^6$ ), 125.65 ( $\text{C}^4$ ), 120.86 ( $\text{C}^7$ ), 47.85 - 43.89 ( $\text{CH}_2$  - chain), 40.41 - 39.8 (CH - chain), 30.85, 21.16 ( $\text{C}^{10}$ ).

FT-IR (in  $\text{cm}^{-1}$ ): 3060 - 3026 ( $\nu_{\text{CH Ar}}$ ), 2920 ( $\nu_{\text{s,asCH}_2}$ ,  $\text{CH}_3$ ), 1761 ( $\nu_{\text{COO}}$ ), 1602 ( $\nu_{\text{C=C}}$ ), 1493 ( $\nu_{\text{C=C Ar}}$ ), 1451 ( $\delta_{\text{CH}_2}$ ), 1366 ( $\nu_{\text{OCO-CH}_3}$ ), 1197 ( $\nu_{\text{CO}}$ ), 1064 ( $\nu_{\text{CO}}$ ), 756 ( $\delta_{\text{CH Ar}}$ ).

## 6.2.5.2 Synthesis of poly(styrene-r-4-hydroxy-styrene)



PPS4-OH

Poly(styrene-r-4-acetoxy-styrene) (**PPS4-OAc**) (3.47 g, 0.02 mol) was dissolved in dioxane (200 mL). The solution was stirred for 0.5 h at room temperature and hydrazine monohydrate (6.43 g, 0.13 mol) was added to the solution. The reaction mixture was stirred for 12 h, then concentrated under vacuum and precipitated in a mixture of water/methanol (1:9, v/v). The product was obtained as a white solid.

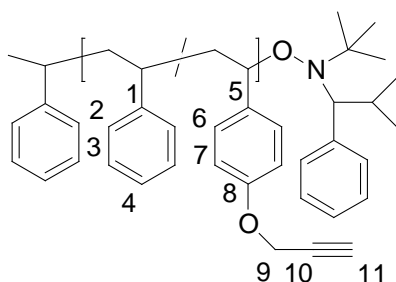
Yield: 71 %

$^1\text{H NMR}$  ( $\text{CDCl}_3$ ): 7.3 - 7.07 (br,  $\text{H}^3$ ,  $\text{H}^4$ ), 6.57 - 6.3 (br,  $\text{H}^2$ ,  $\text{H}^6$ ,  $\text{H}^7$ ), 5.20 - 4.9 (br,  $\text{H}^9$ ), 1.83 (br, CH - chain), 1.6 - 1.41 (br,  $\text{CH}_2$ -chain).

$^{13}\text{C NMR}$  ( $\text{CDCl}_3$ ): 153.24 ( $\text{C}^8$ ), 145.3 ( $\text{C}^1$ ), 137.50 - 135.46 ( $\text{C}^5$ ), 128.78 - 127.90 ( $\text{C}^1$ ,  $\text{C}^2$ ,  $\text{C}^6$ ), 125.6 ( $\text{C}^4$ ), 114.92 ( $\text{C}^7$ ), 47.85 - 43.35 ( $\text{CH}_2$  - chain), 40.41 - 39.8 (CH -chain).

FT-IR (in  $\text{cm}^{-1}$ ): 3532 ( $\nu\text{OH}$ ), 3060 - 3026 ( $\nu\text{CH Ar}$ ), 2920 ( $\nu_{\text{s,as}}\text{CH}$ ), 1602 ( $\nu\text{C=C Ar}$ ), 1493 ( $\nu\text{C=C Ar}$ ), 1451 ( $\delta\text{CH}_2$ ), 756 ( $\delta\text{CH Ar}$ ).

## 6.2.5.3 Synthesis of poly[styrene-r-4-propargyl-oxy-styrene]



PSPS4-Oprg

Poly(styrene-r-4-hydroxy-styrene) (**PSPS4-OH**) (10 g,  $10 \cdot 9.46^{-3}$  mol),  $K_2CO_3$  (3.92 g, 0.03 mol), and 18-crown-6 (0.054 g,  $10 \cdot 2.05^{-4}$  mol) were placed in a 150 mL flask and dissolved in DMF (40 mL). The mixture was degassed several times and kept under nitrogen atmosphere. While stirring for 15 min at room temperature, propargyl bromide (1.4 g, 0.02 mol) was added to the solution under nitrogen atmosphere. The mixture was stirred at 50 °C for 12 h, and cooled to room temperature. The remaining  $K_2CO_3$  left in the reaction medium was removed by filtration. The polymer solution was concentrated under reduced pressure and afterwards dissolved in  $CH_2Cl_2$  and precipitated in methanol. The product was obtained as a white solid.

Yield: 80 %

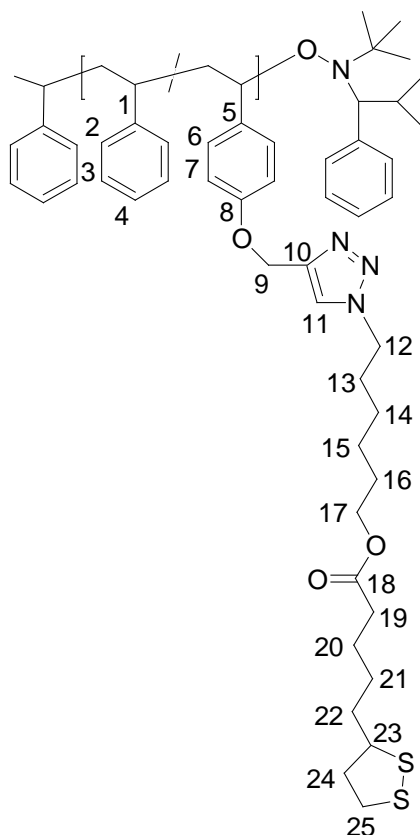
$^1H$  NMR ( $CDCl_3$ ): 7.3 - 7.08 (br,  $H^3$ ,  $H^4$ ), 6.5 - 6.3 (br,  $H^2$ ,  $H^6$ ,  $H^7$ ), 4.59 (br,  $H^9$ ), 2.45 (br,  $H^{11}$ ), 1.83 (br, CH - chain), 1.6 - 1.42 (br,  $CH_2$ -chain).

$^{13}C$  NMR ( $CDCl_3$ ): 156 ( $C^8$ ), 145.31 ( $C^1$ ), 141.82 - 138.3 ( $C^5$ ), 129.08 - 127.72 ( $C^1$ ,  $C^2$ ,  $C^6$ ), 125.05 ( $C^4$ ), 114.45 ( $C^7$ ), 78.95 ( $C^{10}$ ), 75.25 ( $C^{11}$ ), 55.9 ( $C^9$ ), 47.85 - 43.89 ( $CH_2$  - chain), 40.41 - 39.8 (CH -chain).

FT-IR (in  $cm^{-1}$ ): 3288( $\nu C\equiv C$ ), 3059 - 3025 ( $\nu CH$  Ar), 2921 ( $\nu_{s,as}CH_2$ ), 2120 ( $\nu C\equiv CH$ ), 1659 ( $\nu CO$  Ar), 1601 ( $\nu C=C$  Ar), 1493 ( $\nu C=C$  Ar), 1452 ( $\delta CH_2$ ), 1217 ( $\nu COC$ ), 1029, 757 - 697 ( $\delta CH$  Ar).

## 6.2.6 Multifunctional polymer through precursor by 1,3-dipolar cyclo-addition

### *PSPS4-Lip*



Poly(styrene-*r*-4-propargyl-oxy-styrene) (**PSPS4-OPrg**) (0.11 g,  $1 \cdot 10^{-4}$  mol), 5-[1,2]dithiolane-3-yl-pentanoic acid-6-azido-hexyl ester (0.10 g,  $4.23 \cdot 10^{-4}$  mol),  $\text{Cu}(\text{PPh}_3)_3\text{Br}$  (0.01 g,  $2.37 \cdot 10^{-5}$  mol) and DIPEA (0.06 g,  $4.78 \cdot 10^{-4}$  mol) were dissolved in dioxane (15 mL). The mixture was stirred at room temperature for 3 days. The solution was concentrated in vacuum and precipitated in ethanol. The product was obtained as a red-brownish solid.

Yield: 93 %

Empirical formula:  $[\text{C}_{10.72}\text{H}_{12.23}\text{O}_{0.51}\text{N}_{0.51}\text{S}_{0.34}]$

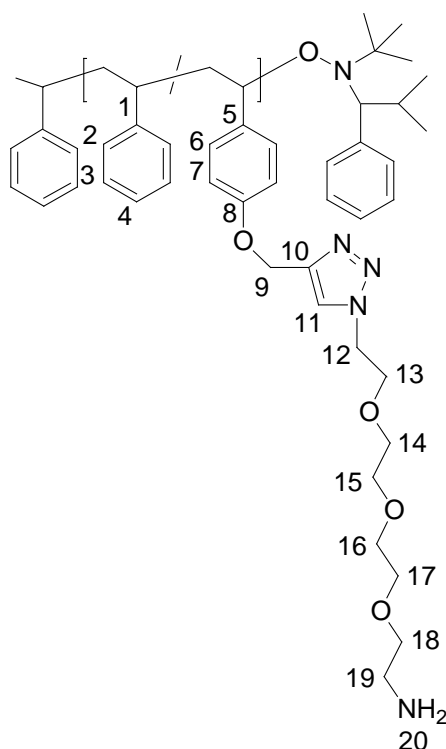
$^1\text{H NMR}(\text{CDCl}_3)$ : 7.55 (br,  $\text{H}^{11}$ ), 7.3 - 7.07 (br,  $\text{H}^3$ ,  $\text{H}^4$ ), 6.57 - 6.3 (br,  $\text{H}^2$ ,  $\text{H}^6$ ,  $\text{H}^7$ ), 5.12 (br,  $\text{H}^9$ ), 4.32 (br,  $\text{H}^{12}$ ), 4.06 (br,  $\text{H}^{17}$ ), 3.57 (br,  $\text{H}^{23}$ ), 3.15-

3.11 (br, H<sup>25</sup>), 2.45 (m, H<sup>24</sup>), 2.31 (t, H<sup>19</sup>), 1.91 (m, H<sup>24</sup>); 1.83 (br, CH-chain), 1.68 (H<sup>20</sup>), 1.6 - 1.41 (br, CH<sub>2</sub>-chain), 1.46 (H<sup>14</sup>, H<sup>15</sup>, H<sup>21</sup>).

<sup>13</sup>C NMR(CDCl<sub>3</sub>): 173.2 (C<sup>18</sup>), 156 (C<sup>8</sup>), 145.31 (C<sup>1</sup>), 144.47 (C<sup>10</sup>), 141.82 - 138.3 (C<sup>5</sup>), 129.08 - 127.72 (C<sup>1</sup>, C<sup>2</sup>, C<sup>6</sup>), 125.05 (C<sup>4</sup>), 122.29, 114.45 (C<sup>7</sup>), 64.00 (C<sup>17</sup>), 62.20 (C<sup>9</sup>), 56.33 (C<sup>23</sup>), 50.20 (C<sup>12</sup>), 47,85 - 43.89 (CH<sub>2</sub> - chain), 40.41 (C<sup>24</sup>), 40.32– 39.8 (CH –chain), 38.43 (C<sup>25</sup>), 34.53 (C<sup>22</sup>), 34.02 (C<sup>19</sup>), 30.10 (C<sup>13</sup>), 28.69 (C<sup>21</sup>), 28.39 (C<sup>16</sup>), 26.10 (C<sup>14</sup>), 25.37 (C<sup>15</sup>), 24.65 (C<sup>20</sup>).

FT-IR (in cm<sup>-1</sup>): 3059 - 3025 (νCH Ar), 2919 (ν<sub>s,as</sub>CH<sub>2</sub>), 1727 (νCOO), 1602 (νC=C Ar), 1584 (-N=N-), 1509 (νC=C Ar), 1451 (δCH<sub>2</sub>), 1303 (ν CN), 1237 (νCO), 757 - 699 (δCH Ar).

### *PSPS4-TrONH<sub>2</sub>*



Poly [styrene-*r*-4-propargyl-oxy-styrene] (**PSPS4-OPrg**), (0.1 g, 1·10<sup>-4</sup> mol), 11-azido-3.6.9-trioxaminedecene-1-amine (0.09 g, 4.12·10<sup>-4</sup> mol), Cu(PPh<sub>3</sub>)<sub>3</sub>Br (0.02 g, 2.17·10<sup>-5</sup> mol) and DIPEA (0.09 g, 4.79·10<sup>-4</sup> mol) were dissolved in dioxane (15 mL).



The mixture was stirred at room temperature for 3 days. The solution was concentrated in vacuum and precipitated in ethanol. The product was obtained as a green-blue solid.

Yield: 87 %

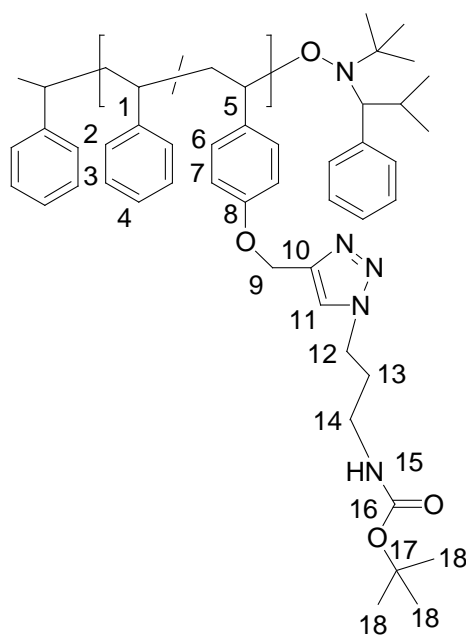
Empirical formula:  $[C_{9.65}H_{11.00}O_{0.6}N_{0.6}]$

$^1H$  NMR ( $CDCl_3$ ): 7.70 ( $H^{11}$ ), 7.3 - 6.85 (br,  $H^3$ ,  $H^4$ ), 6.45 (br,  $H^2$ ,  $H^6$ ,  $H^7$ ), 5.07 (br,  $H^9$ ), 4.97 (br,  $H^{20}$ ), 4.45 ( $H^{12}$ ), 3.76 (br,  $H^{13}$ ), 3.49 (br,  $H^{14}$ ,  $H^{15}$ ,  $H^{16}$ ,  $H^{17}$ ,  $H^{18}$ ), 2.41 (br,  $H^{19}$ ), 1.71 (br, CH-chain), 1.30 (br,  $CH_2$ -chain).

$^{13}C$  NMR ( $CDCl_3$ ): 155.63 ( $C^8$ ), 145.3 ( $C^1$ ), 138 ( $C^5$ ), 127.96 ( $C^2$ ,  $C^3$ ,  $C^6$ ), 125.64 ( $C^4$ ), 122.67 ( $C^{11}$ ), 114.35 ( $C^7$ ), 114.26 ( $C^{10}$ ), 70.51 - 70.48 ( $C^{14}$ ,  $C^{15}$ ,  $C^{16}$ ,  $C^{17}$ ), 69.85 ( $C^{18}$ ), 69.15 ( $C^{13}$ ), 63.55, 62.27 ( $C^9$ ), 58.40, 42.90 ( $C^{19}$ ), 47.85 - 43.89 ( $CH_2$ -chain), 40.43 (CH-chain).

FT-IR (in  $cm^{-1}$ ): 3286 ( $\nu$  NH), 3082 - 3025 ( $\nu$ CH Ar), 2921 ( $\nu_{s,as}CH_2$ ), 1601 ( $\nu$ C=C Ar), 1583 ( $\nu$  -N=N-), 1509 ( $\nu$ C=C Ar), 1452 ( $\delta$ CH<sub>2</sub>), 1263 ( $\nu$ CO), 758 - 698 ( $\delta$ CH Ar).

### *PSPS4-t*-BOC



Poly[styrene-*r*-4-propargyl-oxy-styrene] (**PSPS4-OPrg**) (0.203 g,  $2 \cdot 10^{-4}$  mol), (3-azido-propyl)-carbamic acid tert-butyl ester (0.12 g,  $5.9 \cdot 10^{-4}$  mol),  $\text{Cu}(\text{PPh}_3)_3\text{Br}$  (0.037 g,  $3.99 \cdot 10^{-5}$  mol) and DIPEA (0.077 g,  $6 \cdot 10^{-4}$  mol) were dissolved in dioxane (15 mL). The mixture was stirred at room temperature for 3 days. The solution was concentrated under vacuum and precipitated in ethanol. The product was obtained as an orange-brownish solid.

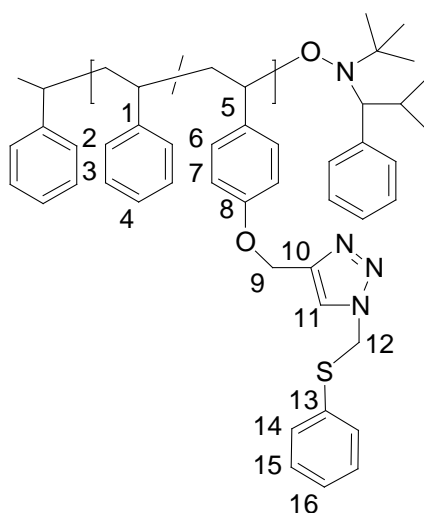
Yield: 46 %

$^1\text{H}$  NMR ( $\text{CDCl}_3$ ): 7.65 (br,  $\text{H}^{11}$ ), 7.3 - 7.07 (br,  $\text{H}^3$ ,  $\text{H}^4$ ), 6.57 - 6.3 (br,  $\text{H}^2$ ,  $\text{H}^6$ ,  $\text{H}^7$ ), 5.11 (br,  $\text{H}^9$ ), 4.81 (br,  $\text{H}^{15}$ ), 4.39 (br,  $\text{H}^{12}$ ), 3.13 (br,  $\text{H}^{14}$ ), 2.07 (br,  $\text{H}^{13}$ ), 1.83 (br, CH-chain), 1.6 - 1.41 (br,  $\text{CH}_2$ -chain).

$^{13}\text{C}$  NMR( $\text{CDCl}_3$ ): 156.24 ( $\text{C}^8$ ), 156.07 ( $\text{C}^{16}$ ), 145.24 ( $\text{C}^1$ ), 144.60 ( $\text{C}^{10}$ ), 141.82 - 138.3 ( $\text{C}^5$ ), 129.08 - 127.72 ( $\text{C}^1$ ,  $\text{C}^2$ ,  $\text{C}^6$ ), 125.05 ( $\text{C}^4$ ), 122.83 ( $\text{C}^{11}$ ), 114.45 ( $\text{C}^7$ ), 79.5 ( $\text{C}^{17}$ ), 62.11 ( $\text{C}^9$ ), 47.85 ( $\text{C}^{12}$ ), 47.59 - 43.89 ( $\text{CH}_2$  - chain), 40.41 - 39.8 ( $\text{CH}$  -chain) , 37.33 ( $\text{C}^{14}$ ), 30.69 ( $\text{C}^{14}$ ), 28.37 ( $\text{C}^{18}$ ).

FT-IR (in  $\text{cm}^{-1}$ ): 3419 ( $\nu\text{NH}$ ), 3059 - 3025 ( $\nu\text{CHAR}$ ), 2921 ( $\nu_{\text{s,as}}\text{CH}_2$ ,  $\text{CH}_3$ ), 1710 ( $\nu\text{COO}$ ,  $\text{NHCOO}$ ), 1601 ( $\nu\text{C}=\text{CAr}$ ), 1584 ( $\nu\text{-N}=\text{N-}$ ), 1508 ( $\nu\text{C}=\text{CAr}$ ), 1451 ( $\delta\text{CH}_2$ ), 1365 ( $\delta(\text{C}(\text{CH}_3))$ ), 1243 ( $\nu\text{CO}$ ), 757 - 698 ( $\delta\text{CH Ar}$ ).

### *PSPS4-ThP*



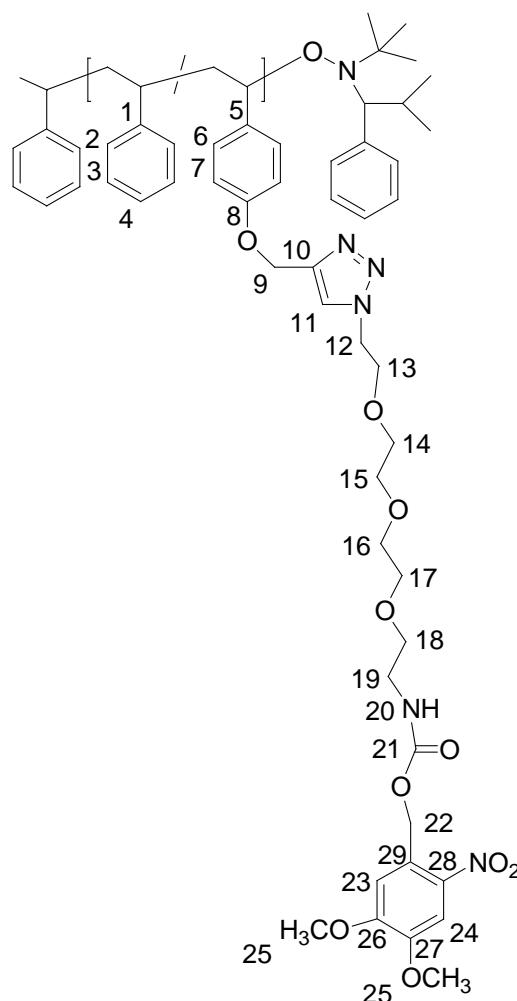
Poly [styrene-*r*-4-propargyl-oxy-styrene] (PSPS4-OPrg) (0.1 g,  $1 \cdot 10^{-4}$  mol), azidomethyl phenylsulfide (0.049 g,  $2.99 \cdot 10^{-4}$  mol),  $\text{Cu}(\text{PPh}_3)_3\text{Br}$  (0.02 g,  $2.13 \cdot 10^{-5}$  mol) and (DIPEA) (0.039 g,  $3.02 \cdot 10^{-4}$  mol) were dissolved in dioxane (15 mL). The mixture was stirred at 60 °C for 3 days under  $\text{N}_2$  atmosphere. The solution was concentrated under vacuum and precipitated in ethanol. The product was obtained as an orange-brownish solid.

Yield: 47 %

$^1\text{H}$  NMR ( $\text{CDCl}_3$ ): 7.55 (br,  $\text{H}^{11}$ ), 7.30 (m,  $\text{H}^{14}$ ), 7.26 - 7.07 (br,  $\text{H}^3$ ,  $\text{H}^4$ ,  $\text{H}^{15}$ ,  $\text{H}^{16}$ ), 6.57 - 6.3 (br,  $\text{H}^2$ ,  $\text{H}^6$ ,  $\text{H}^7$ ), 5.57 (br,  $\text{H}^{12}$ ), 5.08 (br,  $\text{H}^9$ ), 1.83 (br, CH-chain), 1.6 – 1.41 (br,  $\text{CH}_2$ -chain).

$^{13}\text{C}$  NMR( $\text{CDCl}_3$ ): 156 ( $\text{C}^8$ ), 145.31 ( $\text{C}^1$ ,  $\text{C}^{10}$ ), 141.82 - 138.3 ( $\text{C}^5$ ), 132.14 ( $\text{C}^{14}$ ), 131.89 ( $\text{C}^{13}$ ), 129.51 ( $\text{C}^{15}$ ), 129.08 - 127.72 ( $\text{C}^1$ ,  $\text{C}^2$ ,  $\text{C}^6$ ), 128.71 ( $\text{C}^{16}$ ), 128.08 - 127.72 ( $\text{C}^1$ ,  $\text{C}^2$ ,  $\text{C}^6$ ), 125.05 ( $\text{C}^4$ ), 122.06 ( $\text{C}^{11}$ ), 114.45 ( $\text{C}^7$ ), 78.95 ( $\text{C}^{10}$ ), 75.25 ( $\text{C}^{11}$ ), 62.10 ( $\text{C}^9$ ), 55.9 ( $\text{C}^9$ ), 53.88 ( $\text{C}^{12}$ ), 47.85 - 43.89 ( $\text{CH}_2$ - chain), 40.41 – 39.8 (CH –chain).

FT-IR (in  $\text{cm}^{-1}$ ): 3058-3024 ( $\nu_{\text{CH Ar}}$ ), 2919 ( $\nu_{\text{s,asCH}_2}$ ), 1601 ( $\nu_{\text{C=C Ar}}$ ), 1583 ( $\nu_{\text{N=N}}$ ), 1509 ( $\nu_{\text{C=C Ar}}$ ), 1451 ( $\delta_{\text{CH}_2}$ ), 1232 ( $\nu_{\text{CO}}$ ), 748-698 ( $\delta_{\text{CH Ar}}$ ).

*PSPS4-NVOCTrO*

Poly [styrene-*r*-4-propargyl-oxy-styrene] (**PSPS4-OPrg**) (0.164 g,  $1 \cdot 10^{-4}$  mol), (2-{2-[2-azido-ethoxy]-ethoxy]-ethoxy}-ethoxy)-ethyl)-carbamic acid 4,5-dimethoxy-2-nitro-benzyl ester (0.165 g,  $3.72 \cdot 10^{-4}$  mol),  $\text{Cu}(\text{PPh}_3)_3\text{Br}$  (0.023 g,  $2.47 \cdot 10^{-5}$  mol) and DIPEA (0.053 g,  $4.1 \cdot 10^{-4}$  mol) were dissolved in dioxane. The mixture was stirred at room temperature for 3 days under  $\text{N}_2$  atmosphere. The solution was concentrated under vacuum and precipitated in ethanol. The product was obtained as an orange-brownish solid.

Yield: 24 %

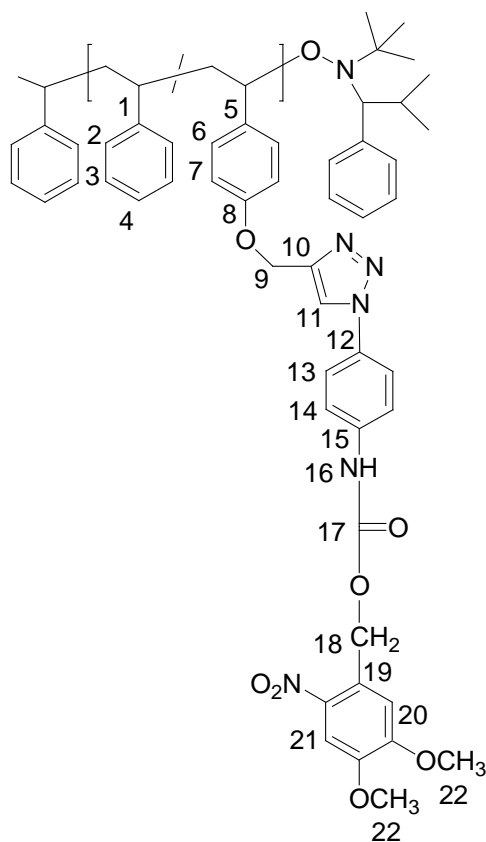
$^1\text{H NMR}(\text{CDCl}_3)$ : 7.75 (br,  $\text{H}^{11}$ ), 7.68 (s,  $\text{H}^{25}$ ), 7.3 - 7.05 (br,  $\text{H}^3$ ,  $\text{H}^4$ ,  $\text{H}^{24}$ ), 6.51 - 6.3 (br,  $\text{H}^2$ ,  $\text{H}^6$ ,  $\text{H}^7$ ), 5.49 (br,  $\text{H}^{20}$ ,  $\text{H}^{22}$ ), 5.09 (br,  $\text{H}^9$ ), 4.51 (br,  $\text{H}^{12}$ ), 3.94-3.91 (br,  $\text{H}^{26}$ ), 3.88 (s,  $\text{H}^{13}$ ), 3.57 (br,  $\text{H}^{14}$ ,  $\text{H}^{15}$ ,  $\text{H}^{16}$ ,  $\text{H}^{17}$ ),

3.53 (br, H<sup>18</sup>), 3.37 (br, H<sup>19</sup>), 1.82 (br, CH-chain), 1.6 - 1.42 (br, CH<sub>2</sub>-chain).

<sup>13</sup>C NMR(CDCl<sub>3</sub>): 156.33 (C<sup>8</sup>), 156.01 (C<sup>21</sup>), 153.51 (C<sup>26</sup>), 148.21 (C<sup>27</sup>), 145.3 (C<sup>1</sup>), 141.26 (C<sup>10</sup>), 139.99 (C<sup>28</sup>), 138.0 (C<sup>5</sup>), 128.0 (C<sup>2</sup>, C<sup>3</sup>, C<sup>6</sup>), 125.64 (C<sup>13</sup>), 125.48 (C<sup>29</sup>), 123.78 (C<sup>11</sup>), 114.20 (C<sup>7</sup>), 110.65 (C<sup>23</sup>), 108.24 (C<sup>24</sup>), 70.51 - 70.24 (C<sup>14</sup>, C<sup>15</sup>, C<sup>16</sup>, C<sup>17</sup>), 69.92 (C<sup>18</sup>), 69.44 (C<sup>13</sup>), 63.55 (C<sup>22</sup>), 62.15 (C<sup>9</sup>), 56.45 (C<sup>25</sup>), 56.40 (C<sup>25</sup>), 50.28 (C<sup>12</sup>), 40.98 (C<sup>19</sup>, CH<sub>2</sub>-chain), 40.2 (CH-chain).

FT-IR (in cm<sup>-1</sup>): 3349 (νNH), 3082 - 3025 (νCH Ar), 2922 (ν<sub>s,as</sub>CH<sub>2</sub>, CH<sub>3</sub>), 1727 (νCOO, NHCOO), 1601 (νC=C Ar), 1582 (ν-N=N-), 1522 (ν<sub>s,as</sub>-N=O), 1510 (νC=C Ar), 1452 (δCH<sub>2</sub>), 1329 (ν<sub>s</sub>NO), 1262 (νCO), 757 - 698 (δCH Ar).

### PSP4-AN



Poly [styrene-*r*-4-propargyl-oxy-styrene] (PSPS4-OPrg) (0.1 g,  $1 \cdot 10^{-4}$  mol), (4-azidophenyl)-carbamic acid 4,5-dimethoxy-2-nitro-benzyl ester (0.102 g,  $2.73 \cdot 10^{-4}$  mol),  $\text{Cu}(\text{PPh}_3)_3\text{Br}$  (0.008 g,  $9.12 \cdot 10^{-6}$  mol) and DIPEA (0.035 g,  $2.73 \cdot 10^{-4}$  mol) were dissolved in dioxane (15 ml). The mixture was stirred at ambient temperature for 3 days under  $\text{N}_2$  atmosphere. The solution was concentrated under vacuum and precipitated in water. The product was obtained as a brown solid.

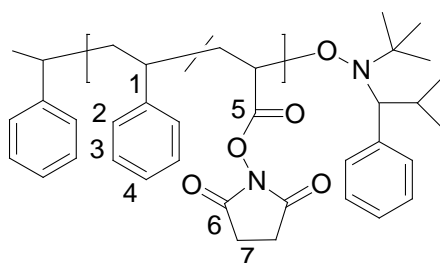
Yield: 72 %

$^1\text{H}$  NMR( $\text{CDCl}_3$ ): 9.91 (s,  $\text{H}^{16}$ ), 7.75 (s,  $\text{H}^{11}$ ), 7.71 (s,  $\text{H}^{21}$ ), 7.50 (d,  $\text{H}^{14}$ ), 7.27 (s,  $\text{H}^{20}$ ), 7.07 (d,  $\text{H}^{13}$ ), 7.05 (br,  $\text{H}^3$ ,  $\text{H}^4$ ), 6.54 (br,  $\text{H}^2$ ,  $\text{H}^6$ ,  $\text{H}^7$ ), 5.44 (s,  $\text{H}^{18}$ ), 5.07 (br,  $\text{H}^9$ ), 3.90 (s,  $\text{H}^{22}$ ), 3.87 (s,  $\text{H}^{22}$ ), 1.82 (br, CH-chain), 1.45 (br,  $\text{CH}_2$ -chain).

$^{13}\text{C}$  NMR ( $\text{CDCl}_3$ ): 156.12 ( $\text{C}^8$ ), 153.49 ( $\text{C}^{23}$ ), 152.87 ( $\text{C}^{17}$ ), 148.43 ( $\text{C}^{24}$ ), 145.78 ( $\text{C}^1$ ), 144.32 ( $\text{C}^{10}$ ), 139.78 ( $\text{C}^{25}$ ), 136.85 ( $\text{C}^5$ ), 136.18 ( $\text{C}^{15}$ ), 133.36 ( $\text{C}^{12}$ ), 127.92 ( $\text{C}^2$ ,  $\text{C}^3$ ,  $\text{C}^6$ ), 121.46 ( $\text{C}^{11}$ ), 119.59 ( $\text{C}^{14}$ ), 114.58 ( $\text{C}^{13}$ ), 114.16 ( $\text{C}^7$ ), 111.50 ( $\text{C}^{20}$ ), 108.31 ( $\text{C}^{21}$ ), 63.53 ( $\text{C}^{18}$ ), 62.95 ( $\text{C}^{25}$ ), 62.12 ( $\text{C}^9$ ), 56.35 ( $\text{C}^{22}$ ), 56.14 ( $\text{C}^{22}$ ), 47.85 - 43.89 ( $\text{CH}_2$ -chain), 40.41 (CH-chain).

FT-IR (in  $\text{cm}^{-1}$ ): 3367 ( $\nu\text{NH}$ ), 3081-3025 ( $\nu\text{CH}$  Ar), 2921 ( $\nu_{\text{s,as}}\text{CH}_2$ ,  $\text{CH}_3$ ), 1740 ( $\nu\text{COO}$ ,  $\text{NHCOO}$ ), 1602 ( $\nu\text{C}=\text{C}$  Ar), 1582 ( $\nu\text{-N}=\text{N-}$ ), 1523 ( $\nu_{\text{s,as}}\text{-N}=\text{O}$ ), 1510 ( $\nu\text{C}=\text{C}$  Ar), 1452 ( $\delta\text{CH}_2$ ), 1330 ( $\nu_{\text{s}}\text{NO}$ ), 1278 ( $\nu\text{CO}$ ), 757-698 ( $\delta\text{CH}$  Ar).

## PS-AE



PS/AE

Styrene (14.123 g, 0.135 mol), N-acryloxysuccinimide (2.554 g, 0.015 mol), nitroxide-initiator ( $0.231 \text{ g}, 3.7 \cdot 10^{-4} \text{ mol}$ ), and acetic anhydride ( $0.075 \text{ g}, 7.41 \cdot 10^{-4} \text{ mol}$ ) were introduced in a 250 mL flask. The mixture was degassed with freeze/thaw cycles (4) and then was kept under nitrogen atmosphere. The mixture was immersed in an oil bath preheated at  $120 \text{ }^\circ\text{C}$  for 16 h, and then was cooled to room temperature, dissolved in  $\text{CH}_2\text{Cl}_2$  and precipitated in ethanol. The product was obtained as a white solid.

Yield:	82 %
$^1\text{H}$ NMR ( $\text{CDCl}_3$ ):	7.08 (br, $\text{H}^3, \text{H}^4$ ), 6.59 (br, $\text{H}^2$ ), 2.67 (br, $\text{H}^7$ ), 1.83 (br, CH-chain), 1.42 (br, $\text{CH}_2$ -chain).
$^{13}\text{C}$ NMR( $\text{CDCl}_3$ ):	171.39 ( $\text{C}^5$ ), 168.94 ( $\text{C}^6$ ), 145.28 ( $\text{C}^1$ ), 127.99 ( $\text{C}^2$ ), 127.70 ( $\text{C}^3$ ), 125.65 ( $\text{C}^4$ ), 43.95 ( $\text{CH}_2$ -chain), 40.46 (CH-chain), 25.55 ( $\text{C}^7$ ).
FT-IR (in $\text{cm}^{-1}$ ):	3037 - 3025 ( $\nu_{\text{CH Ar}}$ ), 2928 ( $\nu_{\text{s,asCH}_2}$ ), 1818, 1785 (imide peaks), 1735 ( $\nu_{\text{C=O}}$ ), 1659 ( $\nu_{\text{CO Ar}}$ ), 1601 ( $\nu_{\text{C=C Ar}}$ ), 995 - 870 ( $\delta_{\text{CH Ar}}$ ).

## 7 List of symbols and abbreviations

Ac <sub>2</sub> O	Acetic anhydride
AES	Auger Electron Spectroscopy
AFM	Atomic Force Microscopy
AIBN	2,2'-Azobis-(isobutyronitrile)
APAS	Sodium-4-acryloyl-aminophenyldiazosulfonate
ASP	Set Point Amplitude
ATR	Attenuated Total Reflection
ATRA	Atom Transfer Radical Addition
ATRP	Atom Transfer Radical Polymerization
Boc	<i>tert.</i> -Butylcarbamate-
°C	Temperature in degrees Celsius
CDI	1,1'-Carbonyldiimidazole
CHCl <sub>2</sub>	Dichloromethane
CHCl <sub>3</sub>	Chloroform
CTA	Chain Transfer agent
CuBr <sub>2</sub>	Copper(II)bromid
CRP	Controlled Radical Polymerization
DCC	N,N'-Dicyclohexylcarbodiimide
DHLA	Dihydrolipoic acid
DIPEA	<i>N,N</i> -Diisopropylethylamine
DMAP	4-Dimethylamino-pyridine
DMF	<i>N,N</i> -Dimethylformamide
DMSO	Dimethylsulfoxide
DNA	Deoxyribonucleic acid
DNBOC	Di(nitrobenzyl)oxycarbonyl group
DIPC	Diisopropylcarbodiimide
DIPEA	<i>N,N</i> -Diisopropylethylamine
DPTS	4-( <i>N,N'</i> -dimethyl)-aminopyridinium tosylate
DSC	Differential Scanning Calorimetry
DUV	Deep Ultraviolet



---

EA	Elementary analysis
$E_b$	Binding energy of the electron
$E_{kin}$	Kinetic energy
$E_{X-ray}$	Energy of the X-rays
EBL	Electron Beam Lithography
e.g.	for example
Eq	Equation
$Et_3N$	Triethylamine
EUV	Extreme Ultraviolet
FIB	Focused Ion Beam Lithography
FITC	Fluorescein isothiocyanate
FRP	Free Radical Polymerisation
FT-IR	Fourier-Transformations-Infrarot-Spektroskopie
g	gram
GPC	Gel Permeation Chromatography
h	hour
HCl	Hydrochloric acid
HOBT	1-Hydroxybenzotriazole
i.e.	that is
$I_2$	Initiator
$k_d$	Dissociation rate coefficient of initiators I
$k_p$	Propagation rate coefficient
LB	Langmuir-Blodgett
$\mu$ CP	Microcontact Printing
M	Monomer
MCT	Mercury/ cadmium/ tellurium
ml	millilitre
MMA	Methylmethacrylate
$M_n$	Number average molar mass (g/mol)
$M_w$	Weight average molar mass (g/mol)
$M_w/ M_n$	Molar mass distribution
mol	mole
mol%	Mole percent

---

N	Degree of polymerization
NaHCO <sub>3</sub>	Sodium bicarbamate
NaOH	Sodium hydroxide
NaN <sub>3</sub>	Sodium azide
Na <sub>2</sub> SO <sub>4</sub>	Sodium sulfate
NBOC	Nitrobenzyloxycarbonyl
NHS	N-hydroxysuccinimide
nm	nanometer
NMR	Nuclear Magnetic Resonance Spectroscopy
NMRP	Nitroxide-Mediated Radical Polymerization
NVOC	4,5-Dimethoxy-2-nitrobenzyl-oxycarbonyl
ONB	o-Nitrobenzyl group
p	Pressure (bar)
P	Polymer
PAG	Photoacid generator
PCBs	Printed circuit boards
PD	Polydispersity
PDI	Polydispersity index
PDMS	Polydimethylsiloxane
PRE	Persistent Radical Effect
PRPG	Photoremovable protecting group
QCM	Quartz Crystal Microbalance
RAIRS	Reflection Adsorption Infrared Spectroscopy
R <sub>i</sub> <sup>•</sup>	Propagating radical
R <sub>p</sub>	Reflection coefficients for the parallel component
R <sub>s</sub>	Reflection coefficients for the perpendicular component
-r-	<i>random-</i>
RAFT	Reversible Addition Fragmentation Chain Transfer Polymerization
Rq	Roughness („root mean square (RMS)“)
Rsp	Set-Point Amplitude Ratio
RT	Ambient temperature
S	Transfer agent
SAM	Self-Assembled Monolayer

---

SAW	Surface Acoustic wave
SEM	Scanning Electron Microscopy
SIMS	Secondary Ion Mass Spectroscopy
SPR	Surface Plasmon Resonance
STM	Scanning Tunneling Microscopy
T	Temperature
TEMPO	2,2,6,6-Tetramethyl-piperidin- <i>N</i> -oxyl
TFA	Trifluoroacetic acid,
T <sub>g</sub>	Glass transition temperature (°C)
TGA	Thermal Gravimetric Analysis
THF	Tetrahydrofuran
TM	Tapping Mode
TMSPA	3-(Trimethoxysilyl)propylmethacrylate
UHV	Ultrahigh vacuum
UV	Ultraviolet
VDW	van der Waals
wt%	weight percent
XPS	X-ray Photoelectron Spectroscopy
YOYO-1	1,1'-(4,4,7,7 – Tetramethyl - 4,7 - diazaundecamethylene) - bis - 4 - [3 - methyl - 2,3 - dihydro - (benzo-1,3-oxazde) - 2- methylidene]
$\gamma$	surface interfacial tension (energy) (mJ/m <sup>2</sup> )
(iΔ)	Phase of the light
$\Phi$	Workfunction of the spectrometer
$\Theta$	Contact angle (deg)
$\rho$	Film density of the chromophere
$\epsilon$	Molar absorption coefficient.
$\Psi$	Amplitude of the light

## 8 REFERENCES

- [Abb94] Abbot, N.; Kumar, A.; Whitesides, G. M. *Chem. Mater.* **1994**, 6, 596.
- [AhT04] Ah Toy, A.; Vana, P.; Davis, T.P.; Barner-Kowollik, C. *Macromolecules*, **2004**, 37, 744.
- [All85] Allara, D. L.; Nuzzo, R. G. *Langmuir* **1985**, 1, 45.
- [All85a] Allara, D. L.; Nuzzo, R. G. *Langmuir* **1985**, 1, 52.
- [Ard90] Arduengo, A. J. III; Moran, J. R.; Rodriguez-Parada, J.; Ward, M. D. *J. Am. Chem. Soc.* **1990**, 112, 6153.
- [Arn89] Arndt, Th.; Schupp, H.; Schepp, W. *Thin Solid Films* **1989**, 178, 319.
- [Aro02] Arotcarena, M.; Heise, B.; Ishaya, S.; Laschewsky, A. *J. Am. Chem. Soc.* **2002**, 124, 3787.
- [Arv94] Arvanopoulos, L. D.; Greuel, M. P.; Harwood, H. J. *Amer. Chem. Soc. Polym. Preprints* **1994**, 35, 549.
- [Aul04] Auletta, T.; Dordi, B.; Mulder, A.; Sartori, A.; Onclin, S.; Bruinink, C. M.; Peter, M.; Nijhuis, C. A.; Beijleveld, H.; Schonherr, H.; Vancso, G. J.; Casnati, A.; Ungaro, R.; Ravoo, B. J.; Huskens, J.; Reinhoudt, D. N. *Angew. Chem. Int. Ed.* **2004**, 43, 369.
- [Bah99] Bahatia, R.; Garrison, B. J. *Langmuir* **1997**, 13, 4038.
- [Bai89] Bain, C. D.; Troughton, E. B.; Tao, Y. T.; Evall, J.; Whitesides, G. M.; Nuzzo, R. G. *J. Am. Chem. Soc.* **1989**, 111, 321.
- [Bai89a] Bain, C. D.; Whitesides, G. M. *Angew. Chem. Int. Ed. Engl.* **1989**, 28, 506.
- [Bal05] Balmer, T. E.; Schmid, H.; Stutz, R.; Delamarche, E.; Michel, B.; Spencer, N.; Wolf, H. *Langmuir* **2005**, 21, 622.
- [Bar62] Barltrop, J. A.; Schofield, P. *Tetrahedron Lett.* **1962**, 16, 697.
- [Bar66] Barltrop, J. A.; Plant, P. J., Schofield, P. *Chem. Commun.* **1966**, 822.
- [Bar01] Barner-Kowollik, C.; Quinn, J.F.; Morsley, D.R.; Davis, T.P. *J. Polym. Sci. Part A: Polym. Chem.*, **2001**, 39, 1353.
- [Bar03] Barner-Kowollik, C.; Davis, T.P.; Heuts, J.P.A.; Stenzel, M.H.; Vana, P.; Whittaker, M. *J. Polym. Sci. Part A: Polym. Chem.*, **2003**, 41, 365.

- [Bar98] Barclay, G. G.; Hawker, C. J.; Ito, H.; Orellana, A.; Malenfant, P. R. L.; Sinta, R. F. *Macromolecules* **1998**, 31, 1024.
- [Bau01] Baumann, M.; Schmidt-Naake G. *Macromol.Chem. Phys.*, **2001**, 202, 2727.
- [Bea92] Beamson, G.; Briggs, D. "High resolution of organic polymers" The Sienta ESCA 300 Database, J. Wiley & Sons, Chichester, New York, Brisbane, Toronto, Singapur, **1992**, ISBN 0-471-93592-1.
- [Bee04] Beer, P. D.; Cormode, D. P.; Davis, J. *J. Chem. Commun.* **2004**, 414.
- [Beh96] Behm, J. M.; Lykke, K. R.; Pellin, M. J.; Hemminger, J. C. *Langmuir* **1996**, 12, 2121.
- [Ben99] Benoit, D.; Chaplinski, V.; Braslau, R.; Hawker, C. J. *J. Am. Chem. Soc.* **1999**, 121, 3904.
- [Ben00] Benoit, D.; Grimaldi, S.; Robin, S.; Finet, J. P.; Tordo, P.; Gnanou, Y. *J. Am. Chem. Soc.* **2000**, 122, 5929.
- [Ben00a] Benoit, D.; Harth, E.; Fox, P.; Waymouth, R. M.; Hawker, C. J. *Macromolecules* **2000**, 33, 363.
- [Ben94] Bensimon, A.; Simon, A.; Chiffaudel A.; Croquette, V.; Heslot, F.; Bensimon, D. *Science*, **1994**, 265, 2096.
- [Ber95] Berggren, K. K.; Bard, A.; Wilbur, J. L.; Gillaspay, J. D.; Helg, A. G.; McClelland, J. J.; Rolston, S. L.; Phillips, W. D.; Prentiss, M.; Whitesides, G. M. *Science* **1995**, 269, 1255.
- [Bha93] Bharathi, S.; Yegnaraman, V.; Rao, G. P. *Langmuir* **1993**, 9, 1614.
- [Big46] Bigelow, W. C.; Pickett, D. L.; Zisman, W. A. *J. Colloid Interface Sci.* **1946**, 1, 513.
- [Bla57] Blackman, L. C. F.; Dewar, M. J. S. *J. Chem. Soc.* **1957**, 171.
- [Bla57a] Blackman, L. C. F.; Dewar, M. J. S.; Hampson, H. *J. Appl. Chem.* **1957**, 7, 160.
- [Blo35] Blodgett, K.B. *J. Am. Chem. Soc.* **1935**, 57, 1007.
- [Blo37] Blodgett, K.B., Langmuir, I. *Phys. Rev.* **1935**, 51, 964.
- [Boc02] Bochet, C. G. *J. Chem. Soc., Perkin Trans.* **2002**, 1, 125.
- [Bra99] Brandts, J. A. M.; van de Geijn, P.; van Faassen, E. E.; van Koten, G.; Boersma, J. *J. Organomet. Chem.* **1999**, 584, 246.

- [Bra02] Braun, F.; Eng, L.; Loppacher, S.; Trogisch, S.; Voit, B. *Macromol. Chem. Phys.* **2002**, 203, 1781.
- [Bra03] Braun, F.; Eng, L.; Trogisch, S.; Voit, B. *Macromol. Chem. Phys.* **2003**, 204, 1486.
- [Bru94] Brust, M.; Walker, M.; Bethell, D.; Schiffrin, D. J.; Whyman, R. *J. Chem. Soc, Chem. Commun.* **1994**, 801.
- [Bru95] Brust, M.; Bethell, D.; Schiffrin, D. J.; Kiely, C. *J. Adv. Mater.* **1995**, 7, 795.
- [Bry92] Bryant, M. A.; Joa, S. L.; Pemberton, J. E. *Langmuir* **1992**, 8, 753.
- [Cha03] Chabinyk, M. L.; Love, J. C.; Thywissen, J. H.; Cervelli, F.; Prentiss, M. G.; Whitesides, G. M. *Langmuir* **2003**, 19, 2201.
- [Che99] Chen, X. Y.; Jankova, K.; Kops, J.; Batsberg Pedersen. *J. Polym. Sci., Part A* **1999**, 37, 627.
- [Che03] Chen, Y.; Ohlberg, D. A. A.; Li, X.; Stewart, D. R.; Jeppesen, J. O.; Nielsen, K. A.; Stoddart, J. F.; Olynick, D. L.; Anderson, E. *Appl. Phys. Lett.* **2003**, 82, 1610.
- [Che06] Cheng, J. Y.; Ross, C. A.; Smith, H. I.; Thomas, E. L. *Advanced Materials* **2006**, 18(19), 2505.
- [Cho95] Chou, S. Y.; Krauss, P. R.; Renstrom, P. J. *Appl. Phys. Lett.* **1995**, 67, 3114.
- [Cho96] Chou, S. Y.; Krauss, P. R.; Renstrom, P. J. *J. Vac. Sci. Technol.* **1996**, B14, 4129.
- [Chi98] Chiefari, J.; Chong, Y. K.; Ercole, F.; Krstina, J.; Jeffery, J.; Le, T. P. T.; Mayadunne, R. T. A.; Meijs, G. F.; Moad, C. L.; Moad, G.; Rizzardo, E.; Thang, S. H. *Macromolecules* **1998**, 31, 5559.
- [Chi99] Chiefari, J.; Mayadunne, R.T.A.; Moad, G.; Rizzardo, E.; Thang, S. H. PCT Int. Appl. WO 9931144 A1 990624; *Chem. Abstr.*, **1999**, 131, 45250.
- [Coh86] Cohen, S. R.; Naaman, R.; Sagiv, J. *J. Phys. Chem.* **1986**, 90, 3054.
- [Coo93] Cooper, J. M.; Greenough, K. R.; McNeil, C. J. *J. Electroanal. Chem.* **1993**, 347, 267.

- [Dav99] Davis, B. G.; Khumtaveeporn, K.; Bott, R. R.; Jones, J. B. *Bioorg. & Med. Chem.* **1999**, *7*, 2303.
- [Dei03] Deiters, A.; Cropp, T. A.; Mukherji, M.; Chin, J. W.; Anderson, J. C.; Schultz, P. G. *J. Am. Chem. Soc.* **2003**, *125*, 11782.
- [Dem93] Demoz, A.; Harrison, D. J. *Langmuir* **1993**, *9*, 1046.
- [Des00] Destarac, M.; Charmot, D.; Franck, X.; Zard, S.Z. *Macromol. Rapid Commun.* **2000**, *21*, 1035.
- [Dev13] Devaux, H. *Smithsonian Institute Ann. Rep.* **1913**, 261.
- [DiV04] DiVentra, M.; Evoy, S.; Heflin, J. R. "Introduction to nanoscale science and technology", Kluwer, Boston, MA, **2004**.
- [Dix99] Dixon, K. W, in *Polymer Handbook*, 4th ed., J. Brandrup, E. H. Immergut, and E. A. Grulke, Wiley, New York, 1999, p. II/12.
- [Don02] Donovan, M. S.; Sumerlin, B. S.; Lowe, A. B.; McCormick C. L. *Macromolecules*, **2002**, *35*, 8663.
- [Dub92] Dubois, L. H.; Nuzzo, R. G. *Annu. Phys. Chem.* **1992**, *43*, 437.
- [Dus05] Dusseiller, M. R.; Schläpfer, D.; Koch, M.; Kroschewski, R.; Textor, M. *Biomaterials* **2005**, *26*, 5917.
- [Eas76] Eastmond, G.C. in "Comprehensive Chemical Kinetics", eds. C.H. Bamford, C.F.H. Tipper, Vol. 14A, chap. 1, Elsevier, Amsterdam, **1976**.
- [Eas76a] Eastmond, G.C. in "Comprehensive Chemical Kinetics", eds. C.H. Bamford, C.F.H. Tipper, Vol. 14A, chap. 3, Elsevier, Amsterdam, **1976**.
- [Eas76b] Eastmond, G.C. in "Comprehensive Chemical Kinetics", eds. C.H. Bamford, C.F.H. Tipper, Vol. 14A, chap. 2, Elsevier, Amsterdam, **1976**.
- [Edw89] Edwards, T. R. G.; Cunnane, V. J.; Parsons, R.; Gani, D. *J. Chem. Soc, Chem. Commun.* **1989**, *15*, 1041.
- [Eng80] Engel. P. S. *Chem. Rev.* **1980**, *80*, 99.
- [Eva91] Evans, S. D.; Goppert-Berarducci, K. E.; Urankar, E.; Gerenser, L. J.; Ulman, A.; Snyder, R. G. *Langmuir* **1991**, *7*, 2700.
- [Fen94] Fenter, P; Eberhardt, A; Eisenberger, P. *Science* **1994**, *266*, 1216.
- [Fis86] Fischer, H. *J. Am. Chem. Soc.* **1986**, *108*, 3925.
- [Fis97] Fischer, H. *Macromolecules*, **1997**, *30*, 5666.
- [Fis99] Fischer, H. *J. Polym. Sci., Part A: Polym. Chem.* **1999**, *37*, 1885.
- [Fis01] Fischer, H. *Chem. Rev.* **2001**, *101*, 3581.

- [Fla84] Flack, W.W.; Soong, D.S.; Bell, A.T.; Hess, D.W. *J. Appl. Phys.* **1984**, 56, 1199.
- [Fod91] Fodor, S. P. A.; Read, J. L.; Pirrung, M. C.; Stryer, L; Lu, A. T.; Solas, D *Science*, **1991**, 251, 767.
- [Fra74] Franklin, B.; Brownrigg, W. & Favish *Phil. Trans. R. Soc.* **1974**, 64, 445.
- [Fra04] Franssila, S. *Introduction to Microfabrication*, John Wiley & Sons, New York **2004**.
- [Fre73] Frens, G. *Nat. Phys. Sci.* **1973**, 241, 20.
- [Gat05] Gates, B. D.; Xu, Q.; Stewart, M.; Ryan, D.; Willson, C. G.; Whitesides, G. M. *Chem. Rev.* **2005**, 105, 1171.
- [Gay95] Gaynor, S. G.; Wang, J. S.; Matyjaszewski, K. *Macromolecules* **1995**, 28, 8051.
- [Gay96] Gaynor, S. G., Edelman, S.; Matyjaszewski, K. *Macromolecules* **1996**, 29, 1079.
- [Geo93] Georges, M. K.; Veregin, R. P. N.; Kazmaier, P. M.; Hamer, G. K. *Macromolecules* **1993**, 26, 2987.
- [Geo93a] Georges, M. K.; Veregin, R. P. N.; Kazmaier, P. M.; Hamer, G. K. *Polym. Mater. Sci. Eng.* **1993**, 68, 6.
- [Geo94] Georges, M. K.; Veregin, R. P. N.; Kazmaier, P. M.; Hamer, G. K.; Saban, M. *Macromolecules*, **1994**, 27, 7228.
- [Ger96] Gerdy, J. J.; Goodard, W. A. *J. Am. Chem. Soc* **1996**, 118, 3233.
- [Gey01] Geyer, W.; Stadler, V.; Eck, W.; Gölzhäuser, A.; Grunze, M.; Sauer, M.; Weimann, T.; Hinze, P. *J. Vac. Sci. Technol., B* **2001**, 19, 2732.
- [Gic05] Gichner, T.; Mukherjee, A.; Wagner, E.D.; Plewa, M.J. *Mutat. Res.* **2005**, 586, 38.
- [Gin04] Ginger, D. S.; Zhang, H.; Mirkin, C. A. *Angew. Chem. Int. Ed. Engl.* **2004**, 43, 30.
- [Giv93] Givens, R.S.; Athey, P.S.; Matuszewski, B.; Kueper, L.W.; Xue, J.Y.; Fister, T. *J. Am. Chem. Soc.* **1993**, 115, 6001.
- [Glo00] Gloor, A. P., Hoare, S. M., Lawless, K., Steinauer, R. A., White, P.; Yong, C. W., "Novabiochem synthesis notes ". **1994**.



- [Gra04] Gray, M. K.; Zhou, H. Y.; Nguyen, S. T.; Torkelson, J. M. *Macromolecules* **2004**, 37, 5586.
- [Gu95] Gu, Y.; Lin, Z.; Smentkowski, V. S.; Waldeck, D. H. *Langmuir* **1995**, 11, 1849.
- [Gur97] Gurrieri, S; Wells, K. S.; Johnson, I. D.; Bustamante, C. *Anal Biochem.* **1997**, 249, 44.
- [Had95] Haddleton, D. M.; Waterson, C.; Derrick, P. J.; Jasieczek, C. B.; Shooter, A. J. *Chem. Commun.* **1997**, 683.
- [Har96] Harwood, H. J.; Christov, L.; Guo, M.; Holland, T. V.; Huckstep, A. Y.; Jones, D. H.; Medsker, R. E.; Rinaldi, P. L.; Saito, T.; Tung, D. S. *Macromol. Symp.* **1996**, 111, 25.
- [Har12] Hardy, W. B. *Proc. R. Soc. A.* **1912**, 86, 610.
- [Har01] Harth, E.; van Horn, B.; Hawker, C.J. *Chem. Commun.* **2001**, 823.
- [Hau02] Haugland, R. P. *Molecular Probes Inc.*, Eugene, Oregon, USA **2002**.
- [Haw96] Hawker, C.J.; Barclay, G.G.; Orellana, A.; Dao, J.; Devonport, W. *Macromolecules*, **1996**, 29, 5245.
- [Haw96a] Hawker, C.J.; Barclay, G.G.; Dao, J. *J. Am. Chem. Soc.* **1996**, 118, 11467.
- [Haw01] Hawker, C.J.; Bosman, A.W.; Harth, E. *Chem. Rev.* **2001**, 101, 3661.
- [Hie06] Hien, O.; Komber, H.; Voit, B.; Krasteva, N.; Yasuda, A.; Vossmeier, T. *JNPN* **2006**, 2/4, 109.
- [Hil93] Hill, W.; Wehling, B. *J. Phys. Chem.* **1993**, 97, 9451.
- [Hui64] Huisgen, R.; Grashey, R.; Sauer, J. in *S. Patai: Alkenes. Interscience*, New York, **1964**, 1, 739.
- [Hul02] Hull, R.; Chraska, T.; Liu, Y.; Long, D. *Mater. Sci. Eng.C.* **2002**, 19, 383.
- [Ihr98] Ihre, H.; Hult, A.; Frechet, J. M.; Gitsov, I. *Macromolecules* **1998**, 31, 4061.
- [Ihs93] Ihs, A.; Uvdal, K.; Liedberg, B. *Langmuir* **1993**, 9, 733.
- [Ihs94] Ihs, A.; Liedberg, B. *Langmuir* **1994**, 10, 734.
- [Jac95] Jackman, R. J.; Wilbur, J. L.; Whitesides, G. M. *Science* **1995**, 269, 664.
- [Jun98] Jung, Ch.; Dannenberger, O.; Xu, Y.; Buck, M.; Grunze, M. *Langmuir* **1998**, 14, 1103.

- [Kal03] Kaltenpoth, G.; Himmelhaus, M.; Slansky, L.; Caruso, F.; Grunze, M. *Adv. Mater.* **2003**, 15, 1113.
- [Kap95] Kapuscinski, J. *Biotech. Histochem.* **1995**, 70, 220.
- [Kat92] Katz, E.; Itzhak, N.; Willner, I. *J. Electroanal. Chem.* **1992**, 336, 357.
- [Kat95] Kato, M.; Kamigaito, M.; Sawamoto, M.; Higashimura, T. *Macromolecules* **1995**, 28, 1721.
- [Kaw00] Kawasaki, M.; Sato, T.; Tanaka, T.; Takao, K. *Langmuir* **2000**, 16, 1719.
- [Kaz97] Kazmaier, P. M., Daimon, K., Georges, M. K., Hamer, G. K., Veregin, R. P. N. *Macromolecules* **1997**, 30, 2228.
- [Keo98] Keoshkerian, B.; Georges, M. K.; Quinlan, M.; Veregin, R.; Goodbrand, R. *Macromolecules*, **1998**, 31, 7559.
- [Kha45] Kharasch, M. S.; Jensen, E. V.; Urry, W. H. *Science*, **1945**, 102, 128.
- [Kim98] Kim, C. S.; Oh, S. M.; Kim, S.; Cho, C. G. *Macromol. Rapid. Commun.* **1998**, 19, 191.
- [Kluth99] Kluth, G. J.; Carraro, C.; Maboudian, R. *Phys. Rev. B* **1999**, 59, R10449.
- [Kol01] Kolb, H. C.; Finn, M. G.; Sharpless, K. B. *Angew. Chem. Int. Ed.* **2001**, 40, 2004.
- [Kol03] Kolb, H. C.; Sharpless, B. *Drug Discovery Today* **2003**, 8(24), 1128.
- [Kot99] Kotani, Y.; Kamigaito, M.; Sawamoto, M. *Macromolecules* **1999**, 32, 2420.
- [Kra03] Krämer, S.; Fuierer, R. R.; Gorman, C. B. *Chem. Rev.* **2003**, 103, 4367.
- [Kum93] Kumar, A.; Whitesides, G. M. *Appl. Phys. Lett.* **1993**, 63, 2002.
- [Lai92] Laibinis, P. E.; Whitesides, G. M. *J. Am. Chem. Soc.* **1992**, 114, 1990.
- [Lai92a] Laibinis, P. E.; Whitesides, G. M. *J. Am. Chem. Soc.* **1992**, 114, 9022.
- [Law88] Lawrence, C. J. *Phys. Fluids* **1988**, 31, 2786.
- [Lan04] Langer, R.; Tirrel, D. A. *Nature* **2004**, 428, 487.
- [Lan17] Langmuir, I. *J. Am. Chem. Soc.*, **1917**, 39, 1848.
- [Le98] Le, T.P.; Moad, G.; Rizzardo, E.; Thang, S.H. PCT Int. Appl. WO 9801478 A1 980115; *Chem. Abstr.* **1998** 128, 115390.
- [Lec97] Lecomte, P.; Drapier, J.; Dubois, P.; Teyssie, P.; Jerome, R. *Macromolecules* **1997**, 30, 7631.

- [Lee04] Lee, K.; Pan, F.; Carroll, G. T.; Turro, N. J.; Koberstein, J. T. *Langmuir* **2004**, 20, 1812.
- [Lec97] Lecomte, P.; Drapier, I.; Dubois, P.; Teyssié, P.; Jérôme, R. *Macromolecules* **1997**, 30, 7631.
- [Leu02] Leuteritz, A.; Messerschmidt, M.; Voit, B.; Yin, M.; Krause, T.; Habicher, W.D. *Polymer Preprint* **2002**, 43, 283.
- [Lew04] Lewis, W. G.; Magallon, F. G.; Fokin, V.V.; Finn, M. G. *J. Am. Chem. Soc.* **2004**, 126, 9152.
- [Li84] Li, T.-T. T.; Liu, H. Y.; Weaver, M. J. *J. Am. Chem. Soc.* **1984**, 106, 1233.
- [Li93] Li, D.; Swanson, B.I.; Robinson, J. M.; Hoffbauer, M.A. *J. Am. Chem. Soc.* **1993**, 115, 6975.
- [Lii97] Li, I. Q.; Howell, B. A.; Dineen, M. T.; Kastl, P. E.; Lyons, J. W.; Meunier, D. M.; Smith, P. B.; Priddy, D. B. *Macromolecules* **1997**, 30, 5194.
- [Lin03] Link, A. J.; Tirrell, D. A. *J Am Chem Soc.* **2003**, 125, 11164.
- [Lin04] Lin, S.-Y.; Tsai, Y.-T.; Chen, C.-C.; Lin, C.-M.; Chen, C.-H. *J. Phys. Chem.* **2004**, 108, 2134.
- [Lin04a] Lin, H.; Walsh, C. T. *J. Am. Chem. Soc.* **2004**, 126, 13998.
- [Liu00] Liu, G.-Y.; Xu, S.; Qian, Y. *Acc. Chem. Res.* **2000**, 33, 457.
- [Loo02] Loo, Y. L.; Willett, R. L.; Baldwin, K. W.; Rogers, J. A. *J. Am. Chem. Soc.* **2002**, 124, 7654.
- [Lov05] Love, J. C.; Estroff, L. A.; Kriebel, J. K.; Nuzzo, R. G.; Whitesides, G. M. *Chem. Rev.* **2005**, 105, 1103.
- [Lut01] Lutz, J. F.; Lacroix-Desmazes, P. P.; Boutevin, B. *Macromol. Rapid. Commun.* **2001**, 22, 189.
- [Mal97] Malmström, E.; Miller, R. D.; Hawker C.J. *Tetrahedron*, **1997**, 53, 15225.
- [Mal99] Malkoch, M.; Schleicher, K.; Drockenmuller, E.; Hawker, C. J.; Russel, T. P.; Wu, P.; Fokin, V. V. *Macromolecules* **2005**, 38, 3663.
- [Mao88] Maoz, R.; Netzner, L.; Gun, J.; Sagiv, J; *J. Chim. Phys. (Paris)* **1988**, 85, 1059.
- [Mat 95] Matyjaszewski, K.; Gaynor, S.; Greszta, D.; Mardare, D.; Shigemoto, T. *Macromol. Symp.* **1995**, 98, 73.

- [Mat95a] Matyjaszewski, K.; Gaynor, S.; Greszta, D.; Mardare, D.; Shigemoto, T.; Wang, J.-S. *Macromol. Symp.*, **1995**, 95, 217.
- [Mat95b] Matyjaszewski, K.; Gaynor, S.; Wang, J. S. *Macromolecules* **1995**, 28, 2093.
- [Mat97] Matyjaszewski, K.; Wei, M.; Xia, J.; McDermott, N. E. *Macromolecules* **1997**, 30, 8161.
- [Mat98] Matyjaszewski, K.; Kajiwara, A.; Wang, J.S. WO 9630421; U.S. Pat. 5763548, **1998**, 31, 548.
- [Mat02] Matyjaszewski, K. *Curr. Org. Chem.* **2002**, 6, 67.
- [Mat02a] Matyjaszewski, K.; Davis, T. in *Handbook of Radical Polymerization*, John Willey & Sons, New Jersey, **2002**.
- [Mat02b] Matyjaszewski, K. *Macromolecular Symposia*, **2002**, 183(1), 71.
- [Mat05] Matyjaszewski K; Spanswick J. *Materials today*, **2005**, 8, 26.
- [May99] Mayadunne, R. T. A.; Rizzardo, E.; Chiefari, J.; Chong, Y. K.; Moad, G.; Thang, S. H. *Macromolecules* **1999**, 32, 6977.
- [May00] Mayadunne, R. T. A.; Rizzardo, E.; Chiefari, J.; Kristina, J.; Moad, G.; Postma, A.; Thang, S. H. *Macromolecules* **2000**, 33, 243.
- [Mel03] Mele, E.; Di Benedetto, F.; Persano, L.; Pisignano, D.; Cingolani, R. *Nanotechnology* **2005**, 16, 391.
- [Mer07] Mertig, M. *Micromaterials and Nanomaterials* **2007**, 7, 44.
- [Mes06] M. Messerschmidt, *Ph.D Thesis* TU Dresden, **2006**.
- [Mes08] Messerschmidt, M.; Millaruelo, M.; Komber, H.; Häußler, L.; Voit, B.; Krause, T.; Yin, M.; Habicher, W.D. *Macromolecules* **2008**, 41, 2821.
- [Mic01] Michel, B.; Bernard, A.; Bietsch, A.; Delamarche, E.; Geissler, M.; Juncker, D.; Kind, H.; Renault, J. P.; Rothuizen, H.; Schmid, H.; Schmidt-Winkel, P.; Stutz, R.; Wolf, H. *IBM J. Res. & Dev.* **2001**, 45, 697.
- [Mic02] Michel, B.; Bernard, A.; Bietsch, A.; Delamarche, E.; Geissler, M.; Juncker, D.; Kind, H.; Renault, J. P.; Rothuizen, H.; Schmid, H.; Schmidt-Winkel, P.; Stutz, R.; Wolf, H. *Chimia* **2002**, 56, 527.
- [Mie91] Mielczarski, J. A.; Yoon, R. H. *Langmuir* **1991**, 7, 101.
- [Min75] Minisci, F. *Acc.Chem. Res.* **1975**, 8, 165.

- [Min96] Minamii, N., Yamada, B. in *Polymeric Materials Encyclopedia*, Salamone, J. C. ed. CRC Press, Boca Raton, FL, **1996**, 432.
- [Moa89] Moad, G.; Solomon, D. H. in *Comprehensive Polymer Science*, eds. Eastmond, G. C.; Ledwith, A.; Russo, S.; Sigwalt, P. eds. Pergamon, London, **1989**, 3, 97.
- [Moa96] Moad, C. L.; Moad, G.; Rizzardo, E.; Thang, S. H. *Macromolecules* **1996**, 29, 7717.
- [Moi99] Moineau, G.; Minet, M.; Dubois, P.; Teyssié, P.; Senninger, T.; Jérôme, R. *Macromolecules* **1999**, 32, 27.
- [Mos02] Moses, J. E.; Moorhouse, A. D. *Chem. Soc. Rev.*, **2007**, 36, 1249.
- [Mus95] Muskal, N.; Turyan, I.; Shurky, A.; Mandler, D. *J. Am. Chem. Soc.* **1995**, 117, 1147.
- [New91] Newkome, G. R., Behera, R. K., Moorefield, C. N., Baker, G. R. *J. Org. Chem.* **1991**, 56, 7162.
- [Ngu97] Nguyen, D. M.; Mayer, T. M.; Hubbard, S. F.; Singer, K. D.; Mann, J. A.; Lando, J. B. *Macromolecules* **1997**, 30, 6150.
- [Nuz83] Nuzzo, R. G.; Allara, D. L. *J. Am. Chem. Soc.* **1983**, 105, 4481.
- [Nuz87] Nuzzo, R. G.; Fusco, F. A.; Allara, D. L. *J. Am. Chem. Soc.* **1987**, 109, 2358.
- [Oga85] Ogawa, H.; Chihera, T.; Taya, K. *J. Am. Chem. Soc.* **1985**, 107, 1365.
- [Opi04] Opitz, J.; Braun, F.; Seidel, R.; Pompe, W.; Voit, B.; Mertig, M. *Nanotechnology* **2004**, 15, 717.
- [Ots82] Otsu, T.; Yoshiba, M. *Macromol. Chem. Rapid Commun* **1982**, 3, 127.
- [Ots82a] Otsu, T.; Yoshiba, M.; Tazaki, T. *Macromol. Chem. Rapid Commun* **1982**, 3, 133.
- [Qui85] Quinga, E. M. Y.; Mendenhall, G. D. *J. Org. Chem* **1985**, 50, 2836.
- [Qui89] Quirk, R. P.; Kinning, D. J.; Fetters, L.J. In *Comprehensive Polymer Science*; Aggarwal, S. L., Ed.; Pergamon Press: London, **1989**, 7, 1.
- [Pat70] Patchornik, A.; Amit, B.; Woodward, R. B. *J. Am. Chem. Soc.* **1970**, 92, 6333.
- [Pirr93] Pirrung, M. C.; Lee, Y. R. *J. Org. Chem.* **1993**, 58, 6961.
- [Poc891] Pockels, A. *Nature* **1891**, 43, 437.
- [Poc892] Pockels, A. *Nature* **1892**, 46, 418.

- [Ree78] Reese, C. B. *Tetrahedron* **1978**, 34, 3143.
- [Riz87] Rizzardo, E. *Chem.Aust.* **1987**, 54, 32.
- [Riz95] Rizzardo, E.; Meijs, G. F.; Tang, S. H. *Macromol. Symp.* **1995**, 98, 101.
- [Rob90] Roberts, G. Ed. *Langmuir-Blodgett Films*, Plenum Press, New York, **1990**.
- [Ros02] Rostovtsev, V. V.; Green, L. G.; Fokin, V. V.; Sharpless, K. B. *Angew. Chem.* **2002**, 114, 2708.
- [Ryz07] Ryzhkov, P.; Ostermann, K.; Blüher, A.; Mertig, M.; Rödel, G. *Phys.Sta. Sol.* **2007**, 204, 1863.
- [Sab93] Sabatani, E.; Cohen-Boulakia, J.; Bruening, M.; Rubinstein, I. *Langmuir* **1993**, 9, 2974.
- [Sag80] Sagiv, J. *J. Am. Chem. Soc.* **1980**, 102, 92.
- [Sam92] Samant, M. G.; Brown, C. A.; Gordon, J. G. *Langmuir* **1992**, 8, 1615.
- [San03] Santhanam, V.; Andres, R.P. *Nano Lett.* **2004**, 4, 41.
- [Sch86] Schlotter, N. E.; Porter, M. D.; Bright, T. B.; Allara, D. L. *Chem. Phys. Lett.* **1986**, 132, 93.
- [Sch95] Schlenoff, J. B.; Li, M.; Ly, H. *J. Am. Chem. Soc.* **1995**, 117, 12528.
- [Sch99] Schwedhelm, R.; Schlomka, J. - P.; Woedtke, S.; Adelung, R.; Kipp, L.; Tolan, M.; Press, W.; Skibowski, M. *Phys. Rev. B* **1999**, 59, 13394.
- [Scho99] Schön, J. H.; Kloc, C.; Batlogg, B. *Science* **2001**, 293, 2432.
- [Sche04] Scheel, A.; Komber, H.; Voit, B. *Macromol. Rapid Commun.* **2004**, 25, 1175.
- [Sha04] Shadnam, M. R.; Kirkwood, S. E.; Fedosejevs, R.; Amirfazli, A. *Langmuir* **2004**, 20, 2667.
- [She92] Sheen, C. W.; Shi, J. X.; Martensson, J.; Parikh, A. N.; Allara, D. L. *J. Am. Chem. Soc.* **1992**, 114, 1514.
- [Shi94] Shimazu, K.; Sato, Y.; Yagi, I.; Uosaki, K. *Bull. Chem. Soc. Jpn.* **1994**, 67, 863.
- [Shi01] Shinoda, H.; Matyjaszewski, K. *Macromol. Rapid Commun.*, **2001**, 22, 1176.
- [Sin94] Singh, N. P.; Stephens, R. E.; Schneider, E. L. *Int. J. Radiat. Biol.* **1994**, 66, 23.

- [Sol86] Solomon, D. H.; Rizzardo, E. and Cacioli P. U.S. patent **1986**, 4, 581, 429.
- [Spe03] Speers, A. E.; Adam, G. C.; Cravatt, B. F. *J Am Chem Soc.* **2003**, 125, 4686.
- [Sta62] Staab, H. A. *Angew. Chem. Int. Ed.* **1962**, 1, 351.
- [Ste86] Stewart, K. R.; Whitesides, G. M.; Godfried, H. P.; Silvera, I. F. *Rev. Sci. Instrum.* **1986**, 57, 1381.
- [Str88] Strong, L.; Whitesides, G. M. *Langmuir* **1988**, 4, 546.
- [Str90] Stratmann, M. *Adv. Mater.* **1990**, 2, 191.
- [Sum01] Sumerlin, B.S.; Donovan, M.S.; Mitsukami, Y.; Lowe, A. B.; McCormick, C. L. *Macromolecules*, **2001**, 34, 6561.
- [Sun02] Sun, S.; Chong, K. S. L.; Leggett, G. J. *J. Am. Chem. Soc.* **2002**, 124, 2414.
- [Swa87] Swalen, J. D.; Allara, D. L.; Andrade, J. D.; Chandross, E. A.; Garoff, S.; Israelchvili, J.; McCarthy, T. J.; Murray, R.; Pease, R. F.; Rabolt, J. F.; Wynne, K. J.; Yu, H. *Langmuir* **1987**, 3, 932.
- [Tab80] Tabor, D. *J. Colloid Interface Sci.* **1980**, 75, 240.
- [Til89] Tillman, N.; Ulman, A.; Penner, T. L. *Langmuir* **1989**, 5, 101.
- [Tom99] Tompkins, H. G.; McGahan, W. A. *Spectroscopic Ellipsometry and Reflectometry: A User's Guide.* John Wiley & Sons, New York, **1999**.
- [Tor02] Toroe, C. W.; Christensen, C.; Meldal, M. *J. Org. Chem.* **2002**, 67, 3057.
- [Tro88] Troughton, E. B.; Bain, C. D.; Whitesides, G. M.; Nuzzo, R. G.; Allara, D. L.; Porter, M. D. *Langmuir* **1988**, 4, 365.
- [Tsa02] Tsarevsky, N.V.; Sarbu, T.; Gobelt, B.; Matyjaszewski, K. *Macromolecules* **2002**, 35, 6142.
- [Tur53] Turner, R. B. *J. Amer. Chem. Soc.* **1953**, 75, 3489.
- [Ueg97] Uegaki, H.; Kotani, Y.; Kamigaito, M.; Sawamoto, M. *Macromolecules* **1997**, 30, 2249.
- [Ulm89] Ulman, A. *J. Mat. Ed.* **1989**, 11, 205.
- [Ulm91] Ulman, A. *An Introduction to Ultrathin Organic Films*, Academic Press: Boston, **1991**, Chap. 2.
- [Ulm96] Ulman, A. *Chem. Rev.* **1996**, 96, 1533.

- [Uvd92] Uvdal, K.; Bodo, P.; Liedberg, B. *J. Colloid Inter. Sci.* **1992**, 149, 162.
- [Vee00] Van der Veen, N.J.; Flink, S.; Deij, M.; A.; Egberink, R. J. M.; van Veggel, F. C. J. M.; Reinhoudt, D. N. *J. Am. Chem. Soc.* **2000**, 122, 6112.
- [Ver93] Veregin, R. P. N.; Georges, M. K.; Kazmaier, P. M.; Hamer, G. K. *Macromolecules*, **1993**, 26, 5316.
- [Vof63] Vofsi, D.; Asscher, M. *J. Chem. Soc.* **1963**, 3921.
- [Voi04] Voit, B.; Braun, F.; Loppacher, Ch.; Trogisch, S.; Eng, L. M.; Seidel, R.; Gorbunoff, A.; Pompe, W.; Mertig, M. *ACS Symposium Series* **2004**, 874, 118.
- [Voi07] Voit, B.; Fleischmann, S.; Komber, H.; Scheel, A.; Stumpe, K. *Macromolecular Symposia* **2007**, 254, 16.
- [Vol90] Volmer, M.; Stratmann, M.; Viefhaus, H. *Surf. Interface Anal.* **1990**, 16, 278.
- [Wal91] Walczak, M. M.; Chung, C.; Stole, S. M.; Widrig, C. A.; Porter, M. D. *J. Am. Chem. Soc.* **1991**, 113, 2370.
- [Wal01] Walbert, S.; Pfeleiderer, W.; Steiner, U. E.; *Helvetica Chimica Acta* **2001**, 84(6),1601.
- [Wan86] Wan, P.; Yates, K. *Can. J. Chem.* **1986**, 64, 2076.
- [Wan95] Wang, J. S.; Matyjaszewski, K. *J. Am. Chem. Soc.* **1995**, 117, 5614.
- [Wan95a] Wang, J. S.; Matyjaszewski, K. *Macromolecules*. **1995**, 28, 7901.
- [Wan03] Wang, Q.; Chan, T. R.; Hilgraf, R.; Fokin, V. V.; Sharpless, K. B.; Finn, M. G. *J Am Chem Soc.* **2003**, 125, 3192.
- [Way94] Wayland, B. B.; Pszmik, G.; Mukerjee, S. L.; Fryd, M. J. *Amer. Chem. Soc.* **1994**, 116, 7943.
- [Wei98] Weimer, M. W.; Frechet, J. M. J.; Gitsov, I. *J. Polym. Sci. Polym. Chem. Part A* **1998**, 36, 955.
- [Whi90] Whitesides, G. M.; Laibinis, P. E. *Langmuir* **1990**, 6, 87.
- [Wun 96] Wunderlich, W.; Benfaremo, N.; Klapper, M.; Müllen, K. *Macromol. Rapid Commun.* **1996**, 17, 433.
- [Xia98] Xia, Y.; Whitesides, G. M. *Angew. Chem. Int. Ed .Engl.* **1998**, 37, 550.
- [Xia98a] Xia, Y. N.; Whitesides, G. M. *Annual Review of Materials Science* **1998**, 28, 153.



- [Xia99] Xia, Y.; Rogers, J. A.; Paul, K. E.; Whitesides, G. M. *Chem. Rev.* **1999**, 99, 1823.
- [Xue91] Xue, G.; Huang, X. Y.; Dong, J.; Zhang, J. *J. Electroanal. Chem.* **1991**, 310, 139.
- [Yam00] Yamada, R.; Wano, H.; Uosaki, K. *Langmuir* **2000**, 16, 5523.
- [Zho97] Zhou, C.; Deshpande, M. R.; Reed, M. A.; Jones, L.; Tour, J. M. *Appl. Phys. Lett.* **1997**, 71, 611.
- [Zhu03] Zhu, H.; Snyder, M. *Curr. Opin. Chem. Biol.* **2003**, 7, 55.
- [Zhu04] Zhu, M.; Xing, Q.; He, H.; Zhang, Y.; Chen, Y.; Pötschke, P.; Adler, H. *J. Macromolecular Symposia* **2004**, 210, 251.
- [Zie79] Ziegler, F. E.; Berger, G. D. *Synth. Commun.* **1979**, 9, 539.
- [Zis64] Zisman, W. A. *Adv. Chem. Ser.* **1964**, 43,1.

## List of publications

### Articles

1. „Synthesis and characterization of photolabile aminoterpolymers for covalent attachment onto gold substrates” Sieczkowska, B.; Millaruelo, M.; Voit, B., *Designed Monomers and Polymers* **2005**, 8, 6, 629-644.
2. „Amino Terpolymers for the Preparation of Patterned Functionalized Surfaces and the Attachment of Nanostructures” Millaruelo, M.; Braun, F.; Eng, L.; Mertig, M.; Opitz, J.; Pompe, W.; Sieczkowska, B.; Voit, B. *Macromolecular Rapid Communications* **2005**, 26, F19- F20.
3. „Photolabile Carboxylic Acid Protected Terpolymers for Surface Patterning. Part 1: Polymer Synthesis and Film Characterization Millaruelo, M.; Eichhorn, K.-J.; Sieczkowska, B.; Voit, B., *Langmuir* **2006**, 22, 9436-9445.
4. „Photolabile Carboxylic Acid Protected Terpolymers for Surface Patterning. Part 2: Photocleavage and Film Patterning” Millaruelo, M.; Eng, L.; Mertig, M.; Pilch, B.; Oertel, U.; Opitz, J.; Sieczkowska, B.; Simon, F.; Voit, B., *Langmuir* **2006**, 22, 9446-9452.
5. „Photolabile Functional Polymers for Surface Patterning and Specific Attachment of Nanostructures” Millaruelo, M.; Sieczkowska, B.; Messerschmidt, M.; Mertig, M.; Opitz, J.; Eng, L.; Pompe, W.; Voit, B. *Polymer Preprints* **2006**, 47, 533-534.
6. „Photolabile and thermally labile polymers as templates and for surface patterning” Voit, B.; Braun, F.; Gernert, M.; Sieczkowska, B.; Millaruelo, M.; Messerschmidt, M.; Mertig, M.; Opitz, J. *Polymers for Advanced Technologies* **2006**, 17, 691-693.

7. „New photolabile functional polymers for patterning onto gold obtained by click chemistry” Sieczkowska, B.; Millaruelo, M.; Messerschmidt, M.; Voit, B. *Macromolecules* **2007**, 40, 7, 2361-2370.

### *Patent*

B. Voit, B. Sieczkowska, M. Millaruelo, J. Opitz, J. Voigt, W. Pompe, M. Mertig „Structured polymeric multilayered support for biomolecules, its production method and use” EP20060123899, IPF Dresden.

### *Contribution to conference*

B. Voit, M. Gernert, B. Sieczkowska

„Functional thin polymer film for imagewise structuring” Presented at the Workshop der Nanoforschergruppe, Wittenberg, Februar 02-03, 2004.

B. Sieczkowska

„Photolabile aminopolymers for Nanotechnology on gold substrates” Seminar on current research topic at the Lehrstuhl für Makromolekulare Stoffe, Institute für Technische Chemie TU München, 22-24.10.2004 Thurnau.

M. Millaruelo, F. Braun, M. Mertig, J. Opitz, W. Pompe, B. Sieczkowska, B. Voit:

„Amino Terpolymers for the Preparation of Patterned Functionalized Surfaces and the Attachment of Nanostructures” Macromoleculares Kolloquium Freiburg, Februar 2005.

# VERSICHERUNG

Hiermit versichere ich, dass ich die vorliegende Arbeit ohne unzulässige Hilfe Dritter und ohne Benetzung anderer als der angegebenen Hilfsmittel angefertigt habe; die aus fremden Quellen direkt oder indirekt übernommen Gedanken sind als solche kenntlich gemacht. Die Arbeit wurde bisher weder im Inland noch im Ausland in gleicher oder ähnlichen Form einer anderen Prüfungsbehörde vorgelegt.

Die vorliegende Arbeit wurde in der Zeit von April 2003 bis April 2009 am Leibniz-Institut für Polymerforschung Dresden e.V. im Rahmen des DFG-Projektes zum Thema: „Erzeugung metallischer Nanostructures mittels Assemblierung und Funktionalisierung von Protein und DNA“ unter wissenschaftlicher Betreuung von Frau Prof. Brigitte Voit durchgeführt.

Frühere Promotionsverfahren haben nicht stattgefunden.

Ich erkenne die Promotionsordnung der Fakultät Mathematik und Naturwissenschaften der Technischen Universität Dresden vom 16. April 2003 in vollem Umfang an.

Dresden, 03 Februar 2009

Barbara Sieczkowska